
2809673333

DEVELOPMENT OF ENGINEERING METHODS FOR THE RAPID EVALUATION OF MEMBRANE FILTRATION WITHIN BIOPROCESSES

A thesis submitted to UCL

for the degree of

DOCTOR OF ENGINEERING

by

Ranna Eardley-Patel

November 2008

The Advanced Centre for Biochemical Engineering

Department of Biochemical Engineering

University College London

London WC1E 7JE

UMI Number: U591457

All rights reserved

INFORMATION TO ALL USERS
The quality of this reproduction is dependent upon the quality of the copy submitted.

In the unlikely event that the author did not send a complete manuscript
and there are missing pages, these will be noted. Also, if material had to be removed,
a note will indicate the deletion.

UMI U591457
Published by ProQuest LLC 2013. Copyright in the Dissertation held by the Author.
Microform Edition © ProQuest LLC.
All rights reserved. This work is protected against
unauthorized copying under Title 17, United States Code.

ProQuest LLC
789 East Eisenhower Parkway
P.O. Box 1346
Ann Arbor, MI 48106-1346

I, Ranna Eardley-Patel, confirm that the work presented in this thesis is my own. Where information has been derived from other sources, I confirm that this has been indicated in the thesis.

Signed:.. .....

Date:....1st November 2008.....

Copyright Statement

The copyright of this thesis rests with the author and no quotation from it or information derived from it may be published without the prior written consent of the author.

ABSTRACT

With the advent of high-throughput screening technologies, key constraints associated with identifying potential drug candidates are being removed – the bottleneck in the timely delivery of new drugs will inevitably shift toward process development. Conventionally, the pilot plant studies required for process design only start when there is confidence that the drug candidate will make it to market. This means that this development period is very limited, and the flowsheet that enters the manufacturing phase is often sub-optimal. Collaborative work at UCL has been developing new strategies that aim to change this paradigm. The use of scale-down experiments in the drug discovery phase, in conjunction with modelling techniques, has been shown to be capable of providing more robust process definition early on in development. Such methodologies allow the study of more process options and hence rapid identification of optimal conditions, and thus mitigate the risks associated with equipment capital investment. Further advantages are that the experiments require less material, and can be done prior to, as well as in parallel to, pilot plant development. Scale-down can also be useful for the analysis of existing processes, e.g. for validation and troubleshooting, especially where material is valuable and/or scarce.

This thesis describes the design and development of a scale-down device for membrane filtration, with a focus on tangential flow microfiltration for primary clarification. The device uses a rotating disk suspended above a static membrane surface to generate surface shear, in order to mimic the global, hydrodynamic conditions found in commercial crossflow modules. Results are presented showing how filtration performance of the scale-down device ($3.5x10^{-4}m^2$ membrane area) correlates well with pilot scale data ($0.1m^2$) for a range of representative biological materials including yeast, bacterial and mammalian cell cultures. Methodologies for confident assessment of microfiltration performance are given, which are capable of dealing with different feedstocks, membrane types, and a range of operating strategies, using greatly reduced quantities of feed. The steps required to design and build the next generation of filtration scale-down device for rapid process development are also addressed, along with a discussion of the related business and regulatory issues that shape the industry.

ACKNOWLEDGEMENTS

It is a pleasure to thank the people who have contributed to this thesis, and to the journey through my doctoral studies. It is difficult to overstate my gratitude to my supervisor and mentor, Professor Nigel Titchener-Hooker. His enthusiasm and remarkable ability to put everything into perspective is truly the way that research should be conducted. I am also grateful for the advice and insight of Professor Mike Hoare, especially during the early stages of the project, and Dr Gary Lye for his extensive knowledge of bioprocess filtration theory, and organisation of the departmental filtration focus group.

The manufacture of the TFF USD device would not have been possible without the skill and expertise of Sarah Bailey, Alan Craig and Martin Town of the UCL Biochemical Engineering electronic and mechanical workshops.

This EngD was funded by the Millipore Corporation and the EPSRC. Financial support from The Royal Academy of Engineering and the IChemE's Biochemical Subject Group enabled me to present some of this work at an international conference, and prepare thus me for wider peer review.

I would like to acknowledge the industrial input and information provided by Ralf Kuriyel, Charles Christy, and Daniel LaCasse of the Millipore Corporation. Thank you for persevering with the teleconferences!

I wish to thank Brendan Fish for allowing me to do a placement at Cambridge Antibody Technology Ltd. The contribution of Karen Bannister, Jeannette Langstone, Katherine Maisy, Kalpana Nayyar, Alison Ridley, Carl Spicer, Richard Turner to the work undertaken during this time is gratefully acknowledged.

Many thanks go to Jamal Uddin, Arun Singh and Benedict Hardas for being great experimental project students, and to all the biochemical engineering students who worked with me during those hectic pilot-plant weeks.

Special thanks to my friends and colleagues in the department for getting me started and for keeping me going: Derrick Abraham, Andrew Booth, Daniel Bracewell, Natalie Boulding, James Cody, Sam Denby, Steve Doig, Billy Doyle, Pedro Esponda-Aguilar, Claudia Ferrera-Torres, Philippa Gardener, Benjamin Jake Hodgson, Christine Ingram, Helen Irvine, Nigel Jackson, Diane Kendall, Josh King, Simyee Kong, Sally Lamping, Helen Law, Leigh MacGuire, Julia Markusen, Juan Pablo Acosta Martinez, Sabin Maskey, Chris Mason, Fran Meacle, James Myers, Greg Neal, Anthony Nealon, Joanna Novais, Sam Okagbue, Sam Pickering, Jon Postlethwaite, Heide Salte, Roy Okec, Lars Pampel, Tom Reynolds, Cassandra Rock, James Scarr, Jobin Shaeri, John Ward, Barnaby Zoro.

Thanks to those friends and supporters who made the completion of this thesis worth it, if only because I can now answer "have you finished yet?" affirmatively: Kathleen Caper, Matthew Cheeks, Catherine Clayton, Gerry Czerniawski, Janine Downes, Ann Marie Earwaker, Catrin Harland, Adam Hawthorne, Claire Hill, Lucie March, Sarah Marcus, Paul Nixon, Marta Penas, David Pepper, Elizabeth Petrie, Karin Steimel, William Redgrave, Anthony Vernon.

For a thorough chance to communicate my EngD experience and results, I would like to thank my examiners Dr Mark Bustard and Dr John Liddell for their suggestions, corrections and comments.

Finally, I would like to acknowledge the unconditional support of my family: the late Kamlaba Patel, Uday Patel, Satyen Patel, Ashita Patel, Viral Patel, the late Bhadraben Patel, the late George Eardley, Anne Eardley, Michael Eardley, Mary Eardley, my parents Rameshchandra Vithalbhai Patel and Dharmishtaben Patel, my role models Romaben, Dipeshbhai, and Nishithbhai and my husband Aidan, to whom I dedicate this thesis.

TABLE OF CONTENTS

LIST OF FIGURES

LIST OF TABLES

Chapter 1 General Introduction

1.1 Introduction

This thesis aims to establish methods for the fast prediction of the processing conditions needed to yield acceptable flux and transmission performance of tangential flow membrane operations. The design, development and verification of a scale-down device and experimental methodology to mimic tangential flow filtration (TFF) systems are described. It contributes to the process engineering science base for a new generation of filtration devices with the capacity to produce a step change in the way conventional early stage filtration studies are conducted.

This initial chapter provides the context for this research, giving general information on the current methods and uses of scale-down simulations in bioprocesses. The specific research aims and objectives are then stated along with a description of the thesis structure.

1.2 Scale-down in bioprocesses

The length, complexity and costs of pharmaceutical research and development have continued to increase steadily over the last few decades. The vast majority of drug candidates never reach the market and of those that do, only a third generate enough revenue to compensate for the large research and development costs (Burnett et al., 1991; Bregar, 1996). Much effort has gone into speeding up drug discovery and considerable innovation has lead to the development of combinatorial libraries, high throughput screening techniques and the new disciplines of proteomics and generics. However, in order to avoid a bottleneck at the process development stage similar levels of effort and innovation are required (Nicholson, 1998; Willoughby et al., 2004). The concept of process scale-down provides an opportunity for this since more information can be generated using less material and in less time. The critical challenge is to determine how scale-down can be used to produce accurate, quantitative and reliable process data.

The following pages will examine the requirement and roles of scale-down models in bioprocess development discussing the different requirements for scale-down models, depending on their intended use. Sections 1.2.2 and 1.2.3 subsequently examines methods for the generation of scale-down models and the level of accuracy they are required to have. Several examples of existing scale-down models are described in Section 1.2.4, and the possibility of using these models in conjunction with one another is considered in Section 1.2.5. Further issues pertaining to the use of scale-down models, such as the combination of scale-down devices with other methods of process modelling and hence, the development of an ultra scale-down (USD) methodology are explained in Sections 1.2.6 and 1.2.7 respectively.

1.2.1 Requirement for scale-down in bioprocesses

In traditional process development the scale of operations is gradually increased to arrive at a working production-scale purification process. For economic reasons most process development work is not completed at the final scale, but instead involves extensive use of pilot and laboratory-scale equipment to predict and optimise the performance of the large-scale process. Each stage of the potential production process is tested at laboratory scale, from fermentation to purification, recovery, polishing and formulation.

This usually involves a significant number of large-scale trials to cope with the changes in behaviour or efficiency of production-scale process equipment. The complex nature of biological materials makes them difficult to characterise and their behaviour difficult to predict. The lack of predictive tools has meant that bioprocess design has been a largely empirical process relying heavily on pilot plant trials and the experiences of the design team. This approach is increasingly becoming unfeasible due to the significant costs associated with material consumption in pilot plants, and due to the difficulty of scheduling process trials in already stretched pilot or production facilities.

The response to this dilemma has come in the shape of improvements in equipment, experimental design, and computer modelling. The most popular approach to mitigate these concerns is the use of scale-down models of bioprocess unit operations. Scale-down can be defined as the attempt to mimic the operation of production- scale

equipment in geometrically similar laboratory-scale models that exhibit the same behaviour and performance without requiring the same amount of process material. Ultra scale-down (see section 1.2.7 below) is an extension of this, using models which may not be geometrically similar in conjunction with mathematical models (Boychyn et al. 2001; Lamping, 2003; Reynolds, 2005; Willoughby et al., 2004).

One of the first reported uses of scale-down techniques in bioprocessing was by Oosterhuis et al. (1985) who found that they were able to reproduce performance of a large fermenter by mimicking the fluctuations of nutrient concentrations in smaller vessels. Since then, the concept of scale-down has found wide application in biotechnology, reaching far beyond the original application fermentation development into the simulation of protein purification operations and more recently, whole process sequences. Currently, research groups have started investigating the performance of key unit operations using vastly reduced quantities of feed (millilitre scale), as a result of advances in microfluidics and liquid handling technologies (Lamping, 2003; Chandler and Zydney, 2004). The use of scale-down techniques has several advantages over the other improvement approaches, and these are described below.

Scale-down versus pilot plant studies

If good scale-down mimics of manufacturing equipment can be developed these constitute a more advantageous strategy than pilot-plant studies given the extreme importance of time-to-market, and the high value of the process streams. Scale-down laboratory devices enable the more rapid integration of unit operations into a process resulting in an earlier and possibly more accurate indication of the true overall process performance. Furthermore, this concept allows the very economical exploration of a greater number of process options that can be achieved at pilot-scale in the same amount of time. Scale-down trials save money and time because they require smaller volumes of process materials, are easier to handle, operate and clean, require less personnel resource and reduce energy consumption.

Scale down versus modelling

Unlike purely chemical systems, biological feedstocks have many uncharacterised components in terms of their size, structure, charge, hydrophobicity etc. Even a great percentage of the defined constituents have unknown responses to various

environmental conditions and stresses. This leads to considerable uncertainty (usually ±30%) in generic models. Nevertheless, these models can be very helpful in designing scale-down experiments, the outputs from which can be used to improve the simulation. Varga et al. (1998) utilised this approach to refine the accuracy of a natural yeast homogenisation model to predict for a recombinant strain from ±30% to ±10%. Scale-down models may be utilised with process modelling to accelerate development and corroborate performance of the predicted manufacturing process with respect to some difficult-to-measure variable, and this is considered further in section 1.2.6 and Chapter 2.

Well performing scale-down models are capable of delivering the same information as trials on their large-scale counterparts, but without the expense of time and resources that inevitably goes with pilot or production-scale process trials.

1.2.1.1 The roles of scale-down

Scale-down models can fulfil a number of roles during process development and throughout a bioproduct's lifetime. Bylund et al. (1999) highlighted the two independent circumstances in bioprocess development when a scaling methodology is required: to facilitate scale up of a new process and to evaluate modifications to an existing one. However as scale-down technology improves the models are also becoming useful tools during the early stages of process development and during process validation.

Role 1: Process Development

During bioprocess research and development the aim is to determine a series of steps that will capture the product from the fermentation broth and concentrate and purify it to the required level. Since there are a wide variety of alternative operations that could be used to achieve this there is a need to screen rapidly a large number of options. Scale-down techniques can be used to assist in this task by rapidly assessing the feasibility of a number of different operations and evaluating alternative options. For example, if the feed seems to be shear insensitive, and the yields obtained by the filtration experiments are not sufficient, then an alternative unit operation such as centrifugation ought to be

considered. It must be noted, however, that such considerations are only relevant until the process flowsheet has been specified.

This example serves to highlight the intrinsic value of adopting scale-down methods since they can make the required information available at a much earlier stage of process development than would be possible by conventional pilot-plant based development strategies. Figure 1.1 below outlines the interaction between scale-down tools and process development.

Figure 1.1: Generation and use of scale-down models in process development (adapted from Sweere et al., 1987).

As indicated by the schematic in Figure 1.1, the results of the scale-down analysis form the basis of the practical design of the scale-down simulation. The basis for the selection of aspects that need to be included in the scale-down simulation and approaches to their experimental representation are discussed in section 1.2.2.

As at the early stages of process development the objective is simply to determine which operations are actually feasible, the accuracy requirements are low and the investment in the scale-down model can therefore also be low. Once the flowsheet has been specified, and the interaction between unit operations becomes a criterion for

process optimisation, the quality of the scale-down data needs to increase. This variation in accuracy between different stages is considered further in Section 1.2.3.

Role 2: Optimisation of existing processes

The yield and purity obtained in a particular process is improved via the use of process optimisation (Zhou and Titchener-Hooker, 1999). This is concerned with making observations on the effects of changing process variables in the pilot plant or laboratory and subsequently transferring the results to production scale. However, the question of what to change and by how much is critical. Methods are needed to test the impact of different process changes with minimal use of time and resources, and to evaluate if the regulatory requirements for post-approval changes are feasible to execute.

A scaled-down model of an individual unit operation can be a very useful tool. The potential uses for such a model include evaluating the sensitivity of an operation to changes in feedstock, process optimisation and assessing the impact of any suggested process changes. In more general terms, a scale-down model should allow better understanding of the process. Predicting the effects of changes to an existing process at small scale removes the expense of testing at large scale, and the need to run larger pilot scale tests for troubleshooting and further optimisation and the identification of process limits would be reduced (van Reis et al. 1997).

Obviously, the degree of optimisation possible relies on the quality of the scale-down procedures used. However, in almost all situations scale-down experiments can be used to find specific process parameters that assist with process optimisation. Obtaining these values by experimental means is often easier than by purely theoretical means since the level of understanding required is likely to be lower; in some cases experimentation is the only way to find a particular parameter.

Limitations in the accuracy and reliability of current scale-down models have restricted their use as tools for process optimisation, and pilot or full-scale verification is still necessary. However, these models are nevertheless useful as they can narrow the range of process variables and highlight particular aspects of a process that could be improved. As the accuracy of scale-down techniques improves it may be possible to eliminate large-scale optimisation studies and simply verify the performance of the

process designed at the laboratory-scale. If the model is sufficiently accurate then a biopharmaceutical corporation could demonstrate and validate its equivalence to the production scale process; undoubtedly, the requirements of a scale-down model to do this are significant, since the model will need to accurately simulate all aspects of the performance of the large-scale operation. The development and validation of such a model may be difficult and resource intensive, but the potential savings made by minimising disruption to the manufacturing process would justify this.

Role 3: Validation Studies

Scale-down can also be used for validation studies (van Reis et al., 1997; Winkler et al., 2000). For example, most companies generate a "process capability specification" wherein the known variability of data is determined for a certain number of runs, almost always fewer than ten, usually less than five (Bobrowicz, 1999). This validation effort is flawed in that more runs are required to establish process variability and specifications usually need to be made before scale-up and optimisation changes to the process; accurate scale-down models could resolve both of these issues.

Although validation requirements would be reduced to a certain extent; a small number of large-scale trials would still be required for the regulatory approval process, and such studies will always be best performed in the manufacturing facility to be licensed (Gardner et al., 1996).

1.2.2 Methods of developing scale-down models

The creation of scale-down models is a multi-step procedure shaped both by the requirements of process development and the available resources. The principle of scale- down, i.e. the dedicated simulation of the performance, as well as the shortcomings, of large-scale equipment in bench-scale experiments requires knowledge of those aspects in which the behaviour of common laboratory equipment differs from its large-scale counterpart. The creation of a scale-down model is therefore initiated by a thorough analysis of the operation or process to be simulated. Methodical approaches to conducting this scale-down analysis will be discussed in the subsequent sections.

1.2.2.1 Scale-down analysis

There are two objectives when creating a scale-down model, the first is to identify the scale-dependent aspects of a large-scale operation and the second is to minimise the number of parameters to be scaled.

The identification of scale-dependent aspects of large-scale process behaviour forms a classical chemical engineering problem that has been treated extensively in the literature on process scaling (Atkinson and Mavituna, 1991) and a number of different approaches have been developed and successfully applied in chemical engineering. However, to be useful for biopharmaceutical process development such approaches should fulfil certain requirements as will be discussed below.

The second objective of keeping the number of relevant parameters to be simulated to the minimum possible is less easily accomplished. Since the reaction of the biological material to changes in the processing environment is generally not known, there will be a frequent need for experimental evaluation of the influence of individual parameters on the performance of an operation. As a whole, a scale-down analysis therefore combines theoretical and practical approaches to arrive at a definition of the requirements for a valid scale-down simulation of the process under study.

A number of strategies exist for scaling various operations and each unit operation has its own specific scaling criteria, but some generalisations can be made. Tactical methods for scaling include fundamental methods, semi-fundamental methods, dimensionless analysis, regime analysis, heuristics, trial and error, and combinations of the above (Oldshue, 1985; Atkinson and Mavituna, 1991). An overview of the steps involved in the generation and application of a scale-down model in biopharmaceutical process development is shown in Figure 1.2.

Which of these strategies works best will depend upon the operation being scaled down and the intended use of the scale-down model. The main criterion for the applicability of these methods to the scale-down analysis of biopharmaceutical operations is their ability to tolerate the scarcity of the fundamental knowledge-base of processes in biotechnology. In that regard trial and error probably represents the most generically

applicable technique, but is of little practical value for scale-down analysis since no information on scaling behaviour of the system is obtained.

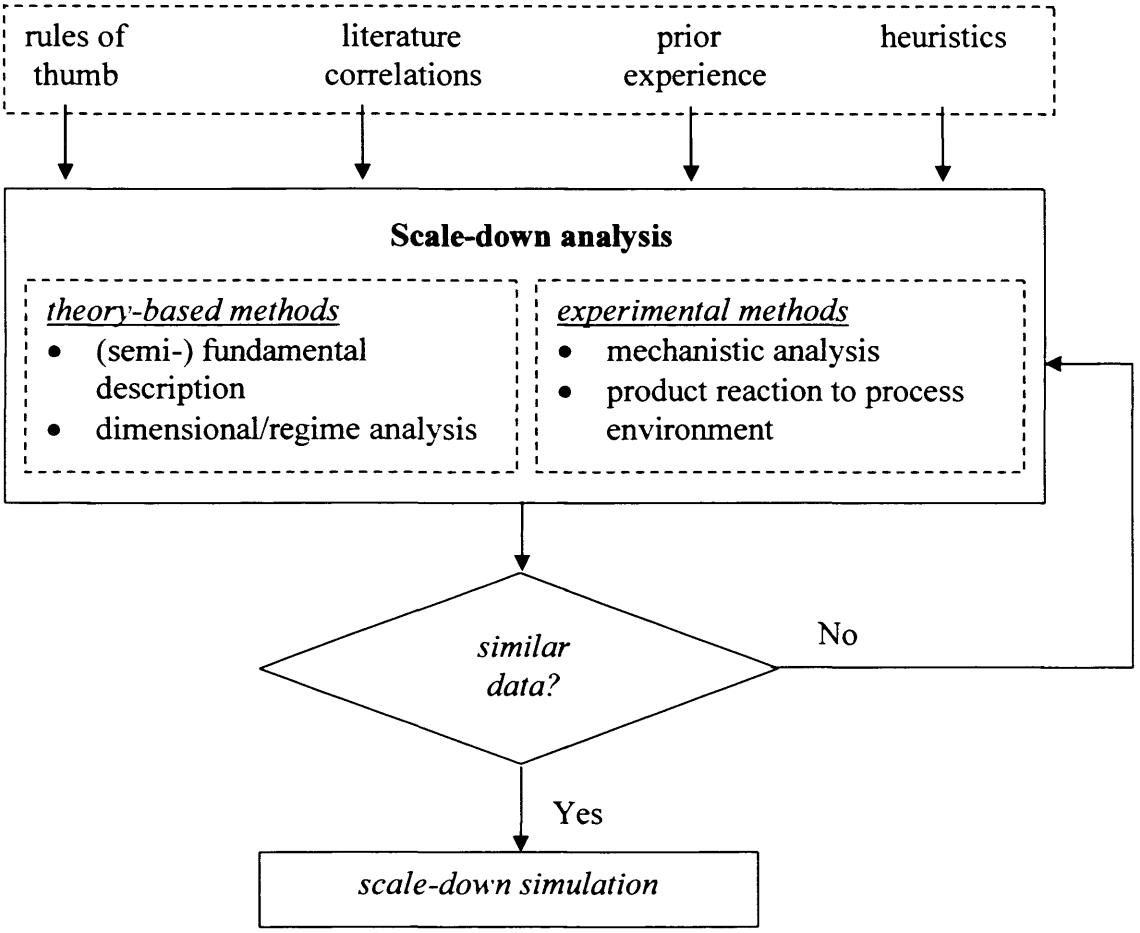

Figure 1.2: Overview of the application of process analysis to the creation of scale-down simulations.

Fundamental methods of scaling are based on a complete mathematical solution of the fundamental equations such as mass balances, transport terms, kinetics and equilibria that describe a process. Since the sheer number of such equations can be large, semi-fundamental methods facilitate the situation by making simplifying assumptions, such as plug flow, a well-mixed reactor etc. Even then, the resulting mathematical framework is often of considerable complexity, making it unwieldy for practical use. More importantly, the level of fundamental understanding required for the generation of accurate descriptions of e.g. cell growth kinetics is rarely available in biotechnology. Fundamental methods themselves are therefore of little practical importance for biopharmaceutical process development, even though they can be used to great effect in combination with other techniques, such as regime analysis or heuristic rules (Atkinson and Mavituna, 1991).

Dimensional analysis is based on the characterisation of a system by dimensionless ratios of groups of parameters. These dimensionless numbers represent the ratio of characteristic times of individual processes within the system. By keeping them constant during scaling the relative importance of individual processes is maintained (Zlokarnik, 1983), but in biotechnological systems however it is rarely possible to arrive at a complete description of a process in terms of dimensionless numbers.

The use of regime analysis, e.g. based on characteristic times, has therefore been suggested to identify the governing regime of the process under study, which then has to be kept unchanged during scaling (Sweere et al., 1987). Since characteristic times can be obtained from a variety of sources including experiments and reasonably accurate correlations from the literature, the method is particularly suitable for application in biopharmaceutical process development. Regime analysis defines the most important mechanism of a scaling problem, rather than eliminating insignificant variables. For example, if the controlling factor is dependent on the fluid dynamics of the system due to resistance to diffusion, then the regime is dynamic e.g. mass transfer through a fouled membrane. In regime analysis, the first stage is to ascertain what the ruling regime is in a particular operation. It is important to define a characteristic parameter on which to base laboratory scale experiments, especially before the construction of any specialised equipment.

In summary, scale-down analysis plays a crucial role in the generation of scale-down models. Since failure to simulate relevant phenomena in the scale-down model will result in misleading results, the objective of scale-down analysis is to identify all aspects of the behaviour of a large-scale operation that need to be included in the scale-down simulation. At the same time however, it is necessary to keep the number if parameters to be included to a minimum in order to facilitate the practical design of the scale-down model.

1.2.2.2 Principles of similarity

Regardless of the scaling method used, the deciding criterion for the successful creation of a scale-down model is the resulting similarity to the large-scale operation. In chemical engineering two systems are termed similar if they are geometrically,

mechanically, thermally and chemically alike (Sweere et al., 1987). Similarity in all four aspects can generally not be achieved for most engineering systems.

Principles of similarity are concerned with the relations between physical; systems of different sizes and it is thus fundamental to the scaling-up or down of physical and chemical processes. It is concerned with discovering the ratios of magnitudes within the system which govern its special and temporal configuration, irrespective of the measured scale. The four states of similarity are discussed below.

Geometric similarity, or miniaturisation, is intuitively the most accessible way of designing scale-down simulations. The use of dimensional analysis during the scale-down analysis, for instance, automatically leads to geometric similarity (Sweere et al., 1987). Geometric similarity is achieved when for every special point in one body there exists a corresponding point in the other. The points are linked by a scale ratio. An example of a criterion for geometric similarity is the maintenance of a constant path length in tangential flow filtration. Geometric similarity of the equipment simulating the real operation may not be required if the ruling regime is better modelled with an alternative geometry; the important criteria at this stage is that laboratory experiments must be representative of what goes on at production scale.

However, since not all processes change equally with the systems dimensions, geometric similarity in scale-down models can produce misleading results. In the example of fermentation scale-down, the small-scale reactors could only simulate either the hydrodynamic conditions in the large-scale fermenter or the mixing conditions, but not both at the same time (Oldshue, 1985). Similarly, miniature models of centrifuges will not reflect the conditions of acceleration and shear that prevail in the production-scale device. However, miniaturisation can in some cases be successful as demonstrated by the reduction of the feed capacity of a pilot-scale disk-stack centrifuge through the insertion of spacer blanks in the centrifuge bowl, thus permitting studies of centrifuge performance on significantly reduced amounts of feed material (Mannweiler and Hoare, 1992).

Considerations leading away from geometric similarity are typically the result of regime analysis and related scaling methods. Their logical consequence is to avoid geometric

similarity in the scale-down model in favour of a more realistic representation of the governing mechanisms. In the case of fermentation this leads to the design of small-scale reactors that permit the simulation of both the hydrodynamic conditions and the mixing regime in the large-scale fermenter, e.g. through the installation of riser tubes or two-compartment reactors (Oosterhuis et al., 1985; Bylund et al., 1999). In centrifugation this concept has recently been taken one step further by fully splitting the scale-down simulation of a large-scale centrifuge in two sub-models (a shear cell and a laboratory centrifuge) that each mimic one aspect of the behaviour of the large-scale device (Boychyn et al., 2001).

Mechanical similarity is an extension of geometric similarity to stationary or moving bodies which are subjected to forces. One type of mechanical similarity is kinematic similarity; this is achieved when the particles within geometrically similar moving systems trace out geometrically similar paths in corresponding intervals of time e.g. the deposition of cells onto a membrane surface.

Thermal similarity is concerned with systems in which there is a flow of heat. It requires geometric and kinematic similarity.

Chemical similarity is concerned with reacting systems in which composition varies. It is achieved when corresponding concentration differences are in constant ratio, and requires geometric, kinematic and thermal similarity.

Similarity criteria are dimensionless quantities and may be derived by dimensional analysis provided that all the variables that govern the system are known. Dimensionless numbers can be used to ensure that a scale-up or scale-down model is fundamentally similar to the original. However, dimensional analysis can lead to false conclusions if a significant variable is omitted from the problem, and alone this method does not give information about the forms of the functions which link individual parameters together (Coulson and Richardson, 1990).

The design of scale-down simulations responds to a number of factors such as the phenomena to be simulated, the requirements for analytical installations and sampling, the amount of material available for testing as well as the availability of resources such

as time and labour. The deciding criterion however is the degree of similarity to the large-scale operation that needs to he achieved. Since similarity in all aspects cannot be realised (see above) scale-down models have to focus on maintaining similarity where it is needed whilst neglecting it elsewhere. The identification of those aspects of similarity that matter for an individual scale-down problem partly results from the scale-down analysis, but may require additional experimentation to ascertain the reaction of the biological material to certain phenomena. The approach to the design of a scale-down model is therefore, to some extent, a result of the method employed during scale-down analysis.

1.2.2.3 Practical design of scale-down mimics

Before creating a scale-down model for a particular operation a thorough understanding of the industrial operation is required. This should identify the important operating parameters as well as highlight the key differences between the industrial operation and commonly used laboratory equipment. After this, the basis for scaling needs to be identified i.e. which aspects of the large-scale operation need to be reproduced in the scale-down mimic?

Nonetheless, determination of the critical operation parameters and recreation of the product environment may not be sufficient to develop a good scale-down model as the equipment used in large-scale industrial operations is often fundamentally different from the experimental apparatus used in a laboratory. For accurate scale-down, engineers seek to create laboratory-scale models, which simulate the behaviour of production-scale devices, particularly the reduced efficiency often encountered during scale-up. This could be accomplished in some cases by fabricating a geometrically similar, small-scale replica of the industrial machine. However, this is often uneconomical, and for some equipment e.g. high-speed centrifuges and filter presses this is simply not feasible. Another strategy is to modify the existing piece of industrial equipment in such a way that it requires only a fraction of the process material to give a similar performance.

It must also be considered that industrial equipment is usually made from stainless steel and the processes are heavily automated and controlled; in contrast laboratory

equipment is often made of glass or plastic and the level of control and automation is much lower. The effects of this on performance may be negligible but they should be considered when comparing a scale-down model to a larger operation. For example the location of sample points and instrumentation can affect the results they yield and biological products have a tendency to adsorb to certain materials. Thus, in order to develop an accurate scale-down model, it is often useful to consider not just a specific piece of equipment but also the ancillaries such as pumps, piping, valves and detectors etc.

The critical challenge is to determine how scale-down models can be used to produce accurate, quantitative and reliable process data.

1.2.3 Accuracy, reliability and extent of scale-down models

A central question in the use of scale-down models relates to the reliability of the data obtained. Reliability in this respect refers both to the numerical accuracy of the parameter values compared to measurements from the large-scale equipment and to the validity of trends or critical parameters found in the scale-down model compared to the actual behaviour of the large-scale device. The numerical accuracy of scale-down models depends on several factors which partly counteract each other. Overall, the control and determination of process parameters at small scale is easier due to the difficulty of obtaining representative measurements of, for instance, spatially distributed variables at large-scale (Sweere et al., 1987). However, at very small scale, the influence of the analytical instruments on process parameters can in itself lead to significant deviations in the measurement parameter values (Gagnon, 1997). Table 1.1 shows some examples of comparisons between scale-down prediction of parameter values and the results of large-scale measurements. Overall, a deviation of scale-down data of less than 10% from the large-scale parameter values seems attainable.

At least equally important as the numerical accuracy of scale-down models is the ability of scale-down data to predict trends in the behaviour of large-scale equipment. Simple scale- down models can usually only provide a "yes/no" answer regarding the importance of a certain phenomenon in the large-scale system (Bylund et al., 1999). The value of such information on large-scale process behaviour, however inaccurate in

absolute parameter values, should not be underestimated since it can save long and fruitless large-scale process trials, or help to avoid surprises during process scale-up.

The ability of scale-down simulations to predict the sensitivity of large-scale process performance to operating parameters depends to a large extent on the effort invested during the generation of the scale-down model. However, some constraints to this exist.

System	Performance Measure	Scaling factor	Accuracy of prediction *	Reference
E. Coli fermentation	Biomass yield	800	-1.2	Bylund et al. (1999)
Soya protein precipitation	Precipitate particle size	740	26.1	Bell et al. (1983)
Yeast homogenate precipitation	Total protein precipitated	700	-6.3	Boychyn (2000)
Centrifugal precipitate removal	Clarification	600	2.3	Boychyn et al. (2001)
High-pressure homogenisation	Cell debris particle size distribution	10	~0	Siddiqi (1998)
Expanded bed adsorption	Product breakthrough curve	~200	6	Willoughby et al. (2004)
Ultrafiltration	Protein yield	212	1.2	van Reis et al. (1997)
Ultrafiltration	Processing time	212	4.8	van Reis et al. (1997)

*Table 1.1 Examples of the accuracy of scale-down prediction of pilot-scale equipment performance. *Accuracy is calculated as % deviation of the scale-down prediction of the individual parameters from their actual value in the large-scale process.*

In situations where two aspects of large-scale process behaviour cannot be scaled simultaneously, but nonetheless both influence the process result, the development of a reliable scale-down model will be difficult. More importantly the existence of non-

scaleable parameters, such as gravity or a characteristic dimension of a system, places a lower limit on the size of scale-down simulations. That such a limiting dimension need not be microscopic is illustrated by the following example. The presence of the walls of a chromatographic column disturbs the uniformity of the packing due to geometric effects in the near wall region, and due to frictional support of the bed by the column wall in a zone extending 20 – 30 particle diameters into the column (Shalliker et al., 2000). For a typical laboratory column of, for instance, 2.5cm diameter and filled with a process chromatography resin of a particle size of 100μm, this translates to an outer shell of 2-3mm thickness of bed disturbance which can give rise to misleading results in small-scale trials.

The numerical accuracy that is actually required from scale-down models is likely to depend on the stage of process development during which scale-down is employed, as highlighted previously in 1.2.1 above. Particularly in the early stages of process development a rapid and reliable assessment of the overall ability of a certain unit operation to deliver the required purification performance is more valuable than an accurate prediction of the precise performance of that operation, which might still be subject to change during the further course of the process development project (Storey, 2000).

As a product prepares for entry into clinical trials the process development team must transfer the manufacturing process that was used in the laboratory into the pilot plant. This change of scale inevitably leads to some undesirable changes in performance due to the different environmental and operating conditions. These changes can be difficult to predict and may delay the production of clinical trial material while thee process is adjusted to rectify its performance. The use of suitable scale-down models can predict these changes in performance; therefore any surprises when scaling up can be avoided and the production of clinical trial material is not delayed. Obviously the level of accuracy required from the scale-down models is much greater at this stage than during actual processing. However, the availability of resources is likely to be greater since the importance of getting the process right at this stage is considerable, and any delays to development are highly undesirable.

To conclude, the reliability of scale-down models is influenced by several factors, such as the scale of operations, the analytical tools and the nature of the system to be scaled. An evaluation of the reliability of scale-down models must take into account the actual requirements of the intended application. The stage of the development project will determine the extent of validation work required to demonstrate both the numerical accuracy and the overall reliability of a scale-down simulation.

1.2.4 Scale-down of bioprocess unit operations

This section aims to give a brief introduction to the scale-down of bioprocess unit operations. Recent examples of where scale-down techniques have been successfully applied to bioprocess equipment are listed in Table 1.2.

Unit Operation	**Literature references**
Fermentation	Bylund 1999; Lamping, 2003
Homogenisation	Siddiqi, 1997; Chan et al. 2006
Jet mixing	Baker, 2001; Meacle 2003
Precipitation	Bell et al., 1983; Boychyn, 2000; Pampel, 2002
Centrifugation	Boychyn, 2000; Hutchinson et al., 2006; Salte et al., 2006
Depth filtration	Reynolds, 2005
Ultrafiltration	van Reis et al., 1997
Expanded bed adsorption	Willoughby et al., 2004
Chromatography (including membrane, ion exchange, adsorption, affinity, annular etc.)	Winkler et al., 2000; Kelley et al. 2004; Reynolds, 2005; Neal, 2005; Siu et al., 2006, Salisbury et al., 2006

Table 1.2 Examples of bioprocess unit operation scale down.

A large amount of work on scale-down models has been produced; a good review of this field is given by Maybury (1999) and Titchener-Hooker et al. (2008). The approaches utilised in each of the above cases vary according to the type of operation and the extent of scale-down (in terms of processing volume). Attempts at scaling almost every bioprocess operation have been made, but their general applicability and

scope of operation is still an area for improvement. In particular, scale-down of tangential flow membrane filtration has been restricted to linear scaling, limiting it's potential for ultra scale-down.

1.2.4.1 Scale-down of the entire unit operation

Most scale-down models only deal with the core function of a unit operation down i.e. the "processing" part of the unit operation and are not suitable for studying secondary operations such as cleaning and regeneration. Industrial processes may also have intermediate holding or transfer stages between key operations, which may involve a number of pumps and valves and a network of pipes. Since these factors can have an effect upon the product e.g. shear damage in pumps or protease activity in a holding vessel, they need to be accounted for is scale-down models.

Conversely, the use of disposable technology in bioprocesses is becoming more popular (Novais, 2001). For example, several companies no longer reuse the membranes used in separation applications, due to the high cost and difficulty of the cleaning step validation (Meacle et al., 1999). The impact of batch-to-batch variations between these disposable items adds an additional parameter to the host of processing variables, and should therefore be able to be assessed by the scale-down methodology.

Finally, the process sequence up and downstream of the operation being scaled-down should be considered in terms of the interaction and constraints they provide the processing step. Examples of the issues arising include the following:

- Variability of the preceding unit operation will impact on the operation of the downstream step.
- More rapid processes at the small-scale may fail to detect the effects of pH, ionic strength, temperature or proteases and other agents on product stability over prolonged times.

Where practical, the above production details should be considered and incorporated into the scale-down experimental methodology. This aspect is extended further to the modelling of process sequences in the folowing section.

1.2.5 Scale-down of whole processes

Scale-down process simulations are principally based on scale-down mimics of individual unit operations. However, even though most of the published work on scale-down focuses on individual unit operations, it is important to realise that the concept of a "stand-alone" unit option has little practical meaning in process development. The purpose and design of any unit operation is defined in the context of the process within which it operates, and is thus equally determined by the output of operations further upstream as by the requirements of downstream processing steps (see section 1.2.4.1). Current approaches to scale-down usually see one operation studied and optimised at a time, this type of approach means that overall process performance is likely to be sub-optimal (Groep et al., 2000). Scale-down simulations of process sequences employed in the recovery of proteins have in recent years received growing attention both in academia and in industrial application (Maybury, 1999; Gadam et al., 2001; Varga et al., 2001; Pampel et al., 2001; Neal 2005).

Creating scale-down models of process sequences can be difficult as process scale-down faces all of the problems encountered in the development of scale-down models of individual unit operations (c.f. section 1.2). In addition to this, the way in which the individual unit operations depend on each other in their performance has to be represented accurately in the laboratory (Zhou and Titchener-Hooker, 1999; Groep et al., 2000). The failure to include relevant aspects of large-scale process behaviour into the scale-down simulation can produce misleading results and hence undesirable surprises during process scale-up. While past experience offers some guidance as to the aspects which are most likely to affect process performance, the complex behaviour of biological macromolecules tends to inflate the number of potentially relevant influences which might need to be included in the scale-down model. A systematic approach is therefore needed which permits engineers to first collect all factors to potentially contribute to process performance and subsequently to conduct a methodical evaluation of the most relevant parameters. Ultimately this would yield a set of essential process parameters and interactions which need to be included in the design of the whole process scale-down model.

In order for whole bioprocesses to be scaled down current scale-down models will need to be improved and very accurate scale-down models that are capable of producing material representative of the large-scale are required. As well as improving accuracy, the scope of scale-down models will need to be increased to incorporate all aspects of a particular process stage.

1.2.6 Interaction of scale-down with process modelling

Process modelling and scale-down share a common objective in their attempt to reduce an operation or process to manageable elements either for mathematical representation or for experimental simulation. The shortcomings of purely theory-based prediction of bioprocess behaviour have been touched upon in the previous sections (see section 1.2.1). Scale-down can help alleviate this situation by providing supporting data at crucial junctures, thus improving the overall reliability of modelling results (Varga et al., 1998; Varga, 2001; Zhou and Titchener-Hooker, 1999a). However, mathematical models can also serve as an important extension of the range of scale-down simulations by providing rapid interpolation and extrapolation of the data obtained in scale-down trials. In particular, computational fluid dynamics are increasing becoming an important tool in the development of scale-down models simulation, where they can provide a degree of insight into the process that would be difficult to obtain on a purely experimental basis (Boychyn et al. 2001; Meacle 2003).

Another point of particular interest is the joint application of scale-down process mimics and economic process models, since both techniques can provide complementary information for process development. Economic process simulations are increasingly being employed in process development not only for the examination of absolute project feasibility but also in the more detailed fashion of comparing alternative process designs for their economic efficiency at large scale (Vasquez-Alvarez et al., 2001). The benefit gained from the use of economic process models in development is maximised the earlier this source of development information is exploited (Fulton, 2001).

Existing tools for considering economic information during process development comprise a wide range drawn from the chemical processing industries and, lately, process simulation software packages specific to bioprocesses (Petrides; 1994). The

core of economic process simulations consists essentially of pricing information for equipment and material used, unit operation models and mass balances to estimate consumption of resources and production as well as a set of rules of accounting used to convert this information into financially meaningful statements. As for other process models, scale-down can play a central role in the application of economic process simulations during process development by providing new and realistic information on the performance of individual unit operations or process sequences. The relation of scale-down to economic process simulations is not one-way though. Economic process information can also be used to advantage in the generation of scale-down models, by highlighting aspects of process behaviour that have a particularly strong bearing on economic process performance and therefore should receive special attention in the development of the scale-down mimics.

Pampel (2000) identified a strong synergy between scale-down experimentation and economic models in process development work to resolve a yield-productivity conflict in the recovery of proteins from transgenic milk. It was shown that in process optimisation work situations could arise where scale-down mimics and economic models have to be used in a complementary fashion in order to resolve key questions of process performance. In such situations both sources of information had to be considered as mutually dependent on each other. The use of modelling within a scale-down methodology is discussed further below and in Chapter 2 of this thesis.

1.2.7 Ultra scale-down concept

Currently, scale-down in bioprocess development is viewed as the use of pilot-scale equipment on a 1 to 100L scale. Ultra scale-down (USD) aims to use 10's of millilitres of material i.e. taking the operation down to laboratory scale. This leap in magnitude presents several challenges to engineers, including hardware design and the development of analytical techniques that can cope with smaller process samples. Below is a summary of the challenges for an USD device:

1) Mimic large-scale performance on 1-100mL scale. The USD device should:
    a) produce material representative of the large scale process
    b) obtain data on the performance of that operation

2) Use data from the device to extrapolate to other process conditions, and hence define windows of operation.
3) Use data to project process solutions (e.g. assess changes to upstream operations) e.g. via USD indices.

Thus USD can be defined as the combination of a scale-down device that mimics the whole unit operation, semi-empirical modelling techniques, and a sub-set of material properties data, which is specific to each bioprocess feed.

Both USD and traditional scale-down methods are quick, simple and inexpensive to perform. However, USD techniques have several advantages over their traditional counterparts. The major limitation of the traditional techniques is that they tend to focus on a few important parameters and rely solely upon calculating how these parameters should be scaled down. As a result of this, traditional scale-down methods often represent an ideal situation that cannot be achieved at large scale since important process considerations are ignored. The effect of this is that the scale-down methods over predict the performance of large-scale equipment. Ultra-scale-down techniques take into account all aspects of large-scale operation including scale-down parameters, mode of operation and ancillary equipment. Factors such as shear in centrifugation (Boychyn et al., 2001), cake structure and formation in depth filtration (Reynolds et al., 2003) and diffusion effects in chromatography may impact upon the performance of an operation and so need to be considered.

USD techniques incorporate these factors either by mimicking them directly within the scale-down devices, or by establishing a correction factor in the associated modelling (Reynolds et al., 2003). Overall, USD techniques through a greater understanding of large-scale processes allow the production of representative process material, improve the quality of process data and enable better process understanding. All this should contribute to more streamlined process development with fewer unforeseen process or operational issues.

Figure 1.3 below depicts the components of USD and compares it qualitatively to current process development procedures. Along the bottom axis are the initial phases of product development. Conventionally, pilot plant development only starts when there is

confidence that the drug candidate will make it to market. This means that time is very limited for process development, often requiring the process to be right first time.

The development and implementation of USD techniques for process development aim to change these rules. The use of scale-down experiments in the drug discovery phase, in conjunction with modelling techniques should lead to more robust process definition earlier on, and is therefore superior to current techniques.

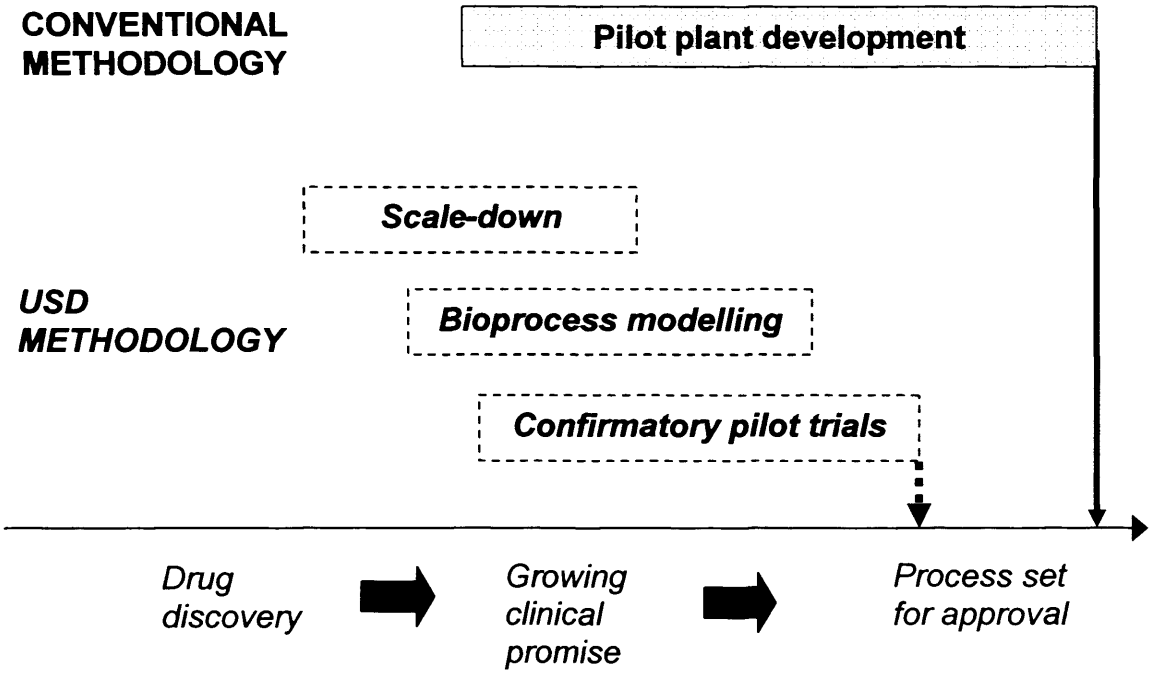

Figure 1.3 Comparison of USD methodology with current techniques.

In essence, the use of USD devices that require millilitres of material means that experimentation can begin in the lab (before the pilot plant is built). Individual unit operations can be optimised and the interactions between upstream and downstream components can be studied, leading to a better overall flowsheet. In addition, it allows the study of more process options and hence rapid identification of optimal conditions, and assessment of unit operation integration, and potentially delayed risk of capital investment.

1.3 Summary and Conclusions

The discussions in Chapter 1 have highlighted the importance of small-scale experimentation for the development of biopharmaceutical processes. Aspects that are important for the use of scale-down models in process development include their generation, and the quality of the data obtained. However, it is also clear that the generation of scale-down models is no trivial undertaking. It is crucial to arrive at a reliable representation both of the primary purpose of an operation as well as secondary, often subtle influences of the process environment on the biological product, all the while keeping the complexity of the scale-down model down to a manageable level.

Two further aspects of scale-down that are of particular interest to process development were highlighted. Section 1.2.5 refers to the possibility of simulating not only individual operations, but also whole process sequences in the laboratory by using appropriate scale-down mimics. The interest in process scale-down results from the convenience and efficiency of conducting whole process studies at bench scale, as well as from the need for a method that permits the identification and investigation of the complex, often long-reaching interactions that occur in large-scale biopharmaceutical processes. The second aspect of the use of scale-down mimics in process development relates to their interaction with other types of process simulations. Section 1.2.6 identified especially the combination of scale-down with computer modelling as an attractive field of study, since the capabilities and requirements of both types of process simulation effectively complement each other.

Section 1.2.7 described the integration of a scale-down device with bioprocess modelling techniques and material properties data to give rise to an ultra scale-down (USD) methodology. The USD concept is based on creating laboratory scale mimics of production-scale processes and identifying and simulating the key features that determine the performance of the large scale process equipment. The overall benefits of an USD methodology can be summarised as follows:

- Minimise labour and feedstock usage i.e. more studies can be conducted at small scale, given the same resources and time constraints as conventional pilot-scale studies;

- Aid to process development and validation, plant troubleshooting, process optimisation, comparability protocols;
- More economical to run multiple trials;
- Sanitisation trials involving spiking with contaminants, which cannot be done with actual production equipment, may be carried out e.g. viral clearance studies;
- Studies can be performed while pilot plant is being commissioned;
- Reduce risks involved with capital expenditure, by providing parameters for equipment selection;
- Process mimicked directly from laboratory to industrial scale and back i.e. studies can provide information for process development, and troubleshooting/optimisation once the process has been scaled up.

1.4 Research aims and objectives

The aim of this thesis is to develop an USD methodology for TFF. The specific objectives used to achieve this are as follows:

- To review and evaluate flux and transmission models for TFF for their suitability of use for a USD methodology.
- To design and build a prototype USD TFF scale-down device which is suitable for various filtration operations such as concentration, diafiltration and normal flow filtration (NFF). This would include the incorporation of suitable instrumentation into the design of the TFF scale-down device, and specification of the ancillary filtration equipment.
- To verify the results obtained from the scale down device against data generated using conventional, pilot-scale equipment, i.e. to commission the system, with "real", complex biological media.
- To define a way to compare different membrane/feed combinations in order to rank the filtration performance e.g. in the form of a USD index for membrane TFF.
- To define a graphical method to present the USD data in a pragmatic and industrially relevant way.
- To show an appreciation and understanding of the impact of the USD concept on bioprocess business aspects.

Further developments in this area, used in conjunction with the work in this thesis should lead to refinements of the USD methodology in order to make it a commercially viable design tool for the rapid assessment and evaluation of TFF for bioprocess applications.

1.5 Thesis structure overview

Chapter 1 has given an overview of the motivation for ultra scale-down (USD) and its benefits. A review of the approaches taken to scale-down several bioprocess unit operations has been presented, and highlighted the lack of application of such methodologies to tangential flow membrane filtration (TFF).

The following chapter presents the theory behind scale-down of TFF for bioprocess applications, culminating in a strategy for the development of a USD methodology for this unit operation. Theoretical considerations for membrane filtration are further extended in Chapter 2 with a review and discussion of the flux and transmission models available for TFF, focusing on microfiltration (a fuller review of the main approaches previously considered in the literature is given in Appendix 1). Parameters for use as a "filtration index" are discussed as a way of assessing the "filterability" of different feeds in relation to each other, in order to comply with the definition for USD. The concept of Windows of Operation is applied, and suggestions for graphical methods by which to present the data generated from the USD experiments and modelling are given.

Chapter 3 presents a scale-down device for TFF and the rationale behind its development. This device is intended for use in conjunction with the modelling approaches described in Chapter 2, and is therefore referred to as the TFF USD (tangential flow filtration ultra scale-down) device.

For ease of reference, the materials and methods used for all the experiments presented in this thesis (Chapters 5, 6, and 7) are collated together in Chapter 4.

Chapter 5 presents data from preliminary experiments using yeast-based feeds (whole cell and homogenate) to test and validate the TFF USD device against conventional filtration equipment. The data is used as inputs into the models described in Chapter 2,

and the output compared to the experimental results. A program listing of one of these models is included in the appendices.

The verification work is continued in Chapter 6, using a complex bacterial feed (an E. coli lysate), extending the scope of operation to diafiltration. In addition, the "filtration index" for this feed is determined from the data generated at both scales.

Chapter 7 completes the verification work undertaken with an industrial partner, by presenting data using mammalian cell broths, and therefore demonstrating the applicability of the TFF USD device for yet another major class of bioprocess feed.

Finally, to place this research into context, Chapter 8 presents a discussion of the related business and regulatory issues that shape the bioprocess industry.

This thesis concludes with recommendations for the steps required to design and build the next generation of filtration scale-down device for rapid process development in Chapter 9.

Chapter 2 Membrane Filtration in Bioprocesses

2.1 Introduction

Now that the motivation for scale-down has been described in Chapter 1, the following pages provide the relevant information required for the scale-down of membrane tangential flow filtration. It begins with a review of the pertinent background theory of membrane filtration. This is followed by an overview of modelling in bioprocess engineering; in particular membrane filtration modelling approaches are presented to give an awareness of the literature data and modelling tools available. This is followed by an examination of several recently published models, which will be reviewed in terms of their pragmatism for use in conjunction with a scale-down model for TFF.

This chapter culminates with a proposal for an USD methodology for TFF, which will be used as the basis of the experimental research described in Chapters 3 to 7. Finally, a method for presenting the results from USD experimentation and/or modelling known as Windows of Operation (WinOps) is discussed, and a format for such a "Window" is suggested for TFF.

2.2 Background theory to membrane filtration in bioprocesses

Membrane filtration is a major unit operation in the bioprocessing industries. Despite its prominence as a separation step its performance is frequently sub-optimal due to lack of knowledge of how best to operate the membrane module in conjunction with the remaining bioprocess sequence. This feature holds true for both upstream (cell culture) stages and the impact on subsequent steps (e.g. high-resolution operations). In addition, whilst many fundamentally-based models exist for membrane flux, few academic workers have tackled the equally pressing problem of product transmission where behaviour can be markedly dynamic and highly system-specific, depending both on the membrane characteristics and those of the process downstream. Filtration theory is a well studied field and some background theory is presented below.

2.2.1 Membrane filtration

Membrane filtration is a popular choice in many bioprocess flowsheets. A good review on the reasons for selecting this unit operation is given in Cheryan (1986). Membrane filtration can be defined as the separation of particles of one size from particles of another size in the range of approximately 0.01 μm through 20 μm. It is a pressure driven separation of solids from liquids (on a size basis) using a porous membrane. The fluid may be either a liquid or a gas. The membrane passes materials, which are soluble and low in molecular weight, and retains colloids, particles and dissolved solids that are larger than the membrane pore size.

Membrane processes may be separated into several sub-classes based on the size of the species being separated; microfiltration (MF), ultrafiltration (UF), reverse osmosis (RO), nanofiltration (NF) and electrodialysis (ED), but for bioprocess applications MF and UF are the key unit operations, and are therefore focused on here. Membrane filtration uses in bioprocesses include:

- Concentration – reduction of process stream volume.
- Cell harvesting/recycling or washing.
- Cell removal – to limit bioburden.
- Buffer exchange – to prepare the process stream for further downstream processing or formulation.
- Debris removal – to protect e.g. chromatography columns.
- Product sterilisation.

The pore sizes of MF membranes range from 0.05μm to 10μm which makes it useful for the retention and concentration of microorganisms, cellular fragments, precipitates, etc (Mateus et al., 1993); applications of MF include therefore cell harvesting, cell debris removal, waste-water treatment and non-thermal sterilization (Mulder, 1996). These applications include even the processing of more fragile cells, such as mammalian cells, since the loss of viability is not significant when a peristaltic (Ng and Obegi, 1990) or a rotary lobe pump (Rudolph and MacDonald, 1994) is used.

The pore sizes of the membranes used in UF range from 1nm to 0.05μm, which corresponds to 1 to 1000kDa size retention (Millipore, 1992). It is typically used to separate, purify and concentrate large molecules such as proteins in solution,

polysaccharides, antibiotics and pyrogens. It can also be used to process cells and colloidal suspensions (Mateus et al., 1993).

Membranes with pore sizes in the range 300-1000kDa are at the boundary between MF and UF membranes and can present better performance than MF for clarification. In fact, since pore plugging is affected by components of similar or smaller diameter than the pores, it will be less prone to occur when operating with tighter membranes (Marshall et al. 1997).

2.2.1.1 Membrane materials and module configurations

Membrane material selection is dependent on several factors including particulate size, hydrophobicity and the concentration of feed. Selection of the proper module design is a choice that depends on many factors. Some membrane materials are only available in certain module designs. Depending on the findings of initial membrane screening studies one may find that a particular membrane type works best for an application. Membrane material may then dictate module selection. Other considerations include cost, space constraints, ease of use at the final scale, solvent resistance, and ability to clean, autoclave or steam-in-place (CIP or SIP).

Membranes can be found in different module configurations as shown in Table 2.1. Different modules are appropriate for specific applications and have different hold-up volumes which may affect the overall yield and performance. Descriptions of these are widely available in the literature e.g. Cheryan (1986), and will not be described further here. If possible, more than one membrane material and module design should be evaluated for a particular application during process development.

Table 2.1: Qualitative comparison of various commercially available membrane module configurations (after Mulder, 1996).

2.2.1.2 Modes of operation

The two main ways in which feeds are contacted with the membrane, which creates the pressure gradient that acts as the driving force for the separation, are:

- Normal flow filtration (NFF) or dead-end filtration – the feed is contacted perpendicularly to the membrane surface. Only batch operation is possible.
- Tangential or crossflow filtration (TFF) – the feed is contacted parallel to the membrane surface. Continuous operation is possible.

These modes are shown in Figure 2.1 below and a comparison of the two methods is given in Table 2.2. Since TFF is the more versatile of the two modes, it will be the focus of the discussion below.

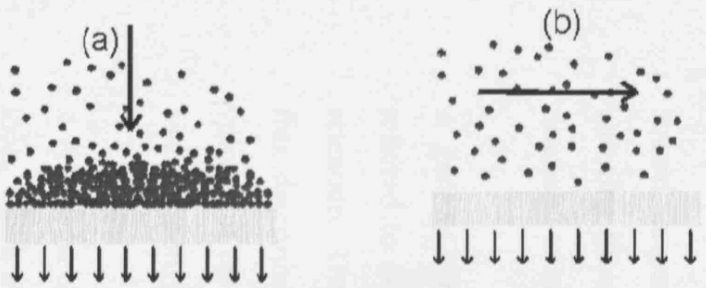

Figure 2.1: Schematic of (a) Normal flow filtration (NFF) and (b) Tangential Flow filtration (TFF).

Process goal	***Clarification***	***Concentration***	***Diafiltration***	***Sterile filtration***	***Benefits***	***Limitations***
NFF Operating steps: Install, Flush, SIP, Integrity Test (IT), Process Feedstock, Recover Product, (Post Use IT)	Yes	No	No	Yes	*Simplicity in scale up and implementation *Multiple selective and scaleable options	*No reuse possibilities *High disposable costs *No high solids loading
TFF Operating steps: Flush, Integrity Test (IT), Buffer Flush, Charge feed, concentration/ Dialfiltration processing, Recover Product, CIP, SIP, Storage	Yes	Yes	Yes	No	*Most efficient option for cell recovery *Robust systems widely available at all scales	*High capital cost *More difficult to operate *Validation requirements greater

Table 2.2: Comparison of NFF and TFF

2.2.2 Basic principles of tangential flow filtration

Crossflow or tangential flow membrane filtration has been a popular topic in biotechnology for over three decades. The terminology of crossflow filtration is not well defined, for the purposes of this thesis tangential flow filtration (TFF) is the appellation chosen. The level of activity is reflected in the large body of literature available on the subject, but examples of scale-up and large-scale applications remain limited. These efforts have been driven by a number of factors, mainly the need to develop processes appropriate for the recovery of new high-value biologically derived products, the syntheses of which were made possible by an explosive advance in biological sciences (see Chapter 1). Changes in the underlying technology have been evolutionary, not revolutionary.

TFF is the most general term to describe the various techniques by which slurries of particles or solutions of macromolecules are recirculated across the surface of a filtration medium with only a fraction of the liquid volume permeating the membrane per pass. Through various mechanisms, depending on the particle sizes in the feed stream, tangential flow reduces the accumulation of materials on the membrane surface, allowing filtration to continue beyond the point that would be possible using traditional dead-end or normal flow filtration (NFF).

A general schematic of TFF is shown in Figure 2.2 below. The filtered stream is referred to as the permeate and the non-permeable portion of the feed is called the retentate. The permeate rate per unit of membrane area is defined as the flux (J). The flux determines the amount of membrane area required for a given separation. The volume of the permeate is usually small compared to that of the feed (this is referred to as a low conversion ratio).

A typical batch crossflow filtration system comprises a tank connected to a recirculation loop, which includes a pump and the membrane, as well as some instrumentation such as pressure gauges, flowmeters and temperature probes (see Figure 4.1 in Chapter 4). In flux control mode a control valve or a second pump is installed on the permeate line. This configuration allows the creation of the high performance tangential flow filtration (HPTFF) system, which has been developed to reduce the pressure drop along the

membrane which can be as high as 50kPa.m^{-1} (Huisman et al., 1997). This system has been developed to facilitate a crossflow both on the feed side and on the permeate side, thus guaranteeing a uniform low transmembrane pressure. HPTFF has been reported to facilitate the separation of species of similar size (van Reis et al., 1999).

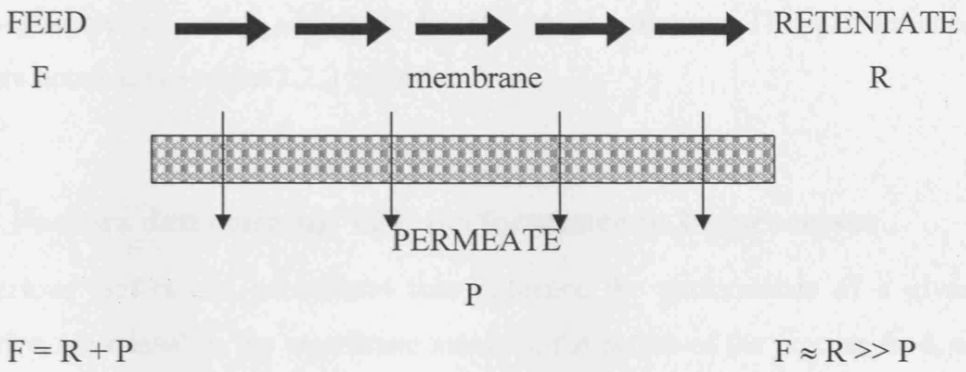

Figure 2.2: General schematic of crossflow or tangential flow filtration

In the case of removal of solid contaminants (e.g. clarification of cell lysates), the solution is recirculated via the loop and the purified stream passes out through the membrane. Further recovery of the product can be achieved with constant volume diafiltration, which is the addition of pure buffer to the tank at the same rate as the permeation rate. This has however the disadvantage of diluting the purified stream.

Concentration of products (e.g. proteins or cell harvesting) is achieved in the same way but in this case the membrane retains the desired product. The diafiltration step is used to wash away any contaminants (Quirk and Woodrow, 1983) and can also be used for buffer exchange, without altering the product concentration.

TFF is a balance of two main parameters, shear rate and pressure. The transmembrane pressure (TMP), which forces material across the membrane and the shear at the membrane surface, which causes a back transport of material thus reducing fouling and gel layer formation (Cheryan 1986). Shear at the membrane surface can be created either by moving the broth past the membrane, by recirculation pumping, or by moving the membrane past the broth, by rotating or vibrating the membranes (Lee et al., 1995). Theoretically, the higher the shear at the membrane the higher the permeate flux that will be achieved. There are however, upper limits, shear can damage cells and cause

aggregations of proteins which lead to impurities and loss of product (Zeman and Zydney 1996). The other factor acting at the membrane is the transmembrane pressure (TMP). The TMP is the pressure difference between the broth side, (feed stream and retentate) and the purified side (permeate).

However, there are many additional factors which influence TFF performance, and these are detailed in section 2.2.3 below.

2.2.3 Factors determining TFF performance in bioprocesses

The various factors and parameters that influence the performance of a given TFF separation are related to the membrane material, the nature of the process feed, and the membrane module configuration.

2.2.3.1 Membrane related parameters

These parameters are related to the membrane material itself.

Product size versus pore size

The pore size of a membrane is the diameter of the particle that is retained by the membrane. Pore sizes are usually measured in micrometers (μm). Pore size ratings refer to the size of the particle or organism retained by the membrane. Some of the more common biological particles filtered and their approximate size ranges are:

- Bacterial cells, 0.1μm to 30μm;
- Viruses, 0.1μm to 0.05μm;
- Red blood cells, 5.0μm to 10μm;
- Yeasts, 0.6μm to 4μm;
- Chinese hamster ovary (CHO) cells, 10μm to 30μm.

When the particle size is increased there is an increase in the flux through the membrane (Kroner et al., 1984). The particulate material that collects at the membrane surface will pack to form a layer of higher porosity. According to the Carman-Kozeny relationship the resistance (R_s) of the solid cake is given by:

$$R_s = \frac{\alpha V_f C_b}{A} \qquad [2.1]$$

The specific cake resistance α is given by:

$$\alpha = 180\left(\frac{(1-\varepsilon)^2 \delta_c}{d_s \varepsilon^3}\right) \qquad [2.2]$$

These equations assume that the particles are rigid and spherical, which is generally untrue of biological materials; proteins are usually compressible and may be linear, globular, branched etc.

Quantifying the size distribution of the feed stream can be difficult, as many typical feeds have a size range close to the limits of detection of sizing equipment (Brown and Kavanagh, 1987). For biological feed streams, parameter variation in the fermentation or lysis stages will lead to variations in the size distribution.

Spread in the pore size distribution of a membrane can reduce the performance of the system as pore plugging will occur if there is an overlap between the pore and particle size distributions (Brown and Kavanagh, 1987).

Use of an ultrafiltration membrane could lead to higher flux performance than a MF membrane (Lee, 1989, Gatenholm et al., 1998), presumably because the retained solids roll along the ultrafiltration membrane surface, as they cannot be trapped in the pores. Similar flux improvements using tighter membranes have been reported by other workers (Brown and Kavanagh, 1987, Bailey et al., 1990).

Tarleton and Wakeman (1993) have seen that there is a higher proportion of finer material in the fouling layer than there is in the bulk liquid and McDonogh et al. (1992) have seen that there is a size gradation in the concentration polarisation layer; the smaller particles are situated closer to the membrane. The size distribution within the layer is thought to cause fouling layer disengagement when the yield strength of the compacted fines is reached. This disengagement leads to a sudden increase in flux.

However, transmission performance is not necessarily improved by using a smaller pore sized membrane. A point may be reached where the effective pore size is reduced to such an extent that the required product is no longer transmitted.

Reismeier et al. (1989) investigated different membranes and feeds mixtures and found that the specific cake resistance increased as the pore size was reduced. The most effective solution to this is to use a membrane with sufficiently large pores to give a reduced specific cake resistance without increasing the degree of pore blocking.

Membrane Porosity

This is the measure of all of the open spaces (pores) in the membrane; generally, membranes have 50 to 90% open space. A nominal pore size rating (c.f. absolute) describes the ability of the filter to retain 60 to 98% of the particulates that are equal to or greater than the rated size (note: Nominal Pore Size Ratings vary widely among different filter manufacturers). Flow rate is directly proportional to the porosity of the membrane i.e. more pores equal a higher permeate flow rate.

Thermal Stability

There is always a maximum temperature at which the membrane and its housing will remain stable. Thermal stability is important when considering sterilisation and cleaning protocols. There is a relationship between chemical compatibility and thermal stability. Many types of membrane material are compatible with a chemical at room temperature, but not at elevated temperatures. Most materials are stable up to 100°C when exposed to aqueous solutions. If organic solvents are used the maximum temperature could be as low as 50°C.

Chemical Compatibility

Chemical compatibility is defined as the ability of a membrane to resist select chemicals, to prevent damage to the pore structure and the membrane material. This also prevents the shedding of particles or fibres. To select the proper membrane and its

housing, the compatibility of the membrane with the fluid must be established. Temperature, concentration, and length of exposure time affect chemical compatibility.

The materials used in the manufacture of membrane materials are carefully chosen for their resistance to a wide range of chemical solutions. An understanding of the compatibility between the fluid to be filtered and the membrane elements is essential.

Surface chemistry effects

Membrane and protein surface chemistry will alter the fouling behaviour of the system. Hydrophilic membranes possess an affinity for water. Hydrophilic membranes can be wetted with virtually any liquid and are the preferred material for aqueous solutions. Hydrophobic filters repel water. A hydrophobic membrane will not wet in water but will wet in low surface tension liquids such as organic solvents. Once a hydrophobic membrane has been wetted by an organic solvent, aqueous solutions will pass through.

If the membrane is hydrophobic then thermodynamics dictate which species will adsorb onto the membrane. The use of hydrophilic membranes has been suggested for improved performance (Kroner et al., 1984; Lojkine et al., 1992; Fane and Fell, 1987; Van den Berg and Smolders, 1988). Other pre-treatment methods may also be used to provide favourable surface chemistry (Fane et al., 1991). The presence of surfactant molecules (such as antifoam used in the fermentation) in the process stream may lead to a loss in membrane filtration performance, as these will adsorb onto the membrane. A significant decline in flux is seen when surfactant dispersions are filtered (Akay and Wakeman, 1993; Fane et al., 1992).

Batch-to-batch variability

The membrane manufacturing process is complex and slight variations can be expected between different membranes, and from coupons cut from different areas of the same membrane sheet. This is especially true between membranes from different manufacturers.

Extractables

Extractables are contaminants that elute from the membrane material or device that may adversely affect the quality of the permeate. These contaminants may include wetting agents in the membrane material, manufacturing debris, sterilisation residuals, adhesives or additives in polymer or housing components, colorants, and mould release agents, etc.

Leaching out of extractables generally occur at temperatures over 50°C. The type and amount of extractables vary with the type of liquid being filtered. Extractables can affect filtration in almost every application e.g. in cell culture they can kill cells, and they can affect the recovery of microorganisms. They are a serious concern, especially for regulatory and validation issues.

2.2.3.2 Feed related parameters

These can be further sub-divided into stream properties e.g. temperature, pH, viscosity, product concentration, and product properties e.g. hydrophobicity, shape (globular, linear), size, compressibility.

Component Shape

The shape and mechanical characteristics such as compressibility of the feed components are factors that influence filtration behaviour. For example, the particle size difference between the product and the contaminants will determine the efficiency of the separation. The compressibility of the proteins present will also determine the nature of the fouling or gel layer that forms at higher transmembrane pressures.

Viscosity

This determines a liquid's resistance to flow. The higher the viscosity of a liquid (at a constant temperature and pressure), the lower the flow rate and the higher the differential pressure required to achieve a given flow rate.

Temperature

The temperature can alter the flux in one of two ways (Kroner et al., 1984). Temperature increases can promote protein aggregation by altering the solubility of proteins and other solutes in then feed. Temperature changes will also affect the viscosity of the process stream, in some cases dramatically. This will lead to higher fluxes if other factors remain unchanged (Kroner et al., 1984; Lojkine et al., 1992).

Chemical environment

The chemical environment can influence the performance when proteins are present in the feed, such as the pH and ionic strength of the buffer solution will alter the surface charge on proteins present. When the protein is at its pI (isoelectic point) the degree of adsorption is higher (Bowen and Gan, 1992; Hanemaajer et al., 1989). This is thought to be a result of the absence of charge shielding of the protein, which stabilises the structure, reducing the degree of deformation. When the protein is deformed it is likely to adsorb on the membrane in order to shield the exposed hydrophobic groups. The presence of charge shielding molecules will also increase the effective size of the proteins, increasing the permeability of the fouling layer.

Concentration

The higher the concentration of the feed, the higher the effects of concentration polarisation. This dynamic phenomenon directly impacts on flux and product retention.

Electrostatic effects

It has been shown that electrostatic effects dominate permeation behaviour under some circumstances. For several proteins, it has been shown that a maximum transmission is achieved at their isoelectric point; a secondary maximum was observed between the isoelectric points of the protein and the membrane (Burns and Zydney, 1999). Specific ionic composition, as well as pH and ionic strength also affect permeation (Balakrishnan et al., 1993; Menon and Zydney, 1999). These investigations showed that the effective size of the proteins could be manipulated by changing pH, ionic

strength and ionic species, thus changing their extent of electrostatically-based exclusion from the membrane pores.

These investigations were, however, conducted using pure proteins in clean solutions. For real-world biological process streams, it is unlikely that such effects could be predicted (or would be measured) based on the properties of a single broth component, since the presence and interactions of other components e.g. cells, proteins, salts etc. would need to be considered.

Feed Variability

The feed stream for bioprocess unit operations is usually subject to batch-to-batch variations. Attempts should be made to minimise these for obvious reasons, but they will have to be accounted for during the design and optimisation stages.

Another source of feed variation is the presence of process aids such as antifoams, which are used in the fermentation step, or cryopreservation agents, which may be employed during hold-steps. Relatively little has been written about this topic, but it has been often observed that the presence of antifoam during TFF processing will significantly reduce the flux. Among other factors, the extent of this effect will depend on the concentration of the antifoam and the temperature relative to the cloud point. For many common antifoams, such as P2000 (polypropyleneglycol 2000) cloud point is slightly below ambient. Silicone oils, such as Tegosipon T52, do not exhibit cloud point behaviour at temperatures of interest in biological systems (Russotti and Goklen, 2000).

If cell concentration is the basic goal of the process, the problem can be minimised by filtering at a temperature below the cloud point or by increasing membrane area. Passage of an antifoam is typically highly temperature dependent, with almost complete retention by polymeric membranes above its cloud point. The latter of these actions should only be done of changes in membrane material and/or antifoam are not possible.

If the process objective is to recover a soluble component such as a protein in the permeate, the problem becomes much more difficult. Kroner et al. (1986) showed that

the presence of as little as 0.1% P2000 increased the retention for several different enzymes from 5% to 50%. Higher antifoam concentrations and operation at higher TMPs exacerbates the effect. Such higher retentions are undesirable because they result in a disproportionate increase in the extent of diafiltration required to achieve a specified product recovery, increasing not only the scale of the TFF system but downstream volumes as well.

Effect of pH and ionic strength

The separation achieved by MF or UF is mainly size-based but it is also affected by chemical and physical interactions between materials, the membrane and the solvent (Le and Atkinson, 1985). The ionic strength and the pH of the buffers used especially important. For example Menon and Zydney (1999) mention cases where the transmission of bovine serum albumin (BSA) decreases by nearly two orders of magnitude as the NaCl concentration is reduced from 150 to 1.5 mM. Le and Atkinson (1985) also report maximum protein transmission with higher buffer ionic strength in lysate microfiltration. These authors interpret the low transmission at low ionic strength to be a result of an enlargement of the enzyme through swelling or association with other proteins. A similar effect is observed as a result of the pH of the buffer, with reported maximum transmission near the isoelectric point of the protein (Menon and Zydney, 1999; Le and Atkinson, 1985). This effect is also attributed to swelling. On the other hand Huisman et al. (2000) observed a minimum for BSA transmission at its isoelectric point. This was attributed to the high fouling levels resulting from increased hydrophobic interactions and aggregation.

Effects of ionic strength and pH are therefore dependent on the magnitude of the electrostatic and hydrophobic interactions between the different components in the system. As a result, studies made with pure protein solutions as the feed material may not address the complexity of real industrial process streams. For example Kuberkar and Davis (1999) noted that transmission decreases when another protein species is added to the protein solution, possibly through formation of a secondary protein membrane. However protein layer formation could be prevented by addition of whole yeast cells, which probably formed a cake on the membrane surface and thereby prevented protein aggregates from approaching and fouling the membrane.

2.2.3.3 System related parameters

These parameters are related to the filtration equipment and operating procedures.

Operating mode

There are two common modes in which TFF is operated in industry. They are:

- Constant pressure – Flux is allowed to decline with time, and pump speeds are varied to maintain constant TMP.
- Constant flux – A pump is placed on the permeate line, and TMP is allowed to vary within specified limits.

The second of these is currently favoured in bioprocess industries, as it minimises membrane fouling.

Differential Pressure

This is the difference between the pressures on each side of the membrane. A high pressure on one side forces the filtrate through the membrane to the lower pressure on the other side; as the membrane begins to clog or foul, differential pressure increases.

$$\Delta P = P_{INLET} - P_{OUTLET} \qquad [2.3]$$

Transitional TMP can be defined as the pressure at which the species concentration at the membrane surface C_w, rises to the "gel" concentration for that species, C_{max}, according to gel polarisation theory. Operating at this point, it would be expected that the thickness of any polarisation layer would be minimised while obtaining the maximum flux possible. Increasing TMP above the transitional value increases the thickness of the polarisation layer, without an improvement in flux. According to the concentration polarisation model, there should be no penalty for operating further out in the pressure-independent regime (apart from the increase in pumping duty). However, it is suspected that the polarisation layer compacts over time and becomes an irreversibly bound fouling layer (Nagata et al., 1998), which would result in a time dependent decrease in filtration performance.

Transmembrane Pressure (TMP)

The pressure drop across the membrane determines the flowrate of material through the membrane. TMP is defined as:

$$TMP = \frac{P_{INLET} + P_{OUTLET}}{2} - P_{PERMEATE} \qquad [2.4]$$

TMP is a measure of the pressure acting on the materials in the broth, in the direction of the membrane surface. Again, theoretically the higher the TMP the stronger the force acting on the broth and the higher the permeate flux (see equation [2.5] below). However a limit is reached, for a given shear rate, there is a point at which the TMP is forcing material to the membrane surface faster than the back-transport away from the membrane is removing it. This is called concentration polarisation and the region where increasing TMP no longer increases permeate flux marks the experimental limit at that shear rate.

At low TMP the degree of polarisation will be such that the polarised material is removed by back-transport (mechanisms that have been proposed include Brownian diffusion, shear enhanced diffusion, inertial lift and tubular pinch theories).

Eventually a pressure will be reached where the rate of solute convection towards the membrane exceeds the rate of back transport, the rate limiting flux is then reached, and the flux is then unchanged by further increases in TMP, the membrane is then said to be concentration polarised. This form of flux behaviour was first described for ultrafiltration (UF) (Porter, 1972), but has also been seen in many microfiltration (MF) applications (Brown and Kavanagh, 1987; Shimizu et al., 1993).

Operation at higher TMP's leads to lower flux and transmission performance, as polarisation and other fouling effects will be increased (Lee et al., 1995). It has been demonstrated by several workers that the start-up TMP of a membrane process can significantly affect the long-term performance. If high TMP is used at the start, the high initial fluxes will lead to more polarisation, and ultimately to lower fluxes (Attia et al., 1991; Haarstrick, 1991; Field, et al., 1995). If the initial TMP is lower then it is often possible to operate for longer periods without significant loss of performance. This can

be achieved by controlling flux flowrate, and gradually increasing the TMP as any fouling occurs (Maiorella et al., 1991; van Reis et al., 1991).

In TFF there will be a pressure drop along the length of the module due to frictional effects. This can lead to a TMP gradient along the length of the membrane, resulting in a lower TMP at the outlet than the inlet. Use of countercurrent permeate flow or HPTFF (see section 2.2) can eliminate the effects of the retentate side pressure drop. This type of system was used by Gésan-Gesiou et al. (1993) who saw that it initially led to lower fouling of the membrane, presumably because polarisation effects were controlled by keeping TMP constant along the length of the membrane.

Flux

As an alternative to controlling the TMP to dictate filtration performance, the permeate flux may be controlled. The flux (J) through the membrane may be expressed by application of Darcy's law, where membrane and the fouling layers (including concentration polarisation and fouling) are considered as two resistances in series, R_m and R_f respectively:

$$J = \frac{\Delta P - \Delta \prod}{\mu\left(R_m + R_f\right)} \qquad [2.5]$$

where J is the volumetric flux ($m.s^{-1}$), ΔP is the hydraulic pressure difference between the feed and permeate sides of the membrane (Pa), also known as the transmembrane pressure (TMP), μ is the dynamic viscosity (Pa.s), R_f is the fouling resistance ($m.s^{-1}$), R_m is the membrane resistance ($m.s^{-1}$), and $\Delta\Pi$ is the osmotic pressure difference between the feed and permeate sides of the membrane (Pa). $\Delta\Pi$ is negligible for microfiltration.

The flux at which to operate is chosen to be *sub-critical flux*. The critical-flux hypothesis is that on start-up there exists a flux below which a decline of flux with time does not occur (Field et al., 1995). It can be determined by stepping up the flux rate and is the flux at which TMP becomes unstable.

Recirculation velocity

The flow of feed tangential to the membrane acts to minimise the build up of material at the membrane surface. Increasing the recirculation velocity (v_c) increases the rate of mass transfer by reducing the concentration boundary layer thickness, so that higher fluxes can be obtained for the same TMP. The transmission performance is not necessarily improved by increasing v_c. Fouling and polarisation on the membrane surface is reduced by the increased crossflow, but there will be no effect on any internal fouling of the membrane, which determines the transmission performance (Attia et al., 1991). Flux is related to recirculation rate by a function of the form (Lojkine et al., 1992):

$$J \propto v_c^n \qquad [2.6]$$

Various values for the constant n are quoted in the literature, depending on the experimental system.

The TMP at which the transition between pressure and mass transfer control increases with recirculation velocity. Thus, operation at higher rates would be expected to lead to improved performance, in practice recirculation rate is limited by the pumping requirements, and also by limitations in the shear stress the product can be exposed to before damage occurs.

2.2.3.4 Phenomena causing flux decline

Flux decline could be attributed to one or more of the following:

- Cake formation
- Concentration polarisation
- Physical pore plugging
- Surface or fouling through chemical adsorption

The performance of a filtration membrane changes with time presenting a typical flux decline: there is a sharp initial drop followed by an apparent steady state after a few hours of operation (Patel et al., 1987). The discrepancies between ideal and real behaviour are due mainly to concentration polarisation and fouling effects described

below. Actual process fluxes can be less than 5% of the pure water fluxes (Mulder, 1996).

Concentration polarisation is a reversible process, but in practice a continuous decline in flux is observed, as well as significant changes in protein transmission, which is controlled by a combination of increasing wall concentration and solute transport (Chen, 1998). Concentration polarisation arises when proteins or other large solutes create a further resistance to the flow of permeate in addition to those of the membrane and the boundary layer. These components are rejected by the membrane and form gel-type layers on the membrane (Cheryan 1986), resulting in a detrimental effect on MF and UF performance. The modelling of this phenomenon is described in section 2.3 and Appendix 1.

The term "fouling" is widely used to encompass any phenomenon that is deleterious to membrane performance. The term "fouling" will be restricted to phenomena that cannot be reversed under common conditions of TFF operation. Fouling includes adsorption, pore blocking, precipitation and cake formation (Mulder, 1996; Zeman and Zydney, 1996).

The simplest mode of fouling is pore plugging i.e. when a fraction of the recirculation particles are sufficiently small to enter the pore structure of the membrane, but cannot pass through it (Hermia, 1982).

Flow reduction due to irreversible accumulation of particles on the membrane surface is common. This type of fouling can be due to particle-particle or particle-membrane interactions, such as adsorption. Protein aggregation may occur due to pumping (shear damage) or as a result of strong electrostatic and/or hydrophobic interactions (Kelly and Zydney, 1997). Fouling will occur as a result of the deposition of these aggregates on the membrane surface. Marshall et al. (1997) concluded that proteins reduce performance of UF membranes through deposition on the membrane surface as a dynamic cake layer, whereas they reduce the performance of MF membranes through pore plugging.

For MF membranes, it has been suggested that the mechanism of protein fouling is also concentration dependent, with pore plugging dominant under dilute conditions while surface deposition is more prominent at higher concentrations (Bowen and Hall, 1995). Particle aggregation is very specific to the system under study and generalisations are difficult. Hydrophobic membranes are generally considered to be more prone to protein adsorption fouling; use of hydrophilic or modified membranes can moderate this effect.

The hydrophobicity of cells can vary greatly among different species. It is also possible to change the cell surface characteristic through variations on growth medium, especially through changes between defined and complex media (see section 2.2.3.2 above). In some cases it may be found that a soluble broth component is adsorbing to the cell or membrane surface and mediating the aggregation interaction. The effect of this occurrence can be amplified by cell deformation. This results in a reduction or elimination of interstitial spaces restricting flow. It may be expected that animal cells would be most susceptible to this type of effect, but filtration is typically performed at low TMP's to avoid cell lysis. A similar effect for systems containing a broad distribution of rigid particles can also be considered; this is true during the filtration of mycelial broths or broth lysates (homogenates). It is also well documented that soluble components form a gel layer at the membrane, which becomes the controlling resistance to flow.

Permeation fouling is fouling with respect to the permeation of soluble components through the membrane. This is important since many harvest applications seek the recovery of these species in the permeate. Despite the use of microfiltration membranes with pore sizes in the micron range, it is not uncommon to encounter incomplete permeation of solutes such as proteins and smaller components. This is most frequently attributed to the formation of a gel layer.

According to Chen (1998) long term membrane fouling may be reduced if initial solute deposition is controlled. This can be achieved in a low fouling or polarization regime by controlling start-up, pressure, wall concentration or flux (Chen 1998). Constant flux operation provides better results than constant pressure operation because it avoids overfouling during initial stage of filtration (Field et al., 1995; Defrance and Jaffrin,

1999a). Effectively MF membranes have inherently high permeability values and rapid fouling will occur if the initial flux not limited (van Reis et al., 1997).

Field et al. (1995) considered the fouling effects on the flux to be the sum of irreversible and reversible fouling effects. According to these authors, as the TMP is increased and provided that a critical value of flux is not exceeded the behaviour is reversible, i.e., pressure can be reduced and the same fluxes are again observed. If the critical flux is exceeded, reducing the TMP does not restore the original flux, operation at a constant flux just below its critical value will allow a compromise between high fluxes and long term operation without fouling (Defrance and Jaffrin. 1999b).

In light of these phenomena, several approaches have been developed in order to minimise them, and these are discussed in the following section.

2.2.4 Mitigation of flux decline phenomena

Membrane performance may be improved using turbulence or reversal of transmembrane pressure. For example the periodical removal of the transmembrane pressure by closing the permeate valve and circulating the feed solution through the membrane module can result in good flux recovery. However the performance of this method depends on the filtration period and the stopping period (Zahka and Leahy, 1985; Tanaka et al., 1995). Tanaka et al. (1995) improved flux recovery during the microfiltration of yeast through the introduction of air bubbles, which enhance the sweeping effect resultant from the stopping of permeation.

Flux recovery can also be achieved by replacing the feed stream with a rinsing buffer (Novais, 2001). Nakanishi and Kessler (1985) investigated the effect of different variables in the efficacy of this method in the ultrafiltration of skimmed milk, and included transmembrane pressure, convective transport to the membrane due to the permeation (opened or closed permeate valve) and temperature. Their results indicate that high velocities and low TMP can achieve more than 98% removal of the deposit composed of milk proteins. Also Shorrock and Bird (1998) observed that the majority of the cellular cake can be removed with this method after the microfiltration of yeast

under strongly fouling conditions. The removal of the fouling resistance also appeared to be removed more rapidly at higher temperatures (50°C and 60°C).

Other methods make use of intermittent operation of the feed pump to increase the flux (Tanaka et al., 1995) or imposing vibrations on the filtration module (Schluep and Widmer, 1996). One popular method is back flushing (or back pulsing), where the permeate flow direction is changed at a given frequency in order to remove the fouling layer resulting in a higher average flux (Fischer, 1996; Meacle et al., 1999). This method is however not applicable to delicate membranes (e.g. polymeric) that might rupture when the flow is reversed (Kumzovich and Piergiovanni, 1996).

More recently devices generating Dean vortices have been exploited to reduce the extent of fouling (Kluge et al., 1999; Gehlert et al., 1998). In such modules spiral wound or helical coil design is used so that the retentate is forced to twist inducing a secondary flow with counter-rotating vortices. These re-entrain the deposits back into the bulk solution. The limitation of these devices is the additional pumping energy required, although it has been reported that their performance per unit energy is higher than that of traditional designs.

As fouling reduces plant throughput and membrane selectivity (Marshall et al., 1997), eventually the membrane requires extensive cleaning or replacement, and this is discussed further in section 2.2.5.

2.2.5 Membrane cleaning

Since membranes lose performance as a consequence of fouling effects they have to be cleaned (regenerated) between batches if they are to be reused. Membrane cleaning is a critical issue when considering the economics of the process; for many biological applications, membranes must be regenerated reproducibly and efficiently so that process performance is consistent with respect to flux and permeation. Cleaning methods have to be repeatable and consistent and their effectiveness is usually evaluated by comparing the pure water flux or normalized water permeability (NWP) after cleaning with the NWP before the process (Millipore, 1998a). However, this approach does not always give the best indication. Cheryan (1986) reported that although only

40% to 50% of water flux could be recovered after TFF of *Aspergillus niger* broth, flux of the process stream was not severely affected.

The temperature and pH limits that the membrane material can tolerate need to be considered when evaluating various cleaning protocols. Also, the volumes and cost of the cleaning reagents will affect the economics of the unit operation. These factors must therefore also be considered when selecting a membrane for a particular application. Membrane regeneration protocols must be evaluated empirically; a good starting point is to follow the membrane manufacturer's instructions. Typical cleaning agents include nitric, phosphoric and hydrochloric acid, sodium hydroxide, sodium hypochlorite and enzyme detergents that contain proteases. Depending on the feed components, other enzymes can also be used. These protocols must be robust i.e. suitable for validation requirements.

Although chemical cleaning is considered the most important method to restore the membrane's performance (Mulder, 1996), it is time consuming and costly as it typically requires multiple steps (Rudolph and MacDonald, 1994) including:

- system flushing of process material with buffer,
- system cleaning with recirculating base,
- system flushing of base with reverse osmosis (RO) water,
- system cleaning and recirculating with acid,
- system flushing of acid with RO water,
- testing efficacy of cleaning by checking NWP.

For this reason the downtime associated with dealing can account for a significant percentage of total cycle time (see Table 2.3).

Additionally the cleaning procedure needs to be validated, which is also cost and time consuming. For this reason some companies do not always reuse the membranes (Meacle et al., 1999), and disposable options are becoming increasingly popular (Novais, 2001)

Table 2.3: Typical operating cycle for filtration (adapted from Millipore Technical Brief, 1992).

The choice of the membranes may also be affected by their susceptibility to cleaning, when re-use is required. For example Bailey and Meagher (2000) found in a comparison of different membranes that the best performing membrane (cellulose acetate) could not be chosen due to difficult cleaning as a result of the sensitive nature of the polymer.

As a result, this element of the unit operation must not be ignored during scale-down of TFF. The scale-down methodology should facilitate the evaluation of different membrane types, and their regeneration parameters. In hardware terms, the scale-down device must be able to cope with the higher flowrates and temperatures encountered during cleaning, and also the materials of construction must be compatible with the chemicals used.

2.2.6 Optimising TFF performance

When examining the feasibility of utilising TFF two main issues are of concern: filtrate flux and product transmission (or retention). Regardless of the application, it is desirable to achieve as high a flux as possible for several reasons. High flux is beneficial from an economic standpoint since greater flux requires less membrane area and often less pumping capacity. Smaller membrane requirements and a smaller pump will decrease capital costs as well as the cost of the utilities associated with the cooling

and cleaning systems. Furthermore, equipment footprint will be minimised, which will in turn reduce facility cost. Also, a short cycle time may be required, especially if product stability is an issue.

Product transmission (or retention) is an obvious consideration since the goal of any downstream unit operation is to obtain as high a yield as possible. It is helpful to clearly define goals with respect to retention or permeation of product as well as other feed components before examining the feasibility of a TFF process. Initial experiments should be designed to look at these aspects. Using membrane manufacturer recommendations on parameters such as feed volume per membrane area (defined as load), TMP, and crossflow rate are a good starting point for experimentation. After determining whether or not TFF is a feasible operation, optimisation of these parameters can begin.

In these initial experiments, it is important that concentration is carried out to a degree which will be representative of the final desired concentration factor, various membrane materials and pore sizes should be examined in these initial screening experiments. Flux may be strongly dependent on membrane material and/or pore size depending on what the main inhibitor of flux is, and will therefore guide membrane selection (see section 2.2.3. It will also allow determination of the range of fluxes one may encounter for a particular application.

2.2.6.1 Implications for the TFF USD methodology

In the experiments conducted to examine flux and transmission behaviour with a variety of membranes, samples of the retentate and permeate need be assayed for product and other compounds of interest. Hence, the ability to sample from the inlet and outlet streams of the TFF scale-down device is required; this has significant implications when small volumes of feed are involved (see Chapter 3).

Also, it would be advantageous to be able to test the membrane material post-processing to determine whether or not chemical adsorption was occurring, or assess cleaning effectiveness. The ability to remove the membrane from the device for e.g. examination

under a microscope could provide valuable insights into the process; currently membranes can only be tested in this way by destruction of the cartridge they are held in (R. Kuriyel, Millipore Corporation, personal communication, 2001).

The optimisation procedure does not only have ramifications for the scale-down device, but also for the other USD methodology components. For a given feed and membrane material arrangement, there will be an optimal point of operation that will give the best performance in terms of flux and transmission. These are the key performance indicators for the unit operation. Once this combination has been fixed, the optimisation of the other processing parameters can begin. In order to optimise a TFF step, there is a trade-off between the following parameters, which are all inter-related:

- Membrane area
- Processing time
- Diafiltration buffer volume
- Product purity
- Product concentration
- Operating cost

Where these trade-offs are made are process specific, and the large number of variables highlight the need for pragmatic representation of the data produced during process development in order to make informed choices. This requirement is considered further in section 2.6. Another method of examining the interaction between these variables is through process modelling, which is reviewed in section 2.3 below.

2.3 Modelling in bioprocesses

More accurate process modelling can enable accelerated design and optimisation of bioprocesses. This has lead to an impetus to develop computer tools for the biotechnology industry (Zhou and Titchener-Hooker, 1999). In order for this to be achieved, accurate and reliable models for individual unit operations are required. Due to the complexity of biological interactions, these models often require empirical data and guidelines are needed as to how bioprocess models are best used in conjunction with scale-down models to enable USD methods. For example, the model parameters

that a scale-down device might provide should be defined. Also, the interactions between modelling and scale-down trials will influence any experimental strategy; fully-factorial design of experiments may not be required if it is possible to extrapolate information from a sub-set of data using the mathematical models developed.

Generally, the purpose of computer tools and modelling is to evaluate and extrapolate from existing data information that would be time consuming or costly to attain from pilot plant experimentation alone. Feasibility studies and parameter sensitivity are areas that could be investigated without the requirement of using scarce and costly process material. Also, time and labour savings should be made.

There are fundamentally two types of models, physical or mathematical. Physical models (in this study, these are scale-down mimics) try to replicate the physical processes that occur in unit operations. These scale-down devices, which imitate the behaviour of industrial scale units operations have been previously discussed in Chapter 1. Mathematical models give a mathematical description of an operation relating the process outputs with its inputs. Mathematical models can be further divided into theoretical and empirical categories.

Theoretical Models are based on a fundamental understanding of the underlying physical, chemical and biological process in operation. The advantage of theoretical models is that they can easily be adjusted to allow for new situations. However, true theoretical models often take a large effort to develop due to the understanding that is necessary. Once a theoretical model has been developed it is necessary to evaluate the performance of the model against experimental data.

Empirical Models are produced simply by finding a relationship between the inputs and outputs from a set of designed experiments for a unit operation. The empirical model can be in the form of a correlation or a neural network (where artificial neurons relate inputs to outputs – see Appendix 1). The advantage of empirical models is that they are much easier to develop than theoretical models when the underlying processes are too complicated and difficult to understand. However empirical models are only valid for the conditions under which they are developed and therefore the application of such models is limited.

The hybrid of these two categories is known as "semi-empirical" modelling, and is where model parameters are experimentally determined. Scale-down devices can be used in conjunction with each type for model verification, experimental data production, and model parameter evaluation respectively. A complete review of model development and evaluation is given by Varga et al. (1998) and a schematic to the development method is given in Figure 2.3 below.

Essentially, when a model is developed, it is analysed to test the sensitivity of parameters and accuracy against real data in order to validate it. Any discrepancies can be used to refine the model, in an iterative process, until the outputs are acceptable i.e. the accuracy of prediction meets the level defined by the model user. In bioprocess engineering much effort has been devoted to the development of models. However, this effort has mainly been focused on the fermentation stage of bioprocesses to date. Downstream processing has been relatively neglected, as it is less well understood (Gritis and Titchener-Hooker, 1989), particularly as novel downstream unit operations are often used in bioprocesses.

Narodoslawsky (1991) states that a major problem with bioprocess simulation is a lack of comparison between models and actual industrial process data. Typically the unit operations in bioprocesses are batch or semi-continuous and therefore require dynamic models (Petrides, 1994). Additionally biological material is often complex and labile (damaged by shear, heat and pH) and also there is very little physical property data for biomaterial or methods for predicting their likely values (Petrides, 1994). Hence, semi-empirical methods have to be employed, in order to experimentally determine these parameters.

In short, bioprocess modelling is not a trivial endeavour, and is still very much work in progress for many unit operations. The following section presents an overview of modelling approaches to membrane filtration, and aims to give an appreciation of the challenges faced by researchers in this field.

*Figure 2.3: Traditional approach to model development (after Varga et al, 1998). * Model validity may be assessed e.g. against a certain percentage accuracy of prediction.*

2.3.1 Overview of membrane filtration modelling approaches

Membrane filtration is a major unit operation in the bioprocessing industries. Whilst many fundamentally-based models exist for predicting membrane flux, few academic workers have tackled the equally pressing problem of product transmission where behaviour can be markedly dynamic and highly system-specific, depending both on the membrane characteristics and those of the process upstream.

Membrane filtration, particularly TFF, is a very complex process. Some of the variables that influence permeation flux and retention are membrane type and chemistry, module geometry, particle size distribution, nature of particles, interaction between particles and with the membrane, fluid dynamics, operating mode, pressure, temperature, pH and ionic strength of the media. This is a formidable set of variables, and to date no unified theory exists to provide a rigorous expression for permeate flux and retention for TFF.

There is an immense body of work describing attempts to model membrane filtration, and the main approaches are described in more detail in Appendix 1. Methods based on resistance-in-series (Van den Berg and Smolders, 1988; Song and Emeliech, 1995; Cheryan, 1986), concentration polarisation (Chen, 1998; Porter, 1972), flux (Zydney and Colton, 1986; Brown and Kavanagh, 1987; Davis and Leighton, 1987; Belfort et al., 1994), fouling (Hermia, 1982), force balance (Stamakis and Tien. 1993; Hwang et al., 1996), transmission (Ferry, 1936; Okec, 1998; Novais, 2001), statistical (Okec, 1998), neural networks (Dornier et al., 1995; Niemi et al., 1995; Meyer et al., 1998; Delgrange et al., 1997) and computational fluid dynamics (Karode and Kumar, 2001; Wiley and Fletcher, 2002) are discussed.

In addition to the many operational variables encountered during TFF, filtration behaviour is also dependent on the mode and phase of operation. Figure 2.4 below outlines these different modes.

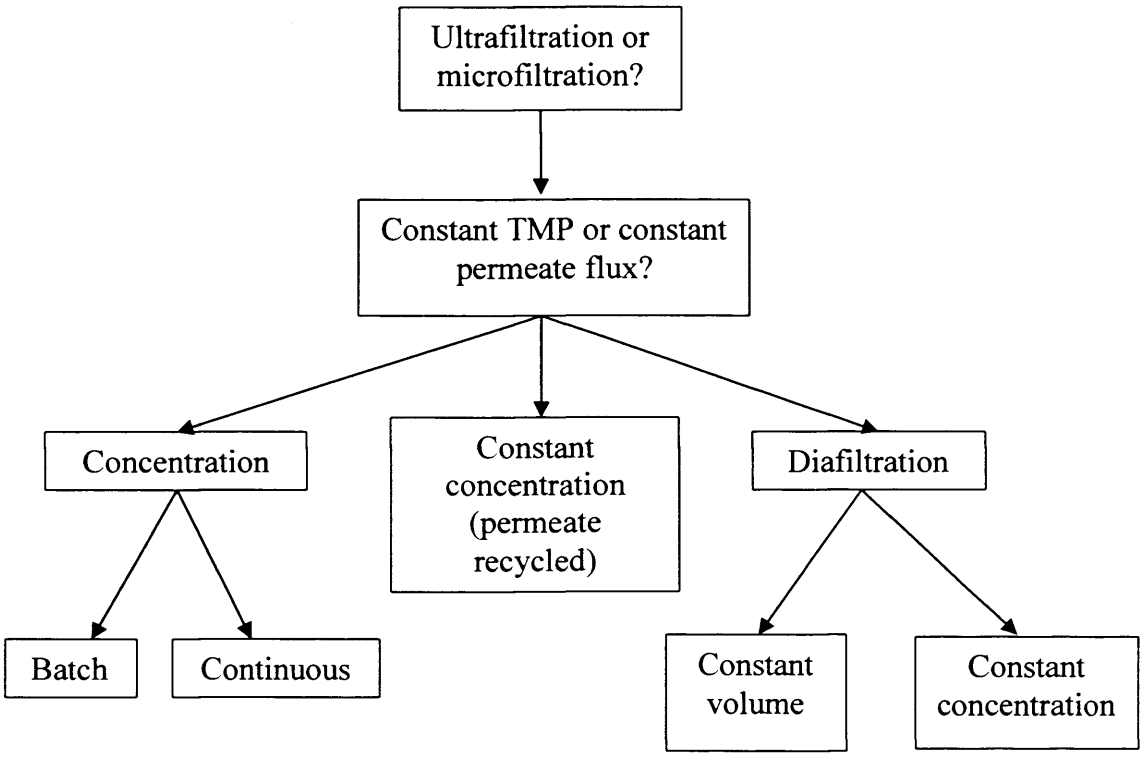

Figure 2.4: Modes of tangential flow filtration

Differences in model calculations also need to be made to account for differences in membrane geometry, such as spiral and tubular polymeric modules (Krishna Kumar et al., 2004), hollow fibre bundles (Silva et al., 2000), and coiled hollow-fibre designs (Kluge et al., 1999; Baruah et al., 2005).

Existing theories render the problem tractable by concentrating, at best, on only a few aspects of the problem. Therefore, for any given case, different theories may yield widely divergent results. In applying a theoretical model, extreme care must be exercised to check the specifics of the case critically so as to evaluate the dominant parameters and compare these with model assumptions. It is quite possible, particularly with complex suspensions such as biological feeds, that no one class of phenomena is dominant. In such a case, an existing model may not give the true picture and a new model may need to be evolved to capture the dominant phenomena. Usually, for microfiltration at constant transmembrane pressure, there is a rapid decline of

permeation flux due to concentration polarisation and pore constriction, followed by a quasi steady-state where there is a gradual decline in permeate flux due to particle deposition and an increase in particle concentration (and hence viscosity) of the bulk solution (Belfort et al., 1994; Nagata et al., 1988).

Several models exist that attempt to evaluate the quasi steady state permeate flux. These models are based on equilibrium between transport to and back-transport of particles from the membrane wall. It is important to note that these models are valid in the laminar flow regime for fully retentive membranes, deal with pressure independent permeation flux regime, and ignore any particle interactions with the membrane. Prediction of permeation flux in the pressure-dependent and transient regimes has also been addressed in the literature (Romero and Davis,1988 and 1990).

The main features of TFF performance that have been observed in practice and hence, must be reflected by a model are:

- Pressure independence of the flux once a certain pressure is reached
- Power law relationship between flux and crossflow velocity
- Quasi-steady state obtained when the retentate concentration is constant
- Flux and transmission decline due to concentration polarisation and fouling.

Most microfiltration models have their origins in ultrafiltration theory; few are fully fundamental, although some workers (Bowen et al., 1996, Song and Elimelech, 1995) have made advances in the application of fundamentals to microfiltration. The general problem with fundamental approaches is that the assumptions used in the model development are normally not valid in many practical applications, e.g. that the polarising solids are spherical and non-interacting. Much of the fundamental work by Bowen et al. (1996) requires detailed knowledge of thermodynamic properties of the system. In the case of multicomponent streams, such as biological feeds, these parameters are essentially impossible to determine.

While abundant models of TFF processes are available, few of them are useful in making predictions of filtration behaviour of a particular fermentation broth and membrane product *a priori*. The models generally account for those elements that

contribute to reversible decreases in flux, i.e. aspects that can be described using mass transfer analysis. Contrary to most practical applications, most models ignore cell-cell, cell-membrane, and other component interactions and other physical interactions and therefore they do not account for irreversible phenomena, which contribute to what is generally termed as fouling.

The specific nature of bioprocesses, such as cell aggregation under certain conditions, accumulation of cells and/or proteins at the membrane surface, extent of cell lysis etc. means that they must be evaluated on a case-by-case basis. As such, there is no substitution for experimentation, and therefore semi-empirical models are expected to provide the most useful data. For bioprocess applications, microfiltration at constant flux is the most popular mode of operation and hence only models capable of handling these conditions were investigated further in this thesis.

2.3.2 Recently published TFF models

With the acknowledgement that *a priori* models for TFF are unlikely to be accurate for bioprocess applications, several recently published models were evaluated for use as part of an USD methodology for TFF. The aim was to select a set of pragmatic flux and transmission models with which to predict performance of existing and new TFF separations using minimal experimental data derived from appropriate USD trials.

The following sections briefly describe two of these models and comments are made of how they would be used in conjunction with a scale-down device.

2.3.2.1 Hydraulic resistance-in-series model

Carrère et al. (2001) describe the microfiltration process via a hydraulic resistance-in-series model developed for modelling the clarification of lactic acid producing fermentation broths. The permeate flux was expressed by

$$J = \frac{TMP}{\mu_p (Rm + Ra + Rp + Rc)} \qquad [2.7]$$

where TMP is the transmembrane pressure, and μ_p is the permeate viscosity. Rm is the hydraulic resistance of the membrane, obtained from the filtration of pure water, and Ra

is the resistance due to the adsorption of matter onto the membrane e.g. proteins from the feed solution. The latter parameter is time dependent and tends towards a steady-state value, Ra_{ss}, correponding to the adsorption equilibrium, and can be described by

$$Ra = Ra_{ss}(1-e^{-bt}) \qquad [2.8]$$

The next contribution to resistance in equation [2.7] is Rp, or the resistance due to concentration polarisation. This is again an experimentally determined parameter, and the authors combine this parameter with Ra to extend equation [2.2] to give

$$Ra + Rp = (Ra_{ss} + Rp_{ss})(1-e^{-bt}) \qquad [2.9]$$

where Rc is the resistance of the deposit formed at the membrane surface

$$Rc = \frac{m}{A}\alpha_0 \qquad [2.10]$$

where m is the mass of the deposited layer, and α_0 is the specific cake resistance, which is dependent on transmembrane pressure as follows

$$\alpha_0 = \alpha TMP^n \qquad [2.11]$$

The compressibility index of the cake is n, and α is an experimentally determined constant and is a factor of the dominant particle size and shape. The cake layer mass m can be obtained by integration of the mass balance across the membrane

$$\frac{dm}{dt} = \left(JC - \frac{D}{\delta}(C_m - C)\right)A \qquad [2.12]$$

where A is the membrane area, C and C_m the bacterial cell concentratins in the retentate and at the membrane wall respectively, and δ the cake thickness. Since the concentration in the bulk is much lower than at the membrane wall, equation [2.12] can be simplified to

$$\frac{dm}{dt} = \left(JC - \frac{D}{\delta}C_m\right)A \qquad [2.13]$$

By assuming the complete retention of cells, the variation in retentate cell concentrtaion in a batch system can be calculated from

$$C = \frac{C_0 V_0}{V_0 - A\int_0^t J dt} \qquad [2.14]$$

where V_0 is the feed volume. However, these equation ignore species transmission, and therefore some further model development was necessary.

To include transmission as a variable, the starting point is to split equation [2.14] up into

$$\frac{dV}{dt} = -AJ \qquad [2.15a]$$

$$C = \frac{C_0 V_0}{V} \qquad [2.15b]$$

The overall volumetric mass balance is given by

$$V_0 = V_R + V_P \qquad [2.16]$$

Assuming the volume of the cake layer is negligible compared to the other terms, component balance would be

$$C_0 V_0 = C_R V_R + C_P V_P \qquad [2.17]$$

The experimentally observed transmission may be defined as

$$T_{obs} = \frac{C_P}{C_R} \qquad [2.18]$$

Substituting [2.16] and [2.18] into equation [2.17], and rearranging for C_R gives

$$C_R = \frac{C_0 V_0}{V_R + T_{obs}(V_0 - V_R)} \qquad [2.19]$$

This equation may be used instead of equation [2.15b]. The value of T_{obs} is a constant. For constant volume diafiltration, the relationship

$$T_{obs} = T_0 e^{at} \qquad [2.20]$$

has been described (Novais, 2001), where T_0 and a are experimentally determined parameters.

The above system of equations can be solved using MATLAB (Mathworks Ltd, UK) software (Carrère et al., 2001) or Visual Basic (Microsoft Corporation), which was done to produce the data in Chapter 5 (see Appendix 2 for program listing). The experiments required to determine the model parameters are summarised in Table 2.4.

Equation	**Parameter**	**Method of Determination**
[2.7]	Rm	Water flux measurements.
[2.9]	(Ra_{ss} + Rp_{ss}) and b	Fitting of model results to data from TFF of permeate from previous experiments.
	Ra_{ss}	Placing the membrane in contact with the feed for 24 hours (Meireles et al., 1991).
[2.11]	α	Fitting of model results using least square method (Levenberg-Marquardt algorithm) to data from constant TMP TFF experiments.
	n	NFF experiments to create plots of specific resistance versus TMP.
[2.13]	$(D/\delta)C_m$	Steady-state fluxes obtained during TFF at constant concentration (permeate recycled).
[2.17]	T_{obs}	Ratio of concentration of product in the feed to permeate concentration obtained during TFF at constant concentration (permeate recycled).
	a	Fitting of model results to data obtained during TFF at constant concentration (permeate recycled).

Table 2.4: Synopsis of dedicated experiments for determining parameters for the resistance-in-series model.

Several repetitions of each experiment are required to obtain accurate data, and roughly fifteen experiments would be required to determine the parameters listed above. If this were to be done using conventional pilot-scale equipment, approximately twelve days

and 20L of feed would be required. This would be quite a significant addition to the already constrained process development schedule and would probably not be justified.

Assuming all of these experiments could be done at USD scale (i.e. less than 0.1L of feed) it would be possible to complete these tasks using 1.5L of feed. Using a single scale-down device and disposable membranes i.e. no time required for membrane regeneration, the experiments could be completed within three days.

Carrère et al. (2001) found good agreement of model predictions to performances obtained from independent TFF trials of the *Lactobacillus delbrueckii* fermentation broth. In order to quantify the success of the model, the authors used a mean error value ε_1, where

$$\varepsilon_1 = mean\left(\frac{\left|J_{\text{model}} - J_{\text{experimental}}\right|}{J_{\text{experimental}}}\right) \qquad [2.21]$$

The paper reported some acceptable model errors for constant transmembrane pressure filtration of (average model mean error: 7.7%), but the error was almost three times larger for constant flux filtration (average model mean error: 22%), which is the most popular mode of operation for bioprocesses. Transmission of the lactic acid was not investigated, so this aspect was not evaluated.
The applicability of this semi-empirical modelling approach to other experimental systems would be interesting to see. The results of such analyses are given in Chapter 5 with a yeast-based feed.

2.4.2 Aggregate transport model

Baruah and Belfort (2003, 2004) have published a series of papers on the development of a methodology which they have termed the "aggregate transport" model. It is one of the first examples of a microfiltration model which aims to predict the length averaged, pressure-independent permeation flux *a priori,* as well as predicting yield of a target species for poly-disperse solutions.

Successful validation of model results with transgenic goat's milk were presented (Baruah et al., 2003; Baruah and Belfort, 2004) that verified the ability of the model to predict filtration behaviour during constant volume diafiltration experiments, conducted under constant flux conditions. The model does not require experimental input c.f. the Carrère resistance-in-series model, but some of the model parameters could be more accurate if they were empirically derived. The methodology can be divided into twelve steps which are summarised below. Additional equations excluded from the publication are also included to show the full system of calculations required for the model.

Step 1: Determine the particle size distribution of the feed suspension and evaluation of the equivalent spherical radii. This would usually be obtained from size exclusion chromatography or particle sizing equipment if available.

Step 2: Evaluate the suspension viscosity by experimental methods or estimation using the modified Einstein-Smolochowski equation

$$\frac{\eta}{\eta_0} = 1 + 2.5\phi_b + k_1\phi_b^2 \qquad [2.22]$$

Step 3: Evaluate the maximum back-transport velocity, u_i, for a particle at the proposed operating wall shear rate, assuming full retention for all solutes:

$$u_i = \max[B(a_i, \gamma, \phi_b, \phi_w, L, n), S(a_i, \gamma, \phi_b, \phi_w, L, n), I(a_i, \gamma, L, n) \qquad [2.23]$$

where B, S and I denote the functionalities of the prominent flux equations summarised in Table 2.5. For the first iteration of the model, the value of ϕ_w can be set to 0.64, which is the maximum packing density for rigid mono-disperse spheres (ϕ_m).

Step 4: Estimate the maximum aggregate packing volume fraction for all particles, ϕ_M at the wall. For poly-disperse solutions, this could be much larger than the value of 0.64 used above. For example, for a feed comprising of three sizes of particle such that $a_1 > 10a_2 > 100a_3$ the following relation may be used

$$\phi_M = \phi_m + 0.74(1 - \phi_m) \qquad [2.24]$$

In this special case, $\phi_M = 0.96$.

Step 5: Iterate for all particle sizes and selection of the particle that gives the minimum permeation flux (lowest back-transport velocity) at the given wall shear rate. The corresponding permeation flux is the predicted one.

Step 6: Evaluate the packing density for other particle sizes (a_j for $j \neq 1$) at this permeation flux. The values of ϕ_{wj} can be calculated from

$$J = \max[B(a_i,\gamma,\phi_b,\phi_w,L,n),S(a_i,\gamma,\phi_b,\phi_w,L,n),I(a_i,\gamma,L,n)] \quad [2.28]$$

for all $j \neq 1$. For particles whose back-transport is governed by inertial lift (equation [2.25]) can be estimated by using the mass balance and the propensity of the particle to lift off. For example, if there is only one such particle jI, check if $u_{jI} \geq 10J$. If yes, $\phi_{wjI} = 0$ as the particle is readily lifted from the membrane wall. Otherwise,

$$\phi_{wjI1} = \phi_M - \sum \phi_{wj} \quad [2.29]$$

where $j \neq j$I. If their is more than one particle that is governed by inertial lift, jI1 and jI2, there contributions to the cake at the wall can be approximately apportioned in the direct ration of their volume fractions in the bulk solution and inverse ratio of their back transport by

$$\phi_{wjI1} + \phi_{wjI2} = \phi_M - \sum \phi_{wj} \quad [2.30]$$

$$\phi_{wjI1} : \phi_{wjI2} = \phi_{bjI1} u_{bI2} : \phi_{bjI2} u_{jI1} \quad [2.31]$$

where $j \neq j$I1 or jI2 and u_{jI1}, $u_{jI2} < 10J$. This logic can be extended for more than two particles whose back-transport is governed by inertial lift.

Step 7: Check $\sum \phi_{wi} \leq \phi_M$ and other packing constraints. If packing constraints are satisfied then proceed to Step 8, otherwise use

$$\phi_{wicorrected} = \phi_M \left(\frac{\phi_{wi}}{\sum \phi_{wi}} \right) \quad [2.32]$$

For the particle selected in Step 5, re-evaluate J based on $\phi_{wicorrected}$ instead of 0.64 by repeating Steps 3 and 5.

Table 2.5 Summary of prominent back-transport and lift equations (after Baruah and Belfort, 2003)

Step 8: Evaluate interstitial packing density, $\phi_{wiinterstice}$, of the smallest particle by using

$$\phi_{wi\,\mathrm{int}erstice} = \frac{\phi_{wicorrected}}{1-\sum\phi_{wjcorrected}} \qquad [2.33]$$

Step 9: On the basis of the corrected packing density of each particle, estimate the minimum pore diameter $2r_{minimum}$ from geometric considerations:

$$2r_{\mathrm{min}imum} = a_i\left\{\sqrt{2}\left[\frac{4\left(\frac{4}{3}\right)\pi}{\phi_{wi\,\mathrm{int}erstice}}\right]^{\frac{1}{3}}-2\right\}\sqrt{b^2-4ac} \qquad [2.34]$$

Equation [2.34] is derived from considering face-centred cubic packing for the cake where there are four spherical particles per cube.

Step 10: Estimate the yield of target species (with equivalent radius r_s) in the permeate by calculating the observed sieving coefficient S_o:

$$S_o = \frac{S_a}{(1-S_a)\exp\left(\frac{-J}{k}\right)+S_a} \qquad [2.35]$$

where the actual sieving coefficient S_a is obtained from

$$S_a = \frac{S_\infty \exp(Pe_m)}{S_\infty + \exp(Pe_m)-1} \qquad [2.36]$$

The wall Peclet number, Pe_m, is obtained from

$$Pe_m = \frac{J\delta_m}{D}\frac{S_\infty}{\varepsilon\phi K_d} \qquad [2.37]$$

where δm is taken as the side of the face-centred cube of the particles of radius a_i that forms the controlling cake for transmission. In general, the governing case for flux and product transmission (corresponding to $r_{minimum}$) may be different. Hence,

$$\delta_m = a = a_i\left[\frac{4\frac{4}{3}\pi}{\phi_{i\,\mathrm{int}erstice}}\right]^{1/3} \qquad [2.38]$$

The intrinsic sieving coefficient S∝ is obtained by

$$S_{\infty} = (1-\lambda)^2\left[2-(1-\lambda)^2\right]\exp\left(-0.7146\lambda^2\right) \quad [2.39]$$

where Ferry's coefficient (λ) is the ratio of the two particle radii

$$\lambda = \frac{r_s}{r_{minimum}} \quad [2.40]$$

The parameters ε and ϕK_d is estimated from

$$\phi K_d = (1-\lambda)^{9/2} \quad [2.41]$$

$$\varepsilon = 1-\phi_{w.r.interstice} \quad [2.42]$$

Returning to equation [2.35] the mass transfer coefficient k for the selected particle a_i, can be determined from the following series of equations (Zeman and Zydney, 1988)

$$k = \frac{ShD}{d_h} \quad [2.43]$$

$$Sh = \beta \mathrm{Re}^a Sc^b \left(\frac{d_h}{L}\right)^c = \frac{kd_h}{D} \quad [2.44]$$

$$Sc = \frac{\eta}{\rho D} \quad [2.45]$$

$$\mathrm{Re} = \frac{\rho u d_h}{\eta} \quad [2.46]$$

$$D = \frac{(\kappa T)}{(6\pi\eta a_i)} \quad [2.47]$$

The yield of the target species in a diafiltration experiment can be evaluated after N_d diavolumes by using

$$yield = 1-\exp(-N_d S_{0average}) \quad [2.48]$$

Step 11: There are three possible scenarios corresponding to low, intermediate, and high shear rates. For low shear rates, the observed sieving coefficients are high, so no further refinement of the model is required. For intermediate shear rates, S_o is further corrected

by using the stagnant film flux equation for non-retentive membranes (for $\phi_{wi} >> \phi_{permeate}$):

$$J = k \ln\left[\frac{\phi_{wi} - \phi_{permeatei}}{\phi_{bi} - \phi_{permeatei}}\right] \cong k \ln\left[\frac{\phi_{wi}}{\phi_{bi}(1 - S_o)}\right] \qquad [2.49]$$

for the transmitted species in Step 3. Steps 3-10 are repeated until the values of S_o obtained by equations [2.29] and [2.41] are within 10% of each other. For high shear rates, $S_o \approx 0$, implying no transmission of the smallest particles, and hence no further iterations are required.

Step 12: Construct a plot of predicted J and yield versus wall shear rate for the pressure-independent regime (>Jcrit).

The aggregate transport model is obviously more complex to understand than the resistance-in-series model presented in section 2.3.2.1, although it was possible to construct a spreadsheet for the model using Excel software (Microsoft Corporation) to produce the results presented in Chapter 5. The iterations required may also render this approach impractical as a tool for USD, in terms of pragmatism. However, a only scale-down device could be required for model validation.

Accurate information regarding the wall shear rate is required, which may prove to be difficult to obtain for complex geometries such as commercially available flat-sheet cassettes (see Chapters 3 and 8). In addition, accurate materials property data (particle size distribution and viscosity) is required, and these may not be readily available for complex biological feeds. Finally, the model is applicable to diafiltration, which limits its use for bioprocess TFF operations, where a concentration step is often employed.

The model is expected to provide a conservative estimate, but this may compensate for the neglecting of particle-particle interactions e.g. aggregation and particle adhesion to the membrane. As with the resistance-in-series model (Carrère et al., 2001), the model described above will be tested with another experimental system in Chapter 5 to establish its applicability.

2.4 Ultra scale-down of membrane TFF

This section aims to give a brief overview of the areas to be considered during the development of a scale-down methodology for TFF. This topic is expanded upon further in Chapter 3.

Scaling of microfiltration equipment is difficult for a number of reasons, due to the large number of variables to be considered and their complex interactions. Example parameters include membrane loading (volume of feed processed per unit area of membrane) and the inherent variability of the membrane material at larger scales can also affect reproducibility (Lee et al., 1995; Russotti et al., 1995a).

The scaling and optimisation of tangential flow filtration (TFF) has progressed greatly once the importance of concentration polarisation effects (see section 2.2.2) for membrane performance had been recognised. As a result, measures that are capable of reducing the thickness of the stagnant boundary layer, such as increased tangential flow velocity or turbulence promoters, have been employed to preserve membrane performance at the original level.

However, the downside of these advances is the addition of more factors to consider in order to maintain the similarity of flow conditions when scaling membranes to avoid alterations to the concentration polarisation behaviour (van Reis et al., 1997). In addition to the parameters traditionally kept constant in the scaling of membrane operations, such as the membrane material, the ratio of filtrate volume to membrane surface area, channel geometry, retentate and filtrate pressure (Brose et al., 1996), it is therefore necessary to consider further factors. These include the feed flow rate and temperature, channel height and length, turbulence promoters, potential entrance and exit effects as well as the overall system geometry with regard to flow distribution (van Reis et al., 1997).

The adherence of precise tolerances in the manufacture of membrane modules meanwhile enables the scale-down of membrane systems to proceed according to the principle of multiplication of elements (Sweere et al., 1987), where linear scaling of the system through the addition of identical, small-scale elements is possible (van Reis et

al., 1997). Due to the importance of the membrane material for the separation result, the emphasis in the development of membrane systems meanwhile shifted towards methods that enable the rapid, small-scale screening of a variety of different membranes, similar to scouting procedures employed in chromatography (Han et al., 2000). However, accurate scale-down of membrane filtration operations can only be achieved by maintaining fluid dynamic parameters that are independent of scale (van Reis et al., 1997).

There are some major assumptions made in current linear scale-down methods which limit their applicability in practice; it is assumed that membrane characteristics, degree of fouling, pressure, temperature and crossflow velocity will be duplicated in the larger model to give the same observed flux and separation factor as in laboratory tests. The emphasis on using such scale-down devices is that they are a "design tool" rather than a system for direct scale-up.

In order to truly scale-down TFF, the operation of ancillary filtration equipment such as pumps, connectors, holding vessels etc. should also be reproduced as accurately as possible at the small scale. Construction materials may also differ; stainless steel is preferred at large scale, whilst glass and plastics dominate at laboratory scale. This can influence the retention of components e.g. virus spikes (Sofer, 1998) and needs to be evaluated carefully. Laboratory pumps tend to deliver more accurately than large scale pumps, and are liable to cause changes in buffer temperature with the potential consequences discussed above. Other design-related factors pertain to required functions which may be difficult to realize at large scale, such as the option to completely drain the system of feed without a buffer flush.

In the literature excellent results have been obtained for the reproducibility of microfiltration permeate flux and product transmission for different processing volumes (van Reis et al., 1997; Brose, et al., 1996). These studies have, however investigated simulated or model feeds. It is important that real bioprocess feeds are used in order to understand how a large scale broth will affect membrane performance since rheology, morphology and concentrations of solutes, suspended solids and residual oils will be variables and will affect filtration behaviour. Also, as truly scaleable crossflow filtration is a relatively new process to be adopted by the biotechnology industry, it is

important to show reliable techniques in order to model or simulate the operation of larger equipment i.e. at the pilot or production scale (Mannweiler and Hoare 1992).

It has been suggested that the membrane is as the only constant for both small and large scale filtration (de-los-Reyes et al., 1990). Different geometries behave differently in distinct ways at various scales (Brose et al., 1996), but these differences could be described mathematically and so could be taken into account for a prediction between scales. Consequently, and as a result of the complex nature of the relationship between the different phenomena that occur in bioprocess TFF, computer simulations based on experimental results have been used in order to cope with the large number of variables (Okec, 1998). Other methods to provide a structured approach to scaling experiments include decreasing the number of factors investigated e.g. van Reis et al. (1997) cites constant membrane channel length as a more effective method of linear scale-up.

By taking into account the above discussion, it is possible to compile a sequence to create an USD methodology for TFF; a proposal is given in Figure 2.5 below.

The starting point is to study published data and select/develop dynamic process models for MF for flux and transmission. The model inputs define what experimental data is required, and hence define the requirements for the data that needs to be obtained via experimentation. With the aid of factorial experimental design, an initial protocol can be defined. Data at this stage may be used to improve the original models.

In parallel, a scale-down device needs to be designed and fabricated which can faithfully mimic the global processing conditions of the larger-scale equipment. It is with this device that the scale-down experiments are to be conducted. However, verification with a well characterised feed using conventional (pilot-scale) equipment is necessary initially to validate the data generated. This comparison can be used to refine the process modelling, device and experimental techniques.

The next step is the representation of the data generated in an easily interpreted and pragmatic way that will facilitate the decision making in process development. This includes the comparison of the use of different membrane materials, operating parameters, and perhaps their sensitivity to changes in upstream operations (see Chapter

1 and Section 2.5). Finally, iteration of this loop with more complex feeds and different membrane types should lead to confidence in the ability of the mathematical models and scale-down device to provide a true process mimic, and hence the development of a generic methodology for the USD of membrane TFF.

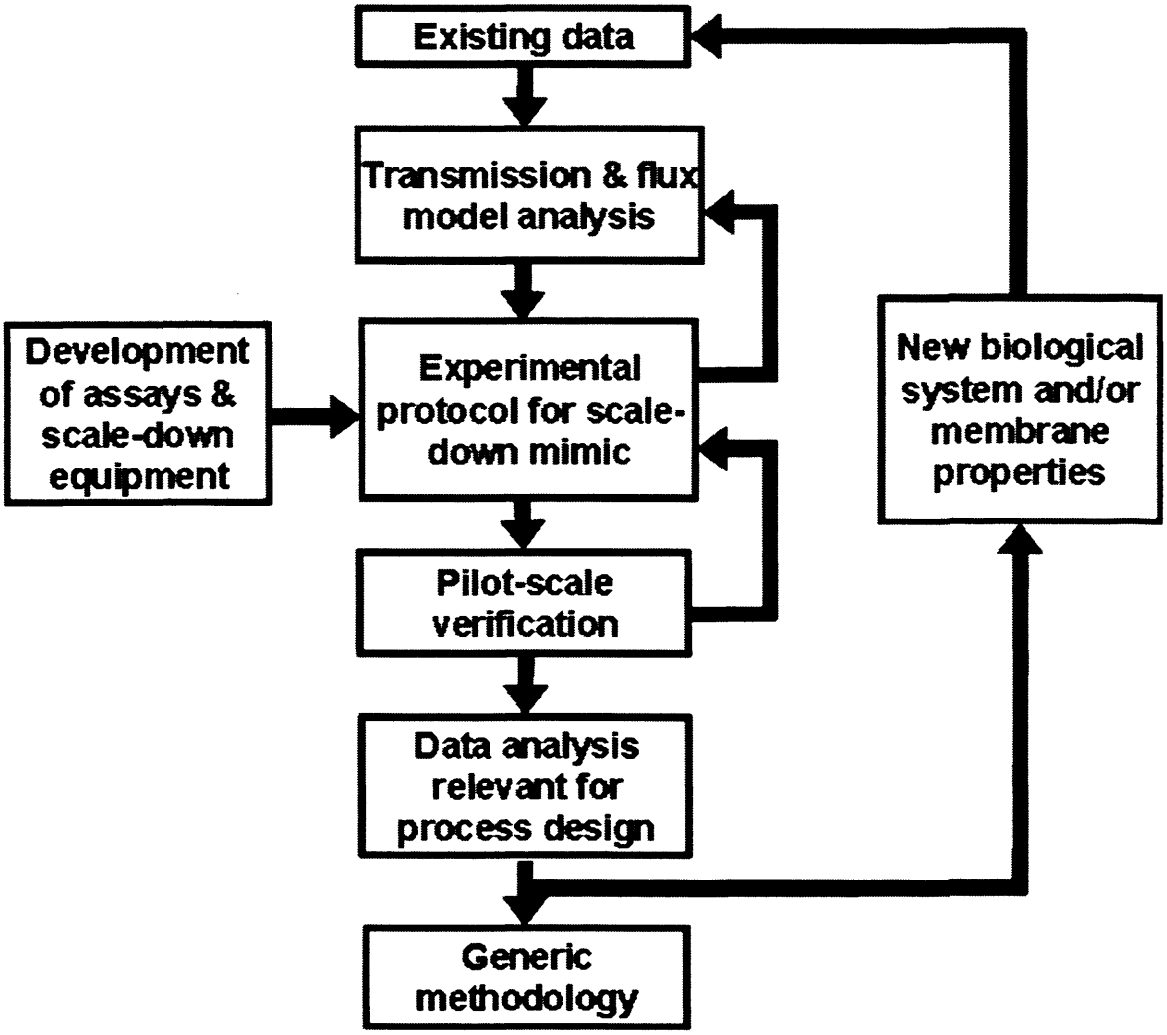

Figure 2.5 Development of an USD methodology for membrane filtration within bioprocesses.

2.5 USD index for TFF

As discussed in Chapter 1, USD indices are required to enable the assessment of changes from upstream operations. For chromatography, this has taken the form of a "fouling factor" or fouling index (Reynolds, 2005). This index is essentially a ratio that gives an indication of how successful the unit operation was in processing a particular feed. An analogy is the use of the dimensionless Reynolds Number to characterise

whether flow in a pipe is laminar or turbulent i.e. how well the fluid is being mixed. It provides a means of comparing one set of operating conditions with another, and could also be used to as an indicator of the impact of variations in upstream operations.

For example, the data obtained from trials using two different membrane materials could be compared; a single indicative number is easier to digest than multiple sets of experimental results. Another example of the use of a USD index could be to quantify the effect of variations in feed concentration on filtration performance – a sub-set of USD trials could be used to demonstrate whether the defined filtration operation could economically process the "worst case" feed. This idea is explored further in Chapter 7, using a mammalian cell culture, which often shows variability in the fermentation culture.

The literature provides three suggestions for a TFF index:

(a) Modified fouling index (MFI): Use plots of t/V versus V from either NFF or constant flux experiments to determine as specific cake resistance "n" or "α" (Brauns et al., 2002).

(b) Critical flux (J_{crit}): Flux stepping experiments to determine the flux below which there is no deposition on the membrane surface (Howell et al., 1991).

(c) Critical ratio of permeation flux to wall shear rate (J/τ_w): Several researchers have shown that that there is a critical ratio between wall shear rate and permeate flux beyond which protein transmission drops drastically and permeation flux does not increase with increasing transmembrane pressure (Gésan-Guiziou et al., 1999).

Only (a) is strictly a "fouling index", which is directly comparable to the index proposed for chromatography (Reynolds, 2005), but knowing the specific cake resistance from a NFF trial may not be useful for defining TFF operation. Membrane fouling has been classified as reversible (cake formation) and irreversible (internal pore plugging, absorption etc.). With bioprocess streams, it is difficult to tell which phenomenon is dominant, and it varies considerably between different feeds and

membrane types. Indeed, more than one regime may be dominant during different stages of processing. Typically, one tries to minimise reversible fouling in order to maintain high fluxes. Information on how fouled a membrane is after processing may useful when developing a cleaning (regeneration) scheme, but only qualitative data is required i.e. whether the manufacturer's recommended procedures does the job or not.

Options (b) and (c) give an insight into the processing conditions required to filter using TFF successfully. However, by also considering the recirculation rate, option (c) is more comprehensive. Figure 2.6 below is a representation of a plot similar to that produced by Gésan-Guiziou et al. (1999), showing the evaluation of the critical operating ratio (J/τ_w) during the microfiltration of skimmed milk. The idea was to plot flux data from constant flux or constant pressure trials conducted, against the calculated membrane wall shear rate. Data was obtained for experiments where operating conditions could be maintained and for those where the conditions did not remain stable.

The division between these two sets of data provides the limit of robust operating conditions. The gradient of this line (critical operating ratio) also offers a convenient ratio of which to compare data from different membrane/feed combinations; greater exploration of the parameter limits is enabled by the use of USD trials. Extrapolation of this line so that it intersects with the x-axis provides the critical erosion shear stress (τ_{wc0}), which is the limit under which there is no transport of particles away from the membrane at zero flux (J = 0 LMH). The value of this is a function of the membrane material and the solution to be filtered i.e. it is a measure of performance which is independent of flux or TMP parameters. It provides the minimum limit of crossflow required to process the material, using the specified membrane material.

Figure 2.6: Representative plot to determine the critical ratio of permeation flux to wall shear stress (J/τ_w) (after Gésan-Guiziou et al., 1999).

Either the critical operating ratio or the critical erosion shear stress obtained from this type of plot could provide a suitable USD index. These values will be determined for different membrane/feed combinations and their application discussed further in Chapters 5, 6 and 7.

2.6 Windows of operation

The amount of data that potentially can be produced from modelling of a unit operation can be large and may be difficult to interpret, and hence the modelling efforts may not be justified in terms of the time required, or use of time and resources for other process development activities e.g. regulatory submission support documentation. In order to avoid this pitfall, the representation of the data must be given careful thought at the outset of the exercise. The methodology flowchart presented in Figure 2.5 (section 2.4) specifies the output of industrially relevant data, and this needs to be presented in a pragmatic format.

The concept of Windows of operation (WinOps) is an attempt to develop simple and easily interpreted graphical techniques using computer algorithms for the design and analysis of bioprocesses (Woodley and Titchener-Hooker, 1996). The desired output of this area of research is a set of computer tools for the analysis of data from either experimental or mathematical bioprocess simulations (Griffiths, 2007). Enabling the user to evaluate the characteristics of the bioprocess will ultimately lead to them being able to determine how best to operate such a process.

The primary focus of this current area of research analyses how the control variables should be set to attain the product at the desired specification. This sort of information is useful for later stages of process development in order to optimise production when relatively large quantities of drug are needed for clinical trials. Although economic viability plays a very important role in examining a bioprocess, it is also essential that the bioprocess is able to meet product purity criteria and also environmental criteria. An inability to achieve these goals could result in severe penalties for the manufacturing companies. An early, but detailed analysis could indeed reveal problems with the capacity of the preliminary design in attaining these goals.

Bioprocesses are generally run batch-wise with limited automatic control, therefore simply finding the optimum operating point and trying to run exactly on it is likely to lead to variability (Samatli et al., 1996). The Window is defined as an operational space, which may be constrained by economics limitations, biological effects or physical laws. The authors demonstrate how putting two variables on graph axes and plotting the region of feasible operation can visually display the WinOp. Control variables are generally placed on the axes of the Window and the output variables are used as constraints.

The advantage of having a feasible region to operate in rather than trying to operate at the optimum point is demonstrated clearly by Samatli et al. (1996) who show a WinOp for centrifugation generated using two control variables on the axis and the optimum point. The optimum point lay on the boundary of the WinOp meaning that a small operating error could lead to the process lying outside the feasible operating region. In addition to control errors biological process have an element of inherent variability

introduced by the cells themselves and it is essential that this be taken into account whilst operating a process.

A further example of the utilisation of WinOps is provided by Zhou and Titchener-Hooker (1999) where a WinOp approach is used for evaluating a sequence of unit operations, using a yeast alcohol dehydrogenase (ADH) process as an example. WinOps for different fermenter growth rates were produced and overlaid on a graph with centrifuge flowrate and homogeniser pressure on the axes. The authors show how the different fermentation conditions lead to very different operating Windows and, counter-intuitively, the highest growth rate produces the smallest operating Window. However, the paper also indirectly highlights a weakness with the WinOp's approach in that bioprocess operations have multiple control variables and a Window plot can only visualise two control variables (the interaction of three parameters could be visualised if another WinOp is overlaid on the same plot).

2.6.1 Windows of operation for TFF

This section suggests a plot for presenting the data from modelling and scale-down experiments to clearly show the feasible region of operation for a TFF separation.

The starting point was to evaluate examples of similar plots in the literature, of which there are few. Van Reis and Saskena (1997) developed an optimisation diagram for membrane separation, based on the inherent trade-off between the product yield and the degree of purification. The axes of these plots were dimensionless parameters i.e. the ratio of sieving coefficients (S), and a new parameter $N\Delta S$, where the number of diavolumes, N is determined from

$$N = \frac{JAt}{V} \qquad [2.43]$$

and ΔS is the difference between the sieving coefficients. A family of selectivity curves can be plotted on these axes to give a purification-yield graph. However, this approach can only be of use for binary solutions where the sieving coefficients are known for each solute; this is hardly ever the case, or even an approximation, for the microfiltration of bioprocess streams.

The difficulty in choosing the axes variables for a WinOp for TFF is that they not only need to be useful for identifying optimal process conditions during industrial operation, but must be obtainable data at the USD scale. The table below lists possible axes titles for a TFF rig of fixed membrane area:

X axis	**Example Units**	**Y axis**	**Example Units**
Wall shear rate	Pa	%Transmission	-
Wall shear stress	Pa.s	Critical flux (J_{crit})	$m^3.m^{-2}.s^{-1}$
Feed crossflow rate	$m^3.s^{-1}$	Critical mass flux	$mg.m^{-2}.s^{-1}$
Linear velocity	$m.s^{-1}$	No. of diavolumes	-

Table 2.6: TFF Window of operation axes candidates.

Continuing from the discussion about the TFF USD index (section 2.5), the obvious axes for a WinOp would then be wall shear rate versus J_{crit}. However, as transmission of the target species is also a key performance indicator (Fischer, 1996), this also needs to be accounted for. The use of critical mass flux (concentration of target species in permeate multiplied by the critical permeate flux) addresses this issue. Figure 2.3 below shows a possible WinOp.

In order to test the suitability of this plot for use in a USD methodology, the WinOp needs to be populated with actual data produced from small-scale experiments and modelling results. This will be attempted in Chapters 5, 6 and 7 with a range of biological feed systems.

1. Lower wall shear stress limit - critical erosion shear stress (τ_{wc0}) under which there is no transport of particles away from the deposit at when there is no permeate flux i.e. J= 0LMH. τ_{wc0} depends on the membrane and the solution to be filtered.

2. Region above critical mass flux curve. This curve can be obtained by flux-stepping experiments, or using a flux/transmission model.

3. Upper wall stress limit (τ_{wcmax}) - product or cells damaged/ pumping cost too high/transcartridge pressure drop unacceptable.

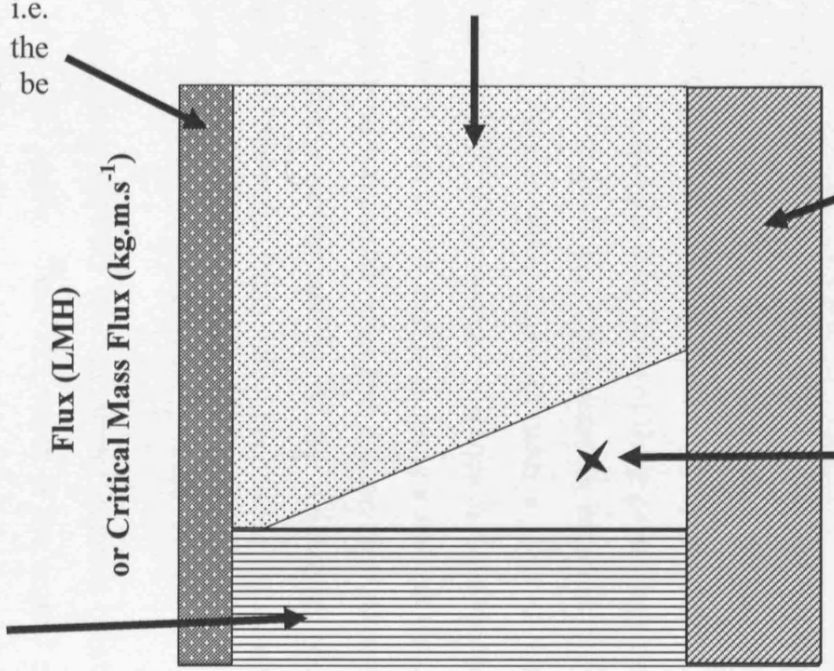

4. Process constraints in terms of processing time (t) time and minimum acceptable yield (% product recovered) e.g. 80% transmission of target species and 50LMH. This region will change if membrane area, process time or transmission limit are altered. It is independent of wall shear stress.

5. Feasible region of operation. One would pick a point on which to base operation conditions near the apex of the peak to maximise flux, but not too close so that variations in feed or membrane batch could be allowed for.

Figure 2.7: Window of operation for crossflow microfiltration.

2.7 Summary and conclusions

Attempts at the scale-down of membrane filtration have been made, but due to the complexity and sheer number of variables involved with this unit operation, work is still in progress. An overview of the background theory for membrane filtration was given as a thorough understanding of this topic is necessary in order to develop an accurate scale-down mimic.

This chapter has also given an overview of the modelling techniques applied to bioprocess applications, particularly to TFF. The key model output parameters for TFF are values for permeate flux and transmission of key species. Critical operating conditions beyond which flux and transmission performance decline provide the upper limits of operation, and the evaluation of these parameters through computer modelling techniques and/or scale-down experiments is required during process development. Two published models were discussed with a view to employing them in a USD methodology for TFF. The resistance-in-series model approach clearly identified points at which empirical data determined from using a scale-down device would be of benefit. The aggregate transport model relies less on empirical data, but is much more complex and requires greater understanding of the underlying equations, and only when confirmatory experimental trials have been done can one have confidence in the numbers generated.

A way of comparing different feed/membrane material combinations was suggested in the form of a USD index. This TFF index is the critical erosion shear stress (τ_{wc0}), which is defined as the crossflow velocity limit under which there is no transport of particles away from the membrane at zero permeate flux conditions.

Finally, a method of graphically representing the data generated by modelling efforts and/or a sub-set of scale-down experiments was proposed. This WinOp for TFF aims to portray industrially relevant data in an easily interpreted form for use during process development activities. The following chapter continues the development of a USD methodology for TFF by describing the development of a scale-down device to mimic the larger scale operation, and hence produce more accurate data for use in conjunction with the models described above.

Chapter 3 Development of a Scale-down Device to Simulate Tangential Flow Microfiltration

3.1 Introduction

In order to develop a USD methodology for the rapid evaluation of tangential flow filtration (TFF), according to the schematic presented in Chapter 2, a device to perform the scale-down experiments is required (see Figure 2.5). The following sections describe the development of a rotating disk device for this purpose.

The design of effective membrane processes typically requires a considerable amount of process development. This can include testing of membranes made from different polymers or with different pore sizes, screening of buffer pH and ionic strength to determine conditions for optimal selectivity and/or product stability, and examination of a range of transmembrane pressures or filtrate fluxes to achieve high throughput while minimising fouling (see Chapter 2). Currently, this type of process development is typically done sequentially, testing one set of conditions followed by another, possibly with the use of a statistical design methodology to minimise the number of experiments needed to explore a wide range of variables.

With multiple parameters influencing membrane processes (pH, type and concentration of solute, buffer choice, pressure, temperature, recirculation rate etc.) and several choices of membrane material (cellulose, polyethersulfone etc.) membrane users would benefit enormously from the successful application of a scale-down methodology.

Once the decision has been made to utilise filtration for a bioprocess purification, it typically takes four weeks to develop a filtration process for a new feed (R. Kuriyel, Millipore, personal communication). The subsequent scale-up of this process to pilot-scale takes yet more time.

3.1.1 Scaling of TFF

Brose et al., (1996) and van Reis et al. (1997) demonstrated that predictable scale-up of membrane filtration could only be achieved by maintaining fluid dynamic parameters, which are independent of scale. This is accomplished by controlling the following:

- *Operating parameters*: feed crossflow velocity, transmembrane pressure, fed-batch ratio i.e. feed to membrane loading, and temperature.
- *Module geometry:* channel length, height, turbulence promoter and entrances/exits, as well as cassette manufacturing and tolerances.
- *Design materials:* membrane material and pore size, turbulence promoter and encapsulant compression.
- *System geometry:* comparable flow distribution in the filter module and ancillary equipment.

It was stated by van Reis et al. (1997a) that for linear scaling of a TFF system, a constant path length is required. Currently the three main vendors of flat sheet TFF systems supply membrane cassettes of varying area based on this premise, and many bioprocess equipment manufacturers advocate linear, or geometric, scaling because of its simplicity.

Scale-down could be accomplished, in some cases, by modifying an existing piece of industrial equipment in such a way that it requires only a fraction of the process material to give a similar level of performance (Mannweiler and Hoare, 1992). Another strategy is to fabricate a geometrically similar, small-scale replica of the industrial machine. This is usually the idea behind pilot-plant equipment.

In the case of membrane filtration, scale-down has taken the form of commercially available devices, such as those listed in Table 3.1 below. These devices are complemented by systems such as the Pellicon XL™ (Millipore), the Sartocon Slice™ (Sartorius), or the Filtron Centramate™ (Pall). These systems integrate the ancillary equipment into a whole filtration rig, which include filter holders, feed reservoirs, recirculation pumps, and pressure gauges. Process monitoring software is also often supplied, making them an attractive option to process development scientists.

Device Format	Description	Mode of filtration	Nominal membrane area (m^2)	Examples (Manufacturer/ Tradename)
Cassette	Flat-sheet cassette	TFF	0.005 to 0.01	Millipore/Pellicon XL™; Pall/Minimate™; Sartorius/Sartocon Slice™; Whatman/ULTRAN™
Hollow fibre	Thin tube loop	TFF	0.0016 to 0.0026	GE Healthcare/Midgee™
Stirred cell	Stirrer bar suspended over flat sheet membrane	NFF	0.0004 to 0.0042	Millipore/Amicon™

Table 3.1: Some existing commercial tangential flow scale-down devices

Using linear scaling, a 400-fold linear scale up of tangential flow filtration has been achieved, without any need for an intermediate stage (van Reis et al., 1997). Successful linear scaling of commercially available cassettes has also been demonstrated (see Figure 3.1). Currently, the smallest available flat-sheet filtration devices contain $0.005m^2$ of membrane area (see Table 3.1); for a representative loading c.f. industrial scale trials, each experiment would require approximately 0.5L of process material. Use of a smaller membrane area is limited by the cartridge geometry. Also, as the cost of each filtration device is not insubstantial, they are not necessarily disposable items, and will therefore need to be cleaned and sanitised before and after each experiment.

To reduce the volume of material required further, non-linear scaling and/or use of novel protocols and devices are necessary. For example, Boychyn (2000) showed that a bench-top centrifuge could mimic the typical performance of a large-scale centrifuge by subjecting the material to shear in a rotating disk device prior to centrifugation. This treatment mimicked the shear damage experienced by the feed in the entrance zone of the industrial machine.

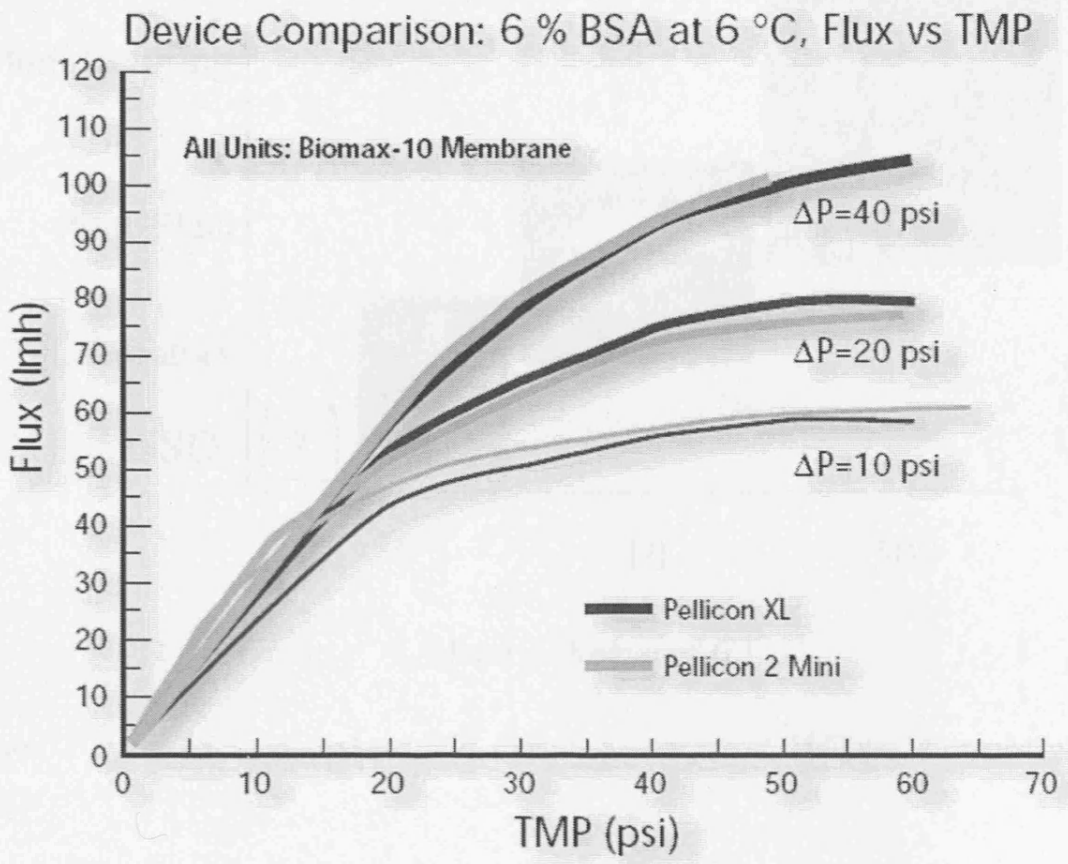

Figure 3.1: Linear scale-down of Pellicon 2 Mini (0.1m^2) to Pellicon XL (0.005m^2) (data courtesy of Millipore Corporation, MA, USA).

For non-linear scaling of tangential flow filtration, the critical parameter to maintain in TFF is the wall shear rate (γ_w) (Fischer, 1996). This should theoretically be possible whilst reducing membrane area, membrane cartridge hold-up and filtration rig hold-up. However, certain parameters remain that are unable to be predicted by current scaling methods such as the impact of pumps, valves and instrumentation, which are intrinsic to any microfiltration operation. To fit within the goals of ultra scale-down i.e. mimic large-scale performance with 1-100mL feed volumes for each experiment (see Chapter 1), a membrane area less than 0.0005m^2 would be required (see Figure 3.2).

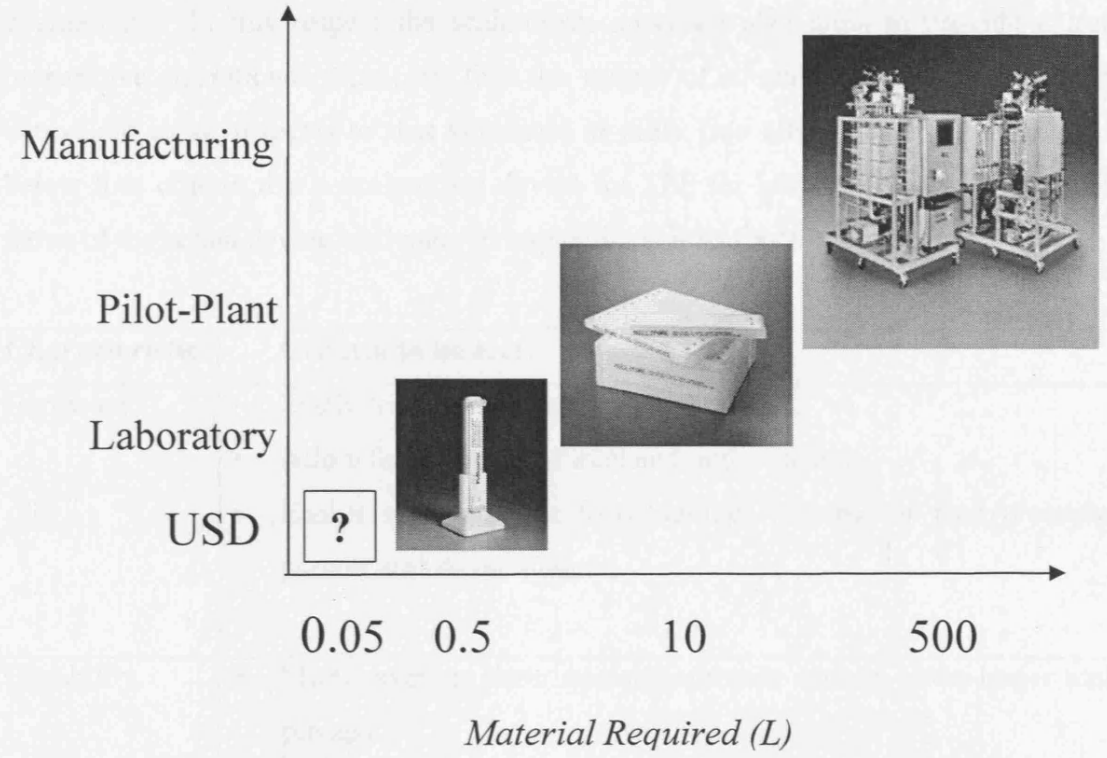

Figure 3.2: Scaling of flat-sheet TFF (pictures courtesy of Millipore Corporation, USA).

3.1.2 Challenges for a TFF scale-down device

Scale-down of TFF would allow rapid feasibility studies and the exploration of more process options c.f. conventional laboratory scale-devices with respect to:

- Membrane material & pore size
- Processing parameters that optimise flux & transmission
- Diafiltration design
- Cleaning protocols

In conjunction, only small volumes of process material would be required, which is desirable during process development, as representative material is often in short supply.

To be a reliable mimic of large-scale, any scale-down device must be able to process the same feeds, in particular with realistic solids loadings. It must also be able to generate material of similar content and specification in contaminant profile to the large-scale

counterpart. In this respect the scale-down approach also aims to provide a truly preparative operational mimic in that the output of a scale-down device must be equivalent in all respects to that generated at scale (see also Chapter 1). Table 3.2 below lists criteria that a scale-down device for TFF for bioprocesses should fulfil in terms of the actual device hardware, its capability and its functionality.

Characteristic	**Criteria to be met**
Hardware	• Easily test different membrane materials. • Allow for sampling of inlet and outlet streams. • Enable representative feed loadings (volume of feed processed perunit area of membrane).
Capability	• Mimic average shear rate at membrane surface of the larger scale process. • Account for material damage due to shear, air/liquid interfaces, retentate recycle, local pressure drops etc. found in industrial scale filtration rigs.
Functionality	• Operate in constant transmembrane pressure (TMP) and constant flux modes. • Perform concentration, diafiltration, recycle. • Capable of membrane regeneration (cleaning and sanitisation). • Capable of normal flow (NFF) or tangential flow (TFF) filtration.

Table 3.2: Attributes of a scale-down device for TFF

3.1.2.1 Caveats of working at small scales

As described in Chapter 1, discrepancies often arise between laboratory predictions and industrial performance. These are commonly due to differing geometries between laboratory-scale and process scale devices and the interaction of process material with ancillary equipment at the larger scale (e.g. shear effects).

Therefore, to surmount these difficulties, several other points should be considered when scaling down TFF to process volumes of less than 0.1L. These include:

•*Membrane uniformity*: Due to the current nature of polymeric membrane manufacture, polymeric membranes do not have a uniform pore size distribution. Hence, for very small areas, the average pore size or MWCO may differ considerable from membrane to membrane, or from between sections of the same membrane sheet. A methodology for assessing variations in the pore size distribution could therefore be employed. As such small membrane areas would be used for a smaller scale device, it is important to account for this variation as any variability will be accentuated. Alternatively, specially developed membranes that have a more even pore size range may be used; for example, Millipore manufacture 3mm diameter membrane disks for life sciences applications that display less batch-to-batch variation compared to conventional membrane disks.

•*Difference in hydraulic permeability*: Chandler and Zydney (2004) found that different membrane geometries exhibited different resistances to water, despite using the same membrane, and this was attributed due primarily to the large parasitic pressure losses in the cartridge and/or to a loss of effective membrane area associated with flow between the pleats.

•*Feed loading*: It is important to keep the fed-batch ratio i.e. the amount of feed processed per unit area of membrane comparable to typical industrial-scale processes. For example, 1.25×10^4L of Chinese Hamster Ovary cells (CHO) were harvested with $180 m^2$ membrane area in TFF mode (van Reis et al., 1991) i.e. a loading value of approximately $70 L.m^{-2}$.

•*Smoothness of feed flow*: For low volumes and flowrates, peristaltic pumps are commonly used. However, the resulting pulsatile flow may not be representative of the pumping characteristics in a large-scale rig, where centrifugal, rotary and gear pumps are common. The effect of pulsed flow on the dynamics of microfiltration has been well documented (Levesley and Hoare, 1995; Fischer, 1996; Meacle et al., 1999).

•*Instrumentation to determine flux, crossflow velocity and pressures*: The contributions of components, such as gauges and rotameters, will have a greater relative effect on hold-up and general rig hydrodynamics at a smaller scale of operation. Where possible, instrumentation should be non-invasive to the process.

•*Taking samples for assay*: Taking a 1mL sample for analysis from 100L of feed is insignificant, but taking the same amount from 10mL and the feed is reduced by 10%. Hence, assays need to be developed that require minimal amounts of material and/or strategies of extrapolation from sparse datasets will be required.

Thus, considerable care must be taken in scaling results from small scale systems employing flat sheet membranes to larger-scale devices with more complex flow patterns.

3.2 Proposal of a scale-down device for tangential flow filtration

Having highlighted the issues to be borne in mind during the design of a scale-down rig, the following section describes the engineering specifications of a scale-down device to mimic tangential flow filtration.

The obvious place to start when scaling down a unit operation is to look at the general principles of similarity (see Chapter 1), the rules of scaling and previous related examples in the literature. It is also worth looking at the scale-down of other unit operations, which have similar process duties e.g. such as centrifugation (Boychyn et al., 1998).

3.2.1 Scale-down approaches

Unfortunately, linear scale-down of flat-sheet TFF is not feasible, whilst maintaining the same channel length as used in industrial-scale filter and the membrane area under $0.0005m^2$ to meet the requirements of a device for USD (see section 3.1.1). For example, the Pellicon (Millipore, USA) series of cassettes have a channel length of approximately 0.155m (C. Christy, Millipore Corporation, personal communication, 2001); the width of a similar cassette with a membrane area of 0.0005 m^2 would be just

under 0.0033 m. Clearly this is not a practical size of membrane to manufacture or handle in the laboratory. It must also be noted that many membranes are usually commercially available as circular disks, the widest diameter currently available being 0.142 m (source: Cole Parmer Product Catalogue, 2005), which could not be cut to the correct length.

Hence, a non-linear approach needs to be considered. Fortunately, the literature suggests a possible solution in the form of a rotating disk filtration system. Lee et al. (1995) investigated the use of a novel rotating disk dynamic filtration system (Pall Corporation, USA) for the microfiltration of recombinant yeast cells. The study demonstrated the superior filtration performance of the new unit, but interestingly identified a critical rotational speed below which behaviour was comparable to that of a flat sheet system, at a given membrane loading level.

The existence of other TFF module formats e.g. hollow fibre, spiral wound, should also be noted. A device that would be general enough to predict behaviour across this range of geometries (not just flat sheet configurations) would be ideal. The development of a scale-down device for TFF based on a rotating disk design is considered below.

3.2.2 Rotating disk filtration

Rotating disk, high shear or so-called dynamic filtration has been in use in the chemical industry for over four decades. The reader is directed to the established work of Murkes and Carlsson (1988) for a comprehensive review of the theory and to Culkin et al. (1998) for examples of industrial hardware and application of this technology. Many novel dynamic filtration systems have been reported in the literature, a selection of which are listed in Table 3.3 below.

In such systems, the high shear rates generated by the rotating disk at the membrane surface yield very high permeate fluxes by minimising concentration polarisation and fouling effects. Unlike traditional TFF, it is possible to control shear intensity independently from the main flow of the suspension through the filtration unit. This offers the advantage of lower pressure drops across the module and the membrane. As a consequence of this decoupling of shear force and pressure generation, shear rates can

be easily optimised and precisely controlled to maximise filtration performance (Vogel et al., 2002).

Description	**Mode of filtration**	**Nominal membrane area (m^2)**	**Literature References**
Rotating disk dynamic filtration system	TFF	0.137	Lee et al., 1995
Controlled shear filtration for animal cell separation	NFF	0.515	Vogel and Kroner, 1999
Rotating disk device	TFF	0.190	Bouzerar et al., 2000
Cone and plate test cell for ultrafiltration	NFF	0.442	Vasan et al, 2002
Rotating disk filter for crossflow microfiltration	NFF	0.500	Pessoa and Vitolo, 1997
Vibrating disk dynamic filtration system	TFF	0.200	Postlethwaite et al., 2004

Table 3.3 Rotating disk devices in the literature

The fluid dynamics of rotating disk filters have also been investigated quite thoroughly. Due to their relatively simple geometry, it has been possible to model rotating disk devices by CFD (Rudniak and Wroński, 1995; Serra et al., 1998; Castilho and Anspach, 2003). These papers described prediction of the fluid dynamics in various rotating disk filtration systems, and use the models developed to estimate shear stresses in such modules and to investigate different designs. Semi-empirical correlations to relate disk rotation to shear rate have also been developed (Schlicting, 1968; Vogel and Kroner 1997; Bouzerar et al., 2000), and these have been shown to provide an adequate estimate of the shear rates generated in such devices. Similar calculations are performed below in order to check the feasibility of the proposed device design performing in a comparable manner to that of a flat-sheet filter.

3.2.2.1 Hydrodynamics of rotating disk devices

Let us consider a disk with rotation speed ω, operating parallel to the membrane surface and located at an axial distance *s* above it (see Figure 3.3 below).

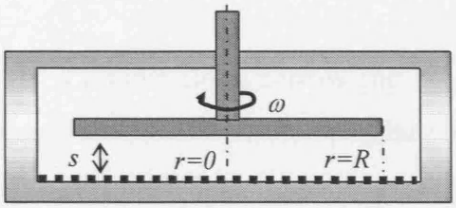

Figure 3.3: Schematic of a rotating disk filter.

The flow is characterised by two Reynolds numbers; the axial and radial turbulence, which are defined by equation [3.1] and [3.2] respectively.

$$\mathrm{Re}_s = \frac{\omega s^2}{\nu} \qquad [3.1]$$

$$\mathrm{Re}_r = \frac{\omega r^2}{\nu} \qquad [3.2]$$

where r is the local radius and s is the gap height between the membrane and the disk surfaces (see Fig. 3.3). The transition Reynolds number based on disk radius and tip velocity was defined as 3×10^5 by Schlichting (1979). However, this value is reduced to 2×10^5, if based on the stationary plate, or in this case, the membrane (Randriampianina et al., 1997).

Assuming that there is no radial net flow and that the surfaces are solid, four different flow types can now be distinguished (Murkes and Carlsson, 1988) which are summarised in Table 3.4 below.

The boundary layers are separated by an inviscid core of fluid with angular velocity $k\omega$, where $0>k>1$. The velocity entrainment factor (k) is an experimentally determined parameter that is a function of the pressure drop across the module, as well as the fluid and disk material and geometry. It can be measured by placement of pressure sensors on the casing of the device (Bouzerar et al., 2000). Values of k between 0.3 and 0.5

have been quoted in the literature for smooth rotating disks (Murkes and Carlsson, 1988, Vogel and Kroner, 1999).

	Region	Re_s	Re_r	s/r
Laminar flow, narrow gap	I	<4	$<2 \times 10^5$	-
Laminar flow, two separate boundary layers	II	>4	$<2 \times 10^5$	-
Turbulent flow, narrow gap	III	-	$>2 \times 10^5$	>0.05
Turbulent flow, two separate boundary layers	IV	-	$>2 \times 10^5$	<0.05

Table 3.4: Flow patterns in rotating disk filters

3.2.2.2 Calculation of shear rate in a rotating disk device

The principle parameter to maintain when scaling TFF is the shear rate at the membrane surface (see Chapter 1, section 1.4 and section 3.1.1 above). Hence, it is necessary to be able to determine the shear rates that are generated in the device.

The following empirically derived equations have been used by several authors to calculate the local shear stress in a rotating disk device:

$$\tau_{w,laminar} = C\rho\nu^{1/2}(k\omega)^{3/2}r \qquad [3.3]$$

$$\tau_{w,turbulent} = C\rho\nu^{1/5}(k\omega)^{9/5}r^{8/5} \qquad [3.4]$$

where C is a constant, values of which are given in Table 3.5 below.

Laminar flow	***Turbulent flow***	***Lit. references***
1.81	0.057	Schiele (1979)
0.77	0.0296	Bouzerar et al. (2000)

Table 3.5: Values of wall shear stress constants (C) for rotating disk device correlations.

The difference in the constants in Table 3.5, as explained by Bouzerar et al. (2000), is due to the calculation of the stress at the surface of the rotating disk, rather than the surface of the stator i.e. the membrane. However, the parameters used, in their

similarity solution for the azimuthal velocity induced near a stationary plate by a rotating fluid, were specific to the device used by Bouzerar et al. (2000).

Based upon laminar flow theory (Lee et al., 1995), the shear rate experienced by a particle within a rotating disk chamber changes with radial position. As noted earlier, a method of mitigating this phenomenon is the use of a conical-shaped rotor (Vogel and Kroner, 1999) since this generates a uniform shear field across the stationary surface (c.f. cone and plate viscometers). Thus, the local radius (r) is no longer a variable parameter.

For a conical rotor of radius R, with a small inclination angle (see Fig. 3.2) (α), Reynolds number is described by

$$\mathrm{Re} = \frac{\omega(h + r\tan\alpha)^2}{\nu} \qquad [3.5]$$

The average shear rate in the gap between the conical rotor and the membrane (h) can be calculated by

$$\dot{\gamma}_{average} = \frac{\omega r}{h + r\tan\alpha} \qquad [3.6]$$

However, for small rotor heights ($h/s_{max}<0.1$) the local average shear rate can be assumed to be constant over the whole gap between the rotor and the stator. The wall shear stress can be estimated by equations [3.3] and [3.4] above. Wall shear rate (γ_w), assuming Newtonian behaviour, can then be determined by

$$\dot{\gamma}_w = \frac{\tau_w}{\eta} \qquad [3.7]$$

The assumption of Newtonian behaviour is valid for dilute suspensions and many fermentation broths, as long as there is no cell lysis.

A basis for comparison of performance for a plane rotor should be considered at half the maximum gap width of the conical rotor (Vogel and Kroner, 1999) i.e. the gap (*s*) between an equivalent plane rotor and the membrane can be calculated using equation [3.8] below (see Figure 3.4):

$$s = \frac{R}{2}\tan\alpha + h \qquad [3.8]$$

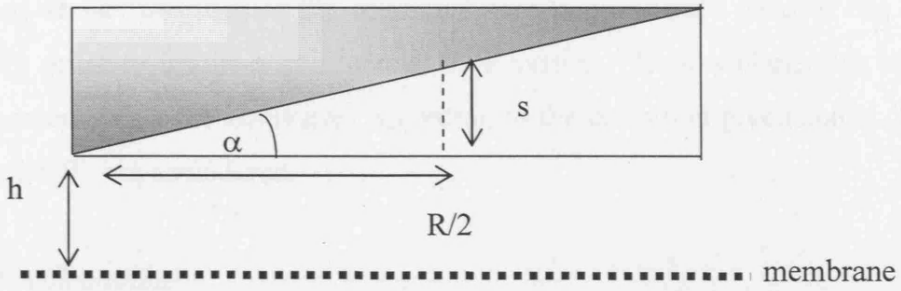

Figure 3.4: Schematic of the determination of an equivalent plane rotor axial gap to a conical rotor.

There have been several attempts in the literature to determine parameters such as torque (T), power input (P), and energy dissipation per unit mass (ε) (Cherry and Papoutsakis, 1986, Lee et al., 1995). In such devices, these enable characterisation of the Kolmogorov microscale of turbulence and therefore provide an insight into the amount of damage caused by the rotor to particles in the feed. However, as the purpose of the microfiltration USD is to mimic conventional TFF, such calculations would only be useful if an equivalent analysis were possible for formats such as membrane cassettes. To date, the latter has not been achieved (see Chapter 9 for a further discussion).

As a corollary, this lack of understanding of the actual shear rates encountered in a "real" industrial TFF system, i.e. in the rig and the membrane device, is another issue that complicates the design of a non-geometric mimic. Shear damage during processing may be caused by the recirculation of the feed through constrictions and components such as pumps, flowmeters and valves. Membrane cassettes may also contain areas of high local shear at the entrance and exit ports (this is analogous to the centrifuge example quoted in Chapter 1). Therefore, pre-treatment of the feed and/or intelligent operation of the USD device may be required in order to mimic the whole unit operation e.g. the exposure of the feed to a high-shear environment before processing to simulate the hydrodynamics encountered of the industrial equipment (Boychyn et al., 2000).

3.2.3 Theoretical calculation of the wall shear rate in a rotating disk filter to mimic a flat-sheet filter

Table 3.8 below is a summary of the results of calculations, using the equations described above, to estimate the rotational speeds one would need to run a rotating device in order to mimic a commercial TFF system. Both a plane disk rotor and a conical rotor, which are equivalent according to the definition given above (Vogel and Kroner, 1999), are considered.

Example calculation:

The maximum wall shear rate in a Prostak™ device (Millipore, MA, USA) when harvesting CHO cells is approximately 4,000s^{-1} (R Kuriyel, Millipore Corporation, personal communication, 2003). What rotational speeds would be required in a USD to mimic these wall shear rates?

It is assumed that the global shear rate is independent of feed flowrate, which is generally the case for dynamic filtration devices (Bouzerar et al., 2000). It is also assumed that because the rotational speeds will be low, and the disk radius small, radial variations in shear are insignificant i.e. r=R (Bouzerar et al., 2000). Hence, the equations developed by Schiele (1979) can be used without integration across the rotor radius to estimate the magnitude of the global shear rate in the device.

Rotor type	***Calculation Method***	Re_r	Re_s	τ_w (N/m^2)	γ_w (s^{-1})	ω ($rads^{-1}$)
Plane	Schiele (1979)	6.3×10^5	3.5×10^4	4	4000	160
Plane	Bouzerar et al. (2000)	-	5.4×10^5	4	4000	318
Conical	Vogel et al. (1999)	6.5×10^5	5.9×10^4	4	4000	160

Table 3.6: Summary of example calculation results, using equation [3.4]. Fluid parameters: $\rho=1000kgm^{-3}$, $\eta=0.001Pa.s$, $\nu=9.8x10^{-7}m^2s^{-1}$.Rotating disk parameters: disk radius=0.015m, conical rotor height from membrane (h) =0.002m, conical rotor inclination angle 4 degrees = 0.07rads, equivalent plane disk height from membrane (s)=0.0023m (equation [3.8]).

According to the definitions described in Table 3.4, the flow patterns in the device at these conditions are in region IV i.e. turbulent flow with separate boundary layers. The values are comparable to those cited in the literature (Vogel and Kroner, 1999) in terms of magnitude. It is interesting to note that the angular velocity calculated by the method developed by Bouzerar et al. (2000) is double the requirement determined by the Schiele method (see Table 3.8). This implies that the wall shear rate at the disk surface is twice the wall shear rate at the membrane surface.

In order to mimic conventional filtration, the wall shear rate at the membrane surface has to be matched, but the possibility of stream component damage due to the high local shear rates at the disk edge has also to be considered. However, this phenomenon may prove to compensate for shear damage due to feed recirculation and entrance/exit effects in a TFF system (see Chapter 1).

The above example supports the concept that it should be possible to attain similar global wall shear rates found in conventional flat-sheet TFF systems by careful selection of the operating conditions of a rotating disk device. At these conditions flux and transmission behaviour should therefore also be comparable. The next stage of investigation entails the construction of such a device and experimental validation of its performance and utility as a scale-down mimic for TFF.

3.3 Design and construction of a scale-down device for TFF

In light of the findings of previous studies on rotary disk filtration units, and the criteria of a device for TFF USD, a device to mimic flat-sheet TFF is proposed in the following section. The design calculations will be described, as well as details of the final mechanical specification for the prototype microfiltration USD.

3.3.1 Device mechanical options

The mechanical options available can be summarised into the following categories:

a) *Materials of construction*: housing, disk, membrane support, mechanical seals etc.;
b) *Filter housing*: size and shape, ability to maintain pressures required during filtration;

c) *Membrane attributes:* size and shape of filter, located either on the rotor or the stator, support method;
d) *Disk attributes*: shape, diameter, position in relation to membrane, position in relation to the filter housing;
e) *Inlet and outlet configuration*: placement of the feed, retentate and permeate ports.

These options are discussed in turn below, with respect to the development of a USD device for TFF.

a) *Materials of construction*

As the device will process biological feeds, it is important to construct it from biologically inert materials. These materials must be cleanable, and be able to withstand any pressure build up due to pumping and restriction of flow of the process fluids. As temperature affects filtration behaviour, the device materials in contact with the process fluid must have a low specific heat capacity i.e. not exchange heat to or from the surroundings or the fluid.

For the purposes of a prototype design, a transparent material for the module housing would allow direct visualisation of the filter chamber, and therefore facilitate the correct priming of the filter and assessment of mixing.

b) *Filter housing*

For simpler fabrication, and analysis of fluid dynamics, a circular housing has been utilised for existing rotating disk filters. The size of the housing will depend on the hold-up requirement of the filtration rig i.e. as small as possible for USD requirements, but will mainly be dictated by the limitation imposed by fabrication techniques.

TFF is a pressure driven separation (see Chapter 2), and therefore the device must be able to maintain the necessary pressures generated on the retentate and permeate sides due to flow restriction by valves (backpressure). Thus, the design of chamber and the mechanical seals on the rotor shaft must be pressure tight.

c) *Membrane attributes*

Devices in which the membrane mounted onto the rotor or the retentate exits through a hollow shaft through the membrane have been described (Murkes and Carlsson, 1988, Lee et al., 1995). However, as fabrication of such devices is complex, they will not be considered in the context of a microfiltration USD; the membrane will be located on the base of the unit.

d) Disk attributes

Bouzerar et al. (2000) also investigated the effects of disk geometry and position in relation to the filter and its housing. The authors found that permeate flux was independent of the disk to membrane (axial) gap, but increased when the gap from disk to housing (radial gap) was increased by 3mm. Brou et al. (2002) also describe the addition of radial vanes to the rotating the disk, which decreased fouling. The application of this modified style of disk to microfiltration of yeast suspensions, and its implications on power consumption and flux has also been studied.

Another important phenomena that has been noted is the variation of shear rate, and hence filtration as a function of radial distance from the axis of rotation (Bouzerar et al., 2000). At low rotational speeds, cake formation is not prevented in the central part of the membrane. The implications on global performance of a range of shear rates across the membrane surface and in the module e.g. at the disk tip, are significant, especially for bioprocess stream components that are prone to damage by high local shear rates and pressure drops, such as cells and proteins (Levy et al., 1999).

In order to mitigate this radial variation Vogel and Kroner (1999) describe the use of a smooth, conically shaped rotor to establish a controlled shear field in which baby hamster kidney (BHK) cells experience a significant hydrodynamic lift away from the membrane surface, whilst maintaining cell viability.

With respect to the TFF USD, maximising flux is not the prime concern, so enhancement of the shear rate by modifications by e.g. radial vanes, is not necessary. However, minimisation of the radial variation of shear across the membrane surface may be important. Although the disk radius of the TFF USD would be much smaller

than the devices described above (and therefore radial variation minimal) it would be wise to consider the use of a conical rotor, if it proved to be feasible to fabricate.

f) Inlet and outlet configuration

The influence of device geometry and angular velocity on rotating disk performance is described by Bouzerar et al. (2000). Several inlet and outlet configurations were tested (see Figure 3.5).

Figure 3.5: Rotating disk module showing inlet and outlet configurations (after Bouzerar et al., 2000). Note that the device is mounted vertically.

At low speeds of rotation (below 500rpm) the variations of permeate flux, and inlet and outlet pressure drop were similar for all five configurations. However, the peripheral pressure for configuration (v) was markedly higher. The authors' objective was to optimise permeate flux, and configuration (v) gave the best performance, especially at higher rotational speeds (up to 1500rpm).

However, the objective of the TFF USD is not to optimise filtration, but rather to mimic conventional filtration. Hence, the position of the ports need only to be designed for ease of access, and to ensure that proper mixing occurs in the filter, and that the filter surface is not bypassed.

Taking these issues into consideration, a prototype TFF USD device was fabricated in-house (Biochemical Engineering Workshop, UCL). A description of this device is given in the following section.

3.3.2 Device Overview

Figure 3.6 shows photographs of the prototype device used for the scale-down experiments in this thesis.

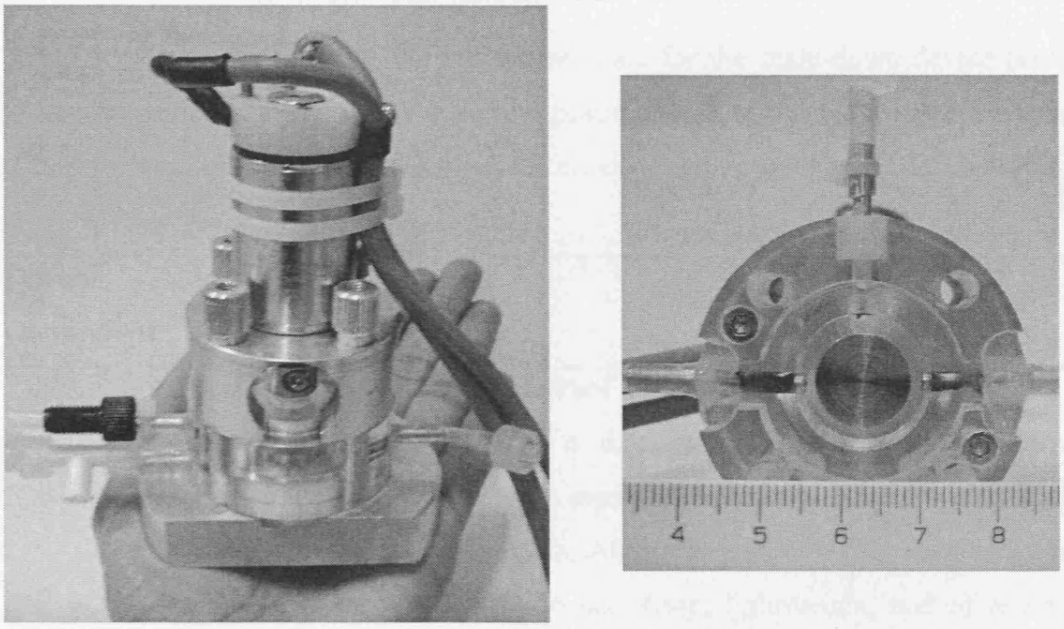

Figure 3.6: Photographs of a purpose-built rotating disk device.

The device has the following features making it superior to existing scale-down devices:

- Uses 25mm membrane disks: Commercially available, disposable membrane disks can be used, obviating membrane cleaning if desired. The area available for filtration is 15 times smaller than commercial scale-down devices (see Table 3.1) and therefore much smaller volumes of feed are required for each experiment.
- Clear filter housing: the Perspex® chamber allows direct visualisation of the feed/retentate; this helps in ensuring proper mixing is occurring, and that all air bubbles are removed during device priming.
- Conical disk: the conical geometry and small diameter of the rotating disk negates radial variation in the shear produced at the membrane surface i.e. a uniform shear field is produced.
- Ability to adjust disk height and geometry: The construction of the rotary shaft seal was designed so the rotor is removable, and therefore can be replaced with rotors of different shapes and sizes, allowing for future modifications.

- NFF capability: By sealing off the inlet and outlet ports, the device can function as a NFF unit, comparable to a stirred cell.

3.3.2.1 Mechanical specifications

Table 3.7 below summarises the options selected for the scale-down device prototype. Once the device had been fabricated and pressure leak tested with compressed air and water, the ancillary equipment to form a scale-down filtration rig could be selected.

Device component	**Discussion**
Filter housing	Perspex was used to construct the filter housing because it is non-corrosive, transparent, easy to machine, and has low water absorption. The support structures were made of an aluminium alloy with stainless steel screws and knurled nuts. Aluminium alloy was chosen because it is non-corrosive, easy to machine, cheap, lightweight, and of reasonable fatigue life. The rotor seal was made of a silcone o-ring mounted into a Delrin® (a general purpose mechanical plastic that has FDA/USDA dairy approval for food contact) support. The internal diameter was 21 mm.
Membrane	As stated above (see Chapter 1), the objective of USD is to scale systems down so they only require 10's of millilitres of process material. With this in mind, and considering commercially available membrane formats as well as the ramifications of small membrane area on overall pore size distributions, it seems sensible to base a microfiltration USD on the widely available 25 mm circular disks (area of ~0.0005 m^2), which most membrane materials can be manufactured to. For a feed loading of 100 Lm^{-2} (typical of industrial applications), this would mean that less than 50 mL of feed would be required for each scale-down experiment.

Device component	Discussion
Membrane support	The membrane will need to be sealed into place; a common method is to use a gasket or o-ring seal (see Figure 3.7). 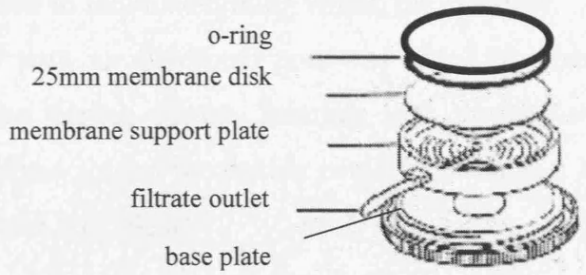 *Figure 3.7: Detail of membrane support* Assuming an o-ring thickness of 2 mm, the available area for filtration would then be 3.46 x 10^{-4} m^2 (this is almost fifteen times smaller than other scale-down devices currently available). As polymeric membranes are fragile, they need to be supported; this was achieved by using a support plate taken from a commercial device (Amicon stirred cell, Millipore, MA, USA), which has grooves etched into it to allow permeate flow, whilst supporting the membrane coupon.
Disk/rotor	As the thickness of the o-ring is 2 mm, a clearance from the chamber wall of 2 mm would allow the disk to rotate above the whole area of the membrane, whilst maintaining a sufficient distance from the housing. The rotating disk above the membrane was therefore designed to be of diameter (R) 17 mm. It was constructed from stainless-steel 316 L; the conical disk itself was 3 mm thick at the centre, with a 5° angle to the horizontal. The rotor shaft was also 3 mm thick, and held into the filter housing with a custom-made Delrin® /silicon lip seal. The axial gap between the membrane and the disk were set by using specially made height-setting spacers (jigs); the disk was suspended 1 mm above the membrane surface for the experiments described in this thesis.

Device component	Discussion
Inlet and outlet configuration	Two opposing pipelines were created in the side of the filter housing, to allow recirculation of the feed/retentate. One port was put higher than the other to facilitate mixing within the chamber. As well as an inlet and outlet port, an additional port was added to enable the removal of air bubbles during system priming, and to enable flow normal to the membrane so that the device could function as a NFF device, as shown in Figure 3.8 below). 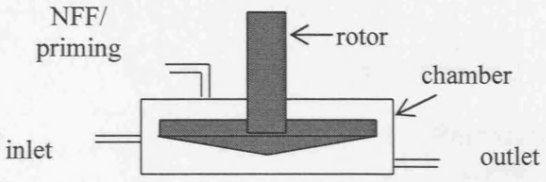 *Figure 3.8: Schematic of feed/retentate port locations on the TFF USD device* The inlet pipes were fabricated from 1mm inner bore stainless steel tubes fixed into the Perspex housing using cyanoacrylate glue.
Disk drive motor	A DC-Micromotor was used to rotate the disk. A speed control card and feed back system was employed to keep speed constant, and a tachometer was added to the unit so that the rotation speed could be measured. The rotation speed range was set to be 0 to 5000 rpm, based on previous shear calculations (see section 3.2.2.2), with an accuracy of ±10rpm.

Table 3.7: Mechanical design on the scale-down device for TFF

3.3.3 Ancillary equipment selection

Figure 3.9 below shows a schematic of the scale-down rig and its ancillary equipment. The arrangement is the same as the conventional filtration rig, but on a smaller scale.

Hence, the same experimental protocols, such as constant volume diafiltration, could be kept the same.

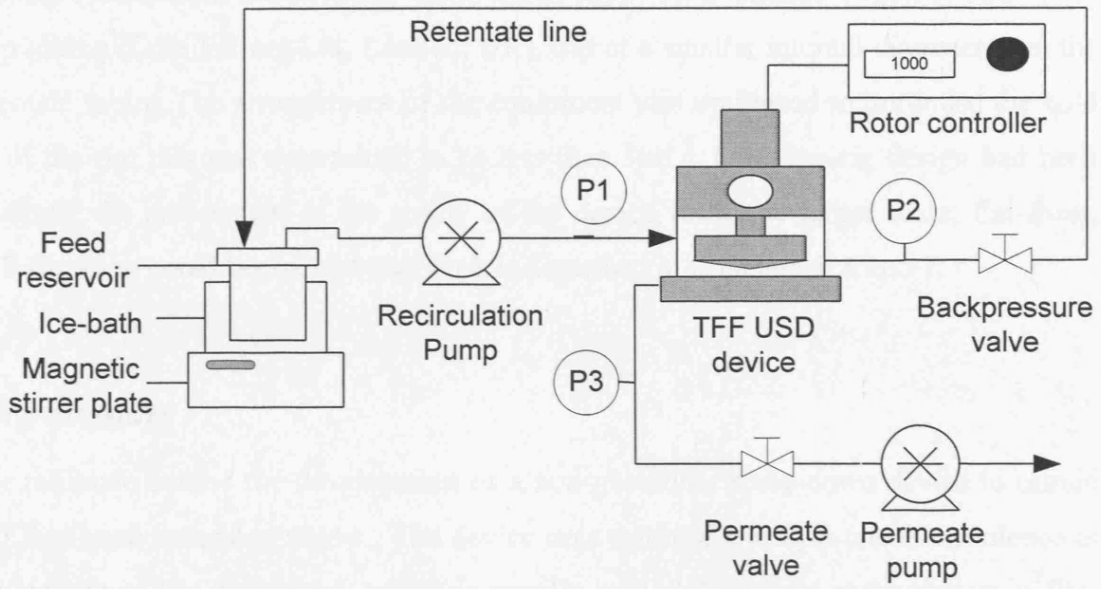

Figure: 3.9: Schematic of the TFF USD filtration rig (not to scale)

The feed reservoir used was a small plastic beaker, which was placed within a larger beaker full of ice (to maintain feed temperature during processing). The feed (retentate) was mixed using a magnetic flea, and placing the reservoir on a magnetic stirrer plate.

The retentate pump selected was a Gilson Minipuls-3 peristaltic pump (Gilson, WI, USA), which uses Ismatec Tygon R-3603 two-stop tubing (Cole Parmer Ltd, London, UK). Tygon was selected due to its biological and chemical inertness i.e. it would not be affected by the feed or cleaning fluids. Gilmont laboratory direct reading flowmeters (Cole Parmer Ltd, London, UK) were used to calibrate the pump. This pump is relatively pulse-free, which is desirable for small-scale operation (see section 3.1.2.1)

The transmembrane pressure was measured by digital manometers (Catalogue no. EW-68603-04, Cole Parmer Ltd, London, UK). These gauges were regularly calibrated according to the manufacturer's instructions using compressed nitrogen gas.

A DC-Micromotor, 10.5 Watt, 24 Volt Linear Controller (LC 3002 System Faulhaber, Electro Mechanical Systems Ltd, Aldermaston, UK) was used to rotate the disk. The disk rotation in rpm was displayed on an LED panel.

Needle valves (Cole Parmer Ltd, London, UK) were used to control the backpressure and the permeate flow. Permeate flow was also controlled by a Pharmacia peristaltic P-1 pump (Amersham Biosciences, UK), which again used Ismatec Tygon R-3603 two-stop tubing (Cole Parmer Ltd, London, UK), but of a smaller internal diameter than the retentate tubing.The arrangement of the equipment was optimised to minimise the hold up of the rig; this was determined to be less than 3mL. Once the rig design had been finalised, the assessment of the ability of the device to mimic larger scale, flat-sheet, TFF filtration could begin, and this work is described in Chapters 5, 6 and 7.

3.4 Summary

The rationale behind the development of a non-geometric scale-down device to mimic TFF has been described above. The device uses a rotating disk to create turbulence at the surface of the membrane, which is usually achieved by feed recirculation in flat-sheet devices. The device was designed to meet the criteria set out for ultra scale-down i.e. mimic large-scale performance with 1-100mL feed volumes for each experiment (see Chapter 1). The TFF USD device approximately provides a 300-fold scale-down to traditional pilot-scale equipment ($0.1m^2$ cassettes), the benefits of which have been outlined in Chapter 1.

The issues surrounding the use of such small scale devices, and small amount of process material have been discussed, and mitigating strategies proposed to address them. These strategies were incorporated into the selection of the TFF ancillary equipment, as well as the device operating procedure, which is described further in Chapter 4.

A theoretical calculation has been presented to support the hypothesis that the rotating disk device can generate the membrane wall shear rates encountered in conventional flat-sheet devices. In order to see whether maintaining this operating parameter can faithfully mimic filtration behaviour in terms of flux and species transmission requires empirical studies. This has been achieved by comparison with commercially available devices, using representative biological process streams (yeast suspension, yeast homogenate, a bacterial lysate, and a mammalian cell broth) in Chapters 5, 6 and 7 respectively. For convenience, the materials and methods used for all these studies are collated in Chapter 4.

Chapter 4 Materials and Methods

4.1 Introduction

The following chapter describes the experimental protocols, equipment, and materials used throughout this thesis. These techniques have been grouped together as such to avoid repetition in each chapter and for ease of reference.

Section 4.1 and 4.3 give details of the filtration equipment and protocols employed, whilst sections 4.4 to 4.7 relate to the feed systems investigated in Chapters 5, 6 and 7.

4.2 Filtration equipment

The TFF USD rig has been detailed in Chapter 3, but the conventional filtration rigs used in thesis are described below.

4.2.1 Pilot-scale

The pilot-scale filtration rig used was a ProFlux® M12 rig (Millipore Corporation, MA, USA), with a baffled reservoir. A schematic is given in Figure 4.1 below. Two Masterflex® L/S™ (Cole-Parmer Instrument Company, IL, USA) peristaltic pumps were incorporated; the retentate recirculation pump was an Easy-Load® II Model 777201-62 and the permeate flux control pump was a Quick-Load® Model 70201-24. The rig also included three pressure transducers to measure inlet, outlet and permeate pressures connected to a digital display. The Pellicon 2-mini cassettes (Millipore Corporation, MA, USA) fitted into a stainless steel cassette holder were used with this rig.

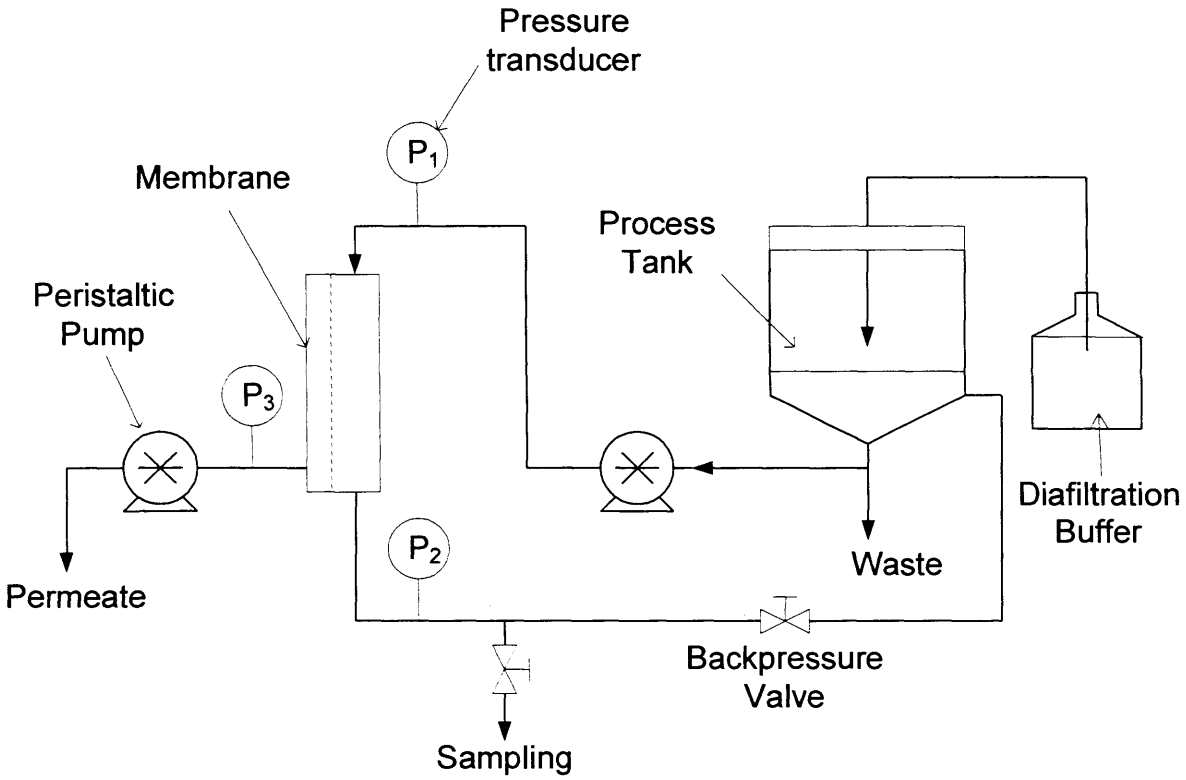

Figure 4.1: Diagrammatic representation of the Proflux M12 rig in one pump format connected to the Pellicon Mini cassette holder. P_1, P_2 and P_3 are the inlet, outlet and permeate pressure transducer respectively.

4.2.2 Laboratory-scale

A LabScale™ TFF System (Millipore Corporation, MA, USA) was also used for the diafiltration studies in Chapters 5 and 6. The rig schematic was similar to the one iillustrated in Figure 4.1 above. Two Watson-Marlow (Watson-Marlow Bredel, Falmouth, UK) peristaltic pumps were incorporated; the retentate recirculation pump was a 505Du pump with a six-roller R2 head, which enabled smoother flow using a special y-shaped tubing element. The permeate flux control pump was a 500Di pump with 4 rollers. The rig also included three bourdon-type pressure transducers to measure inlet, outlet and permeate pressures. The Pellicon XL cassettes (Millipore Corporation, MA, USA) were used with this rig.

4.2.3 Membrane formats and types

Several types of format were used for the studies:

- Pellicon 2 mini (Millipore, USA), flat-sheet cassettes of area $0.1m^2$;
- Centramate (Pall, UK), flat-sheet cassettes of area $0.1m^2$;
- Pellicon XL (Millipore, USA), flat-sheet cassettes of area $0.05m^2$;
- Precut 25mm disks (Millipore, USA; Pall, UK);
- In-house prepared 25mm disks (membrane sheet kindly supplied by D. LaCasse, Millipore, USA). The disks were cut from the middle of the sheet using a titanium die and punch press to reduce variability and great care was taken when handling the sheet not to touch the coupons with bare hands.

Table 4.1 lists the details of the membrane types and formats used for the experiments described in this thesis.

Feed System	Pore size/ MWCO	Membrane Material	Format	Membrane Area (m^2)	Manufacturer
S. cerevisiae whole cell suspension	0.65μm	Durapore®	Pellicon 2-mini cassette, V-screen 25mm disks	0.1 3.46×10^{-4}	Millipore
S. cerevisiae homogenate	0.1μm	Durapore®	Pellicon 2-mini V-screen cassette, 25mm disks	0.1 3.46×10^{-4}	Millipore
E. coli lysate	1000kDa	Biomax®	Pellicon 2-mini V-screen cassette, Pellicon XL cassette, 25mm disks	0.1 0.05 3.46×10^{-4}	Millipore
Mammalian cell fermentation broth	0.2μm	Supor®-200	Centramate cassette, 25mm disks	0.1 3.46×10^{-4}	Pall

Table 4.1: Membrane materials and formats used

All membranes were air-integrity tested and subjected to water permeability tests prior to use. Those not within the manufacturer's recommended ranges were regenerated (cleaned and sanitised) and retested, or in the case of the 25mm disks, discarded.

4.3 Filtration protocols

A typical experimental protocol for the filtration experiments is listed below:

(i) Wet the membrane.
(ii) Air integrity test.
(iii) Water flux tests.
(iv) Buffer conditioning.
(v) With Permeate valve closed, slowly drain buffer and replace with feed.
(vi) Ramp up the feed pump to the desired crossflow velocity, and slowly open the permeate valve.
(vii) Ramp up the permeate pump to the desired setting.
(viii) Perform the filtration experiment.
(ix) Buffer flush.
(x) Water flush.
(xi) Water flux tests.
(xii) Clean the membrane.
(xiii) Water flush.
(xiv) Water flux tests.
(xv) Storage solution flush.

There were several types of filtration experiment, each of which are described below. Also, steps (xii) to (xv) are not applicable to the 25mm disks, which were single-use.

4.3.1 Air integrity testing

These were conducted as per manufacturer's recommendations (Technical procedures, Millipore, USA), using compressed air at 3barg pressure. If air flow through the membrane exceeded 5 x 10^{-8} $m^3.s^{-1}$ ($3cm^3.min^{-1}$) air flow, then the membrane was rejected.

4.3.2 Conventional filtration experiments

Flux was measured using a balance (model BB2400 Metler-Toledo Ltd., Leicester, U.K.) and stopwatch over 1 min intervals after steady state permeate flux had been reached. The feed was kept below 12°C during filtration using a cooling jacket on the reservoir tanks, and agitation ensured that the suspension remained homogeneous.

4.3.2.1 Determination of critical flux

To find the optimal operating conditions for the system, flux was raised by step increments at fixed time intervals and transmembrane pressure (TMP) was monitored. Permeate was recirculated back into the tank to maintain a constant concentration of solids and product (see also Section 4.3.2.2). Permeate samples were taken after flux stabilisation in order to assess the percentage of transmission, defined as the ratio of antibody fragment concentration in the permeate to that in the retentate. The critical flux region was the point at which the TMP increased rapidly at a fixed imposed flux.

4.3.2.2 Total permeate recycle experiments

Buffer conditioning, with a buffer volume equal to 25% of the feed volume, was performed before ramped addition to the process tank of the feed. With the permeate pump off, backpressure valve closed and sampling valve open the buffer flowed out of the system. When the feed approached the sampling valve, this valve was closed rapidly and the backpressure valve opened simultaneously (buffer conditioning is necessary to avoid air pockets in the permeate side, which may have a detrimental effect on transmission (Meagher *et al.*, 1994)). The speed of the feed pump was increased to the desired value and the retentate valve was closed partially in order to maintain some backpressure. At this point (taken as t=0) the permeate pump was started at the desired value and the transmembrane pressure (TMP) was set at by adjusting the retentate valve. The permeate was continuously fed back into the process tank. Samples were taken from the retentate and from the permeate at regular intervals. The inlet, outlet and permeate pressures were monitored throughout the process.

4.3.2.3 Concentration experiments

These procedure was as used in section 4.2.2.2, but the permeate was collected in a separate reservoir i.e. not recycled.

4.3.2.4 Diafiltration experiments

These were conducted in the same manner as the concentration experiments (see section 4.2.2.3), but diafiltration buffer was added to the feed reservoir at the same rate of permeate removal. This was achieved by using an identical pump to that on the permeate line at the same settings, and monitoring tank level visually to ensure a constant volume was maintained.

4.3.2.5 Membrane cleaning

Between experiments the membrane system was flushed with RO water, cleaned and sanitised according to the manufacturers' recommendations with 0.1N sodium hydroxide at 40°C, for 0.5h, flushed with RO water and then followed by 0.1N phosphoric acid at 40°C, for 0.5h (Cassette Maintenance Procedures, Millipore, USA). For the CAT trials (Chapter 7), the membranes were cleaned with a 0.1% SDS solution at 40°C, for 0.5h (Cassette Operating Instructions, Pall, UK).

Pure water flux was measured at different feed flows after cleaning to assess the effectiveness of the cleaning step. The membrane was considered clean once the clean water flux test exceeded 80% of the original value. When lower values of water flux were obtained the cleaning procedure was repeated.

4.3.3 TFF USD experiments

Due to the nature of the TFF USD device, the set-up procedure was different to that of the cassettes, as the membrane disks were removeable. The differences to the conventional procedures are described below.

4.3.3.1 Unit assembly and buffer priming

The membrane disks were into put the membrane support plate (shiny side up), wetted with RO water, and the o-ring placed on top, taking care not to touch the membrane surface. Latex gloves were worn to avoid transferring skin proteins to the equipment.

The support plate was then put into position within the unit, and sealed in place by tightening the knurled screws. The TFF USD device was then attached to the ancillary equipment via small bore Tygon® tubing (Cole Parmer Instrument Company, UK) with C-flex® luer (Cole Parmer Instrument Company, UK) connections.

The unit was hydraulically pressure tested by filling with RO water and checking for leaks. The disk was also rotated to check the shaft seal. The unit was emptied of water, prior to the air integrity test, which was conducted by placing the air supply to the top port of the chamber, and following the procedure as in section 4.2.1.

The unit was primed with buffer by recirculating the buffer around the rig and tilting the chamber so any air bubbles rose to the top of the chamber. The air was vented via the top port. The filtration experiments were then carried out as described in section 4.2.2.

4.3.3.2 NFF experiments

The NFF experiments were conducted by sealing the inlet and outlet ports, and feeding via the top port. Although left in place, the disk was not rotated for these experiments.

4.3.3.3 Cleaning procedures

The disks were disposable, and once the unit was disassembled, and the membrane removes, the parts were rinsed thoroughly in RO Water, 1M sodium hydroxide solution and rinsed again before each experiment. All tubing was disposable also, and prior to the studies at Cambridge Antibody Technology, the unit was autoclaved, and new tubing used. All surfaces of the ancillary equipment were sanitised using isopropyl alcohol.

4.4 *S. cerevisiae* whole cell suspension and homogenate

Yeast alcohol dehydrogenases are tetrameric isoenzymes of a molecular mass of approximately 141kDa. As intracellular soluble proteins, they provide a suitable system for work involving recovery and purification operations of typical bioprocess unit operations. In addition, commercially available packed baker's yeast (*Saccharomyces cerevisiae)* provides a cheap and reproducible starting source material. Feeds were freshly prepared prior to each experiment. All chemicals were obtained from Sigma-Aldrich Ltd, Dorset, UK, unless otherwise stated.

4.4.1 *S. cerevisiae* suspension preparation

Packed baker's yeast (J.W. Pike Ltd., UK) was suspended in phosphate buffer (0.1M KH_2PO_4, pH 6.5) to give a final wet weight concentration of 50 g packed weight L^{-1}. For transmission studies, alcohol dehydrogenase (ADH) from *Saccharomyces cerevisiae* (≥300 units ADH/mg protein, catalogue number A3263, Sigma-Aldrich Ltd., UK) was added to the whole yeast cell suspension to give a final concentration of 200 units.L^{-1} feed.

To prepare the *S. cerevisiae* homogenate suspensions, packed baker's yeast (J.W. Pike Ltd., UK) was suspended in phosphate buffer (0.1M KH_2PO_4, pH 6.5) to give a wet weight concentration of 500g.L^{-1} packed weight and disrupted using a high pressure homogeniser (Manton-Gaulin Model Lab 60, APV, Crawley, Sussex) at 500barg for 5 discrete passes, resulting in at least 98% release of intracellular contents. The temperature of the suspension was maintained at 5-10°C during homogenisation using a glycol cooling system. The yeast homogenate concentration was then adjusted using phosphate buffer to a final wet weight concentration of 50g packed weight L^{-1}.

4.4.2 *S. cerevisiae* suspension analytical techniques

Feed, retentate and permeate samples were collected into eppendorf tubes, which were kept on ice. At the end of each experiment, the samples were spun down at 13 000rpm (~14 000g) for 10 minutes in a Microfuge™ 11 (Beckman, CA, USA) at room

temperature. The recovered supernatants were assayed for total soluble protein content and ADH activity as described below.

4.4.2.1 Total protein assay

Total protein concentrations were determined using the BIO-RAD protein assay (BIO-RAD Laboratories, Hemel Hempstead, Hertfordshire, U.K.). The assay is based on the colour change of a dye (Coomassie Brilliant Blue G-250 in acidic solution) when binding to protein occurs (Bradford, 1976). The dye-binding response to protein concentrations has been found to give an accurate but not entirely linear response. The dye reagent (BIO-RAD Laboratories, Hemel Hempstead, Hertfordshire, U.K.), supplied as a five-fold concentrate, was diluted using RO water.

50μL of sample and 2.5mL of diluted assay reagent were mixed in a cuvette and the absorbance at 595nm was recorded after 5 minutes in a DU® Spectrophotometer, (Beckman Instruments (UK) Ltd., High Wycombe, UK) and blanked against 2.5mL of reagent with 50 μL of RO water. For very dilute samples, or samples taken from scale-down experiments (≤25μg protein.mL^{-1}) a microassay procedure was followed. In this case 0.5mL of sample or standard was mixed with 0.5mL of assay reagent for protein concentration determination. Samples were diluted with phosphate buffer to produce a response ranging from 0.1 to 0.9 absorbance units and assayed in triplicate. The standard error in the assay was usually found to be less than 18%.

Protein concentrations were determined from a standard curve determined for each batch of dye reagent made. Bovine serum albumin (BSA), was used as the protein standard, for which a range of dilutions (0.2 - 1.0mg.mL^{-1} for the standard assays, 5-25μg.mL^{-1} for the microassays) were used.

4.4.2.2 Alcohol dehydrogenase activity

ADH activity was assayed using the method described by Bergmeyer (1983). The rate of reaction was measured spectrophotometrically by monitoring the change in

absorbance of the solution at 340 nm with ethanol as substrate. Nicotinamide-adenine dinucleotide (NAD^+) is reduced during the reaction:

$$\text{Ethanol} + NAD^+ \leftrightarrow \text{Acetaldehyde} + NADH + H^+$$

The enzymatic activity (E) expressed in units of activity per millilitre of solution, is given by equation 4.1.

$$E = \frac{1}{\varepsilon_{340}} \frac{\Delta A}{\Delta t} \frac{V_c}{V_s} D_N \qquad [4.1]$$

where ε_{340} is the extinction coefficient = $6.22 cm^2.\mu mol^{-1}$ and $\frac{\Delta A}{\Delta t}$ is the rate of change of absorbance at 340nm, V_s is the sample volume added to the cuvette, V_c is the total volume in the cuvette and D_N is the dilution factor.

The assay mix contained 0.18M NAD^+, 0.1M glutathione, 0.62M semicarbazide hydrochloride and 3.5% v/v ethanol (BDH, Merck Ltd., Dorset, U.K.). Samples were diluted using phosphate buffer (0.1M KH_2PO_4, pH 6.5) so that the maximum absorbance change was less than 0.7 absorbance units/min. 0.05mL of each sample was added to 3mL of assay mix; this small sample volume was also suitable for samples taken from scale-down experiments. The reaction was monitored for 60s and repeated in triplicate for analytical purposes. The standard error in the assay was usually found to be less than 12%.

4.5 *E. coli* lysate

Previous work at UCL studied the membrane filtration of a periplasmic Fab' antibody fragment expressed by *Escherichia coli* (Novais, 2001). To make use of this existing data, further experiments were conducted using pilot-scale and scale-down filtration rigs. All chemicals were obtained from Sigma-Aldrich Ltd, Dorset, UK, unless otherwise stated.

4.5.1 Bacterial strain and plasmid

The strain used in the fermentation was a wild type *E. coli* W3110 (ATCC 27325) transformed with the plasmid pAGP-4. The plasmid pAGP-4 encoded the chloramphenicol resistance gene (Cm) and the 4D5 Fab' antibody fragment directed against the extracellular domain of $p185^{HER2}$ and derived from HumAb4D5 (Carter et al., 1992). Coding sequences for the Fab' light chain and heavy chain Fd' fragment were arranged in a dicistronic operon under transcriptional control of the *E. coli tac* promoter inducible by addition of isopropyl-β-D-thiogalactopyranoside (IPTG) or lactose. Each antibody chain was preceded by the *E. coli omp A* signal sequence to direct secretion to the periplasmic space.

4.5.2 Fermentation and cell harvesting

A single 450L fermentation was carried out with defined medium. The protocol is described elsewhere in Novais (2001). The cells were harvested from the fermentation broth with a CARR P6 Powerfuge (CARR Separations Inc, Franklin, MA) at 17 000 rpm (19 000g) and at an operating flow rate of 60 Lhr^{-1}. Feed was pumped through the centrifuge using a Watson Marlow 605Di Peristaltic pump (Watson Marlow Ltd., Falmouth, UK). The cell paste was then frozen in 1kg lots and stored at –80°C.

4.5.3 Lysate preparation (periplasmic release)

Periplasmic extraction buffer was prepared by dissolving pre-weighed quantities of Tris[hydroxymethyl]aminomethane (Trizma Base) and Ethylendiaminetetra-acetic acid (EDTA) in water purified by reverse osmosis (RO water, 20-60μ.S.cm^{-1}) to a final concentration of 100mM and 10mM respectively. The pH was adjusted to 7.4 with HCl or H_3PO_4. Frozen *E. coli* cell paste was resuspended in periplasmic extraction buffer, which was preheated to 40°C, to a final concentration of 283g of cells (wet weight) per 2L of buffer (47g dcw.L^{-1}). After thorough mixing using a magnetic stirrer, the mixture was heated to 60°C for 3 hours in a LH Series 210 fermenter (LH Fermentation, Inceltech UK Ltd, Berkshire, UK) stirred at 300rpm. The resulting spheroplast suspension was then left to cool down to ambient temperature and used for filtration

experiments immediately or stored in a refrigerator for up to 2 days. This suspension is referred to as the lysate or feed in this thesis.

4.5.4 Fab' detection and quantification by ELISA

A microplate-based Enzyme-Linked Immunosorbent Assay (ELISA) was used as a means to quantify Fab' antibody fragment. As such small quantities of sample are required for this type of assay, it was suitable for experiments conducted at all scales of filtration. All chemicals were obtained from Sigma-Aldrich Ltd, Dorset, UK, unless otherwise stated.

4.5.4.1 Sample preparation

All feed, retentate and permeate samples were stored at –20°C until required. The impact of overnight freezing versus overnight storage at 4°C has been previously assessed for the lysate (Novais, 2001). The frozen sample did show a higher quantity of Fab' fragment, but the difference between the two measurements was 8%, less than the error of the ELISA assay (assay error ~11%, Bowering, 2000) and hence not deemed significant.

The samples were the thawed at room temperature prior to centrifugation at 13 000 rpm (~14 000 g) for 10 minutes in a Microfuge^{TM} 11 (Beckman, CA, USA). The supernatant was then diluted (usually 1:100) with PBS and analysed as described below.

4.5.4.2 ELISA analysis

NUNC 96 well maxisorp immunoplates (Life Technologies Ltd, Paisley, UK) were coated overnight at 4°C with HP6045 (a murine monoclonal antibody, Celltech Chiroscience Ltd) at a concentration of 2μg ml^{-1} in PBS. After 4 washes with PBS/Tween in a Columbus Plate Washer (Tecan UK Ltd, Reading, UK), purified Fab' standard (2 lanes), a blank of sample conjugate buffer (1 lane) and samples (9 lanes) appropriately diluted in sample conjugate buffer (usually 1 in 100) were added to the top row of the plate. A series of 1 in 2 serial dilution was performed on the plate with

100µl of sample conjugate buffer and the plate was covered with cling-film. It was then incubated for one hour on a 3-D rocking platform STR9 (Stuart Scientific, UK) at room temperature at 30rpm. The wash step was then repeated and 100µl of GD12 peroxidase (The Binding Site Ltd, Birmingham, UK) was added to each well in a dilution of 1 in 2000 of sample conjugate buffer. The plate was again incubated on a rocking platform in the same conditions as before for a further hour. Another wash step was carried out and 100µl of the substrate solution was added to each well. The absorbance at 630nm was recorded with a Titertek Multiskan PLUS MK II microplate reader (Flow Laboratories, High Wycombe, UK) after 5 to 7 minutes. The concentration of Fab' was determined from a standard curve prepared for each plate (see section 4.5.4.4).

4.5.4.3 ELISA buffers

PBS and PBS/Tween was made by dissolving pre-prepared sachets in 1L of RO water. The final pH was 7.1-7.3.

Sample conjugate buffer was prepared by dissolving 6.05g of tris amino-methane, 2.92g NaCl, 1g of casein and 0.1 mL of Tween-20 in 1L of RO water. The pH was adjusted to 7.0 with concentrated HCl and the solution was filtered with 0.22µm filter paper (Whatman, UK) before storage at 4°C.

The substrate solution was prepared immediately before use by adding 100µL TMB solution (10mgL^{-1} of 3,3',5,5'-tetramethylbenzidine) dissolved in dimethylsulphoxide, (DMSO) and 100µL of H_2O_2 (1 in 50 solution of 30% w/w H_2O_2 in RO water) to 10mL of acetate buffer (0.1M sodium acetate/citric buffer pH 6.0).

4.5.4.4 Production of Fab' standards

Purified 4D5 Fab' standards for the calibration of the ELISA assays were obtained from clarified periplasmic extracts of pre-harvested cell paste, using packed bed affinity protein A chromatography. The details of the procedures are given elsewhere (Novais 2001; Bowering 2000) and will therefore not be repeated here.

Purified Fab' was exchanged into a buffer of 100mM acetate pH5.5, containing 125mM sodium chloride and 0.02% sodium azide, for long term storage. The concentration of the resulting solution was determined from the absorbance at 280nm, using the Beer-Lambert equation

$$A_{280} = \varepsilon c l \qquad (4.2)$$

Where: A_{280} = absorbance at 280nm

ε = extinction coefficient = 1.43 for a 1 $mg.mL^{-1}$ solution (Bowering, 2000)

c = concentration ($mg.mL^{-1}$)

l = path length = 1cm

4.5.5 Diafiltration buffers

The diafiltration buffer was prepared by dissolving a pre-weighed amount of sodium chloride (Sigma Chemicals, UK) in RO water to a final concentration of 150mM. This buffer was adjusted to either pH 7.4 or pH 8.3 using a 1M sodium hydroxide solution (Sigma Chemicals, UK).

4.6 Mammalian cell fermentation broth

For reasons of commercial sensitivity, the details of this experimental system are not described here, as they are proprietary to Cambridge Antibody Technology Ltd (C*a*T). The fermentation broth used was a murine hybridoma culture expressing an antibody (MAb) which were stored for several days at 4°C i.e. zero cell viability. The broth was diluted further 1 in 2 with PBS as only small quantities were available for experimentation. The monoclonal antibody (Mab) product concentration was determined by a Protein A chromatography assay.

4.7 Summary

The above sections have outlined the protocols used to generate the results which are presented in the following chapters, beginning with verification of the TFF USD device with yeast-based feeds (Chapter 5).

Chapter 5 Verification of TFF USD Device with Yeast Suspensions

5.1 Introduction

Following the development of a novel device in Chapter 3 to mimic tangential flow filtration, the next step was to test the system using typical bioprocess feeds, and to compare the results with data obtained from conventional devices. Results are presented showing how data from the scale-down device (<50mL) correlates well with pilot-scale results (10L) for a range of representative bioprocess materials. It is demonstrated how typical tangential-flow microfiltration experiments can be conducted using greatly reduced quantities of feed. This work provided the necessary precursor to industrial verification trials undertaken in collaboration with Cambridge Antibody Technology Ltd, which is reported in Chapter 7.

Successful scale-down of any unit operation depends on the availability of relevant material for study i.e. material that is representative of the preceding operation at process scale conditions. Large-scale equipment will probably never perform as well as its ideal laboratory counterpart due to changes in time constants, mode of operation and shear, despite innovative improvements made by manufacturers (Boychyn et al., 2000).

The rotating disk device developed in this study offers the opportunity to account independently for shear degradation during filtration as shear is decoupled from the recirculation rate; during the TFF of fermentation broths, shear stresses often cause damage to cells/proteins, or cause aggregation. Shear effects are often ignored in the control and optimisation of filtration processes, although they may influence the filtration behaviour (Shimizu et al., 1993). Such investigations were not carried out here, as yeast cells and yeast homogenate feeds are relatively shear insensitive c.f. other bioprocess streams, and neither cell lysis, nor product damage have been observed in conventional bioprocess equipment (Lee et al., 1995; Okec, 1998).

This chapter describes the work carried out to compare the performance of the TFF USD and commercially available cassettes operating under similar conditions, using common bioprocess feeds (*S. cerevisiae* suspensions), and evaluate the models

described in Chapter 2. The first section describes the estimation of wall shear rates in a conventional flat-sheet device, as non-linear scaling of TFF requires that the shear rate at the membrane surface be maintained (see Chapter 3). The filtration systems, materials and experimental methods used are described in detail in Chapters 3 and 4. Flux data will be presented as units of LMH ($L.m^{-2}.h^{-1}$). Although these are not strictly S.I. units, they are the industry standard, and are almost universally employed in the literature.

5.2 Estimation of wall shear in a filtration cassette

Scaling of membrane filtration unit operations, whether scaling linearly or non-linearly requires keeping shear at the membrane surface (wall shear) constant (Brose et al., 1995, van Reis et al., 1997). Hence, in order to scale up or down, or change membrane module type, it is necessary to calculate the shear rates generated in manufacturing scale equipment, at the desired operating conditions. The following section describes a method to estimate these values for a Pellicon 2 mini, V-screen, cassette (Millipore, USA). This was the conventional device chosen to compare the TFF USD device against.

A typical membrane filtration cassette comprises of a stack of rectangular membranes arranged in pairs in which two discrete systems of flow passages are provided for conducting liquids along opposite surfaces of each membrane; that is to say, a first system for conducting feed liquid or retentate, and a second system for conducting permeate. The longitudinal edge portions of adjoining membranes of each two successive pairs are bound together in a cured binder along the entire length of the edges such that a fluid tight seal is formed between these adjoining membranes in a marginal zone behind these edges. The construction of commercially available devices is proprietary to the manufacturer, and therefore precise details of cassette construction are not readily available in the public domain. This is a major obstacle to the definitive characterisation of such devices and necessitates the use of approximate methods.

The Pellicon 2 mini module has a membrane area of $0.1m^2$ incorporated within a rectangular cassette. Mass transfer is enhanced by the presence of a net-like turbulence promoter (V-screen), also called a spacer, which is inserted between each membrane

fold. The V-screen is an open-channel spacer suitable for high viscosity feeds and high product concentrations. Freudenberg™ borders (non-woven support substrate) provide a gap in the feed channel, minimising the potential intrusion of the screen into the membrane (C. Christy, Millipore Corporation, personal communication, 2001). The membrane unit is encased in a rigid end-cap, to provide sealing compatibility with the associated filter holder hardware. A schematic of the cross-section of the cassette is illustrated in Figure 5.1.

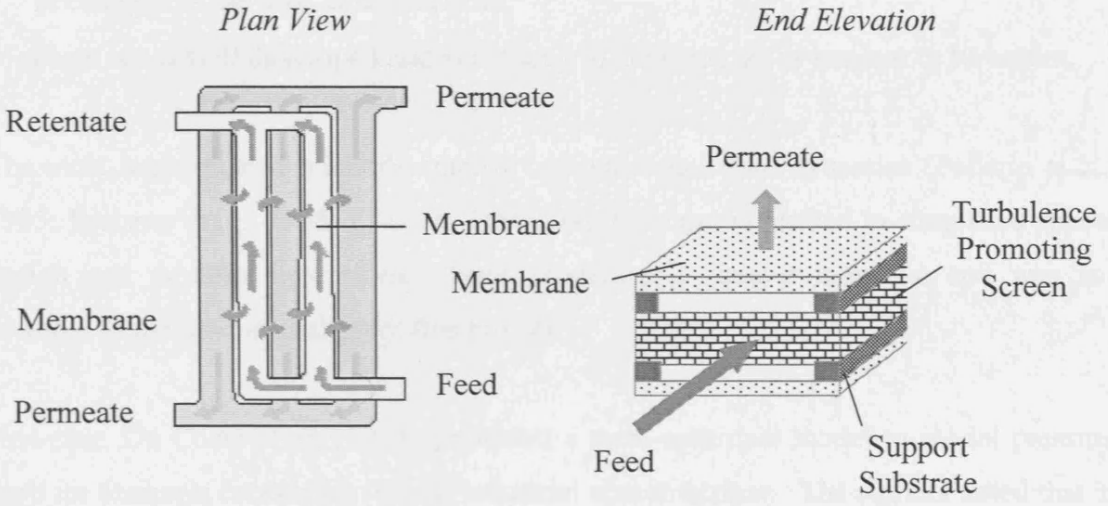

Figure 5.1: Schematic of the feed channel of a Pellicon 2 mini, V-screen, cassette.

Due to the complex geometry, calculation of the wall shear rate is not a trivial matter, although some attempts have been made in the literature. Current methods include:

- Pressure drop calculations (Da Costa et al., 1994);
- Computational fluid dynamics (CFD) (Serra et al., 1995; Li et al., 2004);
- Biological probes: insect cells, mammalian cells (Vandanjon et al., 1999; Kelly et al., 2004).

The most common approach is to correlate shear rate to pressure losses along the channel length, or transcartridge pressure drop (ΔP_{tc}). The simplest method is to consider the filtration channel as a rectangular duct. Many authors have used the following equation to estimate wall shear based on the calculated open channel dimensions (Patel et al., 1987; Lee et al., 1995; Parnham and Davis, 1995):

$$\tau_w = \frac{6u}{b} \qquad [5.1]$$

where u is the feed velocity and b is the effective channel height (based on the pressure drop within the feed channel). The pressure drop of the device is determined experimentally. Such calculations are complicated by the following factors:

- Only part of the pressure losses are due to friction at the wall.
- The presence of a screen affects the effective channel width and cross-sectional area.
- The channels in all screened devices are subject to some slight deformation resulting in changes in the flow characteristics.
- Flow is not well developed and is difficult to characterize as laminar or turbulent.

The most sophisticated methods employ computational fluid dynamics (Pellerin et al., 1995; Weisner et al., 1998; Li et al., 2002), but their use is limited to simplified spacer design and module dimensions. Such modelling is labour intensive and was not possible in the time available for this project.

However, Da Costa et al. (1994) presented a semi-empirical model to model pressure drop for channels containing several industrial spacer designs. The authors noted that in spacer-filled channels, the transcartridge pressure drop is not all due to frictional losses at the walls. Viscous drag and form drag due to the spacer and kinetic losses due to directional flow change also contribute to pressure losses along the length of the cassette. According to their estimations of pressure drop components (Da Costa et al., 1994), viscous drag on the channel walls (ΔP_f) contributed approximately 2 to 7 % of the pressure drop (depending on spacer type and fluid velocity) e.g. for feed velocities around $1 ms^{-1}$.

$$\Delta P_f = 0.07 \Delta P_{tc} \qquad [5.2]$$

Nevertheless, equation [5.2] may give a conservative estimate as Karode and Kumar (2001) suggest that the relative contribution of the pressure drop terms used by Da Costa et al. (1994) may not have been correct, even though overall channel pressure drop was successfully determined.

Hence, a rough value for wall shear rate may be estimated by determining transcartridge pressure drop, although caution is advised in the use of such approximate values to

equate flux performance between devices. Actual testing will always be required when employing this method.

As suggested above, another approach to estimate the shear rates encountered in a complex geometry is to use a biological probe (Vandanjon et al., 1999; Kelly et al., 2004). This idea is explored further in Chapter 9. Nevertheless, again only an approximate range of the shear rate in the cassette can be estimated using this method.

5.2.1 Calculation of hydraulic mean diameter

Most pressure drop equations are derived for circular pipes. For turbulent flow in a duct of non-circular cross-section, the *hydraulic mean diameter* (d_H) may be used in place of the pipe diameter and the formulae for circular pipes can then be applied without introducing a large error (Coulson and Richardson, 1990). This method of approach is entirely empirical. The parameter d_H is generally defined by:

$$d_H = \frac{4 \times \text{cross-section of the flow channel}}{\text{wetted circumference}} \qquad [5.3]$$

For a rectangular channel of height h, and width w, this becomes

$$d_H = \frac{2hw}{h+w} \qquad [5.4]$$

However, for laminar flow this method is not applicable, and exact expressions relating the pressure drop to the velocity can be obtained for ducts of certain shapes only. Hence, the Reynolds number should be checked using equation [5.5]

$$\mathrm{Re} = \frac{\rho u d_H}{\mu} \qquad \mathrm{Re}>2000 \text{ for transition or turbulent flow} \qquad [5.5]$$

Newer definitions of hydraulic diameters for turbulence promoter are available in the literature but they have been developed for specific types of spacer geometry e.g. circular rods (Zimmerer and Kottke, 1996).

Table 5.10 lists the dimensions used in the calculations for the Pellicon 2 mini cassette.

	inches	*m*
Channel height (h)	0.03	0.000762
Channel width (w)	1.2	0.03048
Channel length (l)	6	0.1524
Area available for crossflow (m^2)		*2.32×10^{-5}*

Table 5.1: Pellicon 2 mini cassette dimensions (C. Christy, Millipore Corporation France, personal communication).

Using this information and equation [5.4], the value of d_H = 0.0015m for the Pellicon 2 mini cassette was calculated and used in the analysis below.

5.2.2 Experimental determination of wall shear rate

Supposing a fluid is flowing through a circular pipe of length l and radius r (diameter d) over which the change in pressure due to friction is ΔP_f, then a force balance on the fluid in the pipe gives (Coulson and Richardson, 1990):

$$-\Delta P_f \pi r^2 = 2\pi r l(-\tau_w)$$

$$\text{or } \tau_w = \Delta P_f \frac{r}{2l} = \Delta P_f \frac{d}{4l} \qquad [5.6]$$

where τ_w is the wall shear stress.

Replacing d with d_H gives the following equation for a rectangular geometry:

$$\tau_w = \Delta P_f \frac{d_H}{4l} \qquad [5.7]$$

So from equation [5.4] this becomes

$$\tau_w = \Delta P_f \frac{(hw)}{2l(h+w)} \qquad [5.8]$$

Shear stress (τ) and shear rate (γ) are related by the following equation

$$\gamma = \frac{\tau}{\mu} \qquad [5.9]$$

where μ is the fluid dynamic viscosity.

There are correlations for estimating pressure drop when the fluid velocity is known, but for a complex and unknown geometry, such as the Pellicon 2 mini cassette, experimental determination of pressure drop on the retentate side of the cassette is required. Thus, the wall shear rate can be estimated.

De-ionised water was recirculated through the cassette at different flow rates, and the inlet, outlet and permeate pressures were recorded. The Proflux M12 filtration rig was employed, details of which are give in Chapter 4. During operation, the permeate port was closed so that the transmembrane pressure was zero i.e. fluid flow was only along the cartridge. Table 5.2 gives the measured values of pressure drop and the calculated wall shear rate in the Pellicon 2 mini cassette at the conditions tested.

The wall shear rate values in Table 5.2 compare well with those estimated by CFD modelling of a spacer filled channel (Karode and Kumar, 2001). Shear rates at the channel faces for several spacers at an inlet velocity of $1ms^{-1}$ were between 100 and $7000s^{-1}$. However, it should be noted that the flow at these feed velocities are not turbulent (Re<2000) so it may not be valid to use the mean hydraulic diameter substitution. As a result, such an approximate calculation of wall shear rate cannot be relied upon to equate flux performance between devices; experimental validation is required.

Flowrate ($L.h^{-1}$)	**velocity ($m.s^{-1}$)**	**Reynolds number**	**TMP (kPa)**	**γ_w (s^{-1})**
31.8	0.38	271	21	3210
49.8	0.60	424	28	4281
76.2	0.91	649	34	5351
105	1.26	895	48	7491
139.2	1.66	1186	62	9631

Table 5.2: Experimentally estimated wall shear rates in the Pellicon 2 mini cassette.

The empirical approach finally used was to infer the wall shear rate values of the cassette from comparative data produced by the TFF USD device. Flux (J) versus

transmembrane pressure (TMP) (excursion curves), were generated with the conventional TFF device, and similar plots were generated with the TFF USD by at a selected rotating disk speed. The determination of the shear at the membrane in the TFF USD is somewhat easier (see Chapter 3), and if filtration performance is identical, then it should be reasonable to assume that the wall shear rate is equivalent i.e. the effective global shear rate in the cassette can be estimated.

5.3 Transmembrane pressure correlation constants

The key driving force of a filtration is the transmembrane pressure (TMP). This is defined as the differential between the average global pressure on the retentate side and the pressure on the permeate side (see equation [2.4], Chapter 2).

$$TMP = \frac{P_{INLET} - P_{OUTLET}}{2} - P_{PERMEATE} \qquad [5.10]$$

In order for a scale-down device to mimic larger equipment, one would expect it to be able to generate similar TMP values i.e. to achieve a target flux value the same TMP would be required. However, this may not be the case, especially for a non-geometric scale-down device such as the TFF USD. The reasons for this are considered below.

Pressure gradients along the cassette

The operation of conventional flat-sheet cassette filtration involves a dynamic relationship between feed recirculation rate, the resultant retentate side pressure drop and flow patterns on both side of the membrane. This generates a gradient of pressures along the length of the cassette, but the industry standard is to calculate TMP as the average of the inlet and outlet pressures on each side of the membrane (see equation [5.10]). Although co-current flow was used to minimise the TMP gradient along the cassette (see Chapter 2), there will be local variations of TMP depending on the position along the channel.

The TFF USD device decouples the wall shear rate from the feed recirculation rate, and has much simpler flow patterns (see Chapter 3). Consequently, the TFF USD device operation can only aim to mimic the average, global filtration behaviour of a cassette device.

Differences in membrane hydraulic resistance

Normalised water permeability (NWP), is the established method used to determine the resistance of the membrane to fluid flow, as well as for assessing the cleanliness of a cassette. This method involves measuring the passage of clean water through the membrane under standard pressure and temperature conditions. NWP is calculated by:

$$NWP = \frac{R * F}{A * TMP} = \frac{J * F}{TMP} \qquad [5.11]$$

where R is the water flux through clean membrane ($L.h^{-1}$), F is a temperature correction factor (= 1 at 25°C), A is the membrane area (m^2), and TMP is the transmembrane pressure (kPa). By measuring NWP over a range of TMP values, a plot of flux versus pressure drop data can be obtained. Linear regression of the data gives the hydraulic permeability (the reciprocal of which is the membrane resistance).

Chandler and Zydney (2004) calculated hydraulic resistance (from NWP measurements) using a variety of membranes in different NFF formats a pleated XL-2 capsule (Millipore, MA, USA), membrane disks, 96-well plates and syringe filters. The resistance values differed significantly between the devices, despite them containing similar membranes (same material of construction and pore size). The resistance of the pleated XL-2 capsule was significantly greater than that obtained with the other formats. This increase in resistance was suggested to be due to parasitic pressure losses in the entrance or exit to the capsule in combination with the pressure losses and/or to a loss of effective membrane area associated with flow between the membrane pleats.

Experimental data obtained with small circular disks cut from the membranes contained within the XL-2 module and then placed in a 25mm stirred cell, were in much better agreement with the data for the flat-sheet membranes, although these values were still about 30% smaller than the water flux evaluated in the other formats. The reason for this discrepancy may have reflected an unusually large resistance to flow for the particular lot of membrane used in the XL-2 capsule examined in the study, or it could have been associated with the stresses on the membrane caused by the pleating operation.

The Pellicon 2 device format has a few factors that increase the apparent hydraulic membrane resistance. Firstly, there is a screen (turbulence promoter) in the feed channel of the device (see Figure 5.1); the screen actually blocks off a fraction of the membrane area, typically 25-50%. The second factor is the permeate channel restriction; the permeate channel is limited in height so it causes a pressure drop due to flow restriction, also increasing the measured resistance. Hence, the calculated membrane resistance of the coupon held in the TFF USD device should be much lower than that of the membrane within the cassette device. Consequently, the effect of the apparent hydraulic membrane resistance is examined below.

However, the actual membrane permeability is not exploited in bioprocess TFF applications (D. LaCasse, Millipore Corporation USA, personal communication, 2004), as it is the concentration polarisation (or gel) layer that is the main barrier to filtration (Balakrishnan et al., 1993). Thus, the effect of the discrepancy in the water permeability on the overall scaling strategy is not expected to affect transmission or flux trends, but would affect the observed TMP values from each device. The measured TMP data from cassette filtration would be proportionally higher than TFF USD TMP data, for equivalent flux rates, in the pressure dependent regime. This is to say, at sub-critical flux values, where the relationship between flux (J) and TMP should be similar to the pure solute fluxes (Porter, 1977; Cheryan, 1986), the TFF USD TMP data would have to be multiplied by the ratio of the hydraulic resistance values.

Figures 5.2 shows water permeability data obtained with a Pellicon 2-mini cassette and a membrane coupon of the same membrane material held in the TFF USD device (see Chapter 4 for the experimental protocol). Linear regression of the data gives the hydraulic resistance of each membrane. For the Pellicon 2 mini cassette $R_{m,cassette}$ = 0.09LMH.kPa^{-1} (3.24 x 10^{-9}m^{-1}), and for the TFF USD membrane coupon, $R_{m,TFFUSD}$ = 0.007LMH.kPa^{-1} (2.52 x 10^{-10}m^{-1}).

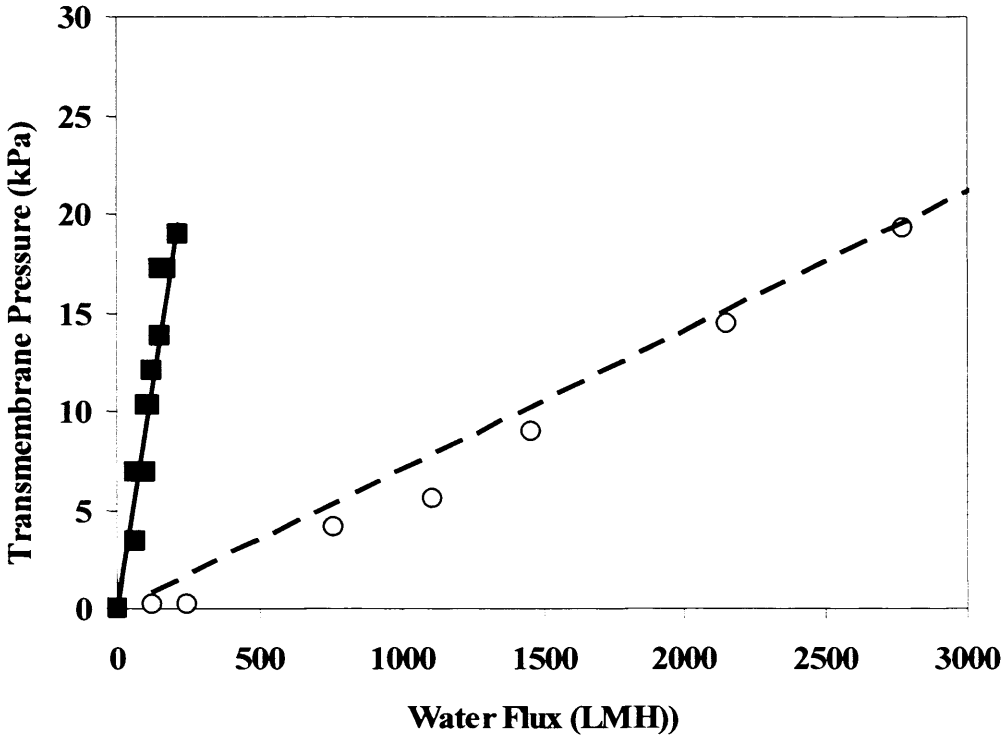

Figure 5.2: Determination of hydraulic membrane resistances for 0.65μm hydrophilic Durapore membranes (Millipore, MA, USA) in a Pellicon 2-mini v-screen cassette (■), and membrane coupons of the same material held in the TFF USD device (○). Linear regression lines give $R_{m.cassette}$ *(———) = 0.09LMH.kPa*$^{-1}$ *(correlation coefficient* R^2 *= 0.93) and* $R_{m.TFFUSD}$ *(- - -) = 0.007LMH.kPa*$^{-1}$ *(*R^2 *= 0.98).*

System pressure

The complex geometry of a filtration cassette and the position of the pressure measuring instruments contribute to the measured TMP value. These include pressure losses that occur in the inlet and outlet pipework, cassette holder, entrance and exits within the cassette, and within the narrow cassette channels. The contribution of these components are difficult to quantify and pinpoint precisely, but combined can dramatically affect the measured TMP of the cassette device. The measured TMP ($TMP_{observed}$) in a cassette format is expected to be much higher than the real TMP (TMP_{actual}) that the membrane is exposed to (D. LaCasse, Millipore Corporation USA, , 2004 communication).

This phenomenon is apparent at the start of a filtration when the flux rate is zero (i.e. the permeate valve is shut, t = 0), there is a measurable TMP value. This is the pressure

required purely to recirculate the feed around the retentate side of the filter, without necessarily providing any driving force for filtration (TMP). This value is expected to be much greater for the complex cassette geometry, than for the relatively simple TFF USD device. In order to compare TMP data from both scales, it would be necessary to also account for this difference.

In light of the above discussion, even though flux values can be equated between the two devices, the same will not hold true for TMP values. For comparison of TFF USD TMP values with those obtained from the pilot-scale equipment, compensation for the constant difference in system pressure ($k_{TMP,t=0}$) and the ratio of the hydraulic permeabilities (k_{Rm}) is required i.e.

$$TMP_{cassette} \approx TMP'_{TFFUSD} = (TMP_{TFFUSD} * k_{Rm}) + k_{TMP,t=0} \quad [5.12]$$

where

$$k_{TMP,t=0} = (TMP_{cassette,t=0} - TMP_{TFFUSD,t=0}) \quad [5.13]$$

and

$$k_{Rm} = \frac{Rm_{cassette}}{Rm_{TFFUSD}} \quad [5.14]$$

in order to equate the TMP values.

5.4 *Saccharomyces cerevisiae* whole cell suspension trials

This work is represented by the pilot-scale verification box in Figure 1.7 (see Chapter 1). The aim of these experiments was to compare and contrast filtration performance between a Pellicon 2-mini cassette (Millipore, USA) and the TFF USD device. To present a valid comparison to conventional filtration, the scale-down TFF device needs to demonstrate comparable filtration in terms of concentration polarisation/fouling behaviour, and therefore separation performance in terms of permeate flux and component transmission or rejection.

In order to test the scale-down device, it was important to use a relatively simple, but relevant bioprocess feed stream; a *Saccharomyces cerevisiae* whole cell suspension was selected as a "model" system; the feed is generally reproducible and fouling should be negligible, allowing for easier cleaning and regeneration of the membrane. Also, the system is well documented in the literature and relatively high flux values (50 to 100LMH) were expected, which facilitated measurement on the small scale.

Transmission of a target molecule is just as important as flux behaviour in bioprocesses, as it is often the product of interest. To study this aspect of filtration, the whole cell suspension was spiked with ADH (see Chapter 4), so transmission data could be compared by taking permeate samples at fixed time intervals.

It is important to state that the aim of the comparative experiments was to show whether or not the TFF USD device was capable of mimicking the overall filtration behaviour of the conventional device during typical filtration process development experiments.

5.4.1 Determination of disk rotation speed, recirculation rate and feed volume for the TFF USD device

The TFF USD rig was operated as a conventional rig, where feed flow rate and retentate backpressure are used to control the TMP. In order to make a fair comparison between the devices, the filtration hydrodynamic conditions must be kept similar i.e. wall shear (see section 5.2), recirculation rate and membrane loading (see Chapter 1).

Wall shear rate is decoupled from tangential flowrate in a rotating disk filter; it is the rotating disk that generates the shear at the membrane wall (Vogel et al., 1999). As discussed in Chapter 3, previous studies have suggested that a rotating disk device could mimic a cassette filter, and that there was a critical rotational speed below which behaviour was comparable to that of a flat sheet system, at a given membrane loading level (Lee et al., 1995). The approach taken to identify this TFF USD device disk rotation speed was to operate it at a permeate flux that matched the critical flux point determined at pilot-scale and incrementally decrease the rotation speed until the TMP became unstable i.e. use the wall shear rate as the variable parameter.

However, confirmatory experiments are required to show that the TFF USD device at operated at the selected disk speed is indeed able to mimic the conventional technology during typical filtration experiments e.g. critical flux determination (see below), concentration, and diafiltration (see Chapter 6), before applying the inferred wall shear rate from the TFF USD device, to the conventional filter.

The feed (retentate recirculation) flow rate ($Q_{cassette}$) for the $0.1m^2$ pilot scale device was set at $60L.h^{-1}$, based on the rule of thumb that recirculation rate is usually 6 to $10L.min^{-1}.ft^2$ for bioprocess applications (R. Kuriyel, Millipore Corporation USA, personal communication, 2002). The equivalent flow rate to the pilot scale filter was calculated using the same rule, giving $Q_{TFFUSD} = 0.21L.h^{-1}$. Although this would not generate the equivalent wall shear rate at the surface of the membrane (due to the device geometry), this at least ensured the same feed frequency through the filtration rig i.e. the same number of passes, which may be of importance if trying to reproduce any degradation with shear encountered in the rig.

Finally, the feed loading was also kept the same ($100L.m^{-2}$) during any experiments that were not operated in recycle mode. Each circular 25mm disk held in the TFF USD device had an effective area of $3.46x10^{-3}m^2$ (see Chapter 3) therefore 0.35L of feed was used for each scale-down experiment, c.f. 10L for the pilot-scale experiments.

5.4.2 Results: *S. cerevisiae* whole cell suspension

The following section describe the flux and transmission results obtained during constant feed concentration (permeate recycle) conditions. Full details of the materials and methods for the experiments are given in Chapter 4.

5.4.2.1 Determination of critical flux

The first parameter chosen for the comparison of the two filtration devices was the value for critical flux (see Chapter 1), as this is key information of interest for filtration scale-up. Critical flux is defined as the mean flux (i.e. the permeate flux observed) for which the first deposit appears on the membrane (Field et al., 1995). Such a critical flux corresponds to a transition from concentration polarisation to cake formation (Chen et

al., 1997), or a transition from reversible to irreversible fouling (Defrance and Jaffrin, 1999). The fouling threshold can be studied with a "stepping" flux experiment (Chen, 1998) and can be detected when the TMP starts increasing at a fixed imposed flux. This indicates that irreversible deposition has occurred. The determination of critical flux is required to determine the optimal operating conditions of a TFF process.

Figure 5.3 below shows the results of a flux-stepping experiment obtained to determine the critical flux region for a *S. cerevisiae* cell suspension, spiked with alcohol dehydrogenase (ADH), using the conventional pilot-scale rig (see Chapter 4 for protocol).

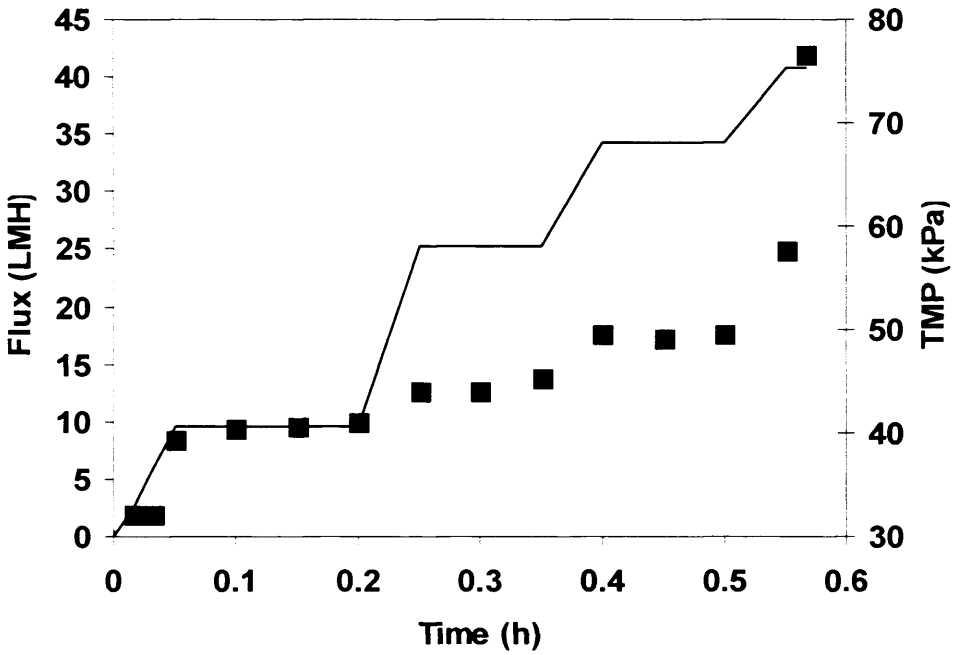

Figure 5.3: Relationship between flux rate (—) and TMP for Pellicon 2-mini v-screen cassette, feed recirculation rate 60L.h^{-1} (■). Critical flux determination with 50g.dcw.L^{-1} S. cerevisiae whole cell suspension, spiked with 30U.mL^{-1} ADH. 0.65μm hydrophilic Durapore membrane (Millipore, MA, USA). Total permeate recycle.

The data shows that the TMP values became unstable at a flux value of 35-40LMH i.e. the critical flux region was identified. In order to determine the equivalent TFF USD disk rotation speed, an experiment was conducted operating it at this flux value, and gradually lowering the disk rotation speed, to identify the corresponding critical wall shear rate. This data is presented in Figure 5.4, and identifies that the TMP behaviour

became unstable at a rotational speed of 500rpm. Also worth noting is the corresponding TMP values generated by the TFF USD device, which are an order of magnitude lower that those obtained using the cassette device, under similar filtration conditions.

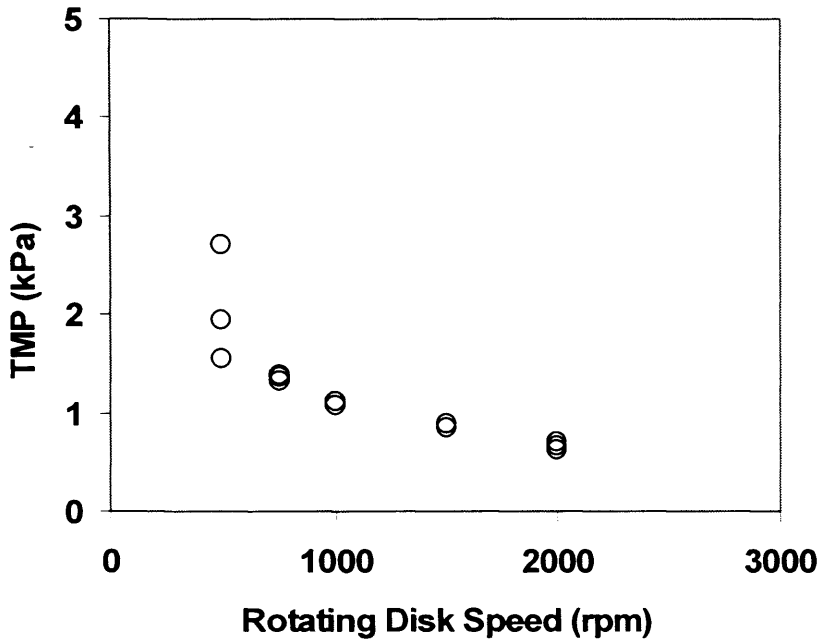

Figure 5.4: Relationship between TFF USD disk rotation speed and TMP, at permeate flux 40LMH, feed recirculation rate 0.21L.h^{-1} (O). Critical wall shear rate determination with 50g.dcw.L^{-1} S. cerevisiae whole cell suspension, spiked with 30U.mL^{-1} ADH. 0.65μm hydrophilic Durapore membrane (Millipore, MA, USA). Total permeate recycle.

Figure 5.5 shows results from a flux-stepping experiment using the TFF USD device at a disk rotation speed of 500rpm, to confirm whether or not this disk rotation speed generated the equivalent filtration behaviour as the conventional cassette device, in terms of critical flux determination. The results identify the critical flux region as being between 35 and 40LMH, which is identical to the values determined from the equivalent cassette data. This supports the hypothesis that a rotating disk device can produce similar filtration behaviour to that of a flat-sheet device (see Chapter 3).

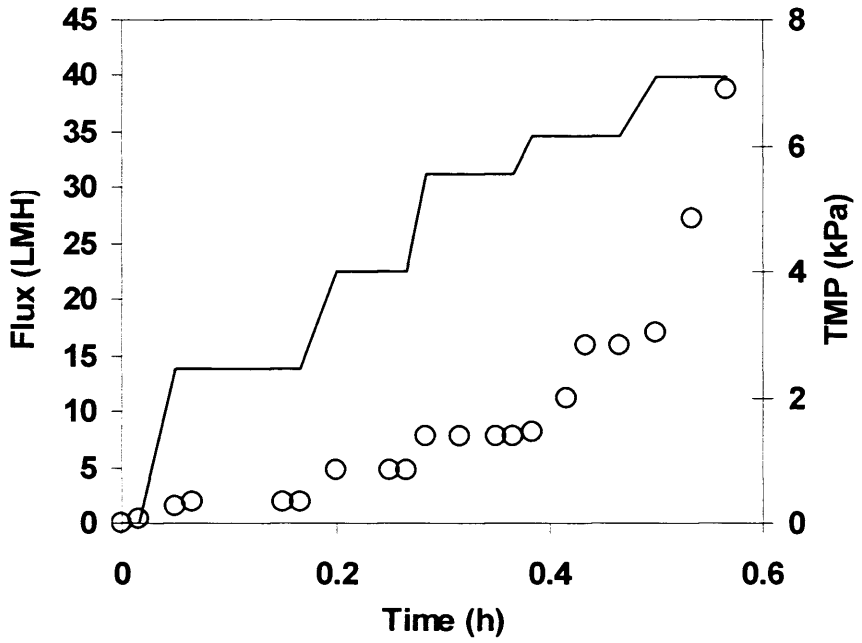

Figure 5.5: Relationship between flux rate (—) and TMP for a 25mm membrane coupon held in the TFF USD device, feed recirculation rate 0.21L.h^{-1}, disk rotation 500rpm (O). Critical flux determination with 50g.dcw.L^{-1} S. cerevisiae whole cell suspension, spiked with 30U.mL^{-1} ADH. 0.65μm hydrophilic Durapore membrane (Millipore, MA, USA). Total permeate recycle.

Despite the critical flux regions being almost identical, the TMP values obtained at similar imposed flux values are an order of magnitude different, as predicted in Section 5.3. Figure 5.6 show a comparison of the data shown in Figures 5.3 and 5.5, in terms of J versus TMP data (excursion curves). However, the TFF USD data has been corrected (TMP'_{TFFUSD}) to account for the TMP compensation constants (see equation [5.12]) using the following parameters: $TMP_{cassette,\ t=0}$ = 32kPa (see Figure 5.3), $TMP_{TFFUSD,\ t=0}$ = 0.01kPa (see Figure 5.5), $Rm_{cassette}$ = 0.1LMH.kPa^{-1} (see Figure 5.1), Rm_{TFFUSD}= 0.07 LMH.kPa^{-1} (see Figure 5.1).

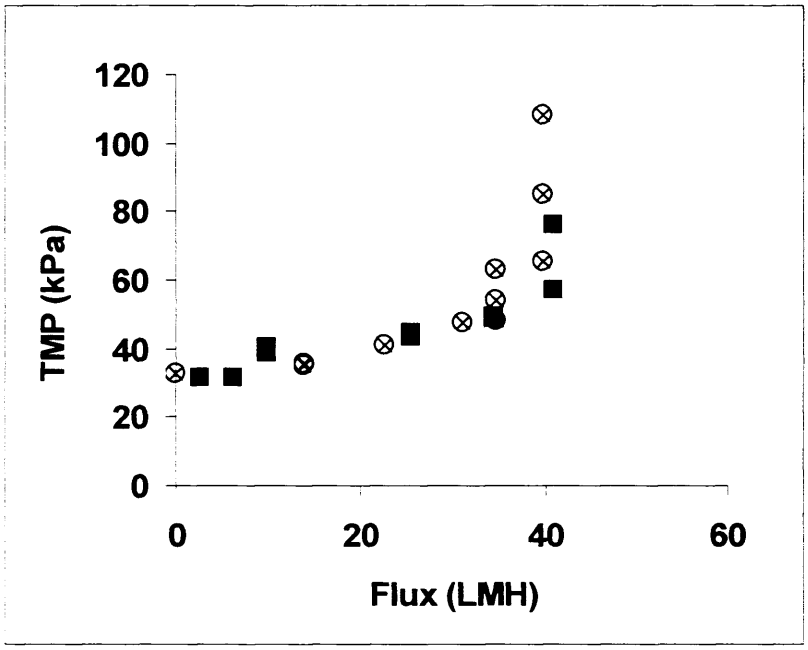

Figure 5.6: Comparison of excursion curves obtained with a Pellicon 2-mini v-screen cassette, feed recirculation rate 60L.h^{-1} (■), and a 25mm membrane coupon held in the TFF USD device, feed recirculation rate 0.21L.h^{-1}, disk rotation 500rpm (⊗). Total permeate recycle filtration of 50g.dcw.L^{-1} S. cerevisiae whole cell suspension, spiked with 30U.mL^{-1} ADH. 0.65μm hydrophilic Durapore membrane (Millipore, MA, USA). TFF USD data corrected for differences in initial system TMP ($k_{TMP,\ t=0}$ =32kPa) and hydraulic permeability (k_{Rm} =12.82) using equation [5.12].

The similarity of the filtration data supports the idea that the TFF USD device can mimic the cassette filtration behaviour, in terms of flux and TMP, albeit compensated to account for initial system pressures.

As an aside, the wall shear rate generated in the pilot scale device can be estimated, as it should be identical to that of the TFF USD device, if the filtration behaviour is identical. The calculated wall shear rate in the TFF USD device at 500rpm was 528s^{-1} (equation [3.4], see Chapter 3), and so it is this value that could be used for scale-up or modelling purposes (see Section 5.6).

5.4.2.2 Comparison of filtration behaviour at constant operation conditions

To confirm that cassette filtration behaviour can be truly mimicked by the TFF USD device, filtration experiments at stable operating conditions (total permeate recycle, sub-critical flux) were performed at both scales. This mode of operation is useful for process characterisation since it maintains the same feed conditions throughout the process.

Figure 5.7 shows TMP behaviour during a total permeate recycle experiment conducted at 20LMH (sub-critical flux, where an actual process may be operated) at both scales. Data is shown for TFF USD experiments where permeate samples were and were not taken for transmission studies, to assess the impact of sampling, which may be of concern at the USD scale (see Chapter 3).

The data shows that TMP at both scales initially increases, as concentration polarisation occurs (Cheryan 1986) reaching a steady value after a stabilisation period (Defrance and Jaffrin, 1999). The stabilisation period is longer for the cassette data, perhaps due to the complex flow paths within the cassette. This confirms that 20LMH is a stable operating condition at both scales (as predicted by the critical flux experiments discussed above). The stabilised TMP values are also similar to those obtained during the flux stepping experiments in Figure 5.3 giving confidence that the filtration is repeatable at both scales.

Comparison of the TFF USD data values from experiments where samples (50μL aliquots) were and were not taken for transmission studies shows that the sampling regime had no significant impact on the filtration behaviour. Ten samples were taken in total, accounting for less than 1.5% of the total feed volume of 0.035L (see section 5.4.1). The ADH transmission during the constant flux experiments shown in Figure 5.7 is presented in Figure 5.8.

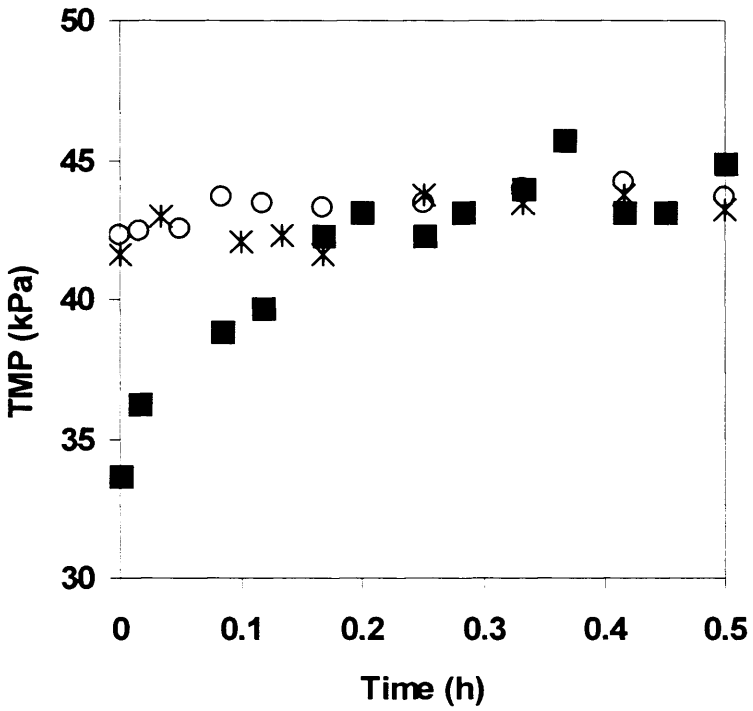

Figure 5.7: TMP behaviour during constant flux filtration at 20LMH. Pellicon 2-mini v-screen cassette, recirculation rate 60L.h^{-1}, with permeate samples taken for offline analyses (■), and a 25mm membrane coupon held in the TFF USD device, recirculation rate 0.21L.h^{-1}, disk rotation 500rpm, with permeate samples taken (O), and without (✳). 50gL^{-1} S. cerevisiae, whole cell suspension, spiked with 30U.mL^{-1} ADH. 0.65μm hydrophilic Durapore membrane (Millipore, MA, USA). Total permeate recycle. Feed to membrane area ratio 100L.m^{-2}. TFF USD data corrected for differences in initial system TMP ($k_{TMP,\ t=0}$ =32kPa) and hydraulic permeability (k_{Rm} =12.82) using equation [5.12].

The transmission level began at 100%, as was expected for the relatively large pore membrane used (c.f. ADH molecule size). However, once stable operating conditions had been reached only around 80% of the ADH permeated through the membrane, as the *S. cerevisiae* cells had formed a concentration polarisation cake layer (see Chapter 2) and perhaps also adsorbed to the membrane (Hanemaaijer et al., 1989). Again, the data from the two devices correlates well, supporting the hypothesis that the pilot-scale device filtration performance can be mimicked by the TFF USD device.

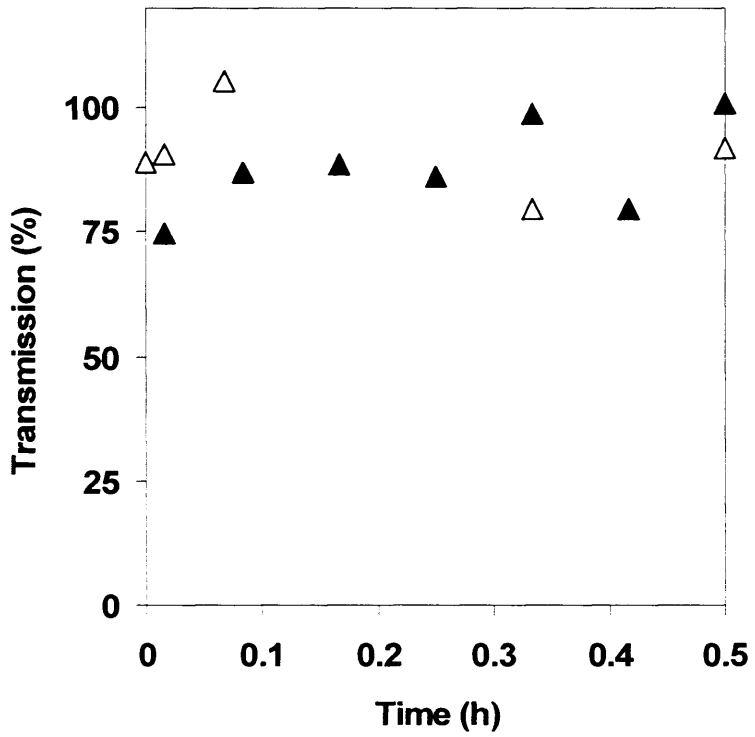

Figure 5.8: Assessment of ADH transmission during constant flux operation at 20LMH, Pellicon 2-mini v-screen cassette, recirculation rate 60L.h^{-1}(▲), and a 25mm membrane coupon held in the TFF USD device, recirculation rate 0.21L.h^{-1}, disk rotation 500rpm (Δ). 50gdcw.L^{-1} S. cerevisiae, whole cell suspension, spiked with 30U.mL^{-1} ADH. 0.65μm hydrophilic Durapore membrane (Millipore, MA, USA). Total permeate recycle. Feed to membrane area ratio 100L.m^{-2}.

Each experiment took the same time to complete, but only a fraction of the feed material was required to obtain the key results with the TFF USD device (see Chapters 1 and 3).

5.5 *S. cerevisiae* homogenate trials

Following the promising results obtained with the *S. cerevisiae* whole cell feed, a *S. cerevisiae* homogenate (details are given in Chapter 4) was also chosen to test the device with a multicomponent feed stream, which would intrinsically capture all of the possible effects of multiple complex contaminant interactions on filtration performance. Such interactions are critical since they will ultimately determine the effectiveness of any large-scale separation (van Reis et al., 1997).

The same series of experiments conducted for the whole cell suspension were repeated for the homogenate using a 1000kDa Biomax membrane, and the data presented in Figures 5.9 to 5.14 below. This membrane material was selected because of the manufacturer's claim of ultra low protein adsorbancy (Millipore Technical Data Sheet - PF1402EN00, 2002), and its pore size should allow the transmission of ADH molecules (141kDa tetramer). Figure 5.9 shows the hydraulic permeability data of this membrane in encased in the two different formats.

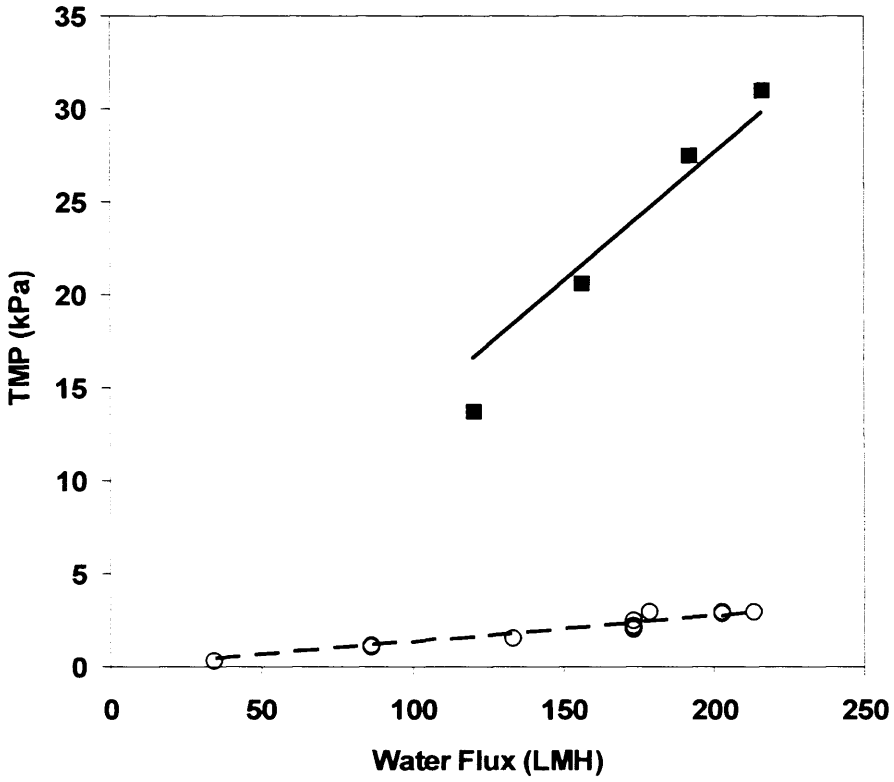

Figure 5.9: Determination of hydraulic membrane resistances for 1000kDa Biomax membranes (Millipore, MA, USA) in a Pellicon 2-mini v-screen cassette (■), and membrane coupons of the same material held in the TFF USD device (○). Linear regression lines give $R_{m.cassette}$ *(——) =* $0.14LMH.kPa^{-1}$ *(correlation coefficient* R^2 *= 0.94) and* $R_{m.TFFUSD}$ *(- - -) =* $0.014LMH.kPa^{-1}$ *(*R^2 *= 0.92).*

As with the 0.65μm Durapore membranes used for the whole cell suspension experiments, there is a marked difference between the hydraulic resistances of the membrane held within the cassette c.f. the coupon held in the TFF USD device. However, the ratio (k_{Rm} = 10) is much lower, which may be a result of the tighter pore

size distribution (1000kDa molecular weight cut-off is approximately equivalent to 0.1μm pore size diameter).

5.5.1 Results: *S. cerevisiae* homogenate trials

Figures 5.10, 5.11 and 5.12 below show the data obtained from critical flux determination experiments using the yeast homogenate suspension, and the determination of the pertinent TFF USD disk rotation speed. The critical flux region appears to be just under 20LMH for the cassette filtration, and the TFF USD device operated at 2500rpm (wall shear rate $5900s^{-1}$, calculated using equation [3.4]).

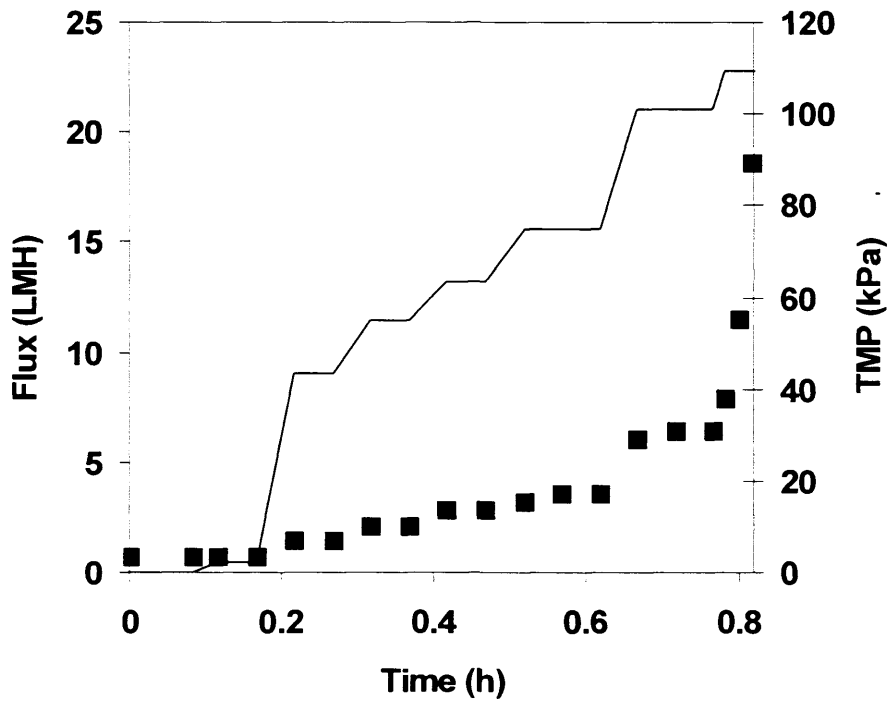

Figure 5.10: Relationship between flux rate (—) and TMP for Pellicon 2-mini v-screen cassette, feed recirculation rate 60L.h^{-1} (■). Critical flux determination with 50g.dcw.L^{-1} S. cerevisiae homogenate suspension. 1000kDa Biomax membrane (Millipore, MA, USA). Total permeate recycle.

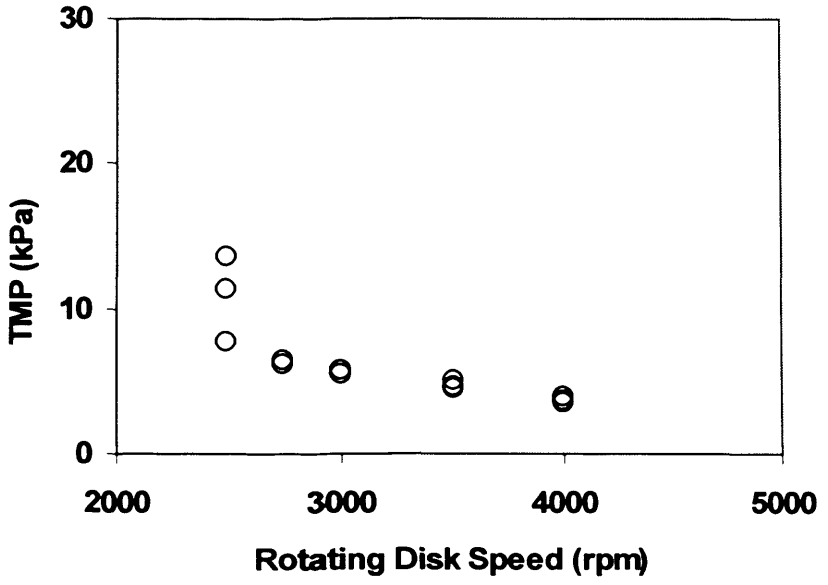

Figure 5.11: Relationship between TFF USD disk rotation speed and TMP, at permeate flux 20LMH, feed recirculation rate 0.21L.h^{-1} (O). Critical wall shear rate determination with 50g.dcw.L^{-1} S. cerevisiae homogenate suspension. 1000kDa Biomax membrane (Millipore, MA, USA). Total permeate recycle.

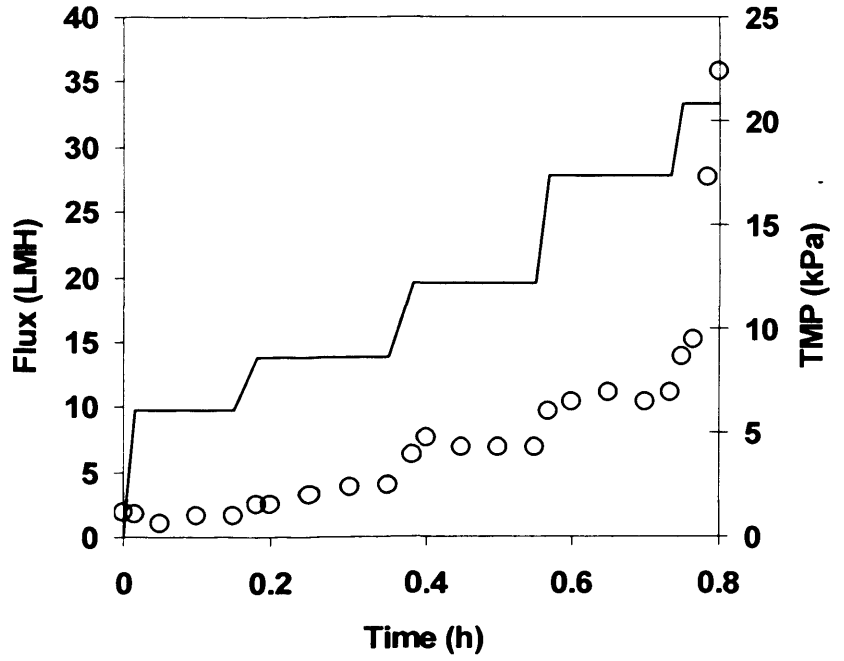

Figures 5.12: Relationship between flux rate (—) and TMP for a 25mm membrane coupon held in the TFF USD device, feed recirculation rate 0.21L.h^{-1}, disk rotation speed 2500rpm (O). Critical flux determination with 50g.dcw.L^{-1} S. cerevisiae homogenate suspension. 1000kDa Biomax membrane (Millipore, MA, USA). Total permeate recycle.

Figure 5.13 shows the comparison of the flux-stepping experiment data, with the TFF USD data compensated for the differences in initial hydraulic membrane resistance and system pressure. Again, there is excellent agreement between the two sets of data, giving confidence in the ability of the TFF USD device's ability to be used as a scale-down model for the cassette device.

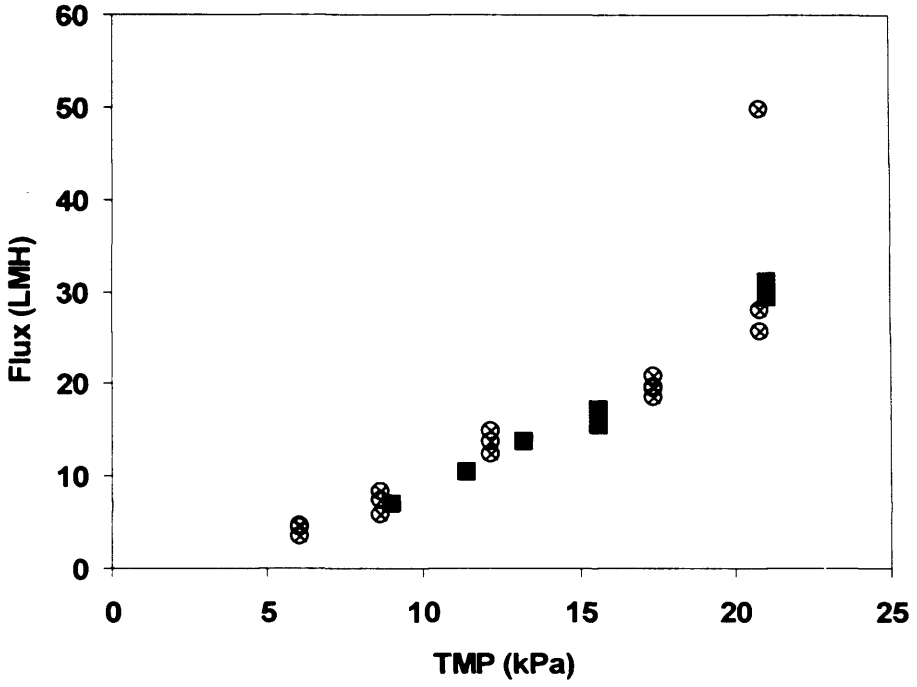

Figures 5.13: Comparison of excursion curves obtained with a Pellicon 2-mini v-screen cassette, feed recirculation rate 60L.h^{-1} (■), and a 25mm membrane coupon held in the TFF USD device, feed recirculation rate 0.21L.h^{-1}, disk rotation 2500rpm (⊗). 50g.dcw.L^{-1} S. cerevisiae homogenate suspension. 1000kDa Biomax membrane (Millipore, MA, USA). Total permeate recycle. TFF USD data corrected for differences in initial system TMP ($k_{TMP,\ t=0}$ =6kPa) and hydraulic permeability (k_{Rm} =12.82) using equation [5.12].

Figure 5.14 illustrates the selectivity of the membrane in both formats, in terms of ADH and total soluble protein during recycle experiments conducted at 17LMH (sub-critical flux). Again, it can be seen that the data from the two devices correspond well. The data shows that less than half of the available soluble protein is transmitted through the membrane, and only about 1% of the product of interest (ADH) is recovered. However, this highlights one the benefits of USD; the early assessment of this membrane type and operating conditions means that time is available to investigate other options to give acceptable yields.

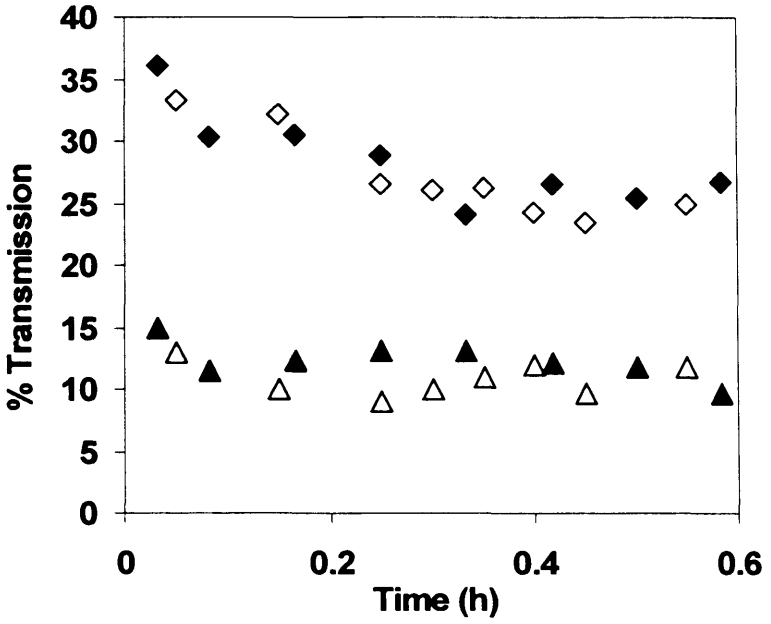

Figure 5.14: Assessment of ADH (▲,Δ) and total soluble protein (◇,◆) transmission during constant flux filtration of 50g.dcw.L^{-1} S. cerevisiae homogenate suspension at 17LMH. Pellicon 2-mini v-screen cassette, recirculation rate 60L.h^{-1}(▲,◆), and a 25mm membrane coupon held in the TFF USD device, recirculation rate 0.21L.h^{-1}, disk rotation 2500rpm (Δ,◇). 1000kDa Biomax membrane (Millipore, MA, USA). Total permeate recycle. Feed to membrane area ratio 100L.m^{-2}.

The next step in the TFF USD methodology outlined in Chapter 2 (Figure 2.5) is the assessment of the semi-empirical models proposed in Chapter 2, using data obtained from the simpler of the two feed systems (whole cell suspension).

5.6 Assessment of TFF models

Once confidence in the ability of the TFF USD to mimic conventional equipment had been established, it could be used to generate data to be used in conjunction with the models described in Chapter 2. The following sections give examples of the attempts made with one of the feed types described above (whole cell suspension), and hence a preliminary evaluation of each of the two models is made.

5.6.1 Resistance-in-series model

The section below describes the application of the hydraulic resistance-in-series model proposed by Carrère et al. (2001).

$$J = \frac{TMP}{\mu_p(Rm + Ra + Rp + Rc)} \qquad [5.14]$$

The model equations were coded using Visual Basic (Microsoft Corporation, USA), and a program listing is included in the Appendix 2. The experiments described in Table 2.4 (Chapter 2), were performed using the TFF USD device and whole *S. cerevisiae* cells spiked with ADH. Table 5.3 lists the determined values i.e. the model inputs.

These input parameters were checked against literature values, and were found to be similar. Using these values, the simulation was run for constant TMP concentration mode to assess flux and transmission behaviour prediction. The data was then compared with actual experimental results, by presenting them in the form of parity plots (see Figures 5.15 and 5.16).

The model over-predicted the values of permeate flux (J) by 40%, using the input values listed. However, the calculated mean error ε_1 (using equation [2.21], see Chapter 2) is 0.05, which is considered a low deviation, suggesting that there is a constant off-set which could be associated with an inaccurate model parameter value e.g. the value of the membrane resistance.

The model under-predicts the transmission values by 8%. However, the values are well within the sensitivity of the ADH assay. In addition, the calculated mean error ε_1 is 0.033, which is considered insignificant.

Table 5.3 Synopsis of dedicated experiments for determining parameters for the resistance-in-series model (Carrère et al., 2001). (See Chapter 2, Table 2.4)

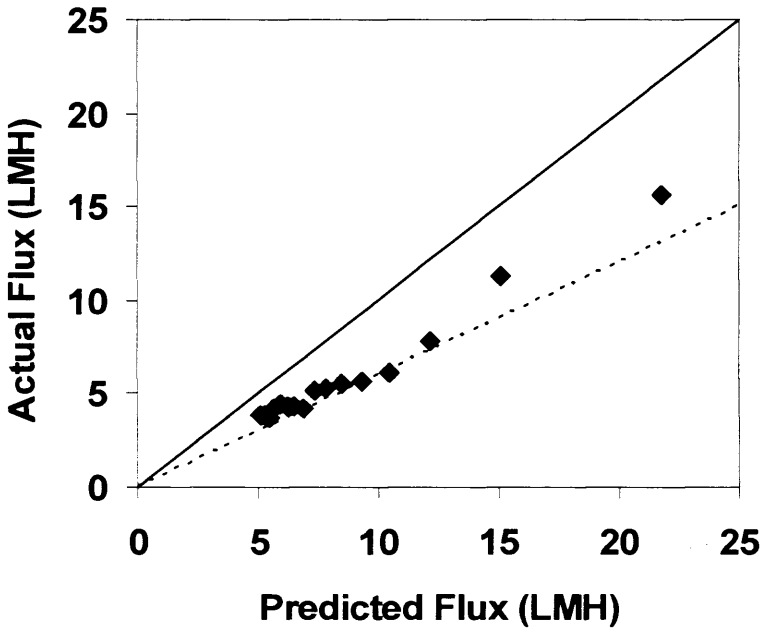

Figure 5.15: Parity plot of resistance-in-series model predictions versus experimental flux measurements (◆) for constant TMP filtration of a whole yeast suspension, using the parameters listed in Table 5.3. Dashed line (- - -) indicates 60% of predicted value.

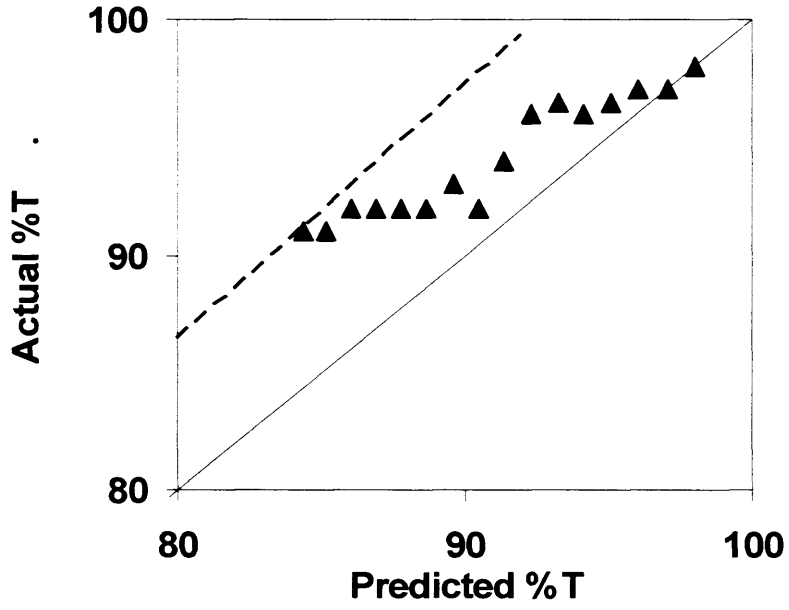

Figure 5.16: Parity plot of resistance-in-series model predictions versus experimental transmission measurements (▲) for constant TMP filtration of a whole yeast suspension, using the parameters listed in Table 5.3. Dashed line (- - -) indicates 108% of predicted value.

However, the modelling effort is only justified if the model is capable of accurately predicting other operating conditions, without having to repeat the same experiments.

Unfortunately, the resistance-in-series model parameter determination protocols are specific to one set of operating conditions. A new set of experiments to determine the parameters would be required if an operating parameter were to be changed e.g. re-evaluation of $(D/\delta)C_m$, T_0, and a would have to be done if the crossflow velocity were to be changed. Indeed, all of the experiments would need to be repeated if one were to change the membrane material. This obviates the need for a method to model the operation, as process development time would be better spent conducting actual trials.

5.6.2 Aggregate transport model

Baruah et al. (2003 and 2004) developed a predictive model for the microfiltration of transgenic goat milk using hollow fibre filters. A spreadsheet was developed to perform the calculations outlined in Chapter 2 using Excel (Microsoft Corporation, USA). However, an obstacle was encountered when attempting to modify the model to cope with the TFF USD geometry. The equations for calculation of the mass transfer coefficient (k_{mtc}) call for the hydraulic diameter (d_H) of the device (see Equation[5.3]). However, for the TFF USD, there is no flow channel as such, and this parameter is therefore incalculable.

As equivalence between the flux and transmission performance of the TFF USD device and a conventional cassette has been demonstrated, it was assumed that the mass transfer coefficient would also be the same. Hence, the geometry of the cassette may be used for the model input parameters, but the USD device would provide the equivalent wall shear rate value.

An attempt to apply the aggregate transport methodology to the *S. cerevisiae* whole cell suspension system was made. The parameters used were as follows:

- *Module Data* (R. Kuriyel, personal communication, 2001): Module length 0.1524m; pore size 0.65μm; hydraulic mean diameter, d_H = 0.115m. Operating conditions:

temperature 298K; shear rate $528s^{-1}$ (based on an equivalent TFF USD experiment conducted at 500rpm).

- *Particle sizes bulk concentrations and intrinsic viscosity* (Okec, 1998): 1.41kDa at 1%, (ADH molecules), 3μm at 3.2% and 7μm at 0.5% (yeast cells). Target particle radius = 14nm, intrinsic viscosity 2.2×10^{-3}Pa.s.

Despite much effort, it was not possible to achieve sensible results with these input parameters. Perhaps this was because of trying to apply the model to the different device geometry (invalid value of d_H) than the hollow fibre format the model was originally developed for.

As a result, it would be reasonable to state that the model methodology in its present format would not be able to fit the USD methodology criteria of being a pragmatic development tool. In addition, the time spent on modelling may have been better spent conducting actual experiments. Also, empirical data is currently more valuable in terms of regulatory application support documentation (Winkler, 2000).

5.7 Summary and conclusions

A prototype rotating disk filter was proposed as a TFF USD device (see Chapter 3). Data from comparative experiments with conventional filtration equipment, using representative bioprocess feeds, imply that the TFF USD is able to mimic the overall cassette performance to the degree required to obtain information for scale-up, in terms of flux and TMP conditions (having compensated for differences in membrane hydraulic resistance, and initial system pressures); hence, the scale-down device has been successfully verified against the conventional technology.

The equating of wall shear rate between the devices was complicated by the inability to estimate accurately the wall shear rate in the cassette, due to its highly complex geometry. Instead, an empirical approach was used to match the filtration behaviour, and thus infer the wall shear rate in the cassette by calculation of the shear rates generated in the rotating disk device. However, this method is not ideal, especially when an objective of USD is to obviate the need for pilot-scale verification.

The latest semi-empirical models available for TFF were evaluated using the simpler of the two feeds. The resistance-in-series approach proved to be able to model the empirical data adequately (insignificant mean errors), but the main drawback of this method is its inability to extrapolate to other operating conditions, without repetition of the parameter-determining experiments. The attempt to apply the aggregate transport model to describe the *S. cerevisiae* whole cell suspension filtration was unsuccessful. Only a pragmatic modelling approach is useful to process development scientists, as empirically derived data is still preferred over simulated data e.g. for use in regulatory submission support documents.

Referring to Figure 2.5 (Chapter 2) the next steps is to test the device further with other bioprocess feeds e.g. bacterial and/or mammalian cell broths. In addition, the experiments described above were conducted in recycle mode; actual processing operations such as diafiltration and concentration need to be investigated to complete the verification of the TFF USD against conventional modules. This work is described in Chapters 6 and 7.

Chapter 6 Verification of TFF USD Device with a Bacterial Lysate

6.1 Introduction

The development of a generic methodology for TFF USD requires several iterations around the flowchart loop (see Figure 2.5, Chapter 2) with various combinations of feed and membrane materials, in order to give confidence that the TFF USD device is a true mimic of conventional equipment. The aim of these experiments was to demonstrate the capability of the TFF USD device with a bacterial lysate system, and new membrane material to show that the system was generic as defined by it's capacity to generate data with a range of bioprocess feed systems and to extend the comparison with pilot-scale data to include diafiltration experiments.

The clarification of a periplasmic antibody fragment (Fab') from an *Escherichia coli* lysate was chosen to test the TFF USD device. Further details of the feed are given in Chapter 4. The scientific and commercial interest in antibodies and antibody-based molecules is significant within the bioprocess sector, with several recombinant products already in the market place. The high affinity and specificity of antibodies for the target antigen has been exploited in a wide variety of therapeutic, diagnostic and industrial applications ranging from the treatment of inflammation and autoimmune diseases to the detection and control of environmental pollution. The Fab' can be detected by a microplate-based ELISA assay, allowing for rapid assay of samples taken to study transmission behaviour. The minute amounts of material required by this sensitive assay made it suitable for the sampling regime required for the USD experiments.

This choice of experimental system was selected for the following reasons:

- Representative of a bioprocess feed of current commercial interest;
- Collaborative work at UCL to provide fermentation material;
- Previous work characterising the system, and the development of reliable production and assay techniques within the department (Bowering, 2000);
- Existing pilot-scale data to corroborate pilot-scale data obtained, and to compare the filtration results with (Novais, 2001).

Unfortunately, the pilot-scale data available was conducted at a membrane loading of $10L.m^{-2}$, which would have meant an equivalent TFF USD feed volume of less than 0.004L, which was clearly not practical to use given the USD system hold-up. Due to the limited amount of lysate material available, the Pellicon XL labscale system was therefore employed, as according to the manufacturer's data (see Chapter 3, Figure 3.1) this device was designed to provide a linear scale-down of the Pellicon 2 mini cassettes. This decision enabled an investigation of the scalability of the Pellicon cassettes, as well as a 20-fold reduction in the amount of *E. coli* lysate used for each conventional experiment.

The results show that the TFF USD device was again able to produce scale-up data comparable to those obtained using conventional filtration devices, despite the increased complexity of the feed.

6.2 Results: *E. coli* lysate

As part of the study to test that a rotating disk device could mimic flat-sheet cassette filtration behaviour, the TFF USD device needed to be tested with a range of representative bioprocess feeds.

As described in Chapter 5, the first step was to identify the wall shear rate required at the USD scale that would give the same critical flux value obtained at pilot-scale. Experiments evaluating the behaviour of transmission of the antibody fragment through the membrane were then performed, both in total permeate recycle mode of operation and constant volume diafiltration.

The following section describe the flux and transmission results obtained from a series of experiments devised to assess the ability of the TFF USD device to mimic clarification of an *E. coli* lysate using commercially available cassette devices (laboratory and pilot-scale) containing 1000kDa Biomax membranes (Millipore, MA, USA). Full details of the materials and methods for the experiments are given in Chapter 4.

6.2.1 Determination of hydraulic permeability correlation factor

Figure 6.1 shows water permeability data from each of the three device formats.

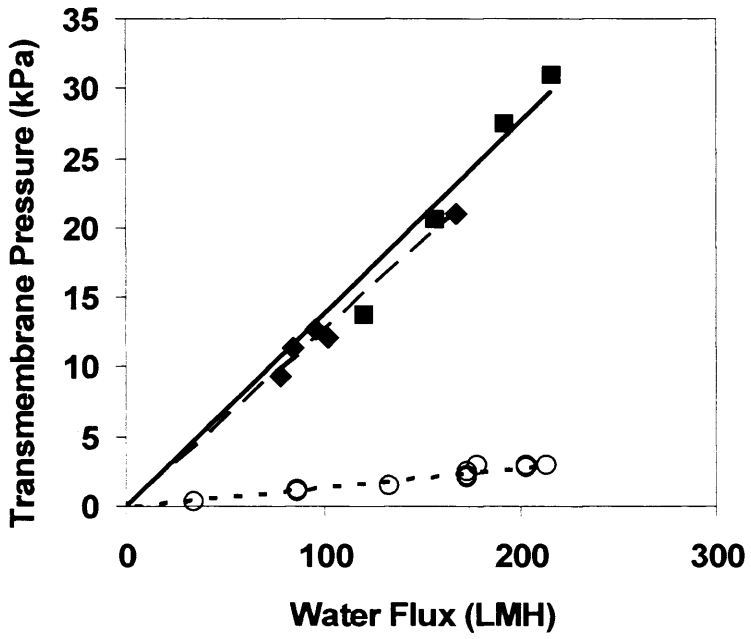

Figure 6.1: Determination of hydraulic membrane resistances for 1000kDa Biomax membranes (Millipore, MA, USA) in a Pellicon 2-mini v-screen cassette (■), a Pellicon XL cassette (◆) and membrane coupons of the same material held in the TFF USD device (○). Linear regression lines give $R_{m.cassette}$ *(——) =* $0.14LMH.kPa^{-1}$ *(correlation coefficient* $R^2 = 0.94$*),* $R_{m.XLcassette}$ *(——) =* $0.13LMH.kPa^{-1}$ *(*$R^2 = 0.98$*) and* $R_{m.TFFUSD}$ *(- - -) =* $0.013LMH.kPa^{-1}$ *(*$R^2 = 0.92$*).*

As expected, the hydraulic membrane resistance of the membranes in the cassette formats are virtually identical, confirming that it is the membrane format (not area) that is responsible for the difference in permeability. Linear regression of this data provided the TMP compensation constants (k_{Rm}) used to convert the TFF USD data so it could be compared with cassette data.

6.2.2 Determination of critical flux and critical wall shear rate

The results of a flux stepping experiment using a 1000kDa Biomax Pellicon 2 mini cassette (pilot-scale) are shown in Figure 6.2 below. The data indicated that the critical flux region is approximately 35-40LMH. This was also the value found by Novais (2001) during a similar experiment.

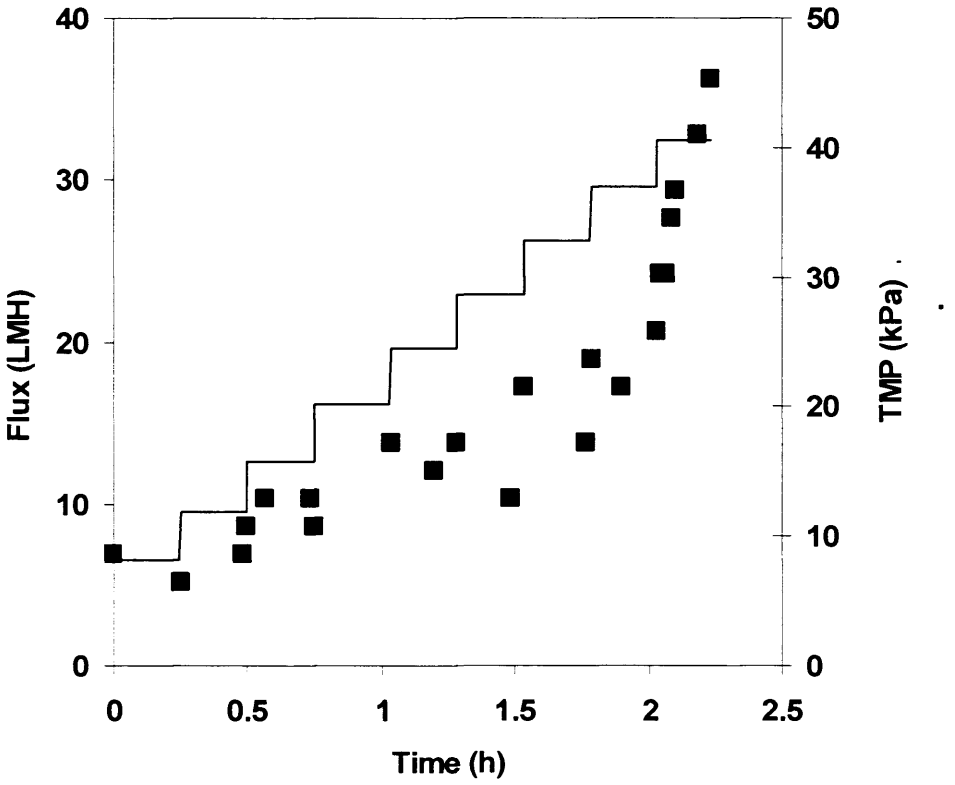

Figure 6.2: Relationship between flux rate (—) and TMP for Pellicon 2-mini v-screen cassette, recirculation rate 60L.h^{-1} (■). Critical flux determination with E. coli lysate (equivalent cell concentration 47gdcw.L^{-1}). 1000kDa Biomax membrane (Millipore, MA, USA). Total permeate recycle. Feed to membrane area 100L.m^{-2} (feed volume 1L).

Figure 6.3 shows the results of a similar experiment conducted with the manufacturer's own scale-down device, the Pellicon XL cassette (membrane area 0.005m^2, 20-fold scale-down). Again, the critical flux region appears to be 35-40LMH, supporting the manufacturer's claim that the Pellicon series of cassettes are linearly scaleable (see also Chapter 3, Figure 3.1). Therefore, it was this flux value that was selected to operate the TFF USD device was at, in order to empirically determine the equivalent disk rotation speed (Figure 6.4).

From this experiment, a disk rotation speed of 3500rpm was chosen to conduct the comparative TFF USD experiments for the *E. coli* lysate system. By using equation [3.4] (see Chapter 3), it is possible to infer that the average wall shear rate in the Pellicon cassette was 9774s^{-1} (turbulent flow, as Re > 2500), which is the key information required for scale-up of the process.

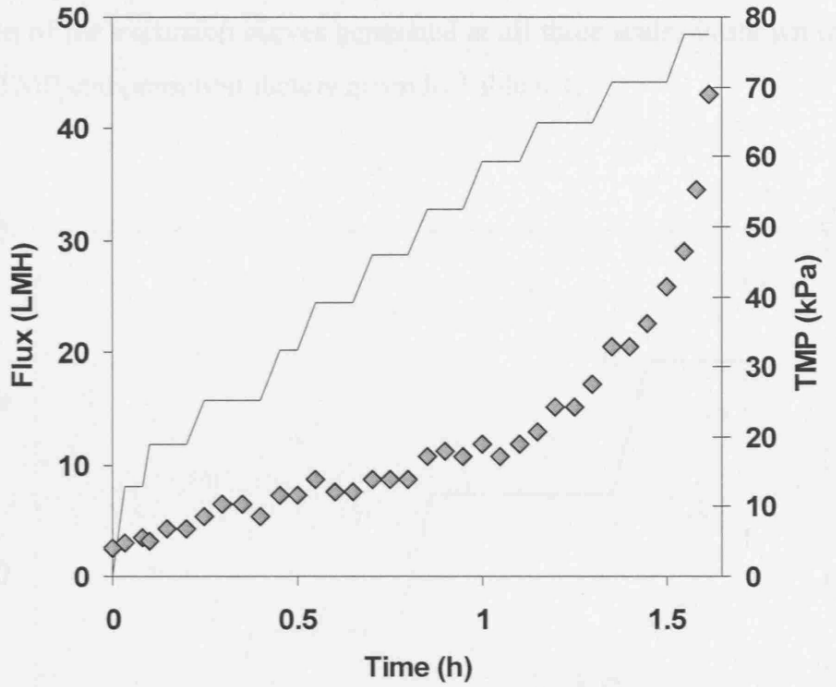

Figure 6.3: Relationship between flux rate (—) and TMP for Pellicon XL v-screen cassette, recirculation rate 3L.h^{-1} (◆). Critical flux determination with E. coli lysate (equivalent cell concentration 47gdcw.L^{-1}). 1000kDa Biomax membrane (Millipore, MA, USA). Feed to membrane area 100L.m^{-2} (feed volume 0.5L).

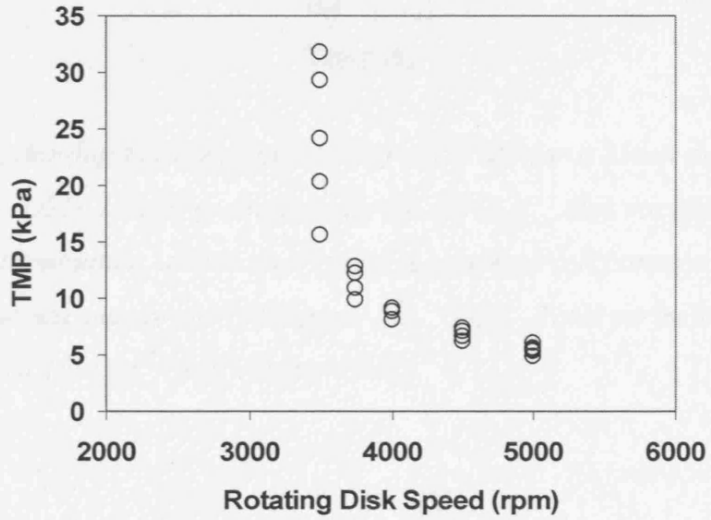

Figure 6.4: Relationship between TFF USD disk rotation speed and TMP, at permeate flux 40LMH, feed recirculation rate 0.21L.h^{-1} (○). Critical wall shear rate determination with E. coli lysate (equivalent cell concentration 47gdcw.L^{-1}). 1000kDa Biomax membrane (Millipore, MA, USA). Total permeate recycle. Feed to membrane area 100L.m^{-2} (feed volume 0.04L).

The data from the flux stepping experiments are presented in Figure 6.5 and a comparison of the excursion curves generated at all three scales is shown in Figure 6.6, using the TMP compensation factors given in Table 6.1.

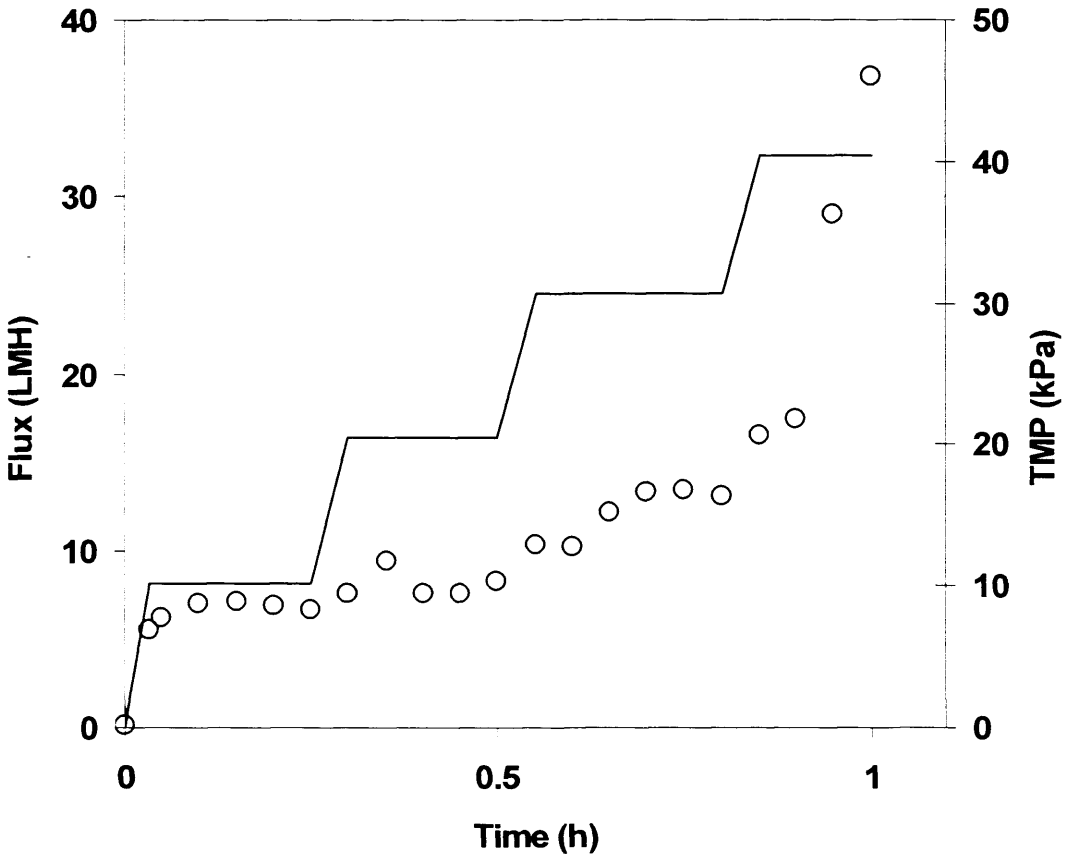

Figure 6.5: Relationship between flux rate (—) and TMP for a 25mm membrane coupon held in the TFF USD device, recirculation rate 0.21L.h^{-1}, disk rotation 3500rpm (O). Critical flux determination with E. coli lysate (equivalent cell concentration 47gdcw.L^{-1}). 1000kDa Biomax membrane (Millipore, MA, USA). Total permeate recycle. Feed to membrane area 100L.m^{-2} (feed volume 0.04L).

Device	Membrane hydraulic resistance k_{Rm} (m^{-1})	Initial system pressure $k_{TMP, t=0}$ (kPa)
Pellicon 2 mini cassette	0.126	6.89
Pellicon XL cassette	0.138	4.00
TFF USD	0.013	0.138

Table 6.1: TMP compensation factors determined from E. coli lysate experiments.

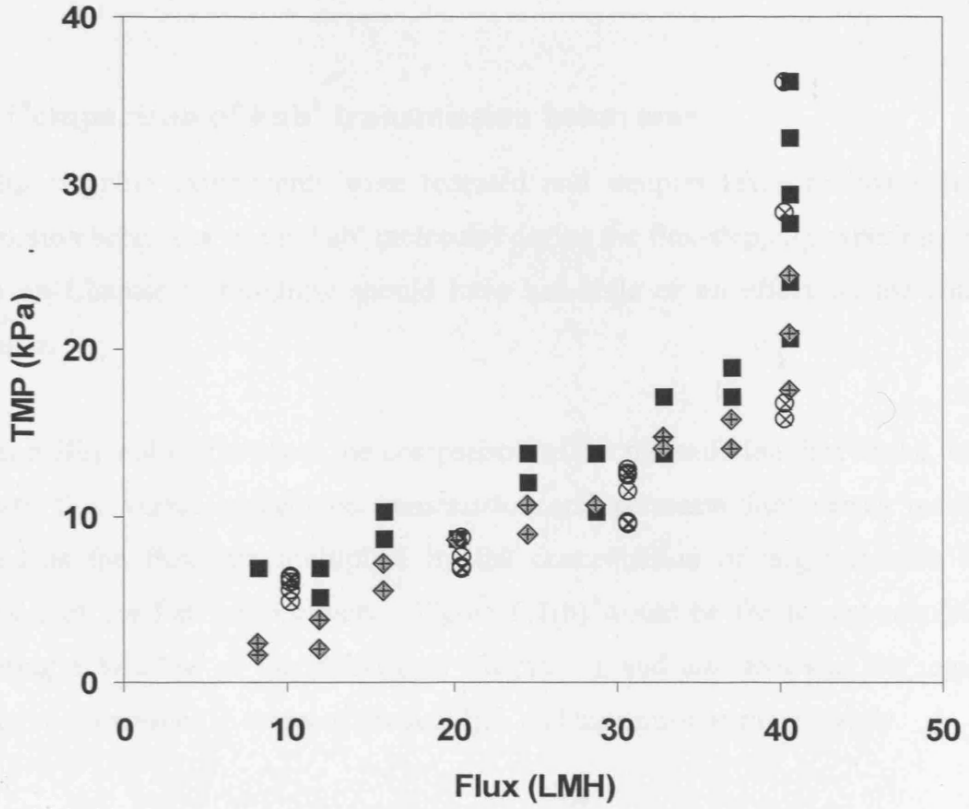

Figure 6.6: Comparison of excursion curves obtained with a Pellicon 2-mini v-screen cassette, feed recirculation rate 60L.h^{-1} (■), a Pellicon XL v-screen cassette, feed recirculation rate 3L.h^{-1} (✦), and a 25mm membrane coupon held in the TFF USD device, feed recirculation rate 0.21L.h^{-1} disk rotation 3500rpm (⊗). 1000kDa Biomax membrane (Millipore, MA, USA). Total permeate recycle filtration of E. coli lysate (equivalent cell concentration 47gdcw.L^{-1}). Pellicon XL and TFF USD data corrected for differences in initial system TMP and hydraulic permeability using values given in Table 6.1 and equation [5.12].

Figure 6.6 confirms several things, the first being that the Pellicon XL cassette is indeed a good linear scale-down of the Pellicon 2 mini cassette. Secondly, the TFF USD device can generate comparable flux and TMP data to the cassette devices non-linear scale-down, despite being a non-linear scale-down and requiring almost 300 times less material. However, the use of the TMP compensation factors is required, and these constants need to be determined for every retentate recirculation rate and membrane combination that is being investigated. The next stage of these comparative experiments was to assess the transmission behaviour of the target molecule of interest (Fab').

6.2.3 Comparison of Fab' transmission behaviour

The flux-stepping experiments were repeated and samples taken to investigate the transmission behaviour of the Fab' molecules during the flux-stepping experiments. As shown on Chapter 5, sampling should have had little or no effect on the filtration behaviour.

Figures 6.7(a) and 6.7(b) show the comparison of the transmission data in the form of permeate flux versus percentage transmission and permeate flux versus mass flux (defined as the flux rate multiplied by the concentration of target species in the permeate) of the Fab' respectively. Figure 6.7(b) would be the format required for generating a Window of Operation (see Chapter 2), and also indicates the region of optimum performance in terms of product flux and transmission more clearly.

The key results is that beyond the critical flux region (35-40LMH), the percentage Fab' transmission ($\%T_{Fab'}$) starts decreasing, and that the maximum $\%T_{Fab'}$ coincides with the maximum mass flux rate of the antibody fragment (see Figure 6.7(b)).

Yet again, the data generated from both devices are similar, despite there being almost a 300-fold difference in scale. The fact that the optimum point for product transmission corresponds to the maximum permeate flux indicates that there is little or no fractionation of species (Fischer, 1996). Based on these results, the lysate should be processed at a controlled flux of less than $40L.m^{-2}.h^{-1}$, but as high as possible so as to allow for a high productivity. These conditions should allow for longer term operation

due to the lower extent of fouling observed below the critical flux (Defrance and Jaffrin, 1999).

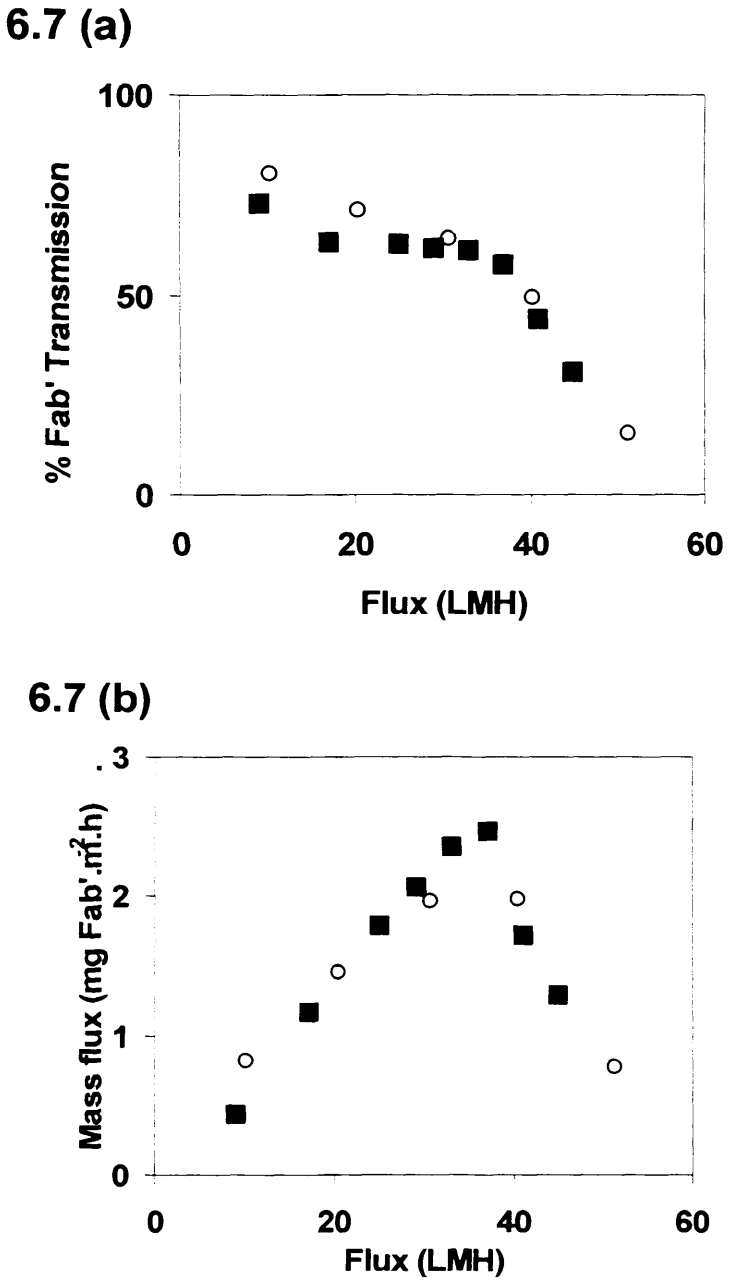

Figure 6.7 (a) and (b): Assessment of Fab' transmission during flux stepping experiments, total permeate recycle. Pellicon 2-mini v-screen cassette, recirculation rate 60L.h^{-1} (■), and a 25mm membrane coupon held in the TFF USD device, recirculation rate 0.23L.h^{-1}, disk rotation 3500rpm (○). E. coli lysate (equivalent cell concentration 47gdcw.L^{-1}. 1000kDa Biomax membrane (Millipore, MA, USA). Data points are the mean value of the results obtained from two or three dilutions of each permeate and retentate sample during the ELISA.

This information was used to perform the diafiltration experiments described in the next section, which were consequently conducted at 34LMH

6.2.4 Diafiltration studies

The next phase of experimentation involved diafiltration of the lysate. The materials used and experimental protocols used are described in Chapter 4. Constant volume diafiltration has often been used to remove soluble proteins from cell lysates (Bailey and Meagher, 2000; Meagher et al., 1994). The advantage of this technique is that is avoids concentration of the non-permeated species, therefore maintaining similar physical properties of the retentate.

Species transmission decreases over time in constant volume diafiltration (Forman et al., 1990; Meagher et al., 1994; Novais, 2001). This decrease is exponential, and Novais (2001) showed that it follows a first order decay relationship

$$T_{obs} = T_0 e^{at} \qquad [6.1]$$

where T_{obs} is the observed transmission of product, T_0 is the initial transmission value at the start of the diafiltration, a is a constant, and t is time (h).

Figure 6.8 shows the transmission results from diafiltration experiments using both the laboratory (Pellicon XL) and pilot scale (Pellicon 2 mini) systems. The similarity of the results suggest that it would be reasonable to continue the experimental comparisons with the Pellicon XL lab-scale device, therefore reducing the demand for the lysate feed material.

Considering the inherent error in the ELISA assay, the two sets of data imply that the transmission performance was the same. Assuming that the transmission behaviour follows an exponential decay (Novais, 2001), the important data points to consider are the initial transmission values. The experiments conducted to obtain the data in Figure 6.8 took 1.1 hours; if only the initial values are required, shorter durations should be acceptable to obtain the model parameters. Table 6.2 shows the model parameters obtained by fitting equation [6.1] to the data, and by only using the first eight points of the Pellicon XL data (diafiltration time = 0.4 hours).

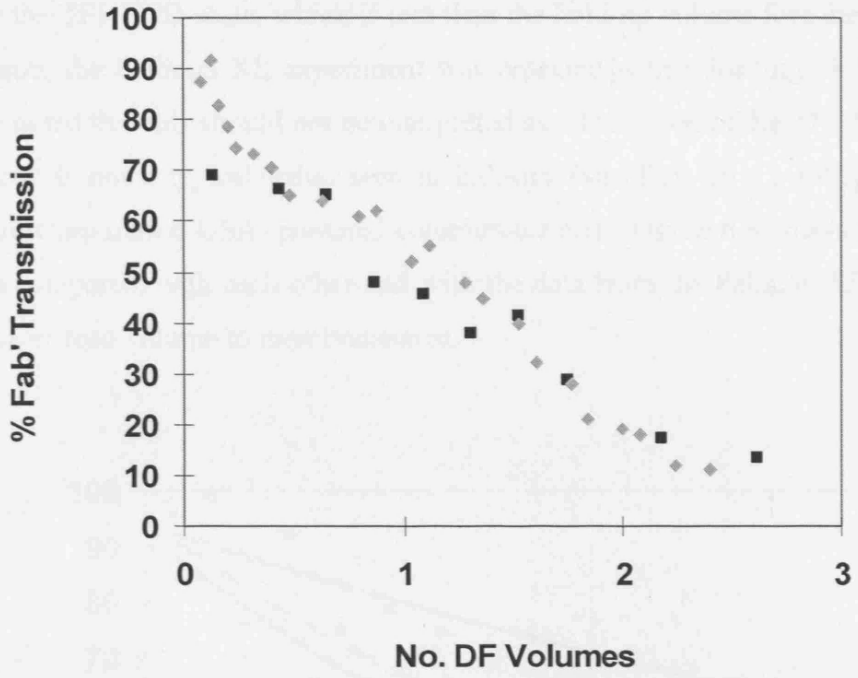

Figure 6.8: Effect of diafiltration volume on percentage transmission of Fab'. Constant volume diafiltration at 34LMH with 150mM NaCl buffer at pH 7.4. Pellicon 2-mini v-screen cassette, recirculation rate 60L.h^{-1} (■), and a Pellicon XL v-screen cassette, recirculation rate 3L.h^{-1} (◆). E. coli lysate (equivalent cell concentration 47gdcw.L^{-1}). 1000kDa Biomax membrane (Millipore, MA, USA). Feed to membrane area 10L.m^{-2}. Data points are the mean value of the results obtained from two or three dilutions of each permeate and retentate sample during the ELISA.

Device	Diafiltration time (h)	Model Equation Parameter		R^2*
		T_0	a	
Pellicon 2 mini	1.1	92	-0.70	0.94
Pellicon XL	1.1	106	-0.82	0.92
Pellicon XL	0.4	94	-0.77	0.91

*Table 6.2: Transmission decay model parameters obtained from fitting Equation [6.1] to data shown in Figure 6.7. *Correlation coefficient between data points and equation curve.*

The model parameters are very similar, and therefore it was decided to conduct further experiments using this shorter experimental time.

As mentioned above, a loading value of $10L.m^{-2}$ equates to a feed volume of less than 4mL on the TFF USD scale, which is less than the hold-up volume fore the device. For this reason, the Pellicon XL experiment was repeated with a loading of $100L.m^{-2}$. It must be noted that this should not be interpreted as a limitation of the TFF USD system, as $10L.m^{-2}$ is not a typical value seen in industry (van Reis et al., 1997; C. Christy, Millipore Corporation USA, personal communication). Figure 6.9 shows how the two datasets compared, with each other and with the data from the Pellicon XL experiment at the lower feed volume to membrane area.

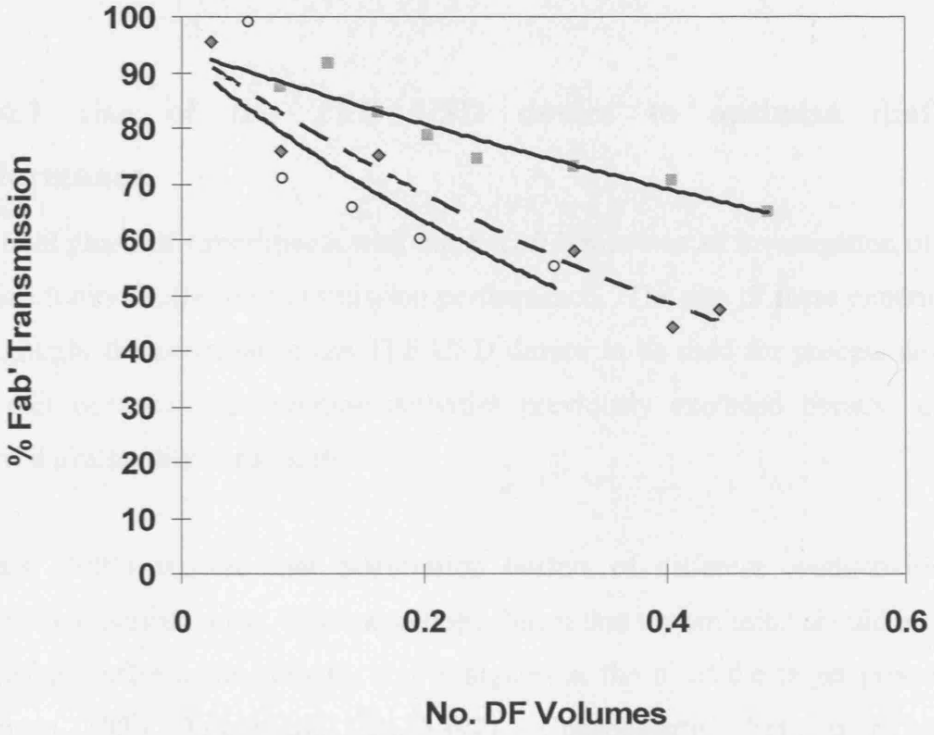

Figure 6.9: Effect of diafiltration volume on percentage transmission of Fab'. Pellicon XL v-screen cassette, feed to membrane area $10L.m^{-2}$, exponential decay curve $\%T = 94e^{-0.8t}$, correlation coefficient $R^2 = 0.91$ (■, ——); Pellicon XL v-screen cassette feed to membrane area $100L.m^{-2}$, $\%T = 95e^{-1.7t}$, $R^2 = 0.95$ (◆,— — —); 25mm diameter coupon held within the TFF USD device, feed to membrane area $100L.m^{-2}$, $\%T = 93e^{-1.9t}$, $R^2 = 0.73$ (○, - - - -). Constant volume diafiltration at 34LMH with 150mM NaCl buffer at pH 7.4. E. coli lysate (equivalent cell concentration $47gdcw.L^{-1}$). 1000kDa Biomax membrane (Millipore, MA, USA). Data points are the mean value of the results obtained from two or three dilutions of each permeate and retentate sample during the ELISA.

The first thing to remark on is that the data obtained at both scales matches well, confirming the ability of the TFF USD device to mimic the transmission behaviour seen with a cassette device. The second point of interest is that although the initial transmission (T_0) values obtained using the Pellicon XL cassette were similar, the decay constant (a) at the higher loading value was greater ($a_{100L.m^{-2}}$ = -1.7 c.f. $a_{10L.m^{-2}}$ = -0.8) i.e. Fab' transmission decayed more rapidly, although the feed concentration was kept constant. This result suggests that either cake deposition or fouling was more rapid. However, as the purpose of these experiments was to validate the TFF USD device, further investigation of the effect of loading on transmission behaviour was not considered.

6.2.4.1 Use of the TFF USD device to optimise diafiltration performance.

The final phase of experiments with the *E. coli* lysate was an investigation of the effect of diafiltration buffer on transmission performance. The aim of these experiments was to highlight the potential of the TFF USD device to be used for process development and unit operation optimisation activities previously excluded because of time or material availability constraints.

Novais (2001) showed that diafiltration buffers of different conductivities altered diafiltration performance. It has also been shown that transmission should increase with increasing buffer ionic strength, and is highest at the pI of the target protein (Le and Atkinson, 1985; Bowen and Gan, 1992). Consequently, diafiltration performance should be improved using a buffer at pH 8.3, which is the isoelectric point of the Fab' molecule (Bowering, 2000). The data shown in Figure 6.10 supports the theory, but there is not a significant improvement in the rate of transmission decay ($a_{pH7.4}$= -1.9 c.f. $a_{pH8.3}$= -1.2). However, there was not a significant difference in the ionic strength of the buffer either.

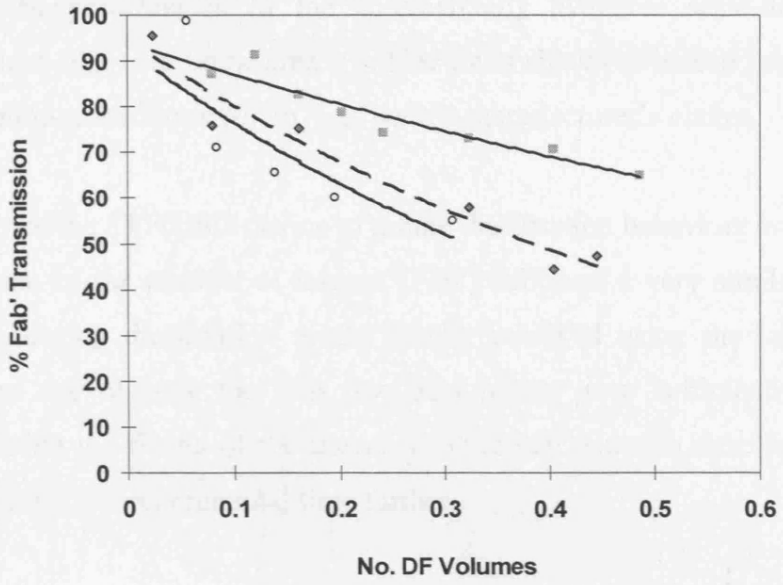

Figure 6.10: Effect of buffer composition on percentage transmission of Fab'. Exponential decay curve for 150mM NaCl buffer at pH 7.4%T = $93e^{-1.9t}$, correlation coefficient R^2 = 0.92 (O, ——), and 150mM NaCl buffer at pH8.3, %T = $97e^{-1.2t}$, correlation coefficient R^2 = 0.92 (●, - - -). 25mm coupon held within the TFF USD device. Constant volume diafiltration at 34LMH. E. coli lysate (equivalent cell concentration 47gdcw.L^{-1}). 1000kDa Biomax membrane (Millipore, MA, USA). Feed to membrane area loading 100L.m^{-2}. Data points are the mean value of the results obtained from two or three dilutions of each permeate and retentate sample during the ELISA.

The effect of buffer composition experiments are exemplary of the type of study that the TFF USD device could be used for during process development. Such investigations are currently not feasible due to scarcity of feed material etc. (see Chapter 1). This aspect is discussed further in Chapter 7.

6.3 Summary and conclusions

The preceding sections have outlined some of the experiments conducted to challenge the TFF USD device with a representative bioprocess feed (bacterial lysate containing Fab'), and successfully confirmed that comparable filtration behaviour to that obtained at pilot-scale (300-fold scale-down) and laboratory scale (60-fold scale-down) can be generated.

In addition, the performance of the commercially available scale-down filtration cassette (Pellicon XL, membrane area = $0.05m^2$) was shown to indeed be a linear scale-down of the pilot-scale device ($0.1m^2$), as per the manufacturer's claims.

The capability of the TFF USD device to mimic diafiltration behaviour was shown, and the transmission of the product of interest (Fab') followed a very similar exponential decay pattern during diafiltration to the results achieved using the laboratory-scale cassette. The use of only the first few data points gave sufficiently comparable parameters during the fitting of the transmission model equation described by Novais (2001), shortening the experimental time further.

The benefits of the TFF USD device were also exploited (small feed requirements and quick equipment turnaround) to conduct a series of exploratory experiments investigating the effect of a change of diafiltration buffer on the mass flux of the Fab'. As predicted by the theory, product transmission did improve when a buffer closer to the pI of the molecule was utilised.

The usefulness and relevance of the TFF USD device would be ultimately shown by successful application in an industrial context. This work is presented on the next chapter in the form of a case study undertaken in collaboration with an industrial partner.

Chapter 7 Case Study: Evaluation of a Mammalian Cell Broth Filtration Using TFF Ultra Scale-Down Techniques

7.1 Introduction

The following chapter describes the work carried out during an EngD industrial placement at Cambridge Antibody Technology Ltd (known as MedImmune, as of October 2007). Cambridge Antibody Technology (C*a*T) is a biopharmaceutical company using its capabilities and technologies in the discovery and development of new and innovative antibody medicines in selected therapeutic areas, such as asthma, rheumatoid arthritis and cancer treatment (http://www.cambridgeantibody.com, 2008).

This collaboration was organised to challenge the TFF USD device and methodology with a mammalian cell culture, another class of biological feed (c.f. yeasts and bacteria). Mammalian cells principally differ from bacterial and yeast cells in that they lack a cell wall. Consequently they are more sensitive to shear stress (Cherry and Papoutsakis, 1986), and are also more temperature labile. Hence, they offer greater challenges for industrial production techniques (Russotti and Göklen, 2000).

The separation of monoclonal antibodies (MAb's) from animal cell cultures, using membrane filtration, has been well documented in the literature (Ng and Obegi, 1990; Maiorella et al., 1991; van Reis et al., 1991; Krishnan et al., 1994; Vogel and Kroner, 1999; Russotti and Göklen, 2000; Baruah and Belfort, 2004), and will not be described further here. The overall placement project aim was to extend the application of the TFF USD technology for the scale-down analysis of flux and product transmission during microfiltration to mammalian cell broths. As a result of the use of the USD experiments, a methodology would be developed for the rapid identification of suitable operating strategies for the clarification of products based upon C*a*T materials known to be problematic with respect to separation.

7.1.1 Objectives

The original objectives for the experiments to be conducted during the placement were as follows:

1. Comparison of the tangential flow filtration ultra scale-down (TFF USD) device with conventional technology (Centramate cassette, Pall, UK).
2. Assessment of broth filtration behaviour with different membrane materials.
3. Definition and determination of a filtration performance index to compare different feed streams
4. The study of flux and transmission behaviour during concentration and diafiltration (DF).
5. An investigation into the effect of different buffers of diafiltration performance.
6. Definition and population of a "Window of Operation" to aid identification of a suitable region for operation.
7. To devise a strategy to identify the optimal fermentation harvest point with respect to filtration performance.

Due to time constraints (and the company fermentation schedule), the investigation to identify the optimal fermentation harvest point (objective 7) was not conducted, but the benefits of doing such a study is discussed further in Chapter 10.

7.2 Results: Mammalian Cell Broth

The following sections describe the results obtained by the experiments conducted to meet the objectives set out above. The materials and methods used are described as much as possible in Chapter 4 (see section 4.6), and the assistance of C*a*T personnel to this work is gratefully acknowledged. To protect any proprietary information, certain data pertaining to the C*a*T fermentation material will be presented in terms of arbitrary units e.g. product concentrations.

7.2.1 Comparison of TFF USD with conventional technology

The commercially available device selected to compare the TFF USD results with was again a flat-sheet cassette (Pall, UK). C*a*T filtration techniques had previously used

hollow fibre cartridges for the particular broth type that was being studied, but membrane coupons of the same material as this were unavailable.

As with the work described in Chapters 5 and 6, the filtration data must be comparable in terms of flux behaviour and product transmission for the TFF USD device to be a good mimic of the conventional filter, even with a challenging mammalian cell culture.

Table 7.1 gives the mean hydraulic membrane resistance values determined from water flux tests carried out before each filtration experiment.

Device	Hydraulic membrane resistance (m^{-1})	Correlation Coefficient R^2
Pall Centramate cassette	1.91×10^{-10}	0.97
TFF USD	1.8×10^{-11} *	0.94

*Table 7.1: Hydraulic membrane resistance of 0.2μm Supor-200 membranes (Pall, UK) in cassette and coupon formats. *Average of data from permeability tests on 14 membrane coupons.*

As with the other membrane materials in previous chapters, the hydraulic resistance of the membrane coupon held within the TFF USD device is an order of magnitude lower than that of the membrane held in the cassette (see Chapter 5).

7.2.1.1 Determination of critical flux and critical wall shear rate

Figures 7.1 and 7.2 below shows data obtained from flux stepping experiments with the Pall Centramate cassette and the TFF USD operated at a disk rotation speed of 900rpm respectively. Both sets of data indicate a critical flux region between 27 and 31LMH.

Figure 7.3 shows a comparison of the two sets of data in terms of the relationship between permeate flux and transmembrane pressure; the TFF USD data has been modified by the TMP compensation factors for hydraulic permeability and initial system pressure (see Chapter 5). Again, there is excellent agreement between the data sets generated with both devices.

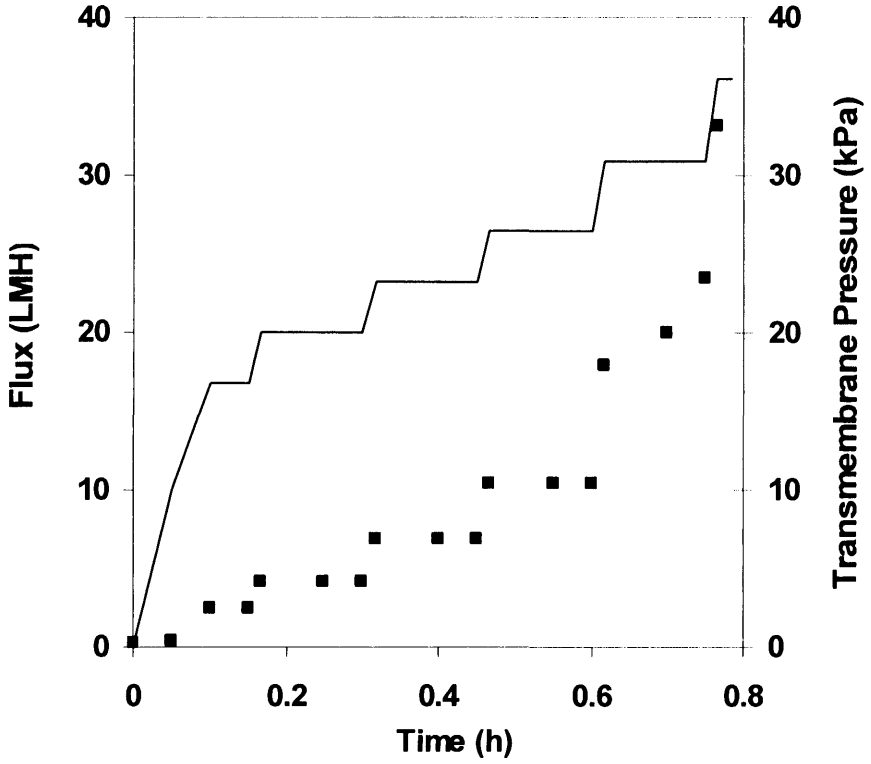

Figure 7.1: Relationship between flux rate (—) and TMP for Centramate cassette, recirculation rate 60L.h^{-1} (■). Critical flux determination with CaT broth (ALI-29OCT04). 0.2μm Supor membrane (Pall, UK). Total permeate recycle. Feed to membrane area 100L.m^{-2} (feed volume 1L).

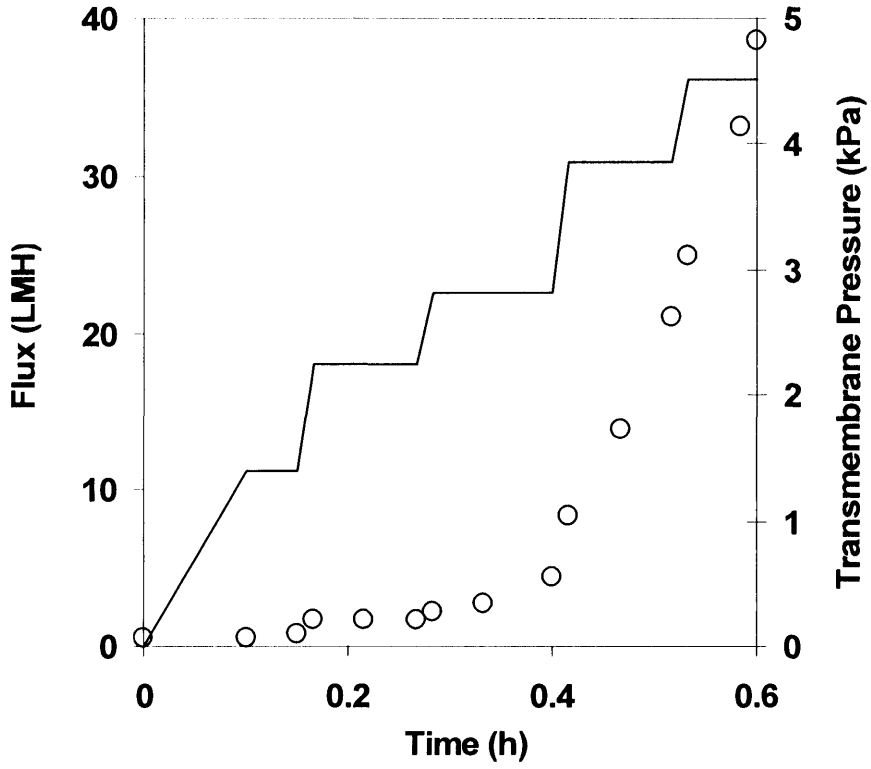

Figure 7.2: Relationship between flux rate (—) and TMP for a 25mm membrane coupon held in the TFF USD device, recirculation rate 0.21L.h^{-1}, disk rotation 3500rpm (○). Critical flux determination with CaT broth (ALI-29OCT04). 0.2μm Supor membrane (Pall, UK). Total permeate recycle. Feed to membrane area 100L.m^{-2} (feed volume 0.04L).

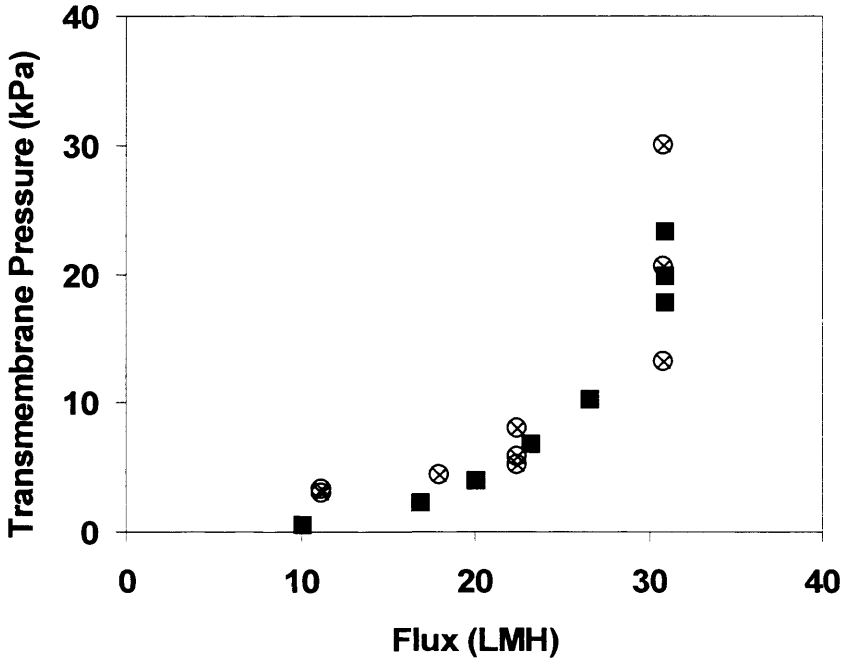

Figure 7.3: Comparison of relationship between flux rate and TMP data obtained with a Centramate cassette (■) and a 25mm membrane coupon held in the TFF USD device at 900rpm (⊗). 0.2μm Supor membrane (Pall, UK). Total permeate recycle filtration of CaT broth (ALI-29OCT04). TFF USD data corrected for differences in initial system TMP and hydraulic permeability using values given in Table 7.1 and equation [5.12].

The calculated shear rate at the membrane wall in the TFF USD device at 900rpm (using equation [3.4], see Chapter 3) is approximately $1400s^{-1}$. This value is in the region that mammalian cell clarification has previously been performed (Maiorella et al., 1991).

7.2.1.2 Comparison of Mab' transmission behaviour

Samples of permeate and retentate were taken during repeats of the flux-stepping experiments to investigate the transmission behaviour of the Mab' molecules. Figure 7.4 shows the comparison of the transmission data from both experiments in the form of permeate flux versus mass flux of the Mab' product. The data shows that TFF USD filtration is capable of mimicking cassette filtration in terms of transmission behaviour, as well as flux performance.

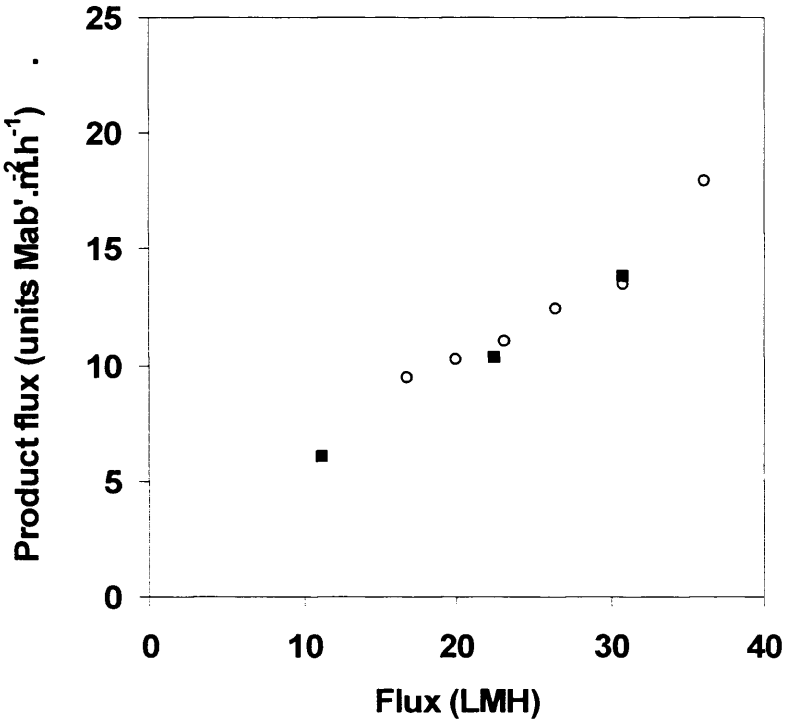

Figure 7.4: Assessment of Mab' transmission during flux stepping experiments, total permeate recycle. Centramate cassette, recirculation rate 60L.h^{-1} (■), and a 25mm membrane coupon held in the TFF USD device, recirculation rate 0.23L.h^{-1}, disk rotation 900rpm (○). 0.2μm Supor membrane (Pall, UK). CaT broth ALI-29OCT04). Data points are the average value of the assay results obtained from two replicates of each permeate and retentate sample.

It is interesting to note that, unlike the Fab'/bacterial lysate system, the transmission of the Mab' appears to continue to increase beyond the critical flux region. This may be due to the higher concentration of cells in the fouling layer causing aggregation of the intracellular proteins, allowing for easier passage of the Mab' molecules (Krishnan et al., 1994). This suggests that the optimum operating point (in terms of product yield) may not be at stable operating conditions i.e. at constant flux or TMP, and thus the use of depth filtration or allowing the filter to foul may be a better option for maximising product yield.

One of the advantages of the TFF USD device is that both of these options could be investigated rapidly, with small amounts of feed material. By capping off the retentate ports, and feeding the broth into the top port of the TFF USD device (see Chapter 3),

depth filtration could be mimicked (see also Chapter 10). Deliberately letting the filter foul to optimise product yield would be allowable if the filters used at production scale were disposable (Meacle et al., 1993; Novais, 2001), or if they could be successfully cleaned after processing (see Chapter 1). This would directly influence the choice of membrane material and module type selected for scale-up studies.

7.2.2 Membrane material selection

A series of experiments were conducted to illustrate how different membrane materials could be assessed using the TFF USD device during initial process development studies. Often, time and feed material restrictions prohibit this type of study for bioprocesses (see Chapter 1). The choice of membrane and pore size is usually selected on the advice of a membrane manufacturer (C. Spicer, C*a*T, personal communication, 2005).

By keeping the feed type (C*a*T broth ALI-29OCT04) and operating conditions constant (permeate recycle, disk rotation speed 1500rpm) three types of membrane coupon were assessed for flux performance (Figure 7.5), product transmission (Figure 7.6), and membrane regeneration after cleaning (Table 7.2). This disk speed (equivalent shear rate at the membrane $3000s^{-1}$) was selected based on the findings of Maiorella et al. (1991) suggesting that this was the critical average wall shear rate above which damage to mammalian cells of different types occurs. The cleaning procedure used is described in Chapter 4, and complied with the recommendations of the membrane manufacturer.

The data shows that there is no significant difference between the filtration performance of the different membranes, despite the wide range of pore sizes (~0.1μm to 0.45μm), suggesting that the secondary membrane of cell debris is the controlling barrier to product transmission (Cheryan, 1986). However, the excursion curves presented in Figure 7.5, show that higher permeate fluxes can be obtained with the 0.2μm Supor membrane; increased throughput would mean shorter processing times.

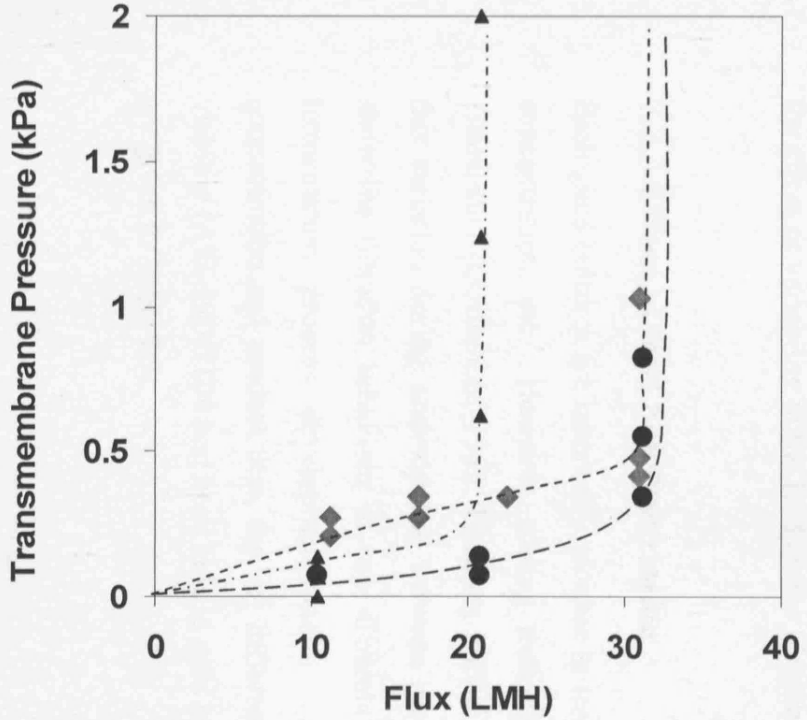

Figure 7.5: Comparison of excursion curves obtained with different 25mm membrane coupons held in the TFF USD device. 1000kDa Biomax (▲), 0.2μm Supor (●) and 0.45μm hydrophilic Durapore (◆) membranes. TFF USD device disk rotation 1500rpm, total permeate recycle filtration of CaT broth (ALI-29OCT04). Curve lines shown for easier interpretation of data.

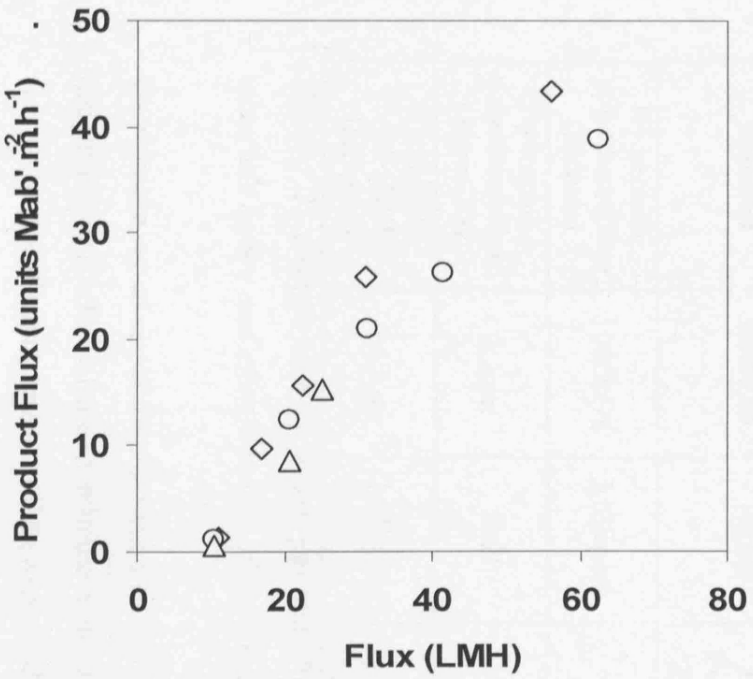

Figure 7.6: Comparison of relationship between permeate flux and product flux obtained with different 25mm membrane coupons held in the TFF USD device. 1000kDa Biomax (△), 0.2μm Supor (○) and 0.45μm hydrophilic Durapore (◇) membranes. Device disk rotation 1500rpm, total permeate recycle filtration of CaT broth (ALI-29OCT04). Data points are the average value of the assay results obtained from two replicates of each permeate and retentate sample.

Membrane Material	Pore size/ MWCO	Manufac -turer	Initial Hydraulic Permeability (LMH/kPa)	Post-cleaning Hydraulic Permeability (LMH/kPa)	%Recovery of Hydraulic Permeability
Hydrophilic polyethersulfone (Biomax)	1000kDa	Millipore	101	88	87
Hydrophilic polyethersulfone (Supor-200)	0.2μm	Pall	233	233	100
Hydrophilic PVDF (HVLP Durapore)	0.45μm	Millipore	496	441	89

Table 7.2: Comparison of water permeability data for various membrane coupon materials before and after filtration of CaT broth ALI-29OCT04.

This simple set of experiments (which took less than a day to complete) gave valuable insight into the effect of the membrane material on the filtration of the C*a*T broth i.e. it was not a significant parameter that warranted further investigation. Having ruled out this variable so quickly using such small amount of material (potentially very early on in the process development cycle, see Chapters 1 and 8), the investigation of other filtration parameters could be conducted in the quest to optimise the purification process. The following section describes the data obtained during an investigation into the effect of variability in the feed on the filtration behaviour.

7.2.3 Effect of feed batch variation

Biological cultures are inherently variable in terms of final cell concentrations, product concentration, etc. However, scaling techniques for fermentation have long been established (Oosterhuis, 1983; Lamping 2003), and much effort is made to minimise this variation during scale-up and between production batches. Figures 7.7 and 7.8 show the filtration behaviour of two different batches of material produced by the fermentation process development team. Although similar in terms of cell concentration and product titre, the key difference between the two feeds was the cell viability (ALI-29OCT04 had been held in cold storage). Details of the two feed batches are given in Table 7.3.

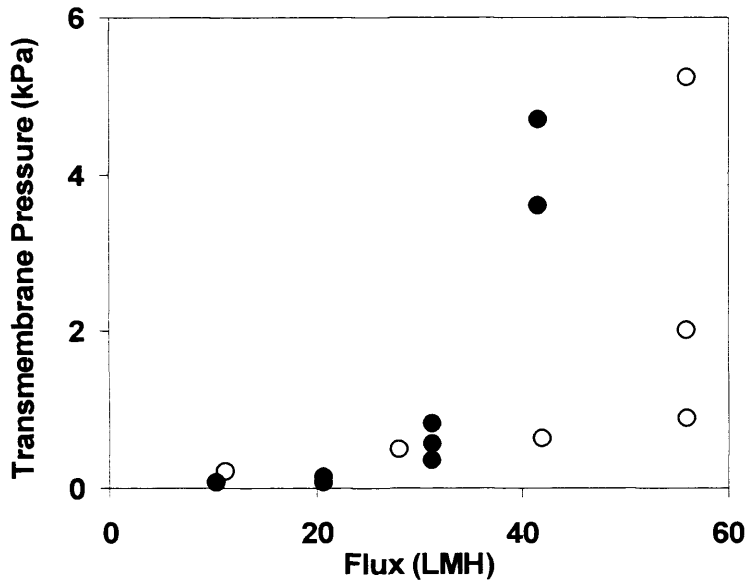

Figure 7.7: Comparison of excursion curves obtained with 25mm membrane coupons held in the TFF USD device. CaT broth ALI-29OCT04 (●) and CaT broth KM-02DEC04 *(○). 0.2μm Supor membrane (Pall, UK). Device disk rotation 1500rpm. Total permeate recycle.*

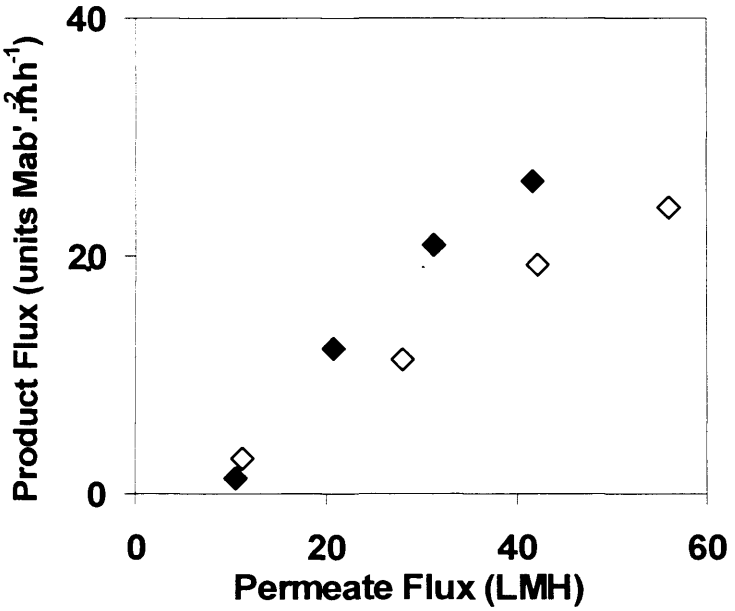

Figure 7.8: Comparison of relationship between permeate flux and product flux obtained with 25mm membrane coupons held in the TFF USD device. CaT broth ALI-29OCT04 (◆) and CaT broth KM-02DEC04 (◇), 0.2μm Supor membrane, device disk rotation 1500rpm, total permeate recycle filtration. Data points are the average value of the assay results obtained from two replicates of each permeate and retentate sample.

Fermentation ID	ALI-29OCT04	KM-02DEC04
Fermentation volume (L)	20	100
Time held in storage at 4°C (days)	28	1.5
Cell concentration (units.L^{-1})	61.8	68.9
Product concentration (units Mab'.L^{-1})	0.53	0.63
Cell viability (%)	< 1	> 60

Table 7.3: Details of CaT broths used in feed batch variation experiments.

The data indicates that cell viability is an important parameter in terms of the filtration operation. Figure 7.7 shows that a much lower critical flux region was identified using the older broth (ALI-29OCT04). This would be expected, as greater quantities of intracellular proteins would be released into the feed, and the lysed cell debris would foul the filter more quickly. However, as Figure 7.8 shows, the difference in product flux is not great. In fact the older broth gave larger product fluxes, despite having a lower initial product concentration (see Table 7.3). This is concurrent with literature examples where although fouling is more severe in the presence of cell debris, the formation of a secondary cake layer prevents the formation of a dense protein layer, therefore improving overall transmission rates (Kuberkar and Davis, 1999).

The impact of the cell viability on filtration performance is discussed further, with relation to the fermentation harvest point in Chapter 10. The effect of the diafiltration buffer on the filtration performance was investigated, and the results presented in section 7.2.4 below.

7.2.4 Concentration/diafiltration studies

Constant volume diafiltration (DF) is often used to separate biological molecules from complex fermentation feeds, to avoid concentration of the non-permeated species (Meagher et al., 1994). The standard operating protocol for filtration of similar *CAT* fermentation broths involved a 10-fold concentration before starting DF, so as to reduce the amount of DF buffer required. Hence, this procedure was used to produce the data presented in Figure 7.9 and 7.10.

The permeate flux value was set at 30LMH, which was below the critical flux region previously identified (see Figure 7.7) for both of the feed batches investigated. During the filtrations, the TMP increased in first 20mins (stabilisation period) then settled to a constant value, confirming the sub-critical flux operation. Again, a greater filtration driving force was required to filter the older broth, which is concurrent with the data presented in section 7.2.3 above.

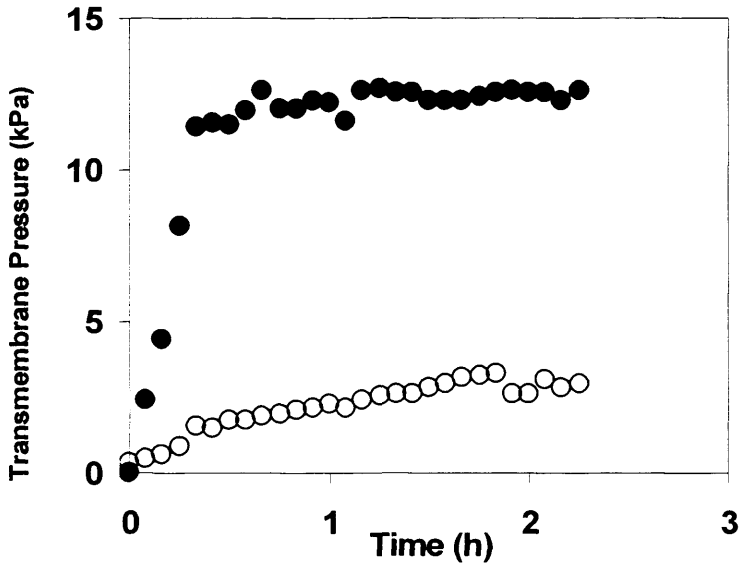

Figure 7.9: Comparison of TMP data during constant flux filtration (1.7h concentration at 30LMH, followed by 0.5h constant volume diafiltration with PBS at 30LMH) obtained with 25mm membrane coupons held in the TFF USD device. CaT broth ALI-29OCT04 (●) and CaT broth KM-02DEC04 (○). 0.2μm Supor membrane. Device disk rotation 1500rpm.

Figure 7.10 shows the product and cell solids concentration profiles obtained during the KM-02DEC04 filtration. The data confirms that the cells are retained within the retentate and as the cell solids were concentrated, so was the product. This indicates that product was partitioning with cells, and that diafiltration may be necessary to optimise product recovery.

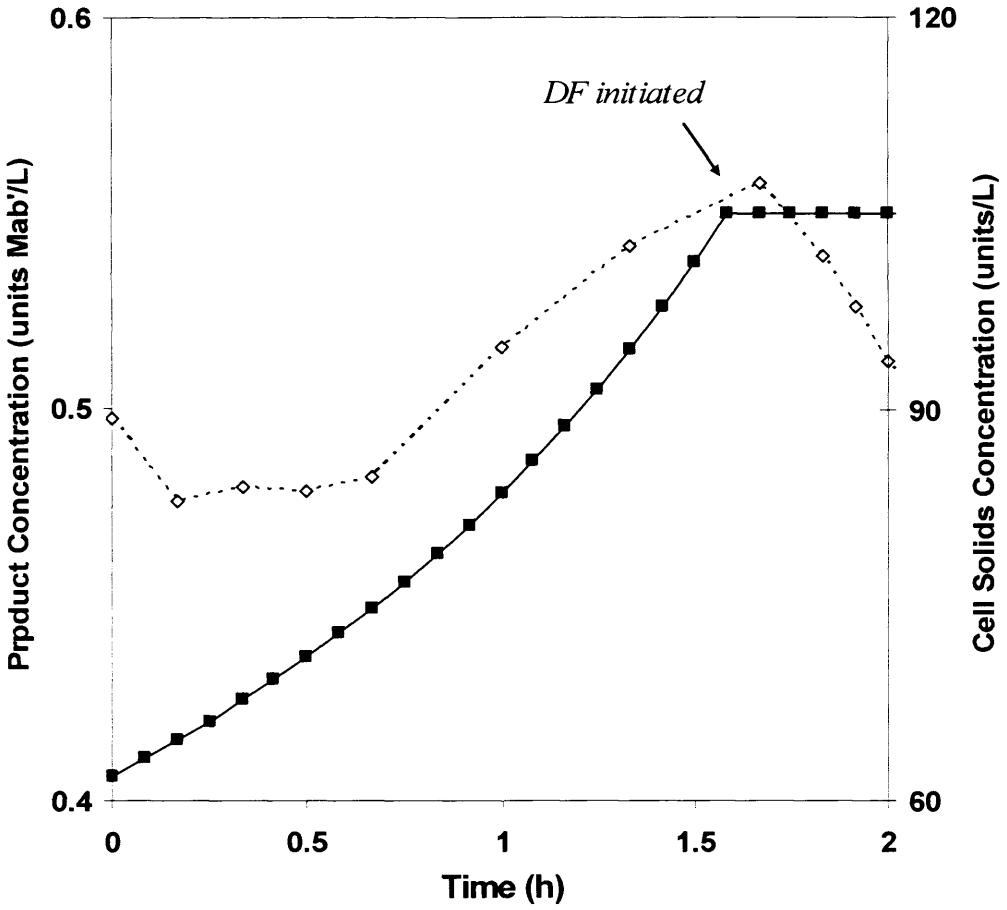

Figure 7.10: Retentate concentration profiles of product (◇) and cell solids (■) during constant flux filtration (1.7h concentration at 30LMH, followed by 0.5h constant volume diafiltration with PBS at 30LMH). CaT broth KM-02DEC04. 0.2μm Supor membrane (Pall, UK). Device disk rotation 1500rpm. Data points are the average value of the assay results obtained from two replicates of each permeate and retentate sample.

Figures 7.11 (a) and (b) shows the product transmission data, in terms of percentage transmission and product concentration in the retentate, obtained during the same experiment. The exponential decay transmission relationship described by equation [6.12] (see Chapter 6) was fitted, showing that product transmission declined rapidly during the concentration phase, but that the use of diafiltration only marginally reduced the rate of decline. Presenting the data in terms of product concentration in the retentate makes it easier to consider the data in terms of product yield (see Figure 7.11(b)).

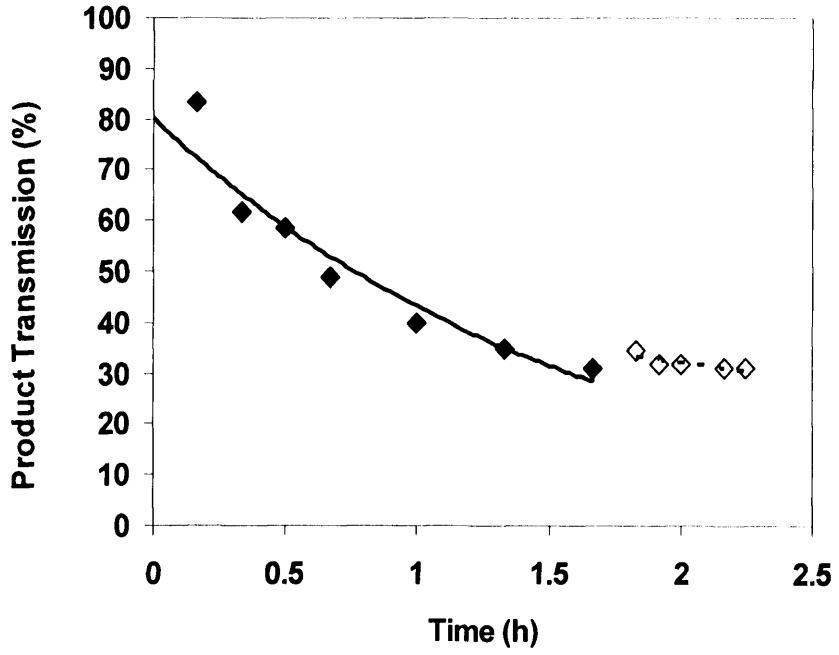

Figure 7.11(a): Product transmission behaviour during constant flux filtration at 30LMH. 1.7h concentration (◆), exponential decay curve $\%T_{conc} = 80e^{-0.6t}$, *correlation coefficient* $R^2 = 0.94$ (——), *followed by 0.5h constant volume diafiltration with PBS (◇),* $\%T_{DF} = 50e^{-0.2t}$, $R^2 = 0.70$ (- - -). *CaT broth KM-02DEC04. 0.2μm Supor membrane (Pall, UK). Device disk rotation 1500rpm. Data points are the average value of the assay results obtained from two or three replicates of each permeate and retentate sample.*

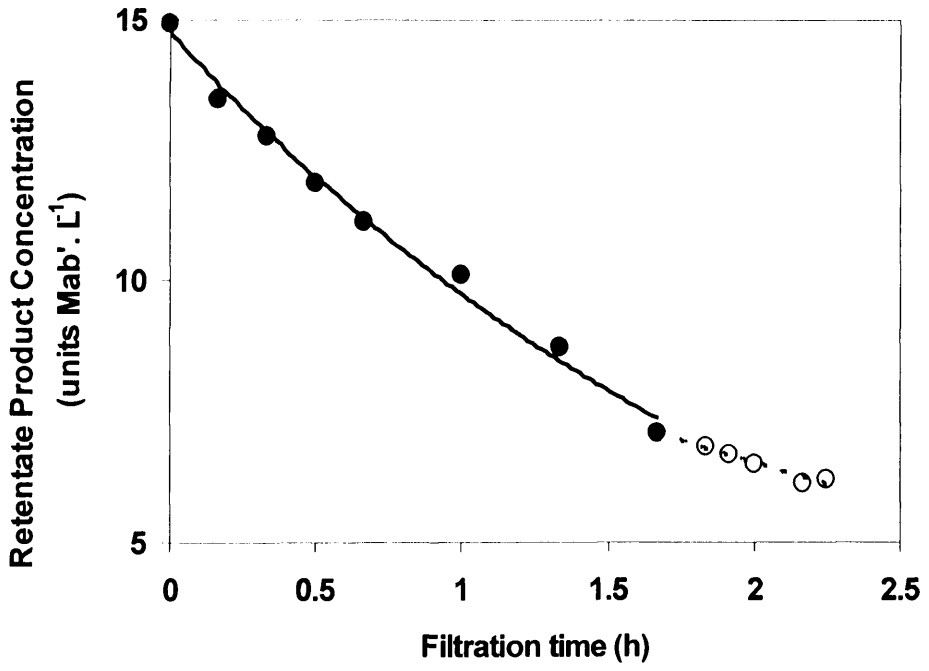

Figure 7.11(b): Product concentration in retentate during constant flux filtration at 30LMH. 1.7h concentration (●), exponential decay curve $[Mab', ret]_{conc} = 14.8e^{-0.42t}$, *correlation coefficient* $R^2 = 0.99$ (——), *followed by 0.5h constant volume diafiltration with PBS (○),* $[Mab', ret]_{DF} = 7.1e^{-0.26t}$, $R^2 = 0.97$ (- - -) *CaT broth KM-02DEC04. 0.2μm Supor membrane (Pall, UK). Device disk rotation 1500rpm. Data points are the average val ue of the assay results obtained from two or three replicates of each permeate and retentate sample.*

The product transmission data is described well by the exponential decay relationship described in equation [6.1] (Chapter 6). Extrapolation of this curve allows the prediction of when transmission would drop below an acceptable level, and therefore the ability to see the trade-off between processing time, DF buffer requirements and product yield.

An example of how this may be done is given in Table 7.4. For example, say that the process development target for the filtration step was 80% product recovery, the number of diavolumes required to achieve this 2. However, if the yield required was 90%, double the number of diavolumes would be required (N=4). It would also mean double the amount of filtrate to be processed by further bioprocess steps e.g. chromatography. The effect of membrane area could also be investigated, but it must be noted that the decay curve coefficients are only valid for the flux rate and concentration time period of the empirical data.

Initial Feed Volume	L	100	100	100
Product Concentration in Feed ($[Mab', ret]_{feed}$)	units Mab'. L^{-1}	15	15	15
Membrane Area (A)	m^2	0.1	0.1	0.1
Operating Flux (J)	LMH	30	30	30
Concentration phase;				
Time (t)	h	1.7	1.7	1.7
Final retentate volume	L	5.1	5.1	5.1
Product Concentration in Retentate ($[Mab', ret]_{conc}$)	units Mab'. L^{-1}	7.2	7.2	7.2
Diafiltration				
Time (t)	h	3.4	6.1	8.5
No. of diavolumes (N)	diavolumes	2	4	5
Volume DF buffer	L	10.2	18.2	25.4
Volume of Filtrate	L	153	233	305
Final Product Concentration in Retentate ($[Mab', ret]_{DF}$)	units Mab'. L^{-1}	3.0	1.5	0.8
Overall Product Yield	%	***80***	***90***	***95***

Table 7.4: Example predictive calculation results for amount of diafiltration buffer (and filtration time) required to achieve specified step yields. Product concentrations calculated from $[Mab', ret]_{conc} = 14.8e^{-0.42t}$ *and* $[Mab', ret]_{DF} = 7.1e^{-0.26t}$.

As suggested in Chapter 1, this information could be also be linked to cost data (e.g. cost of buffer, or cost of membrane area) to look at the trade-off between filtration time and product yield from an economic perspective. This is discussed further in Chapter 9.

7.2.5. Diafiltration buffer studies

The poor transmission data obtained by using PBS as a DF buffer (~40%, see Figure 7.11(a)) warranted an investigation into the effect of the type of buffer used (see also Chapter 6). The feed type and operating conditions were kept constant for each experiment, and pH was also monitored (data not shown as pH values remained constant). The Mab' product pI was approximately 6.6, so the filtration pH profile had to avoid going through this point, as this could cause irreversible damage to the molecule structure (R. Turner, C*a*T, personal communication, 2005).

Figure 7.12 shows the overall step yields obtained during constant flux diafiltrations with three different C*a*T DF buffers. A marked improvement (almost 20%) in yield can be seen with the use of Buffer B, and thus this should be considered as an alternative for the DF operation. However, the effect of this change in buffer environment on the efficacy of the Mab' product molecule would have to be verified beforehand.

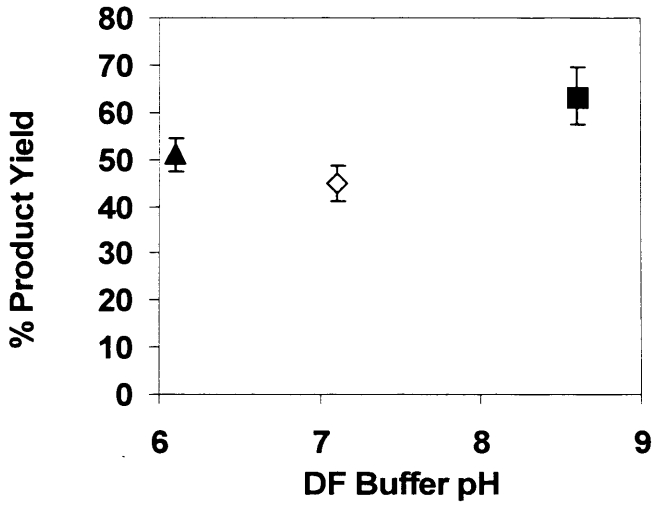

Figure 7.12: Effect of type of diafiltration buffer on product yield. Buffer A pH6.1 (▲), PBS pH7.1 (◇), Buffer B pH8.6 (■). Constant volume diafiltration at 30LMH for 1h. CaT broth KM-02DEC04. 0.2μm Supor membrane (Pall, UK). Device disk rotation 1500rpm. Error bars are the maximum and minimum calculated yields from assay sample replicates.

Further study on the effect of the DF buffer composition would be recommended from these initial findings. The data obtained above was using only 0.1L of feed, in a few hours.

7.3 TFF USD index and WinOp generation for a mammalian cell broth

As discussed in Chapters 1 and 2, the data obtained from scale-down experiments needs to be presented in an industrially relevant form i.e. the key data should be easily interpreted (see Figure 1.6, Chapter 1). In addition, the definition of a USD index for TFF would allow the data obtained from different feed/membrane combinations to be compared by a single figure (see Figure 2.6, Chapter 2), facilitating the use of this information during whole process modelling (see Chapter 1).

Figure 7.13 shows a plot constructed to determine such a filtration performance USD index. The plot differs slightly from Figure 2.6 in that instead of plotting shear stress (τ_w) against permeate flux the shear rate (γ_w) was used (this is acceptable if the broth rheology is Newtonian i.e. constant over the range of shear). In addition, the units of flux converted to a linear velocity ($m.s^{-1}$), so that the gradient of the critical ratio of permeation flux to wall shear rate line can be expressed as essentially a resistance value (m^{-1}). The use of this information is discussed further in Chapter 9.

It is below this line, that the filtration parameters should be set for stable operation at larger scales. The plot can also be used as the basis for a Window of Operation (see Chapter 2, Figure 2.7). A hypothetical WinOp is shown in Figure 7.14 for this feed and membrane combination, based on Figure 7.13.

This visual representation conveys the range of shear rates and permeate flux rates that should be investigated during larger scale trials at a glance (see Chapter 2). It identifies operating conditions which would be robust i.e. repeatable within specified tolerances, which is of great importance during production. The WinOp also simply illustrates that if the process design target flux was e.g. 10 $x10^{-6}ms^{-1}$, the process is not possible with the membrane tested, prompting investigations into different membrane materials, alteration of the fermentation conditions, or even seeking an alternative unit operation for the processing step.

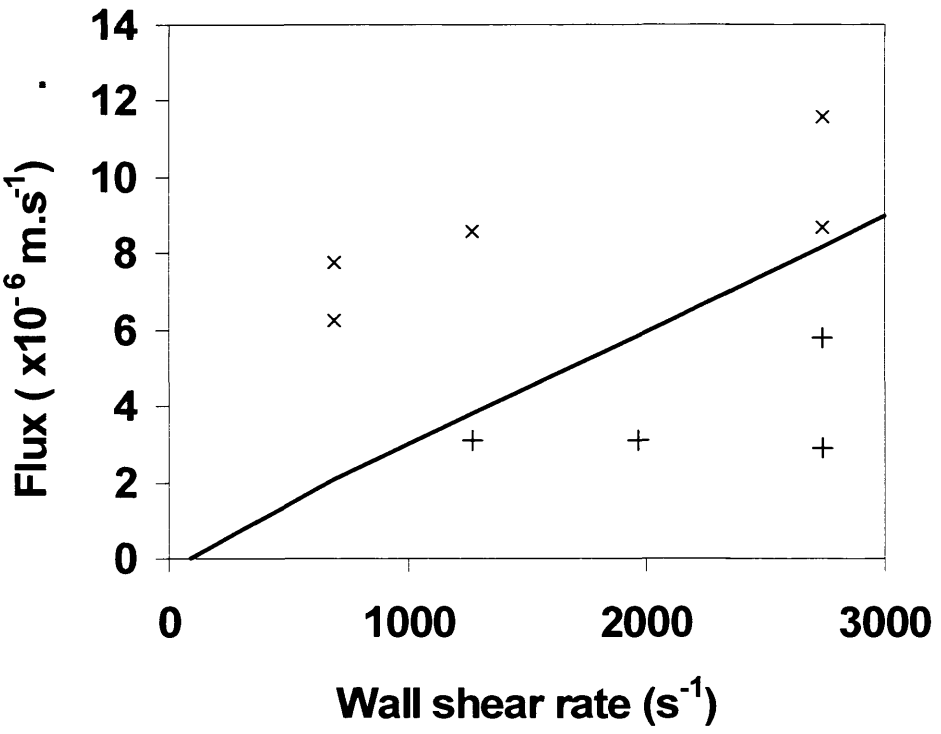

Figure 7.13: Plot to determine the critical ratio of permeation flux to wall shear rate (J/γ_w = 0.37m^{-1}) for constant flux filtration of KM-02DEC04, with a Supor-200 membrane (Pall, UK). Unstable operating points (×), stable operating points (+). Critical erosion shear rate $\gamma_{w,c0}$ = 91s^{-1}.

The gradient of the line dividing stable operating points from unstable operation is the USD index. From Figure 7.13 the value determined for the particular broth was 0.37m^{-2}, and characterises the filtration of this feed with one parameter. This singe value can be used to compare different feed batches or membrane materials side by side. The higher the USD index, the easier the filtration is to perform i.e. higher fluxes using a wide range of recirculation rates gives stable operation.

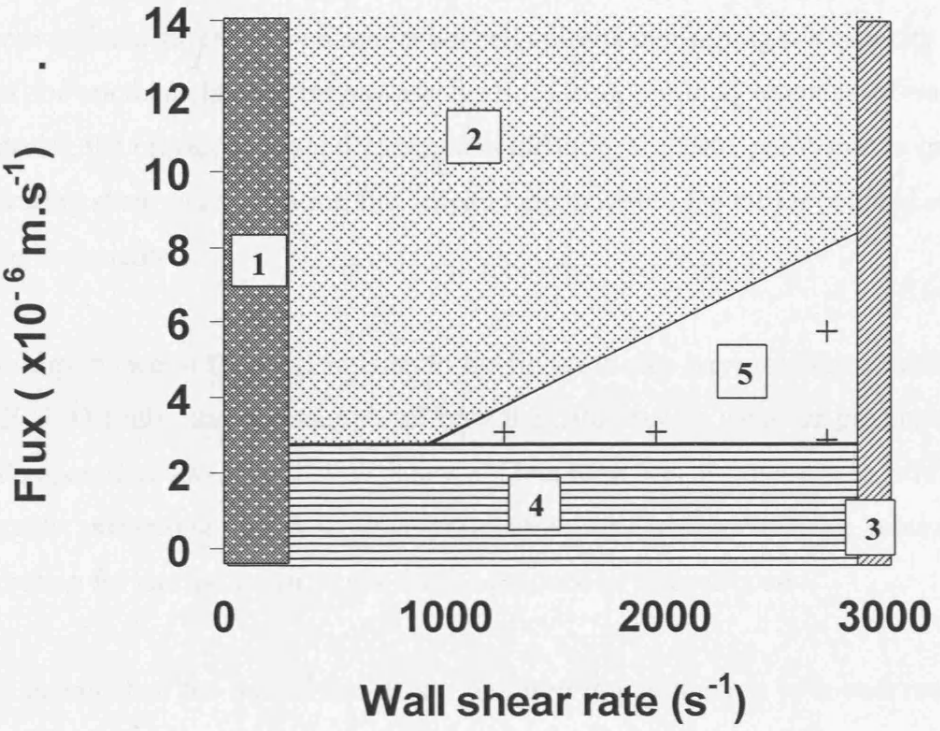

Figure 7.14: Window of Operation for TFF of KM-02DEC04 and Supor-200 membrane, generated using USD data.

Key:

1 Region below critical erosion shear rate (filter would block instantaneously) $\approx 0.91s^{-1}$.

2 Operation unstable (above critical flux) e.g. the membrane would foul rapidly above 5×10^{-6} m.s^{-1} (20LMH) below a wall shear rate of $1800s^{-1}$.

3 Maximum wall shear rate obtainable in large-scale device (or maximum shear rate product can be exposed to (set at $2900s^{-1}$ from literature value)

4 Flux rate too low for a reasonable processing time (15LMH selected here, using a $0.1m^2$ area).

5 Feasible region of operation i.e. design area for scale-up.

7.4 Summary

This practical case study has given examples of the application of the USD device and methodology in a real bioprocess development scenario.

The data presented in this chapter has shown a successful comparison of TFF USD with a conventional filter with a mammalian cell culture, confirming it's capacity to generate data for another class of bioprocess feeds. Using minimal amounts of valuable feed material, the impact of several parameters affecting filtration performance including the operating shear rate, operating flux, membrane material, DF buffer pH, and cell viability were investigated.

The importance of these parameters to the filtration step were quickly established by the TFF USD trials, and an example of how the data may be used for prediction of larger scale operation was given. A Window of Operation was also populated, with the aim of visually presenting the data in a pragmatic way, and identifying robust points of operation for use as design inputs for the production scale process.

The potential of the use of this data to be used in conjunction with cost modelling has been highlighted, and this is discussed further in Chapter 9.

Chapter 8 Business Aspects, Validation and Regulatory Concerns

8.1 Introduction

During an Engineering Doctorate candidates receive training in management, validation and commercial awareness as well as carrying out novel research. In this chapter, knowledge and skills which had been developed during the business and transferable skills course elements of the EngD programme were applied.

In this thesis the design of a novel device for the scale-down of tangential flow filtration has been presented. The work described in the previous chapters details the research conducted on the development and testing of this scale-down device to mimic pilot-scale tangential flow filtration (TFF) operations. The results from this work indicate that such a system could be useful for process development, after some refinements are made. The use of small-scale experiments in conjunction with intelligent data analysis would enable such a device to predict the behaviour of the operation at manufacturing scale. The next step is to define how such a methodology can be best used as a commercial tool for filtration process development and to describe the specifications for such a system. In turn, this will allow a plan for commercialising the product to be created.

In order to develop further understanding of the industrial environment in which TFF development work is performed, the following chapter provides the following:

- An appraisal of current process development practices;
- An assessment of the impact of USD on the management of the process development pathway;
- A discussion of the validation issues surrounding membrane filtration and the use of scale-down devices for regulatory compliance studies;
- A specification of the important features for a TFF USD system to be used for commercial process development.

Finally, the considerations required for the potential commercialisation of a TFF USD device are reviewed.

8.2 Current process development practices

The central challenge in the development of a biopharmaceutical product is to derive from a complex, unstable and inherently variable biological material, a product of defined, reproducible characteristics and predictable effect for use in medical applications (Pisano, 1997). The progress of the biological sciences in understanding the ruling mechanisms of life has enabled an ever wider array of techniques for the customisation of organisms to specific tasks as well as yielding a vast number of new metabolic targets for novel medical treatments. However, this tremendous advance in understanding and research capabilities has not been paralleled by a similar extent of progress in the process sciences. This has lead to the situation where development of processes capable of supplying purified biopharmaceuticals, economically and at large commercial scale, is increasingly becoming the bottleneck in the introduction of novel compounds to the market (Novais, 2001).

Process development procedures for pharmaceutical and biotechnology products have been well documented and reviewed (Pisano, 1997; Wheelwright, 1991; Pampel, 2000; Lamping, 2003, Reynolds, 2005, Neal, 2005, Gardner, 2005) and therefore, only a brief overview is given below.

8.2.1 The traditional biopharmaceutical product development cycle

The development cycle of a biopharmaceutical product takes it from discovery through clinical trials to market launch and continues until manufacturing is stopped either due to lack of demand or for economic reasons. The time to develop and market a new medicine varies widely, with some drugs only taking four years and others taking as long as fifteen years (Wheelwright, 1991). The product development cycle varies for each drug but process development follows a structure defined by the regulatory environment. Figure 8.1 below details a typical development cycle which illustrates the stages that are generic for the manufacture of every bioproduct.

Figure 8.1: The key stages in product development and how they coincide with process development (after Pisano 1997).

Drug discovery forms the beginning of the development cycle. Using the advanced research tools at their disposal, scientists aim to turn biomedical understanding or biomolecular discoveries into promising leads. Recently this process has been greatly accelerated by the advent of comprehensive genome and proteome information and corresponding high-throughput screening techniques. Nonetheless, a well-known rule-of-thumb suggests that out of the 10,000 candidates studied at this point, only about 20 ultimately warrant further investigation.

The predominant objective of pre-clinical development is to accumulate sufficient data to enable a decision as to whether the candidate molecule should be taken onto financially and resource expensive clinical trials. The main activities are laboratory-based, and include preliminary toxicity testing in animal models, an assessment of the pharmacological and pharmacokinetic properties of the compound and initial studies of potential delivery routes.

Clinical trials proceed through three phases. Phase I trials, usually on a small number of healthy human volunteers, are directed at evaluating the drug's safety in terms of side-effects. Phase II trials, usually on a larger group of patients suffering from the condition to be treated, and also involving placebo groups, are conducted to establish dosage and initial efficacy of the drug. Phase III trials are conducted to demonstrate definitive

safety and efficacy of the drug. Phase III trials may require several years to complete (Pisano, 1997).

Following successful completion of Phase III clinical trials, the accumulated data both on clinical aspects as well as the validation of the manufacturing process is submitted to the regulatory authorities for approval. Only then can a company start producing and selling the new drug, and recuperate the investment it has made in research and development (R&D) efforts.

Process development is a parallel activity to product development, and it performs multiple tasks within the overall product development cycle (see Figure 8.1). The goal of process development is to move from a process that has been developed for laboratory developmental work and that is pottentially complex, inefficient and difficult to scale, to one that is practical, efficient, robust and safe (Pisano, 1997). Process development encompasses all the work involved in the transition between the initial discovery phase and final commercial production.

Process development can be divided into three phases:

- *Process synthesis* which entails developing analytical methods, evaluation and exploration of cell line and purification methods at small scale and laboratory scale production of material for preclinical studies.
- *Pilot-plant development* which covers the scale up, evaluation and optimisation of the complete process.
- *Commercial process transfer and start-up*, which involves transferring the technology to the commercial manufacturing plant. This could include tasks such as optimisation of a process under commercial conditions and the validation of the manufacturing process.

Figure 8.1 also shows how these three phases interact with the overall product development cycle. Process development during clinical trials pursues three major tasks which often have conflicting objectives. On one hand, the growing amounts of material to satisfy the short-term demands of clinical trials require significant processing capacities. On the other hand, a process suitable for production at full manufacturing scale has to be developed and data generated for submission to the regulatory

authorities. As Phase III trials approach the need to obtain validation data on a process representative of that ultimately installed in the manufacturing plant rapidly decreases the flexibility of process development to seek alternative options (see section 8.2.2). Since the manufacturing facility has to be commissioned well before the completion of clinical trials, so as to avoid delays during the approval procedure, the pressure on process development to deliver a robust and economic manufacturing process early on becomes even greater.

The growing need for material quickly increases the scale of the process as clinical trials approach. The entrance into clinical trials has historically marked the transfer of the process to pilot-scale production. However, as material demands for clinical trials escalate, more and more processing capacity is committed to satisfy these needs. At the same time, the flexibility in terms of process technology is significantly reduced since the material provided for clinical trials should be produced by similar technological means as the ultimate product. As clinical trials progress, these constraints intensify the need to fix the manufacturing process technology both to supply Phase III trials and to commence validation studies of the manufacturing process. Therefore, while overall process development mostly accompanies the product development cycle, the actual time available for dedicated screening and implementation of process technology is relatively small. In addition, conventional process development methods are being exposed to changing demands and pressures which are considered further below.

8.2.2 Pilot-scale development

Traditionally pilot-scale studies have been exploratory in nature due to the fact that very little is usually known about the purification of the candidate drug in the early stages of development. Of particular importance is the scale of production; this directly influences the performance of a biotech-process, and hence it's viability. These "scale-up" effects are difficult to predict because there is little knowledge about exactly what variables might affect the process, in terms of individual unit operations and interactions between these stages. The emphasis of process development is to get the process sequence and operating parameters defined as quickly as possible.

The time and monetary constraints surrounding pilot plant trials preclude biopharmaceutical companies from thoroughly optimising a process. The current financial and regulatory environments are creating downward pressure on revenues (caused by shorter product life cycles, pressure by governments to produce cheaper drugs and increased competition) and upward pressure on manufacturing costs (caused by the increasing complexity of new drugs and stricter regulatory requirements) (Titchener-Hooker et al., 2001). Hence, the pressure to be first to market and to mitigate the risk of lost capital investment if a drug fails to get to market, outweighs the pressure of having an optimum purification process. The result is often an unwieldy, inefficient, and costly manufacturing process.

In general, pilot plant studies are time consuming expensive and require dedicated equipment (Zhou et al., 1997). Consequently, the traditional stance adopted by biopharmaceutical companies toward process optimisation has been to delay it until there was a reasonable certainty that the drug would be approved. This is in an attempt to avoid committing resources on drugs that would never make it to market. In practice, this meant investing heavily in process development/optimisation only when drugs got to Phase III clinical trials. Pilot-scale development was only considered a success when it did not get in the way of product launch. Creating an optimised process was not a high priority, as this was considered a threat to the aim of keeping process development off the critical pathway to product launch.

The reasons that have previously prohibited biopharmaceutical manufacturers from investing resources on process optimisation are three-fold. Firstly, extraordinary premiums have in the past been paid for successful biological drugs. This, and the possibility of market exclusivity during the lifetime of the product patents, has further reinforced the strategy of concentrating on product innovation rather than process improvement (Pisano, 1997; Wheelwright, 1991). Secondly, process optimisation is difficult and costly to conduct given the complex behaviour of biotechnological products and the high value of the bioproduct and biological reagents. Thirdly, the tight regulatory environment surrounding the production of biopharmaceuticals constrains the ability of companies to introduce significant changes to a process once it has been approved by the regulatory authorities (Mercer and Seely, 2000). As a result, the lack of economic benefit, together with the apparent difficulties described above has, to date,

led biopharmaceutical companies to consider the optimisation of process performance as secondary to that of establishing a validated process in the first place (Farid et al., 2000).

However, shrinking patent lifetimes, and the advent of generic competition combine to exert pressure even on established manufacturers of bioproducts. Consequently, process performance and efficiency has become an area of increasing interest. Whilst the regulatory hurdles surround process changes continue to be high, manufacturers have begun to consider these as a problem to be dealt with rather than avoided. In doing so, process development pursues three main sources of competitive advantage; first to market, high quality (in terms of purity, activity, dependability, or flexibility) and low cost (Wheelwright, 1987). These advantages are mutually dependent and optimisation of one can only be realised at the expense of others (see Figure 8.2).

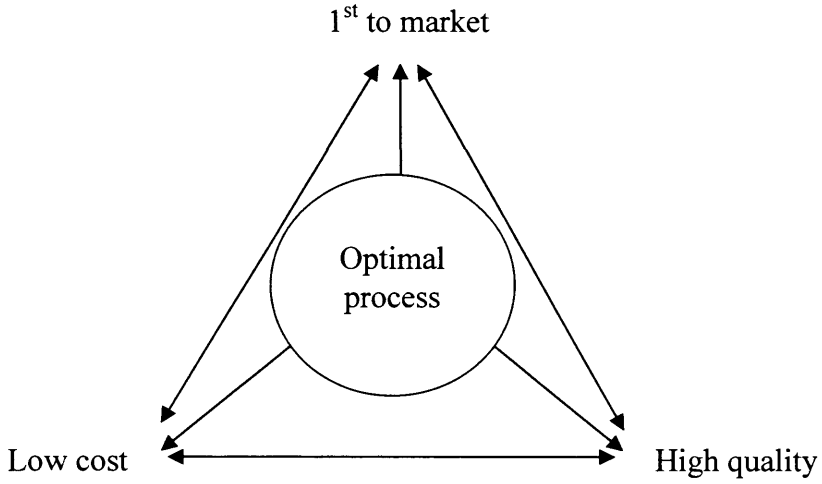

Figure 8.2 Benefits of an optimised manufacturing process showing interdependence of the three main sources of competitive advantage.

In summary, the overall goal of process development is to make as much of the product as required, of the necessary quality, as cheaply as possible and in the shortest amount of time possible. Having a high performance, robust, economic and well understood process established early on can avoid costly delays later on in development (Bobrowicz, 1999). Section 8.3 below discusses how scale-down techniques, in particular ultra scaledown (USD) methodologies, could help to achieve this aim.

8.3 The impact of USD mimics on the management of process development

It has been demonstrated that scale-down, through rapid and simple experiments, can provide much of the information needed during the early stages of process development (Varga et al., 2001). Since process synthesis seeks only to conduct a feasibility study of process alternatives, the data required from scale-down models of individual unit operations would not have to be overly accurate, and more weight would likely be placed on the rapid generation of performance data for a large number of alternative operations (Morrow et al., 2001). For optimum use of the resulting data mathematical models of unit operations could be employed and fed with actual scale-down data at critical junctures in the emerging process.

The availability of USD methodologies has caused a rethink of process development strategies. It has been proved that thorough investigation of the manufacturing process leads to improved yields accelerates throughput and reduces manufacturing cycle times (see Figure 8.3). These improvements all lead to reduced costs of manufacture and provide an advantage in terms of the potential for a company to market first with a new class of drug.

USD mimics, such as those described in Chapters 1 and 3, offer process engineers the opportunity to recreate the conditions of a manufacturing scale process on a laboratory bench top. This means that any process that utilises the unit operations that USD has the ability to mimic can be investigated at the start of the development cycle. In addition, this is at a fraction of the cost in terms of time, material and facilities. The results from these scale-down investigations ensure that process development is kept off the critical path and that a robust, effective purification process is delivered early on with a minimum number of pilot scale trials needed modify it. As a result, a biopharmaceutical company can be first to market. Complementary software would allow inputs from individual operations to be integrated into one whole purification process model. This allows process engineers to make changes to one unit operation and then monitor the effect on the whole process in terms of yield, efficiency and cost (Pampel, 2000; Neal, 2005).

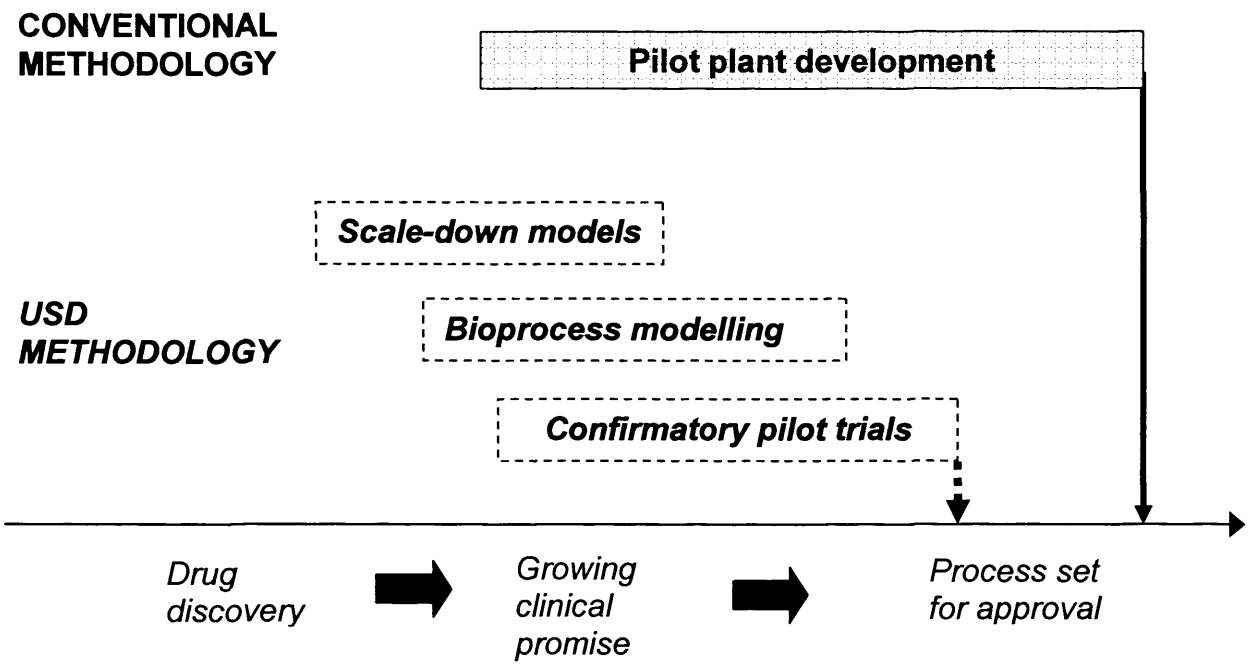

Figure 8.3: The impact of USD approaches on the capacity to gain process understanding in advance of commitment to a particular manufacturing route. Application of USD provides additional time for exploratory studies by comparison with conventional approaches to process development.

8.3.1 Use of TFF USD as a tool for process development

The application of scale-down methods during the individual phases of process development results in different requirements regarding the accuracy of the scale-down models, the level of detail employed and the time available for their generation (see Chapter 1, section 1.2.3). The ability to produce information at a laboratory scale using greatly reduced quantities of feed, that predicts and mimics the industrial scale, has interesting implications for the initial downstream process design and optimisation and how it is managed.

Towards the entrance into clinical trials, process development is faced with the task of transferring a process developed in the laboratory to the pilot plant. Resulting changes to the overall environment, analytical and monitoring capabilities as well as the type of equipment used frequently leads to undesirable changes in process performance, and associated loss of time for their rectification. Scale-down models employed prior to

process transfer can help to avoid most of such surprises, provided that critical parameters can be identified correctly represented during the generation of the scale-down models.

Scale-down models used during process scale-up require both a higher level of detail and a higher accuracy than would be called for during process synthesis. At the same time, the willingness to commit resources to the improvement of scale-down models increases since the potential benefits increase. Models used at this stage would therefore be carefully developed and validated, the prime concern being to detect and subsequently avoid potential issues resulting from the shift to process scale technology.

The TFF USD experiments described in Chapters 5 and 6 would only be used for process research, but this would result in a variety of impacts for the other stages as process definition at an early stage is improved. These impacts are discussed below and have been divided into the key process development tasks shown in Figure 8.1 i.e. process research, pilot-scale development, and technology transfer and start-up.

a) *Impact on process research*: Using the TFF USD for process development would generate far more data than using current methods, thus allowing a better understanding of the system and allowing smoother scale-up. The data would also be of a higher quality if factors, such as shear degradation that occurs in manufacturing scale equipment could be accounted for in the small-scale experiments. The TFF USD device created in this EngD uses disposable membrane disks, obviating the need for cleaning after each experiment, and therefore allowing quicker equipment turn-around. This could mean that different (better) membrane/operating conditions are chosen giving a more efficient process. As the system is so much smaller than current pilot-scale rigs, less feed, buffer and floor space is required.

b) *Impact on pilot development, scale-up and production of material for clinical trials*: If the TFF USD methodology were used correctly, a significant amount of process development work could be completed at a small scale in a very small amount of time. More data on the best process would be obtained before the pilot development stage; at best it would be possible to directly scale-up from the pilot-plant with a process that is very close to the final scale. In addition, it would be beneficial for process validation if

the product finally on the on the market is the same as the product that was used for clinical trials. As process screening increases the speed of development, it should be possible to ensure that even Phase I trials are completed with material produced using a near-final production technique.

c) *Impact on technology transfer and start-up*: As a result of the initial development stages yielding more information and potentially taking less time there should be positive consequences for technology transfer. As the process would be better understood, start-up should run directly as planned with no delays.

Apart from the obvious economic reasons, there are other impacts on the strategy for process development

- The process is locked earlier, and therefore specification of the manufacturing scale process can commence;
- A drug candidate that does not have a viable process can be dismissed at an early stages of process development instead of wasting valuable process development resources;
- Fewer delays in production start-up would allow earlier product launch.

Another consequence of the TFF USD methodology is its use for whole process optimisation. The development of purification techniques tends to run parallel to fermentation optimisation. Traditionally, a clarification filtration process was developed for the broth that gave the maximum yield during fermentation; variables such as harvest time, and media components were not optimised in terms of the filtration. Rapid experiments to assess filtration feasibility would allow input into the decision processes of the fermentation scientists i.e. a feed back loop that would identify the trade-offs between the two unit operations.

Additionally, material must be provided to further the development of operations further downstream, such as chromatography. For the best optimisation of these purification operations, the test material provided must be as similar to that produced using the final production process as possible, as even minor changes to media or impurities could affect the unit operation performance significantly. USD models aim to mimic the manufacturing scale process, and hence satisfy this requirement better than current

methods. Again the trade-offs between the different unit operations could be evaluated in terms of process feasibility and economics, allowing for optimisation of the whole process (see Chapter 9).

In order for the use of scale-down methodologies to be used as an aid for process development, they must comply with the regulations governing the bioprocess industry. These requirements are discussed in the following section, along with the concept of using USD tools to generate the validation data needed to gain process approval.

8.4 Regulatory and validation issues arising from the use of USD mimics during process development

Before a new biological product is brought to market, regulatory approval of the process and the product must be obtained. Regulatory requirements and industry standards have increased dramatically over the past three decades which has led manufacturers to increase their spending in order to achieve a compliant process (Winkler, 2000). The United States' Food and Drugs Administration (FDA) is responsible for licensing all new drugs that are sold in the USA, and is often considered to be the benchmark. There are equivalent regulatory organisations for other parts of the world, such as the European Medicines Agency (EMEA).

One important requirement of all the major regulatory bodies is that the manufacturing process must be fully validated. Process validation is defined by the US Food and Drug Administration (FDA) as "Establishing well documented evidence which provides a high degree of assurance that a specific process will consistently produce a product meeting its pre-determined specifications and quality attributes". Essentially, this means providing evidence that a process does what it was designed to do.

Validation can be a lengthy and expensive process but it is crucial to ensure product safety and quality. As well as regulatory requirements and gaining approval, thorough validation of a procedure has other benefits such as increasing the robustness and reliability of a process and reducing the number of failed batches. Consideration of validation issues should begin as early as possible, usually at the laboratory

development stage since the process will need to be validated before clinical trial material can be manufactured and released.

As a consequence of rapidly changing technology, approaches to validation are also being modified; it is important that a company keeps up to date with the latest trends (e.g. risk based approaches to equipment operation). The vast majority of process validation work is carried out at full or pilot plant scale. However, in some situations it is advantageous either in terms of time, cost or safety to carry out validation studies at small-scale (Sofer, 1996).

The next section discusses the issues surrounding the use of a TFF USD device for validation purposes, and will outline the validation procedures for the unit operation.

8.4.1 Scale-down as a tool for validation

Good scale-down methods can make validation of a large-scale process easier by enabling greater process knowledge and understanding. Since much of the data that would be too expensive to create at large scale can be generated using scale-down techniques a thorough study of the process responses is possible. This makes it easier to define critical process parameters and set operating limits and acceptance criteria for the process.

The accuracy required of a scale-down model used for conducting validation studies is high; equivalency in terms of performance between the model and the full-scale process must be demonstrated. However this can remove some of the burden of validating the full-scale process. For example, to prove the process is consistent, consecutive batches at full or pilot-scale are executed using exactly the same equipment and protocols as would be produced during routine manufacturing. In the USA, this is typically a minimum of three batches; in Europe five batches are required. However, in many cases three runs are not sufficient due to performance differences on scale-up which mean that product specifications or processing conditions have to be adjusted. Scale-down models can be used to set more realistic specifications so that the number of verification runs required can be kept to the minimum. This results in considerable savings in time and resources.

In addition, some validation studies, such as virus removal, are difficult to conduct at large scale (Sofer, 1996). The most comprehensive way to measure virus clearance is using virus spiking studies, where a known virus titre is added to the feedstock for a step and the numbers of viruses present in the feed stream after that step are calculated. Performing this type of study in a full-scale plant would be dangerous and it would be nearly impossible to prove that all the viruses have been removed from the facility. However, an accurate scale-down model of the step could be used to determine the level of virus clearance that could be expected much safer and controlled environment (Morfeld et al., 1996). Others studies, such as chromatography matrix lifetime evaluation, are practically impossible to conduct unless performed in automated scale-down experiments (Sofer, 1996).

USD mimics such as the one developed in Chapter 3 allows initial process development work to be carried out at a very small scale which requires only very small quantities of material. This would allow a company wishing to develop and market a product to conduct more research on purification process should it wish to. This in turn could generate more evidence that the manufacturing process is robust and reproducible since a greater number of experiments could be conducted testing the manufacturing process to verify its design.

However, if this information were to be submitted as a part of the validation process the USD device itself would have to be validated. This would involve the standard installation, operation and performance qualifications required for any piece of bioprocess. In order to do this the manufacturer of any USD device would have to provide evidence and details of the working ranges/conditions within which the device has been tested to show that when used under the tested operating conditions, it will generate results that compare to the full-scale process.

Scale-down models of chromatographic separations have probably gained the widest application in the industry. This popularity mostly relates to their application in scale-down scouting and optimisation as well as process validation studies (Winkler et al., 2000). The benefit of small-scale models for work is most obvious in chromatography due to the high price of packing materials. It was demonstrated that small-scale prospective validation studies could accurately predict the performance of

chromatography resins at manufacturing-scale (O'Leary et al., 2001). The resulting rules for the validation of scale-down chromatography models can therefore serve as a guideline to the requirements that scale-down models of other unit operations will have to satisfy.

8.4.2 Validation of membrane TFF processes

The validation process issues related to membrane filtration in bioprocesses are well documented, and specific guidelines are available for membrane filtration from manufacturers and the appropriate regulatory authorities e.g. FDA, EMEA. Many publications are available which describe how to qualify TFF systems and validate TFF process steps, as well as covering topics such as installation qualification, performance qualification, when to validate, and validation issues for TFF operators. Michaels (1991) provides an industrial perspective of the general principles outlined in the FDA's guideline as applied to the specific problem of validating a TFF process.

The validation of a filtration process starts with the equipment qualification of the filter module. The majority of this (approximately 90%) is completed as part of installation of the equipment but the remaining percentage is product and process specific. Equipment qualification consists of installation qualification (IQ) and operational qualification (OQ).

For a filter module, the IQ and OQ confirm that each component of the system meets the manufacturer's design criteria, including any valves and pumps associated with the device. IQ studies establish confidence that the process equipment and ancillary systems are capable of consistently operating within established limits and tolerance. OQ provides documented verification that the equipment and ancillary systems perform as intended throughout anticipated operating ranges.

Process performance qualification (PQ) is the documented evidence that a process operated within established parameters performs effectively and reproducibly to produce a product that meets predetermined specifications and quality attributes. Process qualification is aimed at ensuring process consistency. Process performance can be defined in terms of a number of parameters/ such as yield and purity of product

which must be reproducible within a defined operating range. Generally parameters that are validated during the PQ are defined within broad ranges during the development stages of a process, but are narrowed as understanding of the process is gained through experience. For TFF these parameters include recirculation rates, membrane loading and either flux or transmembrane pressure.

With the advances in scale-down techniques, it may be possible to use data from smaller scale experiments to reduce the number of PQ trials at full-scale. Section 8.4.3 looks at the factors that need to be considered if a TFF USD methodology were to be used for this purpose.

8.4.3 Design considerations for a TFF USD device to be used for validation purposes

The EMEA defines the different scales use in the development of a manufacturing process:

1) *Laboratory scale* - These are produced at the research and early development laboratory stage; they may be of a very small size (e.g. 100-1000 times less than production scale). The purpose of these batches is the definition of critical product performance characteristics and thereby to enable the choice of the appropriate manufacturing process.

2) *Pilot scale* - Pilot scale batch size should correspond to at least 10% of the future industrial-scale batch. The role of pilot scale batches is to enable smooth passage to the industrial scale product without major production difficulties, by developing and optimising a robust and reproducible manufacturing process.

3) *Industrial scale* - These batches are of the size which will be routinely produced during the marketing phase of the product.

The TFF USD would therefore be classed as a laboratory scale device. Despite the large scaling factor it should be able to provide useful data for process development. It is possible that information gathered from such studies could show an understanding of

a process or could be used to set critical process parameters. However, if this information were to be used for regulatory means, proof of comparability between scales would be required (see section 8.4.1). The type of data that would be required to show comparability between manufacturing scale and USD scale would be:

- Comparability of species fractionation throughout the entire filtration process;
- Comparability of productivity throughout the entire filtration process;
- Comparability of end-product quality.

Each of these points should be tested over a number of scales to ensure that the mimic is valid and to check the extent of the comparability.

8.4.3.1 Materials and apparatus

An accurate scale-down model will include all pipe work and auxiliary equipment associated with the operation. A mimic of a filtration unit will also consist of the material supply lines, pipe work, detectors, valves and pumps. It is important that all these components are represented as any changes to the system could result in a change in performance. It is also preferable to keep materials of construction for any wetted parts the same at both scales. This is because different materials may adsorb proteins or leach contaminating molecules into the process streams. Obviously it is not always possible to use the same materials of construction at the two scales but great care should be exercised to ensure that whatever material is used does not interfere with the process.

The membrane used in the scale-down mimic must be exactly the same as the membrane used in the commercial process i.e. the same manufacturer as well as material and pore rating.

8.4.3.2 Buffers and Feedstock

Every company will have its own, well-established protocols for large-scale buffer preparation. In order to validate a laboratory mimic the same protocols should be shown at a larger scale to ensure all the properties of the buffer are retained. It is also important that the ingredients used in buffer preparation are of the same standard as that used at commercial scale. So if water for injection (WFI) is used to make buffers at the industrial scale it must also be used for the laboratory mimic.

The concentration of salt, protein, product and other components in the feedstock must be identical at both scales. Ideally for validation studies actual feedstock from the industrial process should be used. However, at small scale the addition of material to the feed, such as a viral spike, can have an effect on concentration, ionic strength and pH. The consequences of any changes are variable and may be hard to detect. To avoid any undesirable effects the pH and/or ionic strength should be adjusted to the appropriate values. If it is not possible to get the conditions exactly as they are in the commercial process, then a statistical design of experiments (DOE) approach could be used to determine the sensitivity of the process to the parameters. If the process is insensitive to any given parameter then it may not be essential to maintain that parameter upon scale-down.

8.4.3.3 Operational considerations

There are a great many process parameters that need to be considered when scaling down membrane TFF (see Chapters 1 and 3). Although, the volumetric feed/retentate flow rate should be suitably reduced, either the linear recirculation velocity or residence time (or both) should be maintained in order to replicate the contact times at industrial scale. These affect concentration polarisation, so if they are changed it will be necessary to show that the change has negligible effect on performance.

Another factor to be considered is the temperature of the operation. Temperature can affect the viscosity of solutions, alter the rate of particle aggregation and disrupt the conformation of a protein. It is therefore important that the temperature of the process is controlled at both scales. This applies not just to the membrane module itself but to all elements of the filtration system, e.g. if cleaning buffers are maintained at 50°C at the industrial scale then the laboratory experiments should also keep the buffers at this temperature.

Validation studies that may be performed using the TFF USD include membrane regeneration and module cleaning studies, as well as the core unit operation. Studies to demonstrate the number of times that a filter cassette could be reused may result in operational cost savings. Cleaning studies at small-scale would not only establish that a

certain protocol was effective, but would also allow for the investigation of the impact of different procedures on membrane lifetime.

8.5 Factors to consider for the commercialisation of a TFF USD device

In an increasingly competitive environment process economy is a key issue in the management of bioprocesses. Reducing the number of processing steps can lead to savings in operational cost and processing time and will improve the overall process yield (Novais 2001).

Companies such as Millipore Corporation are market leaders in the production of filtration membranes and devices, which allow the combination of concentration and purification within a single unit operation. However, in order to remain in such a position, it is important that their products for this unit operation are able to keep up with advances in the field and customer requirements.

Below is a discussion of the steps required for the potential commercialisation of the TFF USD device. These are:

- Definition of the product concept
- Assessment of the market and the barriers to market
- Preparation for product launch
- Further product pipeline

8.5.1 Product definition

The device described in Chapter 3 could, with some refinements (see Chapter 9) be developed into a marketable product. However, its benefits are only realisable in conjunction with a small-scale filtration rig and instrumentation and a method of analysing the data generated.

The TFF USD tool should therefore be marketed as part of a complete package comprising of the device itself, a Good Manufacturing Practices (GMP) compliant rig, guidelines for USD methodology experimentation and associated software for analysing, comparing and storing the data generated.

The extent of the development of the "ancillary" product parts will depend on the market sectors which the product is aimed at. For example, if the device were to be marketed as a validation tool, it must meet with the material requirements listed in section 8.4.3.1.

8.5.2 Accessing the market and extracting financial value

This section outlines the issues to consider before the commercialisation of the TFF USD device. It could be used as the starting point for a business plan to attract external or internal organisation support.

8.5.2.1 Market size and share

As discussed above, the TFF USD has the potential to be used during drug discovery, process development, process validation and process improvement. Any institution active in these areas are potential customers for the TFF USD product e.g. academic centres, specialist biotech companies, multinational pharmaceutical companies and contract manufacturing organisations (Neal, 2005).

Financial remuneration for developing the TFF USD package could be in the form of charges for process development services, training courses, as well as the sale of the device, software and ancillary equipment required to conduct these scale-down studies.

Investigation into the number of such institutions would provide the starting point to make an assessment of the potential market available. How much of that market share could be obtained would depend on the competition.

8.5.2.2 Barriers to market - competition

The two areas of potential competition for the TFF USD device are the hardware (the apparatus) and software (equipment control, process simulation) components.

In terms of hardware, there are external and internal competitors. The external competitors are the lab-scale systems available from other filtration equipment manufacturers such as Pall, Sartorius, GE Healthcare, Whatman (see Chapter 3).

Internal competition is from Millipore's own devices, such as the laboratory scale Pellicon XL system and the Advanced Process Development System (APDS) for Tangential Flow Filtration (Kierans and Shaw, 2004).
The competitive advantage of the TFF USD is its ability to evaluate membranes from different manufacturers, which is currently not possible. In addition, it provides the possibility of removing the membrane post-filtration for membrane absorbance tests, e.g. look at product absorption using SEM, without having to destroy a costly cassette. The multi-functionality of the device in terms of its ability to perform TFF and NFF experiments is also a unique feature which differentiates it from existing products.

Software for equipment control is often particular to the device, and is usually inexpensive to develop. Modifications to an existing software package, which is GAMP (relevant production software governing regulations) compliant could be an option, would make product development easier.

The main process simulation packages that are currently used in the biopharmaceutical industry only offer batch operation modelling, and modelling of TFF is often grossly simplified. The software developed for the TFF USD tool would use input parameters based on actual empirical data generated by using the TFF USD device. The resultant process model would hence be superior in validity and comprehensiveness to the simulation models based on theoretical algorithms only.

8.5.3 Preparation for product launch

The initial phase of the commercialisation project would be devoted to developing the hardware and software in order to bring them up to current good manufacturing practice (cGMP) standards. During this time, parallel work with potential customers' process development teams could be undertaken to demonstrate the technology with respect to the major drug classes. Direct comparison with the traditional process development scheme would enable quantification of the cost benefits obtained using the USD methodologies. Product performance must be verified and validated. In addition, application documents explaining how and when the product can be used in real life examples would have to be prepared.

Different areas such as pricing, marketing tools, name, in-house training etc. have to be considered and as the project and final product specifications develop, there is a need to finalise decisions in order to be ready for product launch. It is also imperative that any literature that is prepared for marketing tools be approved by legal and regional departments. Products typically have to be registered and so names must be carefully chosen such that they convey all aspects and selling points.

Preparation discussions revolve around a number of areas. The product price is a crucial decision; too high and it would not be an attractive option to customers and too low and the company would stand to make losses if there were any problems for example with production. It is also important to be able to justify prices to customers by use of economic appraisals. Forecasts for post launch also have an impact on pricing decisions. It is imperative that these forecasts be as realistic as possible as ultimately, deviations from these forecasts could lead to changes in profit and loss and could also lead to bad pricing decisions. The product marketing strategy must also be considered.

Getting a product to market does not necessarily ensure its success or that of the company. The product may fail for a number of reasons such as poor design, lack of resource for continued support, no market need for the product, bad marketing etc. By clearly defining the various project phases for a new product development, risks can be minimised as projects can be terminated at early stages if they are not viewed as potential successes. Careful structuring of a project leads to successful products as all areas are considered before the product "hits the shelves".

8.5.4 Extension of the product pipeline

In order to remain competitive, companies must also seek to develop their products post-launch i.e. improve them in terms of functionality and/or expand their range of application. For example, in terms of the device modification, the addition of torque measurement and/or disk geometry to the rotating disk would allow the device to function as a rheometer to give viscosity data for test fluids. Extension of the disk rotation speeds (shear range), would mean the device could function as a shear device, for centrifuge scale-down experiments (Boychyn et al., 2001).

The ultimate vision would be the ability to integrate with other unit operation USD devices such as bioreactors or chromatography. Similar components e.g. luer-lock connections would make use of the entire range of scale-down equipment attractive. Software could also be developed to allow the results from each individual operation to be integrated together into a whole process model (see Chapter 1).
However, all modifications must be subject to the same product development phases as the original product in order to assess the market demand, and therefore revenue potential as well as the compatibility with the company's core objectives.

8.6 Summary and conclusions

The overall biopharmaceutical development cycle forms the framework within which process development acts to achieve its goals. The development of a biopharmaceutical product follows the overall stages of discovery, preclinical development, clinical trials and approval. Process development is in a central position within the product development cycle with regard to interaction and exchange of information.

Process development summarises the activities surrounding the design, implementation and optimisation of a specific process (Boychyn, 2000). The aim of process development is to create a sequence of operations capable of delivering as much of the desired product as needed, at the required quality and as at low a cost and in as short a time as possible. Against the backdrop of increasing numbers of successful biopharmaceutical products and an ever more competitive market, strong expectations are therefore set on process development as the crucial step in turning laboratory science into functioning, economically viable products (Lendrem, 2000).

As clinical trial times are now shortening due to more efficient design, improved data handling and streamlining of regulatory guidelines the window for process development is also shrinking. Improving the efficiency and hence the process productivity can avoid delays during development, since this production of material use in clinical trials is often the limiting step. Effective process development will also help to avoid scale-up problems and facilitate easier process validation.

The 'standard' development timeline of a new drug is largely dictated by regulatory requirements of the country in which the drug will be sold. These tend to involve rigorous validation procedures, which can be long and costly and have a high failure rate. The TFF USD described in this thesis could be validated if the user could demonstrate that it was a reliable mimic of an industrial filter (see Chapters 5, 6 and 7). Once validated the TFF USD could be used to investigate a number of process variables in the laboratory using minimal time and resources. Several full-scale runs would still be required for process validation as part of process qualification (PQ). However, good scale-down techniques would enable some aspects of the process to be tested and fine-tuned in the laboratory thus minimising the risk of expensive, unforeseen problems at full-scale. Ultimately, the process knowledge and experience gained from scale-down work could keep the number of validation runs to a minimum and facilitate faster regulatory approval.

Speed to market is essential to maximise revenue during patent life (Dunnill and Davies, 1998) and, as a result, there is a demand for novel methods to accelerate process development and validation. USD techniques offer a promising solution to this dilemma.

In summary, successful commercialisation of a TFF USD device would require the development of a product that incorporates the device and data analysis software, which need to comply with GMP and GAMP guidelines. Additionally, to maintain market competitiveness, the extension of the uses of the device, e.g. as a shear cell for centrifugation USD, should also be considered. This discussed further in Chapter 9.

Chapter 9 Conclusions and Possibilities for Future Work

9.1 Introduction

This final chapter provides an overall review of the scientific approach adopted as the framework for the research presented in this thesis (see Figure 9.1). It begins by restating the initial aims and objectives and assessing if these have been achieved, followed by a summary of the main conclusions made throughout this thesis.

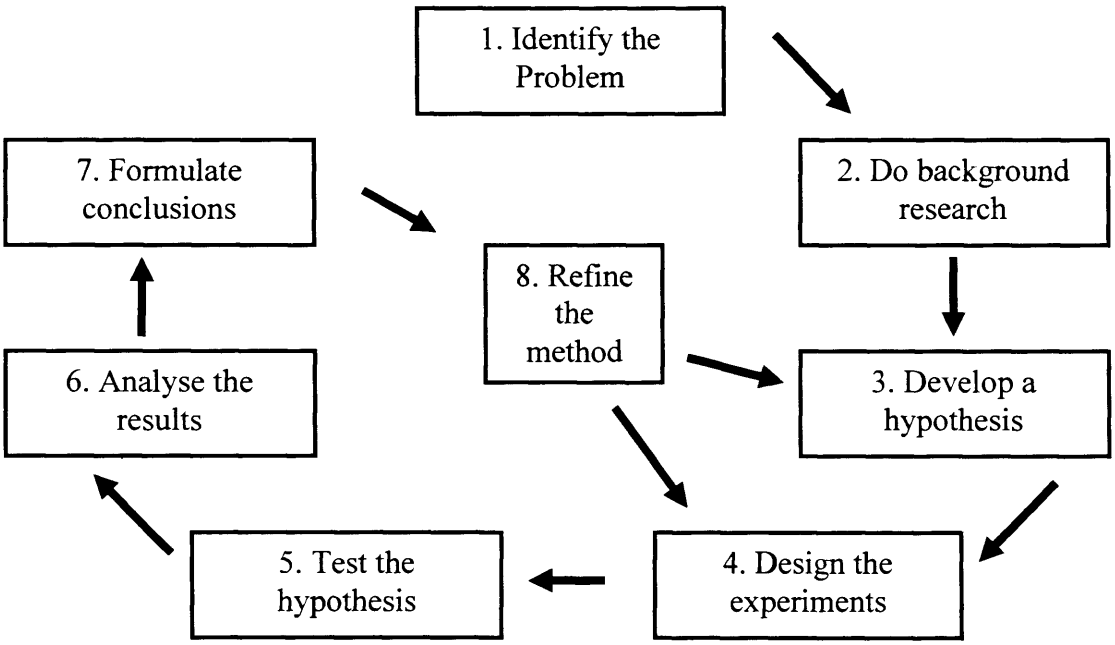

Figure 9.1: Flowchart to illustrate the steps involved in the scientific method.

Recommendations for future development of this research (refinement of the scientific method) are then made covering suggestions for an improved of TFF USD device prototype, comparison with other commercial filtration operations (e.g. vibratory membrane filters), the integration with upstream and downstream unit operations (see Chapter 1), and finally, a method to empirically assess the shear rates found in membrane filtration devices and rigs using a biological shear probe.

9.2 Research achievements

The aim of this thesis was to develop a USD down methodology for TFF. The original objectives set at the start (see Chapter 1, section 1.4) are restated below along with a discussion of how, and to what extent, they have been met.

Objective (step 1, Figure 9.1): Define the need for USD methodologies in bioprocess development

A review of the driving forces for improved process development was given in Chapter 1, and expanded up on and placed in a business context in Chapter 8.

Objective (step 2, Figure 9.1): To review and evaluate flux and transmission models for TFF for their suitability of use for a USD methodology.

A detailed review of the literature pertaining to membrane filtration, particularly for bioprocess applications has been presented (see Chapter 2 and Appendix 1). The complexity of the feed stream parameters and dynamic relationship between the numerous parameters (e.g. permeation rate, solute concentration, TMP etc.) mean that the predictive modeling of membrane filtration is not a trivial matter.

A semi-empirical resistance–in-series model proposed by Carrère et al. (2001) was applied to the yeast whole suspension, and was able to describe the flux and transmission behaviour with reasonable accuracy (see Appendix 2 for program listing). However, the effort required to determine the model input parameters, versus the time it would take to conduct actual filtration trials did not seem justifiable, especially because extrapolation of the model results for different operating conditions is not possible without repetition of the parameter-determining experiments.

A recent predictive model, called the aggregate transport model (Baruah and Belfort, 2003) was also reviewed. Recreation of the results presented in the literature was difficult, and the application to the different filter geometry (cassette versus hollow fibre) and feed stream did not produce sensible results. However, given more time and investigation into the sensitivity of the model to the input parameters, further attempts at applying this model should be made.

The use of the exponential decay relationship proposed by Novais (2001) was successfully applied to describe the behaviour of product transmission during concentration and diafiltration, and an example of how the model results could be utilised was given in Chapter 7.

Objective (steps 3 and 4, Figure 9.1).: To design and build a prototype USD TFF scale-down device which is suitable for various filtration operations such as concentration, diafiltration and normal flow filtration (NFF). This would include the incorporation of suitable instrumentation into the design of the TFF scale-down device, and specification of the ancillary filtration equipment.

The hypothesis of this research was suggested by Lee et al., (1995) stating that there existed a disk speed below which the behaviour of a rotating disk dynamic filtration system was comparable to the performance of a flat sheet cassette device.

The development of such a non-geometric scale down device was presented in Chapter 3, along with a discussion of the caveats of working with such small volumes of material, and definition of the TFF USD filtration rig.

Objective (step 5, Figure 9.1): To verify the results obtained from the scale down device against data generated using conventional, pilot-scale equipment, i.e. to commission the system, with "real", complex biological media.

The work presented in Chapters 5, 6 and 7 has shown how the TFF USD device has been able to mimic commercially available flat-sheet devices in terms of flux, transmission and expected transmembrane pressures (using compensation factors). The verification of the scale-down data with pilot scale trials has demonstrated that filtration behaviour can be reproduced during flux-stepping, recycle, concentration and diafiltration operations, using challenging biological feeds (yeast, bacterial and mammalian cell based), using only a fraction of the material required for conventional process development experiments.

Objective (step 6, Figure 9.1): To define a way to compare different membrane/feed combinations in order to rank the filtration performance e.g. in the form of a USD index for membrane TFF.

The use of a USD index would be useful for the integration of the TFF USD device results into whole process scale-down simulations (see Chapter 1, and section 9.3 below). It also provides a way of ranking the effectiveness of different feed/membrane combinations with a single parameter, making the presentation of trial results more pragmatic for process development decisions. The use of either the critical erosion wall shear rate, or the critical ratio of permeate flux to wall shear rate, (originally proposed by Gésan-Guiziou et al., 1999) was proposed, as these values were relatively easy to determined (see Chapter 7), and fitted the criteria for this index (outlined in Chapter 2).

Objective (step 6, Figure 9.1): To define a graphical method to present the USD data in a pragmatic and industrially relevant way.

The concept of "Windows of Operation" (WinOps) (Zhou and Titchener-Hooker, 1999) was applied to TFF, and proposals made for the plot axes in Chapter 2. Such a WinOp was populated with empirical data (see Chapter 7) to illustrate the feasible region of operation that should be investigated further or used for the scale-up procedure. However, the full extent of how this method of visually representing this data and population with predictive model results, as suggested by Griffiths (2007) was not explored, but warrants further study.

Objective: To show an appreciation and understanding of the impact of the USD concept on bioprocess business aspects.

Chapter 9 presented a discussion of the current procedures and pressures involved in bioprocess development, and an assessment of the impact of USD methodologies on the management of the process development pathway. To place this research in an industrial context, a discussion of the validation issues surrounding membrane filtration and the use of scale-down devices for regulatory compliance studies was also given, and finally the considerations required for the potential commercialisation of a TFF USD device were outlined.

On the whole, the original objectives set out at the start of this thesis were met, and the general outcomes of the work undertaken to achieve this is summarised below.

9.3 General conclusions

The use of a rotating disk device to mimic the filtration of complex biological feeds using commercially available flat-sheet cassette devices is possible. Despite the non-geometric scale down, and use of only a fraction of the valuable feed material (300-fold reduction), a demonstration of how the TFF USD device developed is able to mimic all aspects of filtration behaviour has been given. This included permeate flux rates, product transmission rates and the prediction of the transmembrane pressures that would be seen at the larger scale, with the use of TMP correlation factors.

Good scale-down models can reduce the need for lengthy and expensive pilot-plant trials by allowing much of the process development to be performed in the laboratory. Scale-down experiments can be used to assess different process options, optimise individual unit operations, evaluate operational robustness and accelerate validation. The principle advantage of scale-down is that process development can begin at an early stage in product development since only small quantities of process material are required. The minimal use of resources also reduces the investment involved in the early, high-risk stages of a project.

Other benefits of scale-down include simpler handling and operation, reduced energy consumption, and the ability to carry out a number of experiments very quickly. The biggest limitation of scale-down is the accuracy of the laboratory mimics and demonstrating to the regulatory agencies that the mimics are capable and reliable in producing data representative of the large-scale process.

This thesis has looked at scale-down of TFF to aid rapid and efficient filtration process design. It has been demonstrated that careful design and operation of scale-down mimics to overcome the inherent differences between laboratory and industrial-scale operations can yield reliable process data to aid in process development studies. However current techniques still have room for improvement and there are several other potential uses for this scale-down technology that remain largely unexplored. This following section discusses some of the directions this research could take in the future.

9.4 Possibilities for future work

Suggestions for the future development of this research are made in the following sections. The continuation of the identification of a suitable predictive model to be used within the TFF USD methodology has been stated above so will not be repeated here. Also, concepts such as whole process modelling, and linkage of the USD data to cost models will not be reiterated as they are described fully elsewhere (Pampel, 2000; Novais 2001; Reynolds, 2005), although this is the obvious progression of the research work.

9.4.1 Other uses for the TFF USD device

The comparative experiments described in Chapters 5, 6 and 7 demonstrate the ability of the TFF USD device to mimic flat-sheet cassette devices. However, there is no reason why the device could not be used to mimic other membrane filtration devices such as vibratory membrane filters e.g. a Pallsep dynamic MF system (Pall, UK) where commercially available scale-down models are not yet available.

The experiments to determine the parameters for the resistance-in-series model demonstrated the capability of the TFF USD device to be used for NFF, membrane absorbance tests etc., but these could be extended to investigate other filtration steps such as sterile filtration, or virus reduction steps (depth ultrafiltration).

The feed systems investigated in this thesis were not shear labile at the operating conditions selected. Operation of the TFF USD device to purposely shear the feed to mimic the operation of industrial filtration pumps and valves could be considered. Extension of the disk rotation speed range would mean the device could function as a shear device, e.g. to mimic centrifugation (Neal, 2005).

Finally, with some modification (e.g. addition of torque measurement), the device could also function as a basic rheometer to give viscosity data for test fluids. Further suggestions for hardware modifications are discussed below.

9.4.2 Investigation of the impact of upstream variations

On of the uses of the TFF USD device that became apparent during the placement at CAT was its use to determine the optimum point to harvest the mammalian cell fermentation in terms of filtration yield. This could have been conducted by taking fermentation samples at different time-points, and using the TFF USD protocol, complete the following tasks:

- Determination of operating window for worst sample (most difficult to filter).
- Estimate no. of diavolumes required to achieve a given yield by modelling transmission (see Chapter 7).
- Use costing data to look at trade-off between harvest point and filtration time. Factors to include are the cost of buffers, membrane area required etc.

As described in Chapter 1, scale-down mimics have been developed for other unit operations such as fermentation (Lamping, 2004) and centrifugation (Boychyn, 1998), and these could also be used to study the interaction of the two processing steps. With certain modifications, the TFF USD device could also be used as a shear cell, in order to conduct centrifugation USD (see Table 9.1).

9.4.3 Next generation of TFF USD device prototype

Since the completion of this work, the TFF USD filter has been modified and tested (Ma, unpublished). This device has incorporated the following improvements:

- The ability to vary the chamber volume from 1mL to 3mL using a series of inserts mounted at the top of the unit chamber. This reduces the feed volume required for the TFF USD experiments even further. Reduction of the membrane area could be achieved by using a wider o-ring (therefore achieving greater loadings with less feed material, but still using commercially available membrane coupons.
- The addition of a cooling coil around the motor drive and two cooling jackets at the top and base of the chamber to maintain operating temperature;
- The use of the AKTA Crossflow System (GE Healthcare, UK Ltd, Buckinghamshire, UK) instead of the filtration rig described in Chapter 3. This commercial system allows automatic data recording and greater accuracy of flow and pressure control and measurement through non-invasive instruments. The

associated software has many useful features such as the ability to adjust the permeate pump rate based upon flux or pressure measurements. It enables industrial operating conditions to be mimicked very easily in the laboratory and reduce the laboriousness of experiments. A similar filtration system has also been marketed by the Millipore Corporation (Kierans and Shaw, 2004), for use with the Pellicon XL cassettes, but could be adapted for the TFF USD device.

- Assuming that the feed material is not affected by the hydrodynamic conditions found in the large-scale retentate loop, then retentate recirculation is not required, as the effective crossflow is mimicked by shear at membrane created by disk. The operation of the device in this way has reduced the feed requirement further, and simplified the experimental set-up.

Further modifications that could be made are discussed in the next section.

9.4.3.1 Device hardware improvements

Further improvements to the device need to be made before it could be made into a commercially available device (see Chapter 8). The following section proposes an improved TFF USD device prototype, with the benefit of hindsight. Figure 9.2 shows a schematic of the TFF USD device compared with a suggested improved prototype design.

(a) Original device (b) Improved device

Figure 9.2: Schematics of TFF USD device prototype designs.

In addition, either device could be mounted horizontally, making it easier to prime (avoid air bubbles in the chamber). However, the new format would require a feed channel to be drilled through the rotor shaft to enable NFF, which may make fabrication

more difficult. The advantages of the revised design are listed in Table 9.1, along with some other hardware improvements.

Factor	**Description of Improvement**
Flow hydrodynamics	Shear profile more uniform (no disk edges), which also makes CFD modelling easier.
Calculation of mass transfer coefficient	The equations for calculation of the mass transfer coefficient for modeling purposes call for the hydraulic diameter (d_H) of the device (see Chapter 3). The simpler internal geometry makes this easier to calculate accurately.
Chamber volume	The chamber volume is reduced without the need for inserts. Variation of volume could be achieved by altering the rotating disk height.
Sampling ports	The use of septum based sampling ports would minimise the volumes taken for offline analysis, and speed up the time taken to sample.
Cleanability	The device should be constructed out of materials that can be easily sterilised (i.e. autoclavable), which is desirable for use in industry.
Base attachment	A screw-on base (c.f. Amicon stirred cell design, Millipore, USA), to replace the awkward knurled nuts would facilitate the device set-up.
Connectors	Permanent connectors (e.g. female luer ports) for attachment to tubing, sampling ports or to the filtration rig components.
Disk speed	A disk drive motor allowing a greater range of disk rotation speed would allow the use of the device as a shear cell for e.g. centrifugation USD (see section 9.4.2).

Table 9.1: Additional hardware improvements to TFF USD device prototype.

The simplification of the internal geometry facilitates evaluation of the device hydrodynamics. However, as the purpose of the microfiltration USD is to mimic conventional TFF, such calculations would only be useful if an equivalent analysis were possible for complicate formats such as membrane cassettes. The final section of this thesis describes to empirically assess the shear rates found in membrane filtration devices and rigs using a biological shear probe.

9.4.4 Assessment of shear levels encountered in complex engineering environments: application to tangential flow filtration systems

As highlighted in Chapter 3, the ability to estimate the shear levels encountered in complex geometries, such as a membrane filtration cassette, is limited. This is an issue in membrane filtration in bioprocesses for two reasons: firstly because biological entities (cells, product or contaminants) may be shear sensitive (Joshi et al., 1996), and secondly because the shear rate at the membrane surface is the key parameter to maintain between different scales of operation (van Reis 1997). During tangential flow filtration cells are submitted to shear stresses due to the repeated passage through pumps and flow-control valves. Shear degradation may also occur within the filter module itself, particularly at the entrance region where the feed channels are very small (typically 0.5mm to 0.75mm channel height). Conversely, high shear stresses may be desirable during processing. Some research has been done into the combined lysis and filtration of fermentation broths (Meagher et al., 1994). A practical and simple method of characterising the shear levels encountered at various points in the processing equipment would be useful.

Computation of the actual shear rates encountered in downstream processing equipment is highly complicated; the most sophisticated attempts employ computational fluid dynamics (CFD) (Pellerin et al., 1995; Karode and Kumar 2002). However, little attempt has been made to validate these results with physical data.

Several studies have been conducted using biological entities to estimate the shear levels encountered in processing equipment. The approach uses the fact that such materials may be permanently degraded when exposed to shear (see Table 8.2 below).

The use of plasmid DNA to assess the shear rates encountered in a device is an attractive option, due to advances in the availability of pure solutions of supercoiled plasmid DNA and a reliable and fast fluorescence based assay method to detect plasmid breakage in very dilute solutions (Rock et al., 2004). Shear sensitivity of plasmids is dependent on plasmid size as well as molecule structure: i.e. larger plasmids degrade more easily, and linear forms are more prone to shear degradation than the open-circular form, while the open-circular is more prone than the supercoiled form.

Biological probe	*Processing Equipment*	**Reference**
Red blood cells	Capillaries	Zydney and Coulton 1986
Globular proteins	Centrifuge	Narendranathan and Dunnill, 1982
Mammalian cells (CHO)	Capillaries, Tangential flow filtration (Prostak®)	Kelly et al., 2002
Algal cells	Tangential flow filtration	Jaouen et al., 1999; Vandanjon et al., 1999
Plasmid DNA	Capillaries	Levy et al., 1998, Meacle et al. 2007

Table 9.2 Biological probes to assess shear degradation in the literature

The shear device to produce the breakage curves in the studies presented in Meacle et al., (2007) was a capillary tube system, but a rotating disk device such as the MF USD could also be used. It has been shown that capillaries and rotating disks give consistent levels of DNA degradation at similar levels of fluid stress (Meacle, 2003; Levy et al., 1999). Preliminary experiments were conducted during this EngD, but were not completed due to time limitations. Plasmid degradation in the capillaries was shown to be one of first order decay, as reported by Meacle (2007). It was confirmed that supercoiled plasmid degradation was a function of (i) plasmid size, (ii) level of shear, and (iii) time of exposure to the shear field; degradation was inversely proportional to molecular weight of the scDNA and degradation followed a first order exponential decay.

A flowchart outlining an experimental methodology using a plasmid probe to assess levels of shear-induced degradation in bioprocess equipment is shown in Figure 9.3. As well as estimating the maximum global shear rate encountered during processing, it may also be useful to determine which rig components are responsible for the shear damage; alternative equipment may be an option if the feed is being damaged e.g. the use of a diaphragm valve instead of a needle valve to control backpressure. A methodology to apply this to the identification of regions of high shear stress, and hence reduction of the global shear stresses encountered in a tangential flow filtration rig is shown in Figure 9.4.

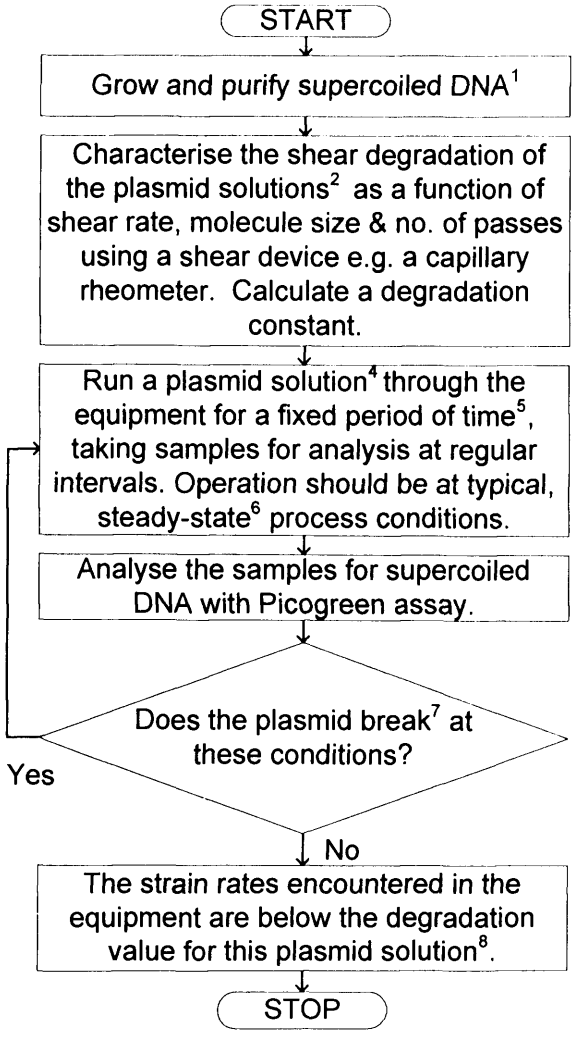

Figure 9.3: Procedure to evaluate the maximum shear rates encountered in bioprocess equipment using a plasmid DNA shear probe

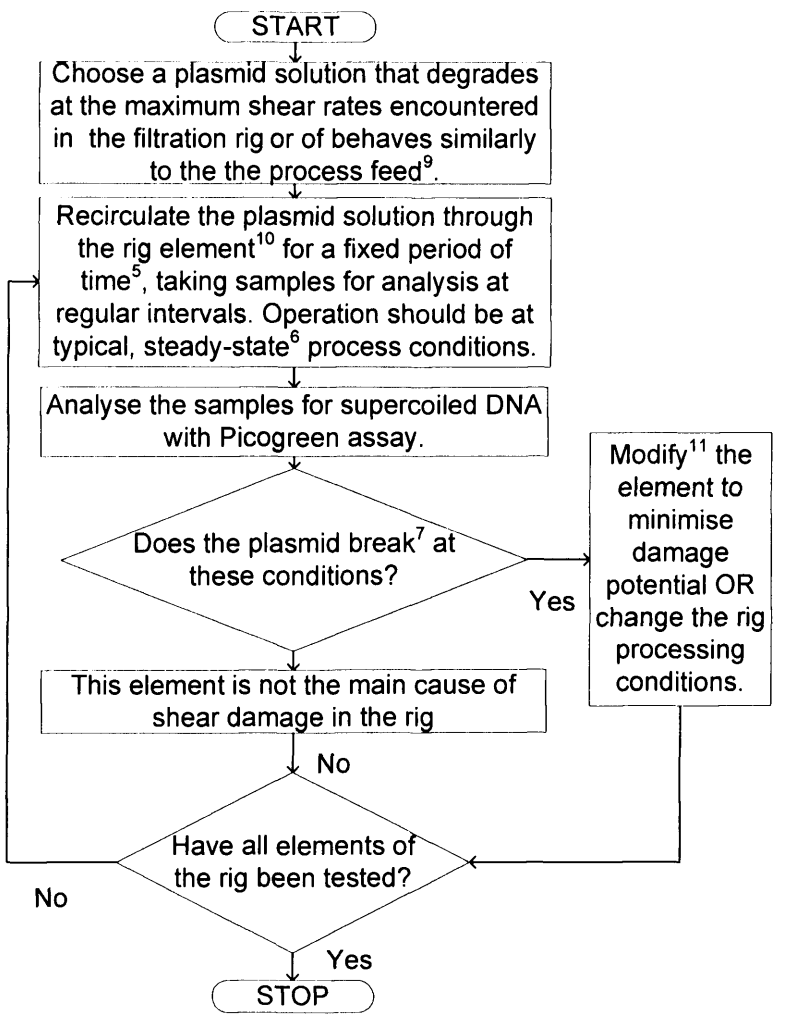

Figure 9.4: Procedure to evaluate the shear rates of membrane filtration rig components using a plasmid DNA shear probe.

Notes for Figures 9.3 and 9.4:

[1] The supercoiled content of the plasmid DNA should be above 90%.

[2] The PicoGreen assay is accurate in the range of 100ng/mL to 500ng/mL. A plasmid solution of 0.2μg/mL is recommended (Meacle, 2003).

[3] A degradation constant must be determined by curve-fitting, or estimation from a single pass.

[4] The first solution selected should be one that is anticipated will degrade. The next solution should have a higher threshold shear stress.

[5] This may be 30 minutes or a typical batch processing time.

[6] Unsteady flows accelerate DNA fragmentation (Lengsfeld et al., 2002). In order to avoid artefacts from poor start-up procedures, it is suggested that the buffer is circulated in the filtration rig until steady state conditions are achieved, and then the plasmid is introduced.

[7] The definition of "breakage" will need to be clearly defined e.g. as a minimum percentage of supercoiled DNA loss.

[8] Corollary: the strain rates in the rig are above the degradation value of the penultimate solution tested in Figure 8.2.

[9] The last plasmid solution that showed degradation in the whole-rig characterisation.

[10] Filtration rig elements include the feed reservoir, feed pump, any instrumentation, the membrane device, any valves and the pipework.

[11] For example, a pinch valve may be used instead of a needle valve to control retentate backpressure.

Preliminary data obtained by recirculation of pure supercoiled plasmid solutions around the M12 Proflux filtration rig and Pellicon 2 mini cassette (data not presented) showed that such experiments are feasible, and prompt the further study of this approach as a generic probe for fluid stress in bioprocess equipment.

9.4.5 Summary of suggestions for future work

To summarise, the research presented in this thesis provides the precursor for the following research:

- Process modelling of TFF and linkage to cost data and eventually to a whole bioprocess modelling approach;
- Population of WinOps with semi-empirical model data and experimental validation of the results;

- Extension of the TFF USD device to also function as a rheometer and/or shear cell for centrifugation USD;
- An investigation into the impacts of changes to upstream unit operations e.g. the identification of an optimum fermentation harvest point in terms of filtration optimisation, and cost efficiency;
- Use of the TFF USD device to mimic other filtration modules, such as NFF, hollow fibre modules, or dynamic filtration devices;
- Hardware improvements to the TFF USD device and ancillary rig to facilitate experimentation;
- Use of a biological probe to assess the shear levels encountered within the complex geometries found in bioprocess equipment.

Appendix 1 Membrane Filtration Modelling

A1.1 Introduction

The following pages provide a literature review of attempts made to model membrane filtration, in terms of flux, fouling behaviour and transmission.

A1.2 Modelling flux

A1.2.1 Resistance-in-series models

The flux of liquid (J) through a porous membrane is directly proportional to the pressure across the membrane (Δp) and inversely proportional to the viscosity (μ) of the permeating fluid. D'Arcy's Law describes this relationship:

$$J=\frac{\Delta p}{\mu R_m} \qquad [A1.1]$$

However, this equation suggests that the flux will increase indefinitely as the Δp increases, which is clearly not the case; this is because the effects of retained material have not been taken into account. The retained material will be transported towards it by convection, due to the flow of permeate, which will create an additional resistance at the membrane R_{CP}, the resistance due to concentration polarisation. Some of the retained material will form an organised layer on top of the membrane to a "cake", which is denoted by the resistance R_C. The cake resistance is dependent on particle size and Δp (for compressible particles). Solutes present in the feed may also be adsorbed onto the membrane and into its pores, creating an additional hydraulic resistance, R_F. These resistances can be combined in series (Van den Berg and Smolders, 1988):

$$J=\frac{\Delta p}{\mu(R_M+R_C(t)+R_{CP}+R_F(t))} \qquad [A1.2]$$

The time dependence of R_C and R_F describe the transient flux decline. R_{CP} will be directly proportional to Δp, but will eventually plateau.

The above equation differs from the comparable UF model because there is no correction for osmotic pressure effects due to the retention of proteins. In most situations these effects are

negligible in MF as the concentration of proteins will not be high enough (Song and Elimelech, 1995). If the concentration is high then

$$J=\frac{\Delta p-\Delta \pi}{\mu(R_M+R_C(t)+R_{CP}+R_F(t))} \qquad [A1.3]$$

Hence, resistance-in-series models correlate flux to TMP accounting for effects of the membrane substrate, concentration polarisation and fouling in a group of additive resistance terms. This model is frequently employed to correlate and compare data obtained with a single experimental apparatus while varying the membrane or feed material. Flux, permeate viscosity and TMP are measured directly, allowing calculation of the total resistance, Rtot.

The intrinsic resistance of the membrane, Rm, is usually measured with a clean water feed prior to introducing the experimental feed, which allows the calculation of the sum of the remaining resistances. The deconvolution of these resistances can be achieved by using an experimental protocol, that limits the contributions of the various terms at certain points in the procedure.

Substitution of more elaborate expressions for individual resistance terms can extend the usefulness of the resistance model. Noting that the thickness of the concentration polarisation layer should be proportional to TMP, Cheryan (1986) replaces R_{cp} with $\Phi(TMP)^n$, where Φ is further specified as a function of the crossflow rate.

Biological materials, such as microbial cells, are compressible and show a decrease in the void fraction and an increase in the specific resistance as the pressure is increased. This makes estimation of the cake resistance difficult. The resistance due to irreversible fouling can only be estimated from experimental data. The total hydrodynamic resistance of the membrane can be used to predict flux using the equation:

$$J=\frac{TMP}{\mu R_{tot}} \qquad [A1.4]$$

where TMP is the transmembrane pressure (Pa) and R_t is the total hydrodynamic resistance (m^{-1}).

R_t can be defined as the sum of the membrane resistance (R_m), the cake resistance (R_c) and the resistance due to blocking of the pores (R_b), which are related by the following equation (Kawakatsu et al., 1993):

$$R_t = R_m + R_c + R_b \qquad [A1.5]$$

The membrane resistance can be measured using the clean water flux. When using pure water equation [A1.4] becomes:

$$J = \frac{TMP}{\mu R_m} \qquad [A1.6]$$

The resistance of the membrane can then be calculated by plotting flux against transmembrane pressure, the gradient of the graph being $1/R_m\mu$. It is more difficult to measure the cake resistance and the resistance due to blocking of the pores.

The formation of fouling cake and boundary layers as has been explained previously, are causes of flux decline. Fouling is caused by solute/solid – membrane interactions that result in a physical adsorption of the solute/solid to the membrane. This can occur at the surface or within the pores (surface or entrapment respectively); the resulting cake impedes the flow of material through it, which can be worsened by the compression of the cake (Kawakatsu et al., 1993). The velocity boundary layer builds up because of friction between the static membrane and the fluid stream which reduces the crossflow velocity at the membrane surface. This in turn reduces the shear and therefore the back-transport of material away from the membrane surface.

Figure A1.1 is a representation of the concentration boundary or gel layer. This gel layer is caused by the transport of solutes to the membrane surface faster than they can be removed by the crossflow and faster than they can pass freely through the membrane. This concentration polarisation can inhibit the passage of solutes across the membrane due to concentration or repulsion by the accumulation of like-charged proteins.

Figure A1.1: A diagram showing the boundary layer effect. A gel-like layer builds up at the membrane. The concentration of cells increases as the membrane is approached, from C_b - the bulk concentration in the feed stream to C_g the gel concentration at the wall (Porter 1972).

In crossflow filtration it is the shear caused by the tangential flow that minimises these boundary layer effects. Flux decay due to fouling and concentration polarisation can be minimised by increasing crossflow (Reismeier et al., 1989; Gyure 1992). Shear can also be increased through the use of cartridge designs which include the use of turbulence promoting spacer screens within the feed channel (da Costa et al., 1991) this causes the formation of vortices which enhance shear at the membrane surface. This can lead to deleterious effects, since vortex formation and high crossflow rates can lead to air entrainment and it has been shown that air-liquid interfaces are the most common cause of protein denaturation in tangential flow filtration systems (Narendranathan and Dunnill 1982). Interactions between protein and the membrane is greater when calf serum albumin (CSA) is denatured and a build up of protein at the membrane surface reduces flux.

A1.2.2 Concentration polarisation models

Concentration polarisation can be modelled with the stagnant film theory (Chen, 1998). According to this model the solutes in the feed are transported to the membrane surface by convective flow and removed by permeation through the membrane or by back diffusion into the bulk (Figure A1.2):

$$JC_b = JC_p - D\frac{dC}{dy} \qquad [A1.7]$$

Where J is the flux through the membrane, C_b and C_p are the concentrations of the solute in the bulk and in the permeate respectively, D is the solute diffusion coefficient dy is the coordinate in the direction perpendicular to the membrane surface. Axial diffusion and axial convection terms in the stagnant boundary layer are considered to be negligible.

Figure A1.2 Schematic representation of the solute transport within the concentration polarization boundary layer (adapted from Zeman and Zydney, 1996, and Le and Atkinson, 1985).

Integration over a boundary laver of thickness δ and defining C, as the concentration at *t* the membrane surface gives:

$$J=k\ln\left(\frac{C_w-C_p}{C_b-C_p}\right) \qquad [A1.8]$$

Where k is the mass transfer coefficient:

$$k=\frac{D}{\delta} \qquad [A1.9]$$

Considering the retained solutes accumulate on the membrane surface a new concept of true transmission (as opposed to the observed transmission) can be introduced:

$$T_{actual}=\frac{C_p}{C_w} \qquad [A1.10]$$

And hence

$$T_{obs}=\frac{T_{actual}}{(1-T_{actual})\exp\left(\frac{-J}{k}\right)+T_{actual}} \qquad [A1.11]$$

The observed protein transmission is therefore expected to increase with increasing concentration polarization as the protein concentration at the membrane surface increases (Huisman et al., 2000).

The membrane may be defined as a semi-permeable barrier between two homogenous phases and its selectivity can be expressed by the retention factor (R):

$$R=\left(\frac{C_f - C_p}{C_f}\right) \qquad [A1.12]$$

Where C_f is the solute concentration in the feed and C_p is the solute concentration in the permeate. The value of R varies between 1 (complete retention of the solute) and 0 (solute and solvent pass through the membrane freely) (Mulder, 1996). Alternatively, the concept of transmission (T) can be used, defined as:

$$1-R=\frac{C_p}{C_f} \qquad [A1.13]$$

The concentration polarisation model assumes that the limiting resistance to flow is provided by a dynamically formed thin layer of retained solutes or solids between the bulk solution and the membrane surface. The dynamic layer is assumed to have a fixed concentration of solutes or solids but varying thickness or porosity. In such a scenario, the permeate flux rate is independent of the pressure driving force or the membrane permeability since the dynamic boundary layer resistance to permeate flow will adjust itself until the convective transport of retained species to the membrane surface equals the back diffusive transport to the bulk stream (Porter, 1972). This balance within the layer is described by

$$JC=D\frac{dC}{dy} \qquad [A1.14]$$

Integration across the boundary layer gives an expression of the permeate flux rate as a function of the wall and bulk concentrations, and the mass transfer coefficient.

$$J=k_m \ln\left(\frac{C_w}{C_b}\right) \qquad [A1.15]$$

The mass transfer coefficient and the wall concentration are unknown and need to be estimated. The wall concentration can be estimated by assuming that the boundary layer resembles a layer of closed-packed spheres having 65-75% solids by volume (Porter, 1972). The mass transfer coefficient can be estimated using analogous solutions for heat transfer such as the Dittus-Boelter correlation for fully developed turbulent flow.

$$k_m = K\, U^{0.8}\, D^{0.67}\, d_m^{-0.2}\, \nu^{-0.47} \qquad [A1.16]$$

Porter (1972) has shown with measurements of fluid velocity as a function of the pressure drop that a definite transition from laminar to fully developed turbulent flow occurs at a Reynolds number of ~2,000. The recirculation rate and the inner membrane diameter are easily determined.

The diffusion coefficients of suspended species can be estimated using the Stokes-Einstein relationship.

$$D = \frac{k_b T}{6\pi\mu_s r_p} \qquad [A1.17]$$

Correlations to estimate the diffusivity of spherical molecules and macromolecules are available in the literature as given by Porter (1972) and Kawakatsu et al. (1993).

It is generally accepted that in UF the concentration of proteins at the membrane will increase until a gel layer forms a concentration C_G, and that once this point is reached, no more protein can enter the polarised layer (Porter, 1972). This concentration of protein can be estimated from the linear plot of J_{lim}, the limiting flux versus ln C_B as the intercept on the ln C_B axis (please see Figure A1.3 below).

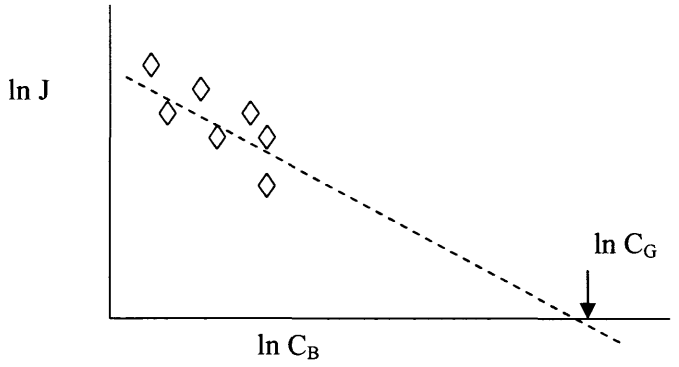

Figure A1.3: Determination of the gel concentration.

However, different workers have obtained different values of C_G, bringing into question the physical significance of the gel concentration. There is therefore still debate over the applicability of concentration polarisation based models.

When these equations are used to predict flux, the values obtained are up to two orders of magnitude lower than measured flux values. This phenomenon has been termed the "flux paradox" (Green and Belfort, 1980). Plots of J versus ln C_B obtained using MF data ((Brown and Kavanagh, 1987) were sigmoidal in nature, rather than linear, showing the breakdown of the gel polarisation with MF.

A1.2.3 Back-transport models

This breakdown is thought to be due to the fact that the back transport cannot be predicted using the Stokes-Einstein equation, as the mass transport away from the membrane is higher (Brown and Kavanagh, 1987, Porter, 1972). Various possible mechanisms for improved back transport have been suggested, some of which are outlined below.

Lateral migration (also known as "tubular pinch") is one such theory. Particles in a flowing suspension will tend to migrate away from the walls of the tube in which they are flowing. This is thought to be a result of inertial forces acting on the particles (Green and Belfort, 1980).

Calculations of these inertial lift forces show that the lift velocity would be smaller in magnitude than the velocity of the permeate towards the membrane (Davis and Birdsell, 1987). Flux performance was successfully predicted for laminar flow by considering the polarised layer as a flowing liquid with a certain viscosity containing a feed of another viscosity (Davis and Birdsell, 1987). By considering the concentration-polarised material as a non-Newtonian fluid, and the bulk liquid as Newtonian, they were able to obtain excellent predictions of flux performance during the UF of latex particles.

Zydney and Colton (1986) considered the nature of the flow of particulates in a suspension. Particles will rotate, collide and overtake neighbouring particles, which are travelling along lower streamlines. Such interactions will lead to a net lateral migration of the particles. As these interactions are dependent on the random position of particles at that time, the motions of individual particles will also be random and can then be modelled by an effective diffusivity coefficient or shear enhanced diffusivity.

Davis and Leighton (1987) proposed that shear induced lateral migration is responsible for the back transport in a laminar flow system where the concentration polarisation layer flows along

the membrane. Davis and Sherwood (1990) used the concept of shear induced diffusivity with concentration dependent viscosities to predict permeate flux. This theory has also been used in the development of a model that can predict the time dependent flux decline (Romero and Davis, 1990), once again for laminar flow conditions. This assumption is the main drawback of the shear enhanced diffusion models reported.

Efforts to models filtration behaviour during cell harvest applications have generally either modified resistance-in-series concepts or the gel polarization model. In concentration polarisation theory, a high concentration of retained species accumulates at the membrane surface and provides additional resistance to flow. Modelling efforts focus on the pressure-independent region of operation, where mass transport effects dominate.

Direct application of this UF model to MF of particulates using Brownian motion particle diffusivity results in significant under prediction of flux c.f. experimental observations. Augmentation of back transport has been attributed to shear-induced diffusion and inertial lift. Comprehensive reviews of the efforts to model these interactions have been written (Belfort et al., 1994) specifically as they apply to MF, and also discuss surface transport models. They conclude that given limited testing of the various models, none can be considered dominant, and that different mechanisms may dominate under different specific conditions.

For practical purposes, it is the functionality that the different models ascribe to key operating parameters such as flux and particle size that is important for the correlation of experimental data. Assuming that the feed suspensions are dilute and composed of non-adhesive spherical particles, which form cake layers that dominate the resistance to flux, the equation for flux to be reduced to

$$J = c\gamma^{n} a^{m} \varphi^{p} L^{q} \eta^{r} \qquad \text{[A1.18]}$$

A comparison can be made of the dependence of flux that the different models predict for key parameters (see Table A1.1).

The Brownian diffusion model predicts a much weaker dependence of flux on shear rate than the other models. The Brownian and shear-induced diffusion models predict similar weak inverse dependences of flux on feed concentration and filter length, whereas the other two models predict no effect of these parameters. All the models predict a different dependence of flux on particle size, although only the Brownian diffusion model counter-intuitively predicts a

decrease of flux with increasing cell size. They also all predict that flux decreases with increasing suspension viscosity, apart from the surface transport model.

Practical experience suggests that all these parameters will play a role in determining the steady-state flux, but that their pure effect anticipated in these models may be masked by the many irreversible phenomena which are likely to contribute to observed performance.

*normalised to prediction by Brownian diffusion

Table A1.1: Parametric dependence of long-term flux for various transport mechanisms (after Belfort et al., 1994).

A1.2.4 Fouling models

Hermia (1982) developed several models, which describe the fouling of membranes during filtration, and hence determine the flux performance. These are summarised in Table A1.3 below.

These fouling models were derived for normal-flow filtration (NFF). Field et al. (1995) have modified these equations for use in tangential or crossflow filtration (TFF) by including terms to account for back transport. These modified equations have then been used to determine the fouling mechanism in different forms of MF.

The accumulation of rejected feed components on the membrane surface as a result of convective flow under an applied pressure gradient, often termed concentration polarisation, is thought to be responsible for the initial sharp decline in permeate flux rates during crossflow microfiltration. The build up of rejected material and the associated boundary layer on the membrane surface is limited by the back diffusion of feed components into the main velocity stream, which runs parallel to the membrane surface. At steady state, the rate of convection of material to the membrane surface equals the diffusion of material from the boundary layer to the main flow path. However, crossflow microfiltration systems exhibit a decline in flux with time under constant operating conditions. This phenomenon can be attributed to a process often termed membrane fouling. Membrane fouling is an irreversible and time-dependent process caused when a membrane adsorbs or its pores are plugged by some feed components (Patel et al., 1987). The narrowing or blocking of pores results in a lowering of the permeate flux rate.

Table A1.2: Membrane filtration fouling models (after Hermia, 1982)

Several models have been developed to describe time dependent nature of filtration processes. Many of these models have been developed for dead-end filtration, but modified versions for use in crossflow filtration by including terms that account for back transport are available. Patel

et al. (1987) used a power law relationship to describe their data obtained from crossflow microfiltration experiments.

$$J_t = J_1 t^{-b} \qquad [A1.24]$$

The fouling index, b, is indicative of the rate of fouling. Higher values indicate higher rates of fouling. The value of b ranges from ~0.1 to ~0.8 for yeast whole cells and yeast homogenate.

Hermia (1982) developed several models to describe the mechanisms of membrane fouling during dead-end filtration. The complete blocking filtration law assumes that each particle reaching the membrane participates in the blocking phenomenon by pore sealing. Thus, particles are not superimposed upon the other, and the portion of the membrane surface area blocked is proportional to the filtered volume. The resulting flux-time relationship is described by equation A1.25.

$$J_t = J_0 e^{-kt} \qquad [A1.25]$$

The intermediate blocking law also assumes that a particle reaching an open pore will seal it, but evaluates the probability of a particle reaching an open pore. Assuming a homogenous suspension, the increment in blocked area due to particles reaching an open pore is proportional to the ratio of unblocked and blocked surface area since the likelihood of a second particle layer settling on an existing layer or on free surface is equal. Equation A1.26 describes the intermediate blocking filtration law.

$$J_t = J_0 e^{-kV} \qquad [A1.26]$$

The standard blocking filtration law assumes that the pore volume decreases proportionally to the filtrate volume by particle deposition on the pore walls. Assuming the membrane consists of a set of pores of constant diameter and length, and using Poiseuille's equation, Hermia derived an expression for the flux as a function of the time of filtration.

$$J_t = \frac{J_0}{(1+kJ_0t)^2} \qquad [A1.27]$$

The cake filtration model assumes the resistance to filtrate flow is composed of a membrane resistance and a cake resistance. The resulting flux-time relationship is described by equation A1.27:

$$J_t = \frac{J_0}{(1+kJ_0^2 t)^{0.5}} \qquad [A1.27]$$

Foley et al. (1995) presented a deposition model developed for crossflow filtration systems that included a back diffusion term. In this model, the net accumulation of matter on the pore walls was expressed as a difference between the rate of deposition and the rate of removal.

$$\frac{dh}{dt} = \nu_D - k_f h \qquad [A1.29]$$

The fouling layer thickness is the difference in pore radii of fouled and unfouled membrane.

$$h = r_0 - r \qquad [A1.30]$$

Integrating equation A1.31 gives an expression for the fouled pore radius as a function of the filtration time.

$$\frac{r}{r_0} = 1 - \frac{\nu_D}{k_f r_0}(1 - e^{-k_f t}) \qquad [A1.31]$$

Most models consider one aspect of the fouling phenomenon. In reality, a combination of effects i.e. increased hydraulic resistance due to concentration polarisation and fouling, pore blocking and osmotic pressure effects will occur simultaneously.

The modelling of fouling has been researched for some time, as has already been discussed, though the mechanisms of fouling are not well understood. Although protein is filtered by the cake formed on the membrane in MF, it is not filtered according to molecular weight. Different factors such as charge, hydrophobicity and formation of aggregates must be involved (Hernandez-Pinzon et al., 1997). Also, in a 'clean' system, blocking of the membrane is not caused by a uniform mono-molecular layer in cattle serum albumen (CSA) solution. It tends to build up around the pore entrances. Fouling by proteins can also be reduced by changing the materials of construction of the membrane. Using a hydrophilic structure reduces the amount of protein binding by changing the surface chemistry in such a way as to reduce the protein-membrane interaction or to operate away from the isoelectric point on the protein which reduces the chance of precipitation and therefore adsorption

A1.2.5 Force balance models

The basic principle of these models is to determine the forces acting on a particle close to the membrane so that it is possible to predict whether it will settle on the membrane (causing fouling) or to be re-entrained into the flow. Stamakis and Tien (1993) developed a solids fouling model for TFF based upon the premise that not all the particles convected towards the membrane will form a cake and lead to fouling; some will be lifted away. A force balance model was developed (forces acting on the particle were due to the crossflow and permeate flow) and successfully applied to published, experimental data. A similar approach was also taken by Hwang et al. (1996). They envisage that forces due to lateral lift will act on the particle, shear induced diffusion, electrostatic interactions with the membrane, a drag force, gravity and Brownian motion. Flux performance was successfully predicted for late particles.

However, neither of these models allowed for particle-particle interactions in the polarised layer. The parameters required for modelling are extremely difficult to determine for biological systems.

A1.2.6 Overview of flux models

The concentration polarisation model is only applicable in the pressure independent region. The resistance model is only applicable in the pressure dependent region. There seems to be two extremes to the models available in the literature; those that are based on fundamental principles, and those that are purely empirical. Which of these are practical in an engineering sense has yet to be resolved.

Models with variable physical properties are well described in the literature. However, the requirement for large numbers of data/parameter estimation means that these models are not suitable for practical applications so will not be described here. Instead, included below is a table below provides a summary of the main, fundamental microfiltration models in the literature and recommendations of the types of systems they are most useful for (after Bowen and Jenner, 1995).

	Theory	Model equation	Model Para -meters	Comments	Feed type recommended for
(a)	Gel-polarisation theory with concentration dependent diffusivity and viscosity.	$J_{\lim} = 1.5\left(\frac{\bar{u}_b D_b^2}{hL}\right)^{1/3} \bar{J}$ $\bar{J} = \left(1 - \frac{C_b}{C_g}\right)$ x $\left[\int_0^\infty D(C)^{-1} \exp\left(-\int_0^\eta \frac{\eta^2 + \bar{J}}{\bar{D}(C)} d\eta\right) d\eta\right]^{-1}$ $\bar{D}(C) = D(C) / D_b(C_b)$ $\eta = y\left(3xD_b / \left(\frac{du}{dy}\right)_b\right)^{-1/3}$	C_g, $D(C)$	For laminar flow, solved numerically. Accuracy of the prediction is limited due to available physical property data.	Macromolecules MW ≥ 10^5 Da
(b)	Gel-polarisation theory with $D = D(C_g)$.	$J_{\lim} = 1.31\left(\frac{\bar{u}_b D(C_g)^2}{hL}\right) \ln\left(\frac{C_b}{C_g}\right)$	C_g, $D(C)$	For laminar flow, solved numerically. An approximation of (a) valid for $C_g/C_b >> 1$; the predictive difference when compared to (a) is ≈ ± 10% between 0.05gcm^{-3} < C_b < 7gcm^{-3}	Macromolecules MW ≥ 10^5 Da

	Theory	Model equation	Model Para -meters	Comments	Feed type recommended for
(c)	Osmotic pressure theory.	$J = \frac{\lvert\Delta p\rvert - \lvert\Delta\pi\rvert}{\mu R_m}$ $\Delta\pi = \pi(C_m) - \pi(C_p)$ $\approx \sum_{i=1}^{3} a_i C_m^i \approx \sum_{i=1}^{3} a_i C_b^i \exp\left(\frac{iJ}{k_s}\right)$		Solved by trial and error. Requires knowledge of the osmotic pressure as a function of concentration to get at least the coefficients a_i; generally good agreement with experimental data.	Macromolecules $10^4 < MW > 10^5$
(d)	Boundary layer resistance theory.	$J = \frac{\lvert\Delta p\rvert}{\mu(R_m + R_{bl})}$ $R_{bl} = \frac{1 - \nu_1/\nu_0}{\mu s_0}\frac{D}{J}$ $\left[C_m - C_b + \frac{K_1}{2}(C_m^2 - C_b^2) + \frac{K_2}{3}(C_m^3 - C_b^3) + \frac{K_3}{4}(C_m^4 - C_b^4)\right]$ $C_m = C_b \exp(J/k_s)$		Solved by trial and error. No gel-formation at the membrane surface is required; excellent experimental agreement with dextran solutions.	Macromolecules $10^4 < MW > 10^5$

	Theory	Model equation	Model Para -meters	Comments	Feed type recommended for
(e)	Empirical model which includes the osmotic pressure theory with a flux dependent mass transfer coefficient and concentration dependent viscosity.	$J_{\lim} = \frac{K\overline{u}_b^{\,y} C_b^{-X}}{\exp(1)X}$ $K = AD^{(1-x)}\rho^{(1-x)}\mu_b^{(x-y)}$	K, X, y or A, x, X, y	Parameters have to be obtained through an experiment; experimental agreement is very good for different solute and membrane types and hydrodynamic conditions.	Macromolecules

	Theory	Model equation	Model Para -meters	Comments	Feed type recommended for
(f)	Shear-induced hydrodynamic diffusion theory with concentration dependent viscosity and effective diffusivity.	$J_{\lim} = J_0 + \frac{1}{L - x_{cr}}$ x $\int_{x_{cr}}^{L} J_0 \left(\frac{3}{2} \frac{(x - x_{cr})}{x_{cr}} + 1 \right)^{-1/3} dx$ $x_{cr} = \frac{\tau_{w0}^3 d_p^4}{16 \mu^3 \phi_b J_0^3} \bar{Q}_{cr}(\phi_b)$ $\tau_{w0}^3 = \frac{3 \bar{u}_b \mu \eta(\phi_b)}{h_e}$ $\bar{Q}_{cr}(\phi_b) = \int_{\phi_b}^{\phi_{\max}} \left(\int_{\phi}^{\phi_{\max}} \frac{\bar{D}(\phi')}{\phi' \eta^2(\phi')} d\phi' \right)$ x $\frac{(\phi - \phi_b)\bar{D}(\phi)}{\phi \eta(\phi)} d\phi$ $\eta(\phi) = \frac{\mu(\phi)}{\mu} = \left(1 + 1.5 \frac{\phi}{1 - \frac{\phi}{0.58}} \right)^2$ $\bar{D}(C) = 0.33 \phi^2 [1 + 0.5 \exp(8.8\phi)]$		For laminar channel flow, solved numerically. Applies for the case of a large cake resistance compared to membrane resistance; J_0 is not specified in the model, therefore, it is suggested that J_0 must be either experimentally determined at limiting conditions or approximated by $J_0 = \Delta p / (\mu R_m)$; good agreement is obtained for many microfiltration experiments under different operation conditions.	Fine particles (and colloids).

	Theory	Model equation	Model Para -meters	Comments	Feed type recommended for
(g)	Film model	$J = k_s \ln\left(\frac{C_m - C_p}{C_b - C_p}\right)$		For mass transfer controlled systems where J_p is independent of pressure. Describes concentration polarisation. Mass transfer coefficient needs to be estimated from literature or experiment.	Fine particles (and colloids).
(h)	Gel polarisation theory	$J_{\lim} = k_s \ln\left(\frac{C_g}{C_b}\right)$		Assumes 100% solute rejection. Limitations include: • Does not distinguish between laminar and turbulent flow; • $Cg = f(C_b, v_{crossflow}) \neq$ constant; • $J_p \neq 0$, when $C_b = C_{g,calculated}$; • No dependence of membrane properties implied. However, still regarded as the most convenient model from a practical point of view.	Fine particles (and colloids).

Table A1.3: Fundamental equations for microfiltration flux modelling

A1.3 Modelling transmission

Ferry (1936) proposed that membranes could be considered as sieves, which pass or stop molecules or particles according to their size. The membrane-sieving coefficient is defined by equation A1.32.

$$\chi = \frac{C_p}{C_b} \qquad [A1.32]$$

Ferry used simple steric considerations to describe the sieving characteristics of perfectly isoporous membranes for monodisperse systems. The sieving characteristics are evaluated in terms of the effective pore size defined as the diameter of the smallest molecular or particulate species, which absolutely fails to penetrate the membrane. The difference between the average pore diameter and the effective pore diameter is attributed to adsorption effects. The membrane structure is assumed to consist of parallel cylindrical capillaries of circular cross-section. Ferry also assumed that the solution remained homogenous throughout filtration.

The filtering solution follows uniformly distributed streamlines in the bulk phase, but these streamlines become concentrated near pore openings. According to Poiseuille flow, the velocity distribution at the centre of any pore to the walls of the pore is given by equation A1.33.

$$u(r) = u_0\left(1 - \frac{r^2}{R^2}\right) \qquad [A1.33]$$

The volumetric flowrate is given by equation A1.34 below

$$Q = \frac{dV_p}{dt} = \int_0^R 2\pi r u(r) dr = \frac{\pi u_0 R^2}{2} \qquad [A1.34]$$

Particles migrating towards a pore, as a result of the suspension flow, will have a probability of penetrating the pore. This probability is equal to unity for particles whose centres fall within a concentric circle having a radius equal to $(R - r_p)$, where r_p is the particle radius, otherwise there is no penetration. This steric limitation introduces a statistical sieving coefficient. Thus, neglecting Brownian motion, the number of particles entering a pore is equivalent to the number of particles whose velocities exceed the hydrodynamic velocity corresponding to that at the limiting probability radius.

$$\frac{dn}{dt} = C_b \int_0^{R-r_p} 2\pi r u(r) dr = C_b \pi u_0 \left[(R - r_p)^2 - \frac{(R - r_p)^4}{2R^2} \right] \qquad [A1.35]$$

The concentration in the permeate is given by

$$C_p = \frac{dn}{dV} = C_b\left[2\left(\frac{R - r_p}{R}\right)^2 - \left(\frac{R - r_p}{R}\right)^4\right] \qquad [A1.36]$$

Thus, the sieving model is described by

$$\chi = 2\left(1 - \frac{r_p}{R}\right)^2 - \left(1 - \frac{r_p}{R}\right)^4 \qquad [A1.37]$$

The retention coefficient curve can be estimated from

$$\sigma = 1 - \chi = [1 - (1 - \lambda)^2]^2 \qquad [A1.38]$$

Several factors have been ignored in the derivation of the sieving model. These include the influence of operating conditions and the effect of concentration polarisation on membrane performance, and the changes in selective behaviour of the membrane with processing time. Also, the criterion for particle penetration may be too restricting. Cherkasov (1990) revealed inadequacies in the sieving model by testing the theory on empirical data obtained from ultrafiltration and microfiltration experiments. The results of his experiments showed a dependence of the retention coefficient on the particle-to-pore size ratio, but this relationship was sigmoidal with a critical relationship.

$$\lambda_{cr} = 0.3 \pm 0.2 \qquad [A1.39]$$

λ_{cr} represents the particle-to-pore size ratio at which there is a sharp fall in membrane permeability.

Literature implies a common mechanism responsible in determining the performance of a membrane system i.e. fouling. Transmission is a function of the total resistance (membrane and cake) and of the operating conditions (flux and transmembrane pressure).

$$Transmission = f\left(\frac{1}{R_{TOTAL}}\right) = f\left(\frac{J}{TMP}\right) \qquad [A1.40]$$

Novais (2001) presents a good literature review on past attempt to describe transmission, and developed a model for an *E. coli* lysate process. The decline in transmission could be modelled by an exponentially decreasing curve which was a function of the initial transmission value (T_0), and filtration time.

$$T_{obs} = T_0 e^{-at} \qquad [A1.41]$$

This experimental work indicated that fouling was likely to be only partially responsible for the decline in transmission. Indeed, an important finding was that small amounts of "non-available" product may be responsible for the decline of the observed transmission. Aggregation or volume increases constitute possible reasons why some product may sot be available for the separation. This result is particularly relevant as the feed material used was a real process stream, as opposed to pure protein solutions, which constitute the basis for most studies found in the literature. This means that experimentally observed transmission does not correspond to the actual %T of the system.

Balakrishnan et al. (1993) suggested that transmission values of greater than 100% indicate enrichment of the protein in the permeate i.e. fractionation of the species was occurring in this UF operation. However, Okec (1998) and Novais (2001) showed that little or no fractionation took place with microfiltration.

A1.4 Statistical models

Algorithms available for least-squares optimisation problems often use the steepest descent method or a Taylor-series method. Palosaari et al. (1986) used a random search method to simulate the reverse osmosis of ethanol and acetic acid. In the method, the best value was initially found by a random search, and subsequent iterations were conducted in a progressively reduced search area. Iterations were continued until the search area was reduced by a given amount. The random search was repeated several times and the most successful random minimisation was accepted as optimal. Once the weighted parameters of the neural network model are determined, simulations of the process can be carried out within the range of variables used in the experiments.

To establish which process variables have the most significant effect on the performance of a membrane system, a method of experimental design can be used. This method allows the abstraction of structured information from physical systems with a minimum of experimentation.

Experimental design is defined as a combination of statistical techniques for the structured analysis of experimental data. Haaland (1989) gives a comprehensive guide to experimental design in biotechnology. A typical design for screening physical systems usually takes the following form:

- Perform experiments in a structured methodical manner;
- For each trial, determine a value for the response factor;
- Calculate values for main effects and interactions by manipulation of the response factors;
- Identify the important main effects and interactions by using pareto charts;
- Determine those experimental factors which are not masked by the experimental error by estimating the noise level and the use of normal probability plots;
- Resolve any interactions between factors by the use of interaction plots.

Full factorial designs are the most commonly used experimental design procedure because they are simple to implement and easy to interpret. The main features include Pareto charts, which identify significant main effects and interactions of process variables, and normal probability plots, which identify main effects and interactions which are large in comparison to the experimental error.

In a typical two level design, i.e. a 'high' setting and a 'low' setting for each variable or factor, experiments are performed for each combination of variable settings. The outcome of each experiment is measured by a value determined for the response factor. A full factorial design investigates all of the possible combinations of settings for each variable, allowing the independent estimation of signals associated with each variable and with a combination of variables (Haaland, 1989). The number of experiments that have to be performed in a k-factor, n-level full factorial design is n^k. The number of experiments in the design is the sample size. The sample size for full factorial designs may become large. In such cases, fractional factorial designs are often used for screening physical systems. Such a design approach will inevitably lead to some information loss and possible ambiguity about variable interactions.

To investigate the effect of 4 factors, including the membrane pore size, the cell concentration, the recirculation rate and the transmembrane pressure, on the performance of the membrane system, a 3-level fractional factorial design was used by Okec (1998). The values were determined by fitting the experimental data to the fouling model described by Patel et al. (1987).

Okec (1998) developed a model, for a yeast/ADH system, based on a statistical approach and uses Pareto charts and normality plots to establish which variables have significant effects on the membrane separation process. A statistical model, based on linear regression, to predict permeate flux rates was developed. Fitting a statistical model to predict the response value involves constructing a linear model using regression analysis.

$$R = \beta + \beta_1 A + \beta_2 B + \beta_3 C + \beta_4 (A*C) + \beta_5 (B*C) + \beta_6 (A*D) + \beta_7 (B*D) + \beta_8 (A*B*D) + \text{error} \quad [A1.42]$$

where R is the residual value

A, B, C, A*C, B*C,... are the significant effects and interactions

β is the intercept term

β_i $(i = 1,...,8)$ m are the model coefficients

The applicability of such a model to a broader range of membrane pore size, cell concentration and recirculation rate is questionable. As the particle size to the membrane pore size ratio (λ) decreases, the filtration mechanism is altered from a predominant screen filter to a predominant depth filter. Kawakatsu *et al.* (1993) concluded that the relationship between the particle size and the membrane pore size was important for determining the steady-state permeate flux rate. They also concluded that in the filtration of compressible particles such as *Sacchromyces cerevisiae*, the steady-state permeate flux rate reached a minimum when $\lambda = 10$. This observation is consistent with the results found by Okec (1998), within the experimental error, since at $\lambda = 8$, the steady-state permeate flux rate is at a minimum for the experiments conducted. If other biological systems exhibit the same behaviour, it would be interesting to determine whether the significant effects and interactions, for the same range of λ, are identical and also if the ratios of the coefficients in equation [A1.42] remain the same.

The use of fractional factorial experimental design as a methodology for assessing the significant effects and interactions of process variables including the membrane pore size, the cell concentration, the recirculation rate and the transmembrane pressure on the performance of microfiltration has been shown. Analysis of the experimental data using a Pareto chart showed that the membrane pore size had the most significant effect on the performance of the physical system examined in this thesis. Of the 15 possible main effects and interactions, 8 were found to have a significant effect on the performance of the system. Process optimisation procedures should begin with the most significant effects and interactions.

Using a statistical approach, a linear model for the prediction of the steady-state permeate flux rate was developed (Okec, 1998). This approach was more accurate than that using a concentration polarisation model characterised by single microfiltration experiments. However, the statistical approach tends to be more specific and requires several experiments to develop.

A1.5 Dynamic modelling of TFF using neural networks or CFD

For a given product/membrane combination, it is often difficult to predict the effects of operating conditions and of the duration of filtration on the fouling rate. A model that can predict the evolution of membrane fouling during filtration as a function of operating conditions and history would therefore be a valuable tool, especially for optimisation of operation parameters.

As described above, membrane fouling is a consequence of a number of dynamic and simultaneous phenomena; convective mass transfer through the membrane, back-diffusion caused by high local concentrations (concentration polarisation), shear-induced hydrodynamic back-transport, electrochemical interactions between the product and the membrane and possible chemical and microbiological instabilities in the feed stream. Considering the diversity of these phenomena, the development of a dynamic model based on the known principles of transfer, that globally represents fouling, is extremely difficult. Therefore, dynamic-knowledge-based models specific to microfiltration are scarce in the literature. The few models proposed so far only define certain phenomena, do not take into account operating conditions as a whole or make use of parameters that are difficult to determine experimentally.

As a result modelling techniques based on the direct analysis of experimental data (descriptive models) appear to be a good alternative to the models based on phenomenological hypotheses (knowledge-based models). As a tool of dynamic simulation, these "black box" models, although not explicative, can be used to represent the experimental results and are suitable to globally describe the considered phenomena. The effects of operating conditions on fouling and its dynamic behaviour are often not linear; hence the classical descriptive linear models cannot be used. Considering their features, connective models or neural networks should allow one to account for the non-linearity of the many phenomena that contribute to flux decline.

Dornier et al. (1995) Niemi et al. (1995) and Meyer et al. (1998) used neural networks model crossflow microfiltration systems. In their work, the output variables included the permeate flux rate and the membrane rejection characteristics. However, different workers used different inputs to describe their models. Dornier et al. (1995) included the transmembrane pressure and the recirculation rate as input variables. Niemi et al. (1995) included the aforementioned variables, the feed concentration and the temperature as input variables.

The main advantage of using neural networks is the ease of implementation and the accuracy of model predictions. However, the training requirements of the simulator and the specificity of generated models are significant drawbacks.

Delgrange et al. (1998) applied neural networks for the prediction of ultrafiltration transmembrane pressure during drinking water production. An artificial neural network (ANN) was also developed for cell harvesting of *Escherichia coli,* through a shear-enhanced module, by Meyer et al. (1997). The effects of seventeen process parameters were investigated. However, a large number of experimental data were required for model development, and the model was not tested against further data. The authors concluded with the major limitation of the neural network approach; every filtration process has to be considered as an individual problem. The model developed is an individual solution and represents a problem-orientated approach.

At the other extreme of dynamic modelling is computational fluid dynamics (CFD); rather than a "black box" approach, it uses finite element analyses and detailed mathematical equations to model fluid flow in different geometries. Ongoing development of commercial computational fluid dynamics software (CFD) and increasing computer power are continuously improving the conditions for the simulation of the three-dimensional and turbulent flow in unit operations. It is now generally accepted that Reynolds- averaging Navier-Stokes equations and modelling the Reynolds-stresses with an appropriate turbulence model is a promising method of flow behaviour modelling (Jenne and Reuss, 1999).

Karode and Kumar (2001) and Wiley and Fletcher (2002) present comprehensive literature reviews of attempts to apply CFD techniques to membrane filtration, as well as CFD models for flow in membrane channels. These models were successfully verified against classical solutions available in the literature, but both publications highlighted the fact that accurate modelling of and concentration polarisation is prohibited by the complex couplings of the flow equations and variable solution properties; overly simplified expressions for the dependence of viscosity and diffusivity on solution concentration produced misleading velocity and concentration profiles.

The demanding mathematics and high order numerical schemes required for valid models has kept CFD in the realms of academia, and as with neural networks, the quality of the output data can only ever be as good as the quality of the input data; such physical properties of biological systems are mostly empirically derived, and therefore limited in their application.

Appendix 2 Resistance-in-series Model Program Listing

Below is the program listing (Visual Basic, Microsoft Corporation, USA), for the resistance-in-series model described in Chapter 2, and used to create the data presented in Chapter 5.

```
Dim A, DP, muperm, V0, C0, tfinal, Rm, Rss, Rass, Rpss, b, alpha, n, JLMH, Cp As Single
Dim Ra, Rp, RaRp, Rc, DdeltaCm, Coeff1, Coeff2, alpha0, dmdt, dVrdt, J, m, C, Cr, V, Vr, Tobs
As Single
Dim t, h As Double
Dim row_copy, column, X_copy As Integer

Sub CONSTTMP()
'Clearing away the old results
Worksheets("tmp model results").Range("b9:f400").Clear

'Membrane, rig and feed details
A = Worksheets("inputs").Range("b3")
DP = Worksheets("inputs").Range("b4")
muperm = Worksheets("inputs").Range("b5")
V0 = Worksheets("inputs").Range("b6")
C0 = Worksheets("inputs").Range("b7")
tfinal = Worksheets("inputs").Range("b8")

'Experimental data
Rm = Worksheets("inputs").Range("f3")
Rss = Worksheets("inputs").Range("f4")
Rass = Worksheets("inputs").Range("f5")
Rpss = Worksheets("inputs").Range("f6")
b = Worksheets("inputs").Range("f7")
Coeff1 = Worksheets("inputs").Range("f8")
Coeff2 = Worksheets("inputs").Range("f9")
alpha = Worksheets("inputs").Range("f10")
n = Worksheets("inputs").Range("f11")
Tobs = Worksheets("inputs").Range("f12")

'Initial conditions
t = 0
X = 0
Vr = V0
Cr = C0
Cp = 0
Ra = 0
Rp = 0
RaRp = 0
Rc = 0
m = 0
DdeltaCm = 0
J = (DP / (muperm * Rm))
alpha0 = alpha * DP ^ (n)

'Iteration loop
h = Worksheets("inputs").Range("j3")
row_copy = 9
column_copy = 2

While t <= tfinal
Worksheets("tmp model results").Range("b4").Value = t
```

```
Worksheets("tmp model results").Range("c4").Value = J
Worksheets("tmp model results").Range("d4").Value = Cr
Worksheets("tmp model results").Range("e4").Value = Vr

If (X Mod 100) = 0 Then

Worksheets("tmp model results").Range("b4").Copy
Worksheets("tmp model results").Cells(row_copy, column_copy).PasteSpecial Paste:=xlValues
Worksheets("tmp model results").Range("c4").Copy
Worksheets("tmp model results").Cells(row_copy, column_copy + 1).PasteSpecial
Paste:=xlValues
Worksheets("tmp model results").Range("d4").Copy
Worksheets("tmp model results").Cells(row_copy, column_copy + 2).PasteSpecial
Paste:=xlValues
Worksheets("tmp model results").Range("e4").Copy
Worksheets("tmp model results").Cells(row_copy, column_copy + 3).PasteSpecial
Paste:=xlValues
row_copy = row_copy + 1
End If

'Permeate flowrate and concentration assumed to be constant over small time steps

DdeltaCm = (Coeff1 * Log(Cr)) - Coeff2
dmdt = (J * Cr - DdeltaCm) * A
dVrdt = -(A * J)
t = t + (0.2 * h)
X = X + 1
RaRp = (Rss) * (1 - Exp(-b * t))
J = (DP / (muperm * (Rm + RaRp + Rc)))
Cr = ((C0 * V0) / (Vr + Tobs * (V0 - Vr)))
Rc = (m / A) * alpha0
m = C * (V0 - Vr)
Vr = Vr + (h * dVrdt)
Wend
End Sub

Sub CONSTFLUX()
'Clearing away the old results
Worksheets("J model results").Range("b9:f400").Clear

'Membrane, rig and feed details
A = Worksheets("inputs").Range("b17")
JLMH = Worksheets("inputs").Range("b18")
muperm = Worksheets("inputs").Range("b19")
V0 = Worksheets("inputs").Range("b20")
C0 = Worksheets("inputs").Range("b21")
tfinal = Worksheets("inputs").Range("b22")


'Experimental data
Rm = Worksheets("inputs").Range("f17")
Rss = Worksheets("inputs").Range("f18")
Rass = Worksheets("inputs").Range("f19")
Rpss = Worksheets("inputs").Range("f20")
b = Worksheets("inputs").Range("f21")
Coeff1 = Worksheets("inputs").Range("f22")
Coeff1 = Worksheets("inputs").Range("f23")
alpha = Worksheets("inputs").Range("f24")
n = Worksheets("inputs").Range("f25")
Tobs = Worksheets("inputs").Range("f26")
```

```
'Initial conditions
t = 0
X = 0
Vr = V0
Cr = C0
Cp = 0
Ra = 0
Rp = 0
RaRp = 0
Rc = 0
m = 0
DdeltaCm = 0
J = JLMH / 3600000
DP = J * (muperm * Rm)
alpha0 = alpha * DP ^ (n)

'Iteration loop
h = Worksheets("inputs").Range("j17")
row_copy = 9
column_copy = 2

While t <= tfinal
Worksheets("J model results").Range("b4").Value = t
Worksheets("J model results").Range("c4").Value = DP
Worksheets("J model results").Range("d4").Value = Cr
Worksheets("J model results").Range("e4").Value = Vr
Worksheets("J model results").Range("f4").Value = J

If (X Mod 100) = 0 Then

Worksheets("J model results").Range("b4").Copy
Worksheets("J model results").Cells(row_copy, column_copy).PasteSpecial Paste:=xlValues
Worksheets("J model results").Range("c4").Copy
Worksheets("J model results").Cells(row_copy, column_copy + 1).PasteSpecial
Paste:=xlValues
Worksheets("J model results").Range("d4").Copy
Worksheets("J model results").Cells(row_copy, column_copy + 2).PasteSpecial
Paste:=xlValues
Worksheets("J model results").Range("e4").Copy
Worksheets("J model results").Cells(row_copy, column_copy + 3).PasteSpecial
Paste:=xlValues
Worksheets("J model results").Range("f4").Copy
Worksheets("J model results").Cells(row_copy, column_copy + 4).PasteSpecial
Paste:=xlValues
row_copy = row_copy + 1
End If

DdeltaCm = (Coeff1 * Log(Cr)) - Coeff2
dmdt = (J * Cr - DdeltaCm) * A
dVrdt = -(A * J)
t = t + (0.2 * h)
X = X + 1
RaRp = (Rss) * (1 - Exp(-b * t))
DP = (J * (muperm * (Rm + RaRp + Rc)))
Cr = ((C0 * V0) / (Vr + Tobs * (V0 - Vr)))
'Cp = (((C0 * V0) - (Cr * Vr)) / (V0 - Vr))
Rc = (m / A) * alpha0
m = m + (h * dmdt)
Vr = Vr + (h * dVrdt)
Wend
End Sub
```

NOMENCLATURE

A	Membrane Area	m^2
a	Exponential Decay Constant For T_{obs}	-
ADH	Alcohol Dehydrogenase	-
A_m	Membrane Area	m^2
BSA	Bovine Serum Albumin	-
C	Concentration Of Retained Species	$g.L^{-1}$
C_b	Bulk Concentration Of Retained Species	$g.L^{-1}$
cGMP	Current Good Manufacturing Practices	-
CIP	Clean-In-Place	-
C_w	Wall Concentration Of Retained Species	$g.L^{-1}$
D	Diffusion Coefficient Of Retained Species	$m^2 s^{-1}$
DCW	Dry Cell Weight	-
DF	Diafiltration	-
DNA	Desoxyribonucleic Acid	-
d_p	Particle Diameter	m
ED	Electrodialysis	-
EDTA	Ethylenediaminetetraacetic Acid	-
ELISA	Enzyme Linked Immunoabsorbant Assay	-
EMEA	The European Medicines Agency	-
F	Feed	-
Fab'	Antibody Fragment	-
FDA	USA Food And Drug Administration	-
HPTFF	High Performance Tangential Flow Filtration	-
IQ	Installation Qualification	-
IT	Integrity Test	-
J	Permeate Flux Rate	$L.m^{-2}.h^{-1}$
k	Constant	-
K_{av}	Apparent Partition Coefficient	-
k_b	Boltzman Constant	$J.K^{-1}$
k_m	Mass Transfer Coefficient	ms^{-1}
L_{mem}	Membrane Module Length	m

LMH	Litres Per Metre Squared Per Hour	$L.m^{-2}.h^{-1}$
Mab'	Monoclonal Antibody	-
MF	Microfiltration	-
MWCO	Molecular Weight Cut-Off	-
NF	Nanofiltration	-
NFF	Normal Flow (Dead-End) Filtration	-
NWP	Normalised Water Permeability	-
OD	Optical Density	-
OQ	Operational Qualification	-
P	Permeate	-
ΔP	Transmembrane Pressure	$N.m^{-2}$
PBS	Phosphate Buffered Saline	-
PQ	Performance Qualification	-
Q	Volumetric Flowrate	$m^3 s^{-1}$
QA	Quality Assurance	-
QC	Quality Control	-
R	Retentate	-
R&D	Research And Development	-
Re	Reynolds Number	-
R_m	Membrane Resistance To Permeate Flow	m^{-1}
RO	Reverse Osmosis	-
R_s	Resistance Of Solid Cake	m^{-1}
R_{total}	Total Resistance To Permeate Flow	m^{-1}
SIP	Sanitise-In-Place	-
SOP	Standard Operating Procedure	-
t	Time	s
T	Absolute Temperature	K
TFF	Tangential Flow Filtration	-
TMP	Transmembrane Pressure	kPa
UF	Ultrafiltration	-
USD	Ultra Scale-Down	-
V	Filtrate Volume	L
WFI	Water for Injection	-

WinOp	Window of Operation	-

Greek Letters

α	Power Constant	-
β	Intercept Term	-
χ	Membrane Sieving Coefficient	-
δ	Boundary Layer Thickness	m
δ_c	Cake Layer Thickness	m
ε	Cake Void Fraction	-
ε_{340}	Extinction Coefficient At 340nm	$cm^2.\mu mol^{-1}$
ϕ	Volume Fraction Of Particles	-
γ	Shear Rate	s^{-1}
λ	Particle-to-Pore Size Ratio	-
ν	Kinematic Viscosity	$m^2.s^{-1}$
σ	Retention Coefficient	-
τ	Shear Stress	$N.m^{-2}$
σ	Retention Coefficient	-
λ	Particle-to-Pore Size Ratio	-
χ	Membrane Sieving Coefficient	-
ν	Kinematic Viscosity	$m^{-2}.s^{-1}$
α	Specific Cake Resistance	m^{-1}
μ_S	Viscosity of the Suspension	$N.s.m^{-2}$
ω	Disk Rotation Speed	$rad.s^{-1}$

REFERENCES

Akay, G. and Wakeman, R. J. **1993.** Ultrafiltration and microfiltration of surfactant dispersions- an evaluation of published research. *Chemical Engineering Research & Design* **71** (A4), 411-420.

Agarwal,G.P. **1997** Analysis of proteins transmission in vortex flow ultrafilter for mass transfer coefficient. *Journal of Membrane Science* **136** (1-2), 141-151.

Aimar, P., Howell, J.A., **1991.** Concentration polarisation build-up in hollow fibers: a method of measurement and its modelling in ultrafiltration. *Journal of Membrane Science* **59**, 81-99.

Alex, T. and Haughney, H. **1998**. New membrane-based technologies for the pharmaceutical industry. In *Filtration in the Biopharmaceutical Industry*, Ed. Meltzer, T.H. and Jornitz, M.W. Marcel Dekker Inc., 745-782.

Altena, F. W., Belfort, G. **1984**. Lateral migration of spherical-particles in porous flow channels - application to membrane filtration. *Chemical Engineering Science* **39** (2), 343-355.

Arnot, T.C., Field, R.W. and Koltuniewicz, A. B. **2000**. Cross-flow and dead-end microfiltration of oily-water emulsions Part II. Mechanisms and modelling of flux decline. *Journal of Membrane Science* **169**, 1-15.

Atkinson, B. and Mavituna, F. **1991**. *Biochemical Engineering and Biotechnology Handbook*, 2nd edition, Macmillan, Basingstoke, Chapter 11.

Bacchin, P. **2004**. A possible link between critical and limiting flux for colloidal systems: consideration of critical deposit formation along a membrane. *Journal of Membrane Science* **228** (2), 237-241.

Bailey, J.E. and Ollis, D.F. **1996**. Product recovery operations. In *Biochemical engineering fundamentals*, 2nd Edition, McGraw-Hill Book Company, 726-797.

Bailey, F.J., Warf R.T., Maigetter, R.Z.**1990**. Harvesting recombinant microbial cells using crossflow filtration. *Enzyme Microb. Technol.* **12** (September), 647-652.

Bailey, S. M. and Meagher, M. M. **1997**. Crossflow microfiltration of recombinant *Eschericoia coli* lystaes after high pressure homogenisation. *Biotechnology and Bioengineering* **56** (3), 304-310.

Bailey, S. M. and Meagher, M. M. **2000**. Separation of soluble protein from inclusion bodies in *Eschericia coli* lysate using crossflow microfiltration. *Journal of Membrane Science* **166** , 137-146.

Baker, A. **2001**. PhD Thesis, University of London.

Balakrishnan,M., Agarwal,G.P., and Cooney,C.L. **1993**. Study of protein transmission through ultrafiltration membranes. *Journal of Membrane Science* **85** (2), 111-128.

Baruah,G.I. and Couto,D. **2002**. Recovery of human monoclonal antibodies from transgenic goat milk. *Abstracts of Papers of the American Chemical Society* **224** 079-BIOT.

Baruah,G.L. and Belfort,G. **2003**. A predictive aggregate transport model for microfiltration of combined macromolecular solutions and poly-disperse suspensions: Model development. *Biotechnology Progress* **19** (5), 1524-1532.

Baruah,G.L. and Belfort,G. **2004**. Optimized recovery of monoclonal antibodies from transgenic goat milk microfiltration. *Biotechnology and Bioengineering* **87** (3), 274-285.

Baruah,G.L., Couto,D., and Belfort,G. **2003**. A predictive aggregate transport model for microfiltration of combined macromolecular solutions and poly-disperse suspensions: Testing model with transgenic goat milk. *Biotechnology Progress* **19** (5), 1533-1540.

Baruah, G. L., Venkiteshwaran, A. and Belfort, G. **2005**. Global model for optimizing crossflow microfiltration and ultrafiltration processes: A new predictive and design tool. *Biotechnology Progress* **21** (4), 1013-1025.

Bashir, I. and Reuss, M. **1991**. Dynamic model for cross-flow microfiltration of microbial suspensions in porous tubes. *Chemical Engineering Science* **41** (1), 189-203.

Belfort G., Davis, R.H., and Zydney, A. L. **1994.** Review: The behaviour of suspensions and macromolecular solutions in crossflow microfiltration. *Journal of Membrane Science* **96**, 1-58.

Bell, D.J., Hoare, M. and Dunnill, P. **1983**. The formation of protein precipitates and their centrifugal recovery. *Advances in Biochemical Engineering,* **26**, 1-72.

Blatt, W. F., Robinson, S. M. **1968**. Membrane ultrafiltration – diafiltration technique and its application to microsolute exchange and binding phenomena. *Analytical Biochemistry* **26** (1), 151-160.

Bobrowicz, G. **1999.** The compliance costs of hasty process development. *BioPharm* **August** 35-38.

Bouzerar, R., Ding, L.H., and Jaffrin, M.Y. **2000**. Local permeate flux-shear-pressure relationships in a rotating disk microfiltration module: implications for global performance. *Journal of Membrane Science* **170** (1), 127-141.

Bouzerar, R., Jaffrin, M.Y., Ding, L.H., and Paullier, P. **2000**. Influence of geometry and angular velocity on performance of a rotating disk filter. *AIChE Journal* **46** (2), 257-265.

Bowen, W. R. and Williams, P. M. **1996**. Dynamic ultrafiltration model of proteins: a colloidal interaction approach. *Biotechnology and Bioengineering* **50**, 125-135.

Bowen, W.R., Cao, X., and Williams, P. **1999**. Use and elucidation of biochemical data in the prediction of the membrane separation of biocolloids. *Proc.R.Soc.Lond.A* **455**, 2933-2955.

Bowen, W. R., Hilal, N., Jain, M., Lovitt, R.W., Mohammad, A.W., Sharif, A.O., Williams, P., and Wright, C. J. **1999**. *Ab initio* prediction of performance of membrane separation processes. In Compton, R.G. and Hancock, G. (eds), Elsevier, 523-541.

Bowen, W. R., Mongruel, A., and Williams, P. **1996.** Prediction of the rate of cross-flow membrane ultrafiltration:a colloidal interaction approach. *Chemical Engineering Science* **51** (18), 4321-4333.

Bowen, W.R., Gan, Q. **1991**. Properties of microfiltration membranes: Flux loss during constant pressure permeation of Bovine Serum Albumin. *Biotech Bioeng* **38** (7), 688-696.

Bowen, W.R., Gan, Q. **1992**. Properties of Microfiltration membranes: The Effects of Adsorption and Shear on the Recovery of an Enzyme. *Biotech. Bioeng.***40**, 491-497.

Bowen, W.R., Hall, N.J. **1995**. Properties of microfiltration membranes: Mechanisms of flux loss in the recovery of an enzyme. *Biotech. Bioeng.***46** (1), 28-35.

Bowen, W.R. and Jenner, F. **1995**. The calculation of dispersion forces for engineering calculations. *Adv. Colloid Interface Sci.* **56**, 201-243.

Bowen, W.R., Jones, M.G., and Yousef, H.N.S. **1998**. Dynamic ultrafiltration of proteins - A neural network approach. *Journal of Membrane Science* **146** (2), 225-235.

Bowering L.C. **2000.** An engineering study of the design, integration and control of antibody fragment production processes. PhD Thesis, University of London.

Boychyn, R.M.**1998**. Scale-down principles for the accelerated design of protein purification processes. PhD Thesis, University of London.

Boychyn, R.M. **2000**. Scale-down principles for the accelerated design of protein purification processes. PhD Thesis, University of London.

Boychyn, R.M., Doyle, W., Bulmer, M., More, J., and Hoare, M. **2000.** Laboratory scaledown of protein purification processes involving fractional preciptation and centrifugal recovery. *Biotechnology and Bioengineering* **69** (1), 1-10.

Boychyn, R.M., Yim, S.S., Ayazi-Shamlou, P., Bulmer, M., More, J. and Hoare, M. **2001**. Characterization of flow intensity in continuous centrifuges for the development of laboratory mimics. *Chemical Engineering Science* **56**, 4759-4770.

Bradford, M. M. **1976**. A rapid and sensitive method fir the quantitation of microgram quantities of protein using the principle of protein-dye binding. *Analytical Biochem.* **72**, 248-254.

Brauns, E., Van Hoof, E., Molenberghs, B., Dotremont, C., Doyen, W. And Leysen, R. **2002**. A new method of measuring and presenting the membrane fouling potential. *Desalination* **150**, 31-43.

Breggar, M.M. **1996**. Navigating regulatory maze requires a proactive strategy. *1996 GEN Guides Editorial*, 277-278.

Brose, D., Dosmar, M., Cates, S., and Hutchison, F. **1996.** Studies on the scale-up of crossflow filtration devices. *PDA Journal of Pharmaceutical Science and Technology* **50** (4), 252-260.

Brou, A., Ding, L.H., Boulnois, P., and Jaffrin, M.Y. **2002**. Dynamic microfiltration of yeast suspensions using rotating disks equipped with vanes. *Journal of Membrane Science* **197** (1-2), 269-282.

Brown, D.E. and Kavanagh, P.R. **1987**. Crossflow separation of cells. *Process Biochem.* **22** 96-115

Burnett, M.B., Santa Marina, V.G., Omstead, D.R. **1991**. Design of a multipurpose biotech pilot and production facility. *Ann NY Academy Sci* **646**, 357-366.

Burns, D. and Zydney, A. L. **1999**. Effect of solution pH on protein transport through ultrafiltration membranes. *Biotechnology and Bioengineering* **64** (1), 27-37.

Bylund, F., Guillard, F., Enfors, S.O. and Larsson, G. **1999**. Scale down of recombinant protein production; a comparative study of scaling performance. *Bioprocess Eng* **20** (377), 389.

Carrère, H. and Rene, F. **1996**. Industrial multi-stage continuous filtration process: influence of operating parameters. *Journal of Membrane Science* **110**, 191-202.

Carrère, H., Blaszkow, F. And Roux de Balmann, H. **2001**. Modelling the clarification of lactic acid fermentation broths by cross-flow microfiltration. *Journal of Membrane Science* **186**, 219-230.

Carter, P., Kelley, R.F., Rodrigues, M.L., Snedecor, B., Covarrubias, M., Velligan, M.D., Wong, W.L.T., Rowland, A.M., Kotts, C.E., Carver, M., Yang, M., Bourell, J.H., Shepard, H.M., and Henner, D. **1992**. High level *Eschericia coli* expression and production of a bivalent humanised antibody fragment. *Bio/Technology* **10** (Feb), 163-167.

Castilho, L.R. and Anspach, F.B. **2003**. CFD-aided design of a dynamic filter for mammalian cell separation. *Biotechnology and Bioengineering* **83**, 514-524.

Chan, G., Booth, A.J., Mannweiler, K., Hoare, M. **2006**. Ultra scale-down studies of the effect of flow and impact conditions during *E.coli* cell processing. *Biotechnology and Bioengineering* **95** (4), 671-683.

Chandler, M. and Zydney, A. **2004.** High throughput screening for membrane process development. *Journal of Membrane Science* **297**, 181-188.

Chang, D., Hsu, F., and Hwang, S. **1995**. Steady-state permeate flux of cross-flow microfiltration. *Journal of Membrane Science* **98**, 97-106.
Chellam, S. and Wiesner, M. **2001**. Evaluation of crossflow filtration models based on shear-induced diffusion and particle adhesion: Complications induced by feed suspension polydiversity. *Journal of Membrane Science* **138**, 83-97.

Chen, V. **1998**. Performance of partially permeable microfiltration membranes under low fouling conditions. *Journal of Membrane Science* **147,** 265-278.

Chen, V., Fane, A.G., Madaeni, S. and Wenten, I. G. **1997.** Particle deposition during membrane filtration of colloids: transition between concentration polarization and cake formation. *Journal of Membrane Science* **125**, 109-122.

Cherkasov, A.N., **1990**. Selective ultrafiltration, *Journal of Membrane Science*, **50**, 109-130.

Cherry, R.S. and Papoutsakis, E.T. **1986.** Hydrodynamic effects on cells in agitated tissue culture reactors. *Bioprocess Engineering* **1**, 29-33.

Cheryan, M. **1986.** *Ultrafiltration handbook*, Technomic Publishing Company, Inc.

Christy, C. **1998**. Pharmaceutical filtration design, applications and examples. *Lecture at UCL Department of Biochemical Engineering.*

Christy, C., 2001 (Millipore Corporation), personal communication.

Clarkson, A.O., Lefevre, P., and Titchener-Hooker, N.J. **1993**. A study of process interactions between cell
disruption and debris clarification stages in the recovery of yeast intracellular products. *Biotech Pro.* **9**, 462-467.

Cole Palmer. **2003**. Product Catalogue.

Coulson and Richardson. **1990.** *Chemical Engineering*, Volume 1, 4th edition, Pergamon Press.

Culkin, B., Plotkin, A., and Monroe, M. **1998.** Solve membrane fouling problems with high-shear filtration.
Chemical Engineering Progress **1**, 29-33.

Cumming, I.W., Holdich, R.G. and Ismail, B. **1999**. Prediction of deposit depth and transmembrane pressure during crossflow microfiltration. *Journal of Membrane Science* **154**, 229-237.

Da Costa, A.R., Fane, A.G., Wiley, D.E. **1994**. Spacer characterization and pressure drop modelling in spacer-filled channels for ultrafiltration. *Journal of Membrane Science* **87**, 79-98.

Da Costa, A.R., Fane, A.G., Fell, C.J.D. and Franken, A.C.M. **1991**. Optimal channel spacer design for ultrafiltration. *Journal of Membrane Science* **62**, 275-291.

Datar, R, and Rosen, C.-G. **1990**. Downstream process economics. In *Separation Processes in Biotechnology*, ed. J. A. Asenjo, Marcel Dekker, Inc., New York, 741 - 793.

Davis, R.H., **1992,** Modelling of fouling of crossflow microfiltration membranes. *Separation and Purification Methods* **21**(2), 75-126.

Davis, R.H., Birdsell, S.A. **1987**. Hydrodynamic model and experiments in crossflow microfiltration. *Chemical Engineering Communications* **49**, 217-234.

Davis, R.H., Leighton, D.T., **1987.** Shear-induced transport of a particle along a porous wall, *Chemical Engineering Science*, **42**, 2, 275-281

Davis, R.H., Sherwood, J.D., **1990**. A similarity solution for steady-state crossflow microfiltration, *Chemical Engineering Science*, **45**, 11, 3203-3209

Defrance, L. and Jaffrin, M.Y. **1999**. Comparison between filtrations at fixed transmembrane pressure and fixed permeate: Application to a membrane bioreactor used for wastewater treatment. *Journal of Membrane Science* **152**, 203-210.

Delgrange, N., Cabassud, C., Cabassud, M., Durand-Bourlier, L. and Laine, J.M. **1998**. Modelling of ultrafiltration fouling by neural network. *Desalination* **118**, 213-227.

Delgrange, N., Cabassud, C., Cabassud, M., Durand-Bourlier, L., and Laine, J.M. **1998**. Neural networks for prediction of ultrafiltration transmembrane pressure - application to drinking water production. *Journal of Membrane Science* **150** (1), 111-123.

de-los-Reyes, G. **1990**. Scale-up considerations for tangential flow filtration processes. *J. Cell. Ciochem. Suppl. 14D.*

Dennis, J. The manufacture of biopharmaceuticals for clinical trials. **1999**. *Manufacturing for Biotechnology Initiative*, Dept of Trade and Industry, Pamphlet.

DiMasi, J.A. **2001**. Risks in new drug development: Approval success rates for investigational drugs. *Clinical Pharmacology and therapeutics* **69** (5), 297-307.

Doran, P.M. **1995**. *Bioprocess Engineering Principles*, 1st Edition, Academic Press.

Dornier, M., Decloux, M., Trystram, G., Lebert, A. **1995.** Dynamic modelling of crossflow microfiltration using neural networks, *Journal of Membrane Science* **98**, 263-273.

Dunnill, P., Davies, E. **1998**. Radical approaches to achieving speed of bioprocess development. *MBI Training Programme*, University College London, London, UK.

Eckstein E.C., Bailey D.G., Shapiro A.H., **1977**. Self-diffusion of particles in shear flow of a suspension, *J. Fluid Mech.* **79** (Part 1) 191–208

Fane, A.G, Fell, C.J.D., **1987**. A review of fouling and fouling control in ultrafiltration. *Desalination*, **62**, 117-136

Fane, A.G., Fell, C.J.D., Hodgson, P.H., Leslie, G., Marshall, K.C., **1991.** Microfiltration of biomass and biofluids: effects of membrane morphology and operating conditions, *Filtration & Separation*, 332-340

Farid, S.S., Novais, J.L, Karri, S., Washbrook, J., Titchener-Hooker, N.J. **2000**. A tool for modelling strategic decisions in cell culture manufacturing. *Biotechnol. Prog.* **16**(5), 829-836.

FDA Biotechnology Task Force on Purification and Scale-Up. **1992**. Industrial Perspective on Validation of Tangential Flow Filtration in Biopharmaceutical Applications. *Journal of Parenteral Science and Technology*, **46** Supplement.

FDA. **1996.** FDA guidance concerning demonstration of comparability of human biological products, including therapeutic biotechnology-derived products. *FDA Center for Biologies Evaluation and Research*, USA.

Ferry, JD, **1936**. Statistical evaluation of sieve constants in ultrafiltration, *Journal of General Physiology* **20**, 95-104.

Field, R.W., Wu, D., Howell, J., and Gupta, B. B. **1995**. Critical flux concept for microfiltration fouling. *Journal of Membrane Science* **100,** 259-272.

Fischer, E. J. **1996**. Impact of separation processes on protein recovery from cells and cell spheroplasts. UCL. PhD Thesis, University of London.

Foley, G., MacLoughlin, PF., and Malone, D. M. **1995**. Membrane fouling during constant flux crossflow microfiltration of dilute suspensions of active dry yeast. *Separation Science and Technology* **30** (3), 383-398.

Forman. S.M., DeBernardez, E.R., Feldberg, R.S., Swartz, R.W. **1990**. Crossflow filtration for the separation of inclusion bodies from soluble proteins in recombinant *Escherichia coli* cell lysate. *Journal of Membrane Science* **48**, 263-279.

Gadam, S., Henrickson, R. and Decker, S. **2001**.Unintended interactions between fermentation and downstream chromatography steps in the purification of virus-like particles. *Abstr. Pap.Amer. Chem. Soc.* **221**, 62-BIOT

Gagnon, P. **1997**. Avoiding instrument-associated aberrations in purification scale-up and scale-down. *BioPharm* **10** (3), 42-45

Garber, K. **2001**. Biotech industry faces new bottleneck. *Nature Biotech* **19**, 184-185

Gardner, P.J. **2005.** The effect of operating parameters and matrix properties on the productivity of an expanded bed adsorption column. PhD Thesis, University of London.

Gardner, A., Gerber, R., Smith, C., McAllister, and Zabriskie, D. **1996**. Use of scale-down models in validation of cell culture processes for production of biopharmaceuticals. *Abstr. Pap. Am. Chem. Soc. 211th Meeting Pt. 1*, BIOT 039.

Gatenholm, P., Paterson, S., Fane, A.G., Fell, C.J.D. **1988**. Performance of synthetic membranes during cell harvesting of *E. coli. Process Biochemistry* **23**(3), 79-81.

Gehlert, G., Luque, S. and Belfort, G. **1998**. Comparison of ultra- and microfiltration in the presence and absence of secondary flow with polysaccharides, proteins and yeast suspensions. *Biotechnol. Prog.* **14**, 931-942.

Geissler, S., Werner, U. **1995**. Dynamic model of crossflow microfiltration in flat-channel systems under laminar flow conditions. *Filtration and Separation* 533-537.

George, S., Larsson, G. and Enfors, S O. **1998**. "Comparison of the baker's yeast process performance in laboratory and production scale." Bioproc. Eng. **18**, 135-142.

Gésan-Guiziou, G., Boyaval, E. and Daufin, G. **1999**. Critical stability conditions in crossflow microfiltration of skimmed milk: transition to irreversible deposition. *Journal of Membrane Science* **158**, 211-222.

Goochee, C.F. **2002**. The roles of a process development group in biopharmaceutical process start-up. *Cytotechnology* **33**, 63-76.

Gooding, C.H. **1991**. Scale-up of membrane systems from laboratory data. *Journal of Membrane Science* **62**, 309-323.

Green, G., Belfort, G., **1980**, Fouling of ultrafiltration membranes: lateral migration and the particle trajectory model, *Desalination*, **36**, 129-147

Griffiths, P. A. **2007**. Developing methodologies for determining operating strategies for bioprocesses. PhD Thesis, University of London.

Gritis, D., Titchener-Hooker, N.J., **1989,** Biochemical process simulation, *Institution of Chemical Engineers Symposium Series*, **144**, 69-77

Groep, M. E., Gregory. M. E, et al. **2000**. Performance modelling and simulation of biochemical process sequences with interacting unit operations. *Biotech Bioeng.* **67** (3), 300-311.

Gyure, D.C. **1992**. Set realistic goals for crossflow filtration. *Chem. Eng. Prog.* **88**, 60-66.

Haaland, P.D., **1989.** Experimental design in biotechnology, Marcel Dekker Inc., New York and Basel,

Haarstrick, A., Rau, U., Wagner, F., **1991.** Crossflow filtration as a method for separating fungal cells and purifying the polysaccharide produced, *Bioprocess Engineering*, **6**, 179-186

Han, W., Gregor, H. P. and Pearce, E. M. **2000**. Interaction of proteins with ultrafiltration membranes: development of a nonfouling index test. *Appl. Polym. Sci.* **77**, 1600-1606.

Hanemaaijer, J.H., Robbertsen, T., Vandenboomgaard, T., Gunnink, J.W. **1989**. Fouling of ultrafiltration membranes – the role of protein adsorption and salt precipitation. *Journal of Membrane Science.* **40** (2), 199-217.

Hermia, J. **1982**. Constant pressure filtration laws - application to power-law non-Newtonian fluids. *Transactions IChemE* **60**,183-187.

Hernandez-Pinzon, I. and Bautista, J. **1992**. Product concentration during tangential flow microfiltration. *Biotechnol. Tech.* **6**, 511-516.

Hernandez-Pinzon, I., Millan, F. And Bautista, J. **1997**. Streptokinase recovery by cross-flow microfiltration: study of enzyme denaturation. *Biosci. Biotech. Biochem.* **61** (8), 1240-1243.

Ho, W.S., Sirkar, K.K. (Eds). **1992**. Microfiltration. In *The Membrane Handbook*, Van Nostrand Reinhold. New York, 455-594.

Hong, S., Faibish, and Elimelech M. **1997**. Kinetics of permeate flux decline in crossflow membrane filtration of colloidal suspensions. *Journal of Colloid and Interface Science* **196**, 267-277.

Howell, J.A., Lojkine, M. And Pritchard, M. **1991**. Cell harvesting using cross flow microfiltration. In *Chromatographic and membrane processes in biotechnology*, ed Costa, C.A. and Cabral, J.S., Kluwer Academic Publishers, 237-252.

Huisman, I.H., Johansson, D., Trägårdh, C. **1997**. Design of a crossflow microfiltration unit for studies of flux and particle transport. *TransIChemE* **75** (A), 508-512.

Huisman, I. H., Prádanos, P., and Hernández, A. **2000**. The effect of protein-protein and protein-membrane interactions on membrane fouling in ultrafiltration. *Journal of Membrane Science* **179**, 79-90.

Hutchinson, N., Bingham, N., Murrell, N., Farid, S., Hoare, M. **2006**. Shear stress analysis of mammalian cell suspensions for prediction of industrial centrifugation and its verification. *Biotechnology and Bioengineering* **95** (3), 483-491.

Hwang, S-J, Chang, D-J, Chen, C-H, **1996,** Steady-state permeate flux for particle crossflow filtration, *Chemical Engineering Journal*, **61,** 171-178.

Jaouen, P., Vandanjon, L., Quemeneur, F. **1999**. The shear stress of microalgal cell suspensions (*Tetraselmis suecica*) in tangential flow filtration systems: the role of pumps. *Bioresource Technology* **68** (2) (May), 149-154.

Jenne M.; Reuss M. 1999. A critical assessment on the use of k-&unknown; turbulence models for simulation of the turbulent liquid flow induced by a Rushton-turbine in baffled stirred-tank reactors. *Chemical Engineering Science,* **54** (17), 3921-3941.

Joshi, J.B., Elias, C.B., Patole, M.S. **1996**. Role of hydrodynamic shear in the cultivation of animal, plant and microbial cells. *Chemical Engineering Journal* **62** (2) (May), 121-141.

Kahn, D. W., Butler, M. D., Cohen, D. L., Gordon, M., Kahn, J.W., and Winkler, M. E. **2000**. Purification of plasmid DNA by tangential flow filtration. *Biotechnology and Bioengineering* **69** (1), 101-106.

Karode, S.K. and Kumar, A. **2001**. Flow visualisation through spacer filled channels by computational fluid dynamics I. Pressure drop and shear rate calculations for flat sheet geometry. *Journal of Membrane Science* **193**, 69-84.

Kawakatsu, T, Nakao, S. and Kimura, S. **1993**. Effects of pore size and compressibility of suspended particles and surface pore size of membrane on flux in crossflow filtration. *Journal of Membrane Science*. **81**,173-190.

Kelly, S. T. and Zydney, A. L. **1997**. Protein fouling during microfiltration: comparative behaviour of different model proteins. *Biotechnology and Bioengineering* **55** (1), 91-100.

Kelly, S.T., Opong, W.S., and Zydney, A.L.**1993**. The influence of protein aggregates on the fouling of microfiltration membranes during stirred cell filtration. *Journal of Membrane Science* **80** (175), 187.

Kelly, S. T. and Zydney, A. L. **1996**. Protein fouling during microfiltration: comparative behaviour of different model proteins. *Biotech Bioeng.* **55** (1), 91-100.

Kelly, W.J., Lorenz, K., Vickroy, T.B. **2004**. Modelling shear-induced damage to CHO cells during tangential flow filtration. *BIOT 393ACS 228th Meeting.*

Kierans, G. and Shaw, B. **2004**.Generating Industry Relevant Data on TFF Processes at Very Small Scale. *PS100ENUS* (Report).

Kirk-Othmer. **1992**. *Encyclopedia of Chemical Technology*, 2nd Ed, Vol. 4, 721.

Kluge, T., Rezende, C., Wood, D., and Belfort, G. **1999**. Protein transmission during Dean vortex microfiltration of yeast suspensions. *Biotechnology and Bioengineering* **65** (6), 649-658.

Knight, P. **1989**. Downstream processing. *Bio/Technology*. **7**, 780-782.

Kossen, M. W. F. **1992**. Scale-up in biotechnology. In *Recent Advances in Biotechnology*, eds. Vardar-Sukan, F. and Suha Sukan, S. Kluywer Academic Publishers, London, 147-182.

Krishna Kumar, N.S., Yea, M.K. and Cheryan, M. **2004**. Ultrafiltration of soy protein concentrate: performance and modelling of spiral and tubular polymeric modules. *Journal of Membrane Science* **244**, 235-242.

Krishnan, M., Kalogerikas, N., Behie, L. A. and Mehrotra, A. K. **1994**. Separation of monoconal IgM antibodies using tangential flow ultrafiltration. *The Canadian Journal of Chemical Engineering* **72**, 982-990.

Kroner, K.H., Schiltte, H., Hustedt, H., Kula, M.R. **1984**. Crossflow filtrate in downstream processing of enzymes. *Process Biochem* **19** (2), 67-74.

Kroner, K.H., Nissinen, V. **1988.** Dynamic filtration of microbial suspensions using an axially rotating filter. *Journal of Membrane Science* **36**, 85-100.

Kuberkar, V.T. and Davis, R.H. **1999**. Effects of added yeast on protein transmission and flux in cross-flow membrane microfiltration. *Biotechnol. Prog.* **15**, 472-479.

Kunas, K.T., & Papoutsakis, E.T. **1990**. Damage mechanisms of suspended animal cells in agitated bioreactors with and without bubble entrainment. *Biotechnology and Bioengineering* **36** (5), 476-483.

Kuriyel, R., Millipore Corporation, 2001. Personal communication.

Kuriyel, R., Millipore Corporation, 2002. Personal communication.

Kuriyel, R., Millipore Corporation, 2003. Personal communication.

Kuruzovich, J.N. and Piergiovanni, P.R. **1996**. Yeast cell microfiltration: optimization of backwashing for delicate membranes. *Journal of Membrane Science* **112**, 241-247.

LaCasse, D., Millipore Corporation, 2004. Personal communication

Lamping, S. R., Zhang, H., Alien, B. and Ayazi Shamlou, P. **2003**. Design of a prototype miniature bioreactor for high throughput automated bioprocessing. *Chemical Engineering Science* **58**, 747-758.

Le, M.S. and Atkinson, T. **1985**. Crossflow microfiltration for recovery of intracellular products. *Process Biochemistry* (February), 26-31.

Lee, S.S., Burt, A., Russotti, G., Buckland, B. **1995**. Microfiltration of recombinant yeast cells using a rotating disk dynamic filtration filtration system. *Biotechnology and Bioengineering* **48** (4), 386-400.

Lendrem, D. **2000**. "Enhancing process development capabilities" *Pharm. Technol Europe* (February), 46-49.

Lengsfeld, C.S. and Anchordoquy, T.J. **2002**. Minireview: Shear induced degradation of plasmid DNA. *J.Pharmaceutical Sciences* **91** (7), 1581-1589.

Levesley, J.A., Hoare, M. **1999**. The effect of high-frequency backflushing on the microfiltration of yeast homogenate suspensions for the recovery of soluble proteins. *Journal of Membrane Science* **158**, 29-39.

Levy, M. S., Collins, I. J., et al. **1998**. Effect of shear on plasmid DNA in solution. *Bioprocess Engineering* **20**, 7-13.

Levy, M.S., Collins, I.J., Yim, S.S., Ward, J.M., Titchener-Hooker, N.J., Ayazi ShamLou, P. and Dunnill, P. **1999**. Effect of shear on plasmid DNA in solution. *Bioprocess Engineering* **20**, 7-13.

Li, F., Meindersma, W., de Haan, A.B., Reith, T. **2002**. Optimization of commercial net spacers in spiral wound membrane modules. *Journal of Membrane Science* **208** (1-2), 289-302.

Li, F., Meindersma, W., de Haan, A.B., Reith, T. **2004**. Experimental validation of CFD mass transfer simulations in flat channels with non-woven net spacers. *Journal of Membrane Science* **232**, 19-30.

Liew, M.K.H., Fane, A.G. and Rogers, P.L. **1997**. Fouling of microfiltration membranes by broth-free antifoam agents. *Biotech. and Bioeng.* **56**, 89-98.

Lindquist, G.M. and Stratton, R.A. **1976**. The role of polyelectrolyte charge density and molecular weight on the adsorption and flocculation of colloidal silica with polyethylenimine. *J. Coll. Int. Sci.* **55**, 45-49.

Lojkine, M.H., Field, R.W. and Howell, J. **1992**. Crossflow microfiltration of cell suspensions: A review of models with emphasis on particle size effects. *Trans IChemE* **70** (Part C), 149-164.

Lu, W.M. and Ju, S.C. **1989**. Selective particle deposition in crossflow filtration. *Sep. Sci. Technol.* **24**.

Lugo, N. M. **1998**. Elements of downstream processing validation. *Biopharm* **11** (6), 18-25.

Luque, S., Mallubhotla, H., Gehlert, G., Kuriyel, R., Dzengeleski, S., Pearl, S., and Belfort, G. **1999**. A new coiled hollow-fiber module design for enhanced microfiltration performance in biotechnology. *Biotechnology and Bioengineering* **65** (3), 247-257.

Maiorella, B., Dorin, G., Carion, A. and Horano, D. **1991**. Crossflow filtration of animal cells. *Biotechnology and Bioengineering* **37** 121-126.

Ma, G. Mimic of a large scale diafiltration process by using ultra scale-down rotating disc filter. Unpublished.

Mannweiler, K. and Hoare, M. **1992**. The scale down of an industrial disk stack centrifuge. *Bioprocess Eng.* **8** 19-25.

Marshall, A.D., Munro, P.A., Tragadh, G. **1997**. Influence of permeate flux on fouling during the microfiltration of beta-lactoglobulin solutions under cross-flow conditions. *Journal of Membrane Science* **130**, 23-30.

Mateus, M., Santos, J.A.L., Cabral, J.M.S. **1993**. Membrane separation processes. In *Recovery processes for biological materials*, ed. Kennedy, J.F. and Cabral, J.M.S. John Wiley and Sons Ltd, 177-222.

Maybury, J. P. **1999**. Scale-down of a bioprocess sequence for the recovery and purification of an intracellular protein. PhD Thesis, University of London.

Maybury, J. P., Hoare, M. and Dunnill, P. **2000**. The use of laboratory centrifigation studies to predict performance of industrial machines: Studies of shear-insensitive and shear-sensitive materials. *Biotech Bioeng.* **67** (3), 265-273.

McDonogh, R.M., Bauser, H., Stroh, N. and Chmiel, H. **1992**. Separation efficiency of membranes in biotechnology: an experimental and mathematical study of flux control. *Chemical Engineering Science* **47** (1), 271-279.

Meacle, F., Aunins, A., Thronton, R. and Lee, A. **1999**. Optimization of the membrane purification of a polysaccharide protein conjugate vaccine using backpulsing. *Journal of Membrane Science* **161**, 171-184.

Meacle, F.J. **2003**. An experimental and computational fluid dynamics atudy of fluid mixing and fluid stress on DNA purification. PhD Thesis, University of London.

Meacle F.J., Zhang H., Papantoniou I., Ward J.M., Titchener-Hooker N.J., Hoare 2007 M.. Degradation of supercoiled plasmid DNA within a capillary device. *Biotechnology and Bioengineering,* 97, 5, 1148-1157,

Meagher, M.M., Barlett, R.T., Rai, V.R., Khan, F.R. **1994**. Extraction of rIL-2 inclusion bodies from *Escherichia coli* using cross-flow filtration. *Biotechnology and Bioengineering* **43** (10), 969-977.

Menon, M.K. and Zydney, A.L. **1999**. Effect of ion binding on protein transport through untrafiltration membranes. *Biotechnology and Bioengineering* **63** (3): 298-307.

Mercer, J. and Seely, R. **2000**. Managing process validation and process changes in the development of a product. *ACS National Meeting,* San Francisco, USA.

Meyer, F., Gehmlich, I., Gunthke, R., Gorak, A. and Knorre, W.A. **1998**. Analysis and simulation of complex interactions during dynamic microfiltration of *Escherichia coli* suspensions. *Biotechnology and Bioengineering* **59** (2), 189-202.

Michaels S.L. **1991**. Validation of tangential flow filtration (TFF) systems. *J Parenteral Science Technol.* **45** (5), 218-23.

Millipore Corporation. **1992**. Membrane based tangential flow filtration systems. *Technical Brief.*
Millipore Corporation. **2000**. Mammalian cell culture clarification: a guide to filter selection (pamphlet).

Morfeld, F., Scutz, R., Josie, D. and Schwinn, H. **1996**. Manufacturing and down scaling process for a virus-inactivated pooled human plasma. *Pharmaceutical Industry* **58**, 433-435.

Morrow, K. J. **2001**. Biopharm manufacturing capacity: seeking solutions for capacity shortage. *Genetic Engineering News* **21**.

Mulder, M. **1996**. *Basic principles of membrane technology*. Kluwer Academic Publishers.

Muller, A., Daufin, G., and Chauffer, B. **1999**. Ultrafiltration modes of operation for the separation of □lactalbumin from acid casein whey. *Journal of Membrane Science* **153**, 9-21.

Murase, T., Ohn, T., and Kimata, K. **1995**. Filtrate flux in crossflow microfiltration of dilute suspension forming a highly compressible fouling cake-layer. *Journal of Membrane Science* **108**, 121-128.

Murkes, J. and Carlsson, C.J. **1988**. *Crossflow Filtration*, John Wiley & Sons Limited.

Murrell, N.J. **1998**. Engineering study of the recovery of shear sensitive biological materials by high speed disk stack centrifuge. PhD Thesis, University of London.

Nagata, N., Herouvis, K.J., Dziewulski, D.M. and Belfort, G. **1989**. Crossflow membrane microfiltration of a bacterial fermentation broth. *Biotechnology and Bioengineering* **34.** 447-466

Nakanishi, K. and Kessler, H.G. **1985**. Rinsing behavior of deposited layers formed on membranes in ultrafiltration. *Journal of Food Science* **50**, 726-731.

Nakanishi, K., Tadokoro, T. and Matsuno, R. **1987**. On the specific resistance of cakes of micro-organisms. *Chem. Eng. Comm.* **62**, 187-201.

Narendranathan, T.J. and Dunnill, P. **1982**. The effect of shear on globular protein during ultrafiltration: Studies of alcohol dehydrogenase. *Biotechnology and Bioengineering* **24**, 2103-2107.

Narodoslawsky, M., Friedler, F., Kiraly, L., Altenburger, H.J., **1993.** SIMBIOS-a new simulation program for biotechnology with novel design, *Chemical and Biochemical Engineering Quarterly*, **7**, 1, 27-30

Nassehi, V. **2001**. Modelling of combined Navier-Stokes and Darcy flows in crossflow membrane filtration. *Chemical Engineering Science* **53** (6), 1253-1263.

Neal, G.E. **2005**. Integrated Scale Down of the Primary downstream purification process and assessment of alternative process options for the production of an ovine polyclonal antibody based anti-venom. PhD Thesis, University of London.

Neusil, J. and Hostalek, Z. **1986**. Enzymes of secondary metabolism and the biosynthesis of macrolide antibiotics. *Folia. Microbiol.* **31**, 402-421.

Ng, P.K. and Obegi, I.A. **1990**. Tangential flow cell separation from mammalian cell culture. *Separation Science and Technology* **25** (6), 799-807.

Nicholson, I.J. **1998**. Outsourcing manufacturing: a strategic rationale. *Biopharm Europe – Conference Proceedings*, Oct 12, Germany.

Niemi, H., Bulsari, A. And Paolsaari, S. **1995**. Simulation of membrane separation by neural networks. *Journal of Membrane Science* **102**, 185-191.

Novais, J.L.F. **2001**. Economic and engineering aspects of disposables-based processing. PhD Thesis, University of London.

O'Kennedy, R.D., Baldwin, C., and Keshavarz-Moore. **2000**. Effects of growth medium selection on plasmid DNA production and initial processing steps. *Journal of Biotechnology* **76**, 175-183.

Okamoto, Y., Ohmori, K. and Glatz, C.E. **2001**. Harvest time effects on membrane cake resistance of *Escherichia coli* broth. *Journal of Membrane Science.* **190**, 93-106.

Okec, R. **1998.** Model development and simulation of membrane separation systems for the recovery of intracellular protein products from crude biological feedstock. Ph.D Thesis, University of London.

Oldshue, J. Y. **1985**. Mixing: Agitation and scale-up of flow-sensitive fluid systems. In *Chemical Engineering*, McGraw-Hill, Inc., New York, 159-168.

O'Leary, R.M., Feuerhelm, D., Peers, D., Xu, Y. and Blank, G.S. **2001**. Determining the useful lifetime of chromatography resins. *BioPharm*, September, 10-18.

Oosterhuis, N. M. G., Kossen, N.W.F., Olivier, A.P.C. and Shenk, E.S. **1985**. Scale-down and optimisation studies of the gluconic acid fermentation by Gluconobacter oxydans. *Biotechnology and Bioengineering* **27**, 711-720.

Opong, W.S. and Zydney, A.L. **1991**. Diffusive and convective transport through asymmetric membranes *AIChE Journal* **37** (10), 1497-1510.

Ould-Dris, A., Jaffrin, M.Y., Si-Hassen, D., and Neggaz, Y. **2000** Effect of cake thickness and particle polydispersity on prediction of permeate flux in microfiltration of particulate suspensions by a hydrodynamic diffusion model. *Journal of Membrane Science* **164**, 211-227.

Palceck, S.P. and Zydney, A.L. **1994**. Intermolecular electrostatic interactions and their effect on flux and protein deposition during protein filtration. *Biotechnol. Prog.* **10**, 207-213.

Palosaari, S., Parviainen, S., Hiironen, J., Reunanen, J., Neittaanmäki, A. 1**986**. A random search algorithm for constrained global optimisation, *Acta. Polytechn. Scand. CH-Series*, **172**, 1-45

Pampel, L.W., Udell, M., Dunnill, P., Titchener-Hooker, N.J. **2000**. A scale-down examination of the use of precipitation and centrifugation for the removal of casein from the milk of transgenic animals. *Food Bioproduct Processing* **78**, 25-42.

Pampel, L. **2002**. A scale-down study of process sequences for the recovery of proteins from transgenic milk. PhD Thesis, University of London.

Parnham, C.S. and Davis, R.H. **1995**. Protein recovery from cell debris using rotary and tangential crossflow microfiltration. *Biotechnology and Bioengineering* **47**, 155-164.

Patel, P.N., Mehaia, M.A., Cheryan, M. **1987**. Cross-flow membrane filtration of yeast suspensions. *Journal of Biotechnology* **5**, 1-16.

Pellerin, E., Michelitsch, E., Darcovich, K., Lin, S. and Tam, C.M. **1995**. Turbulent transport in membrane modules by CFD simulations in 2 dimensions. *Journal of Membrane Science* **100** (2), 139-153.

Pessoa, A. and Vitolo, M. **1998**. Evaluation of cross-flow microfiltration membranes using a rotary disc-filter. *Process Biochemistry* **33** (1), 39-45.

Peters, M. and Timmerhaus, K. **1991**. Plant *Design and Economics for Chemical Engineers*, McGraw-Hill, inc., New York.

Petrides, D. M. **1994**. Biopro Designer: An advanced computing environment for modelling and design of integrated biochemical processes. *Comp. Chem. Eng.* **18**, S621 –S625.

Piron, E., René, F., and Latrille, E. **1995**. A cross-flow microfiltration model based on integration of the mass transport equation. *Journal of Membrane Science* **108**, 57-70.

Piron, E., Latrille, E., and Rene, F. **1997**. Application of artificial neural networks for crossflow microfiltration modelling: "Black-box" and semi-physical approaches. *Computers & Chemical Engineering* **21** (9), 1021-1030.

Pisano, G. P. **1997**. *The development factory*. Harvard Business School Press. Boston, USA

Porter, M.C. **1972**. Concentration Polarization with membrane ultrafiltration. *Ind. Eng. Chem. Prod. Res. Develop.* **11** 234-248.

Postlethwaite, J. **1999**. Scale-down of a Pallsep dynamic microfiltration system. MRes Thesis, University of London.

Postlethwaite, J., Lamping, S.R., Leach, G.C., Hurwitz, M.F. and Lye, G.J. **2004**. Flux and transmission characteristics of a vibrating microfiltration system operated at high biomass loading. *Journal of Membrane Science* **228** (1), 89-101.

Quirk, A.V. and Woodrow, J.R. **1983**. Tangential flow filtration – a new method for the separation fo bacterial enzymes from cell debris. *Biotechnology Letters* **5** (4), 277-282.

Randriamampianina, A., Elena, L., Fontaine, J.P., and Schiestel, R. **1997**. Numerical prediction of laminar, transitional and turbulent flows in shrouded rotor-stator systems. *Physics of Fluids* **9** (6), 1696-1713.

Reismeier, B., Kroner, K.H. and Kula, M.R. **1989**. Tangential-flow filtration of microorganism cell suspension, mathematical model. *J. Biotechnol.* **12**, 153-172.

Reynolds, T. S. **2005**. The accelerated study of bioprocess purification sequences for improved bioprocessing discovery. PhD Thesis, University of London.

Reynolds, T., Boychyn, M., Sanderson. T., Bulmer, M., More, J. and Hoare, M. **2003**. Scale-down of continuous filtration for rapid bioprocess design: Recovery and dewatering of protein precipitate suspensions. *Biotechnology and Bioengineering* **83**, 454-464.

Rock, C.F., Ayazi Shamlou, P., and Levy, M.S. **2003**. An automated microplate-based method for monitoring DNA strand breaks in plasmids and bacterial artificial chromosomes. *Nucleic Acids Research* **31** (11), 1-6.

Romero, C.A. and Davis, R.H. **1988**. Global model of crossflow microfiltration based on hydrodynamic particle diffusion. *Journal of Membrane Science* **39**, 157-185.

Romero, C.A. and Davis, R.H. **1990**. Transient model of crossflow microfiltration. *Chemical Engineering Science* **45** (1), 13-25.

Rosendale, D. M. **2002**. Practical techniques for successful validation of pharmaceutical process equipment. Available from: http://www.vectorcorporation.com/downloads/val-interphex.pdf

Rudniak L. and Wronski, S. **1995.** Influence of hydrodynamics of rotary dynamic filters on separation processes. *Chemical Engineering & Technology.* **18**, 2, 90 - 95

Rudolph, E.A. and MacDonald, J.H. **1994**. Tangential flow filtration for clarification and concentration. In Lydersen, B.K., D'Elia, N.A., and Nelson, K.L. (eds), John Wiley and Sons Inc, pp121-157.

Rumpus, J. **1996**. Dewatering and scale-down of solids in industrial centrifuges. PhD Thesis, University of London.

Russotti, G. and Göklen, K. E. **2000**. Crossflow membrane filtration of fermentation broth. *Merck Research Laboratories*, Rahway, NJ, Marcel Dekker Inc.

Russotti, G., Osawa, A. E., Sitrin, R. D., Buckland, B. C., Adama, W. R., and Lee, S.S. **1995**. Pilot-scale harvest of recombinant yeast employing microfiltration: a case study. *Journal of Biotechnology* **42**, 235-246.

Salisbury, R., Bracewell, D., Titchener-Hooker, N.J. **2006**. A methodology for the graphical determination of operating conditions of chromatographic sequences incorporating the tradeoffs between purity and yield. *Journal of Chemical Technology and Biotechnology* **81** (11), 1803-1813

Salte, H., King, J., Baganz, F., Hoare, M., Titchener-Hooker, N.J. **2006**. A methodology for centrifuge selection for the separation of high solids density cell broths by visualisation of performance using Windows of Operation. *Biotechnology and Bioengineering* **81**

Samatli, N.J., Shah, N., **1996.** Optimal integrated design of biochemical processes, *Computers and Chemical Engineering*, **20**, 315-S320

Santos, J.A.L., Mateus, M., and Cabral, J.M. S. **1991**. Pressure driven membrane processes. In Costa, C.A. and Cabral, J.S. (eds), Kluwer Academic, pp. 177-205.

Schiele, B. **1977**.Untersuchungen zur Filtration feindisperser Suspensionen und zur Stromung im dynamishen Druckfilter. Thesis, University of Stuttgart.

Schlichting, H. **1979**. *Boundary Layer Theory*, McGraw Hill, inc., New York.

Schluep, T. and Widmer, F. **1996**. Initial transient effects during crossflow microfiltration of yeast suspensions. *Journal of Membrane Science* **115**, 33-45.

Schmidt, R.L. **1996**. A stochastic optimisation model to improve production planning and R&D resource allocation in biopharmaceutical production processes. *Management Science* **42** (4), 603-617.

Serra, C.A., Wiesner, M.R., Laîné, J-M. **1999**. Rotating membrane disk filters: design evaluation using computation fluid dynamics. *Chemical Engineering Journal* **72**, 1-17.

Sethi, S. and Wiesner, M. **1996**. MEMSYS: A computer model for performance and cost modelling of low-pressure crossflow membrane filtration processes.

Shalliker, R.A., Broyles, B.S. and Guiochon, G. **2000**. Physical evidence of two wall effects in liquid chromatography. *Journal of Chromatography A*, **888**, 1-12.

Shimizu, Y., Shimodera, K., and Watanabe, A. **1993**. Cross-flow microfiltration of bacterial cells. *Journal of Fermentation and Bioengineering* **76** (6), 493-500.

Shorrock, C.J. and Bird, M.R. **1998**. Membrane cleaning: chemically enhanced removal of deposits during yeast cell harvesting. *Food and Bioproducts Processing* **76** (C1), 30-38.

Shuler, M.L. **1987**. Bioprocess engineering. In: *Encyclopaedia of Physical Science and Technology Vol.2.*, Ed. Meyers, R.A. Academic Press.

Shultis, K. **2002**. The dilemma of process development. *Drug Discovery Today*,**16**, 850-653.

Silva, C.M., Reeve, D.M., Husain, H., Rabie, H.R. and Woodhouse, K.A. **2000**. Model for flux prediction in high-shear microfiltration systems. *Journal of Membrane Science* **173**, 87-98.

Sigma Aldrich. **2003**. Product Catalogue.

Singer, V.L., Jones, L.J., Yue, S.T. and Haughland, R.P. **1997**. Characterization of PicoGreen reagent and development of a fluorescence-based solution assay for double-stranded DNA quantitation. *Anal.Biochem* **249**, 228-238.

Siu, S.C., Baldascini, H., Hearle, D.C., Hoare ,M. and Titchener-Hooker,N.J. **2006**. Effect of fouling on the capacity and breakthrough characteristics of a packed bed ion exchange chromatography column. *Bioprocess Biosystem Engineering* **28**, 405-414

Siwak, M. (Millipore Corporation) **1995**. Calculation of Wall Shear Rate in Turbulence Promoted TFF Devices.

Smidova, D., Mikulasek, P., Wakeman, R.J., and Velikovska, P. **2004**. Influence of ionic strength and pH of dispersed systems on microfiltration. *Desalination* **163** (1-3), 323-332.

Sofer, G. **1996**. Validation: ensuring the accuracy of scaled-down chromatography models. *BioPharm*, October 1996, 51-54.

Sofer, G. **1998**. Validation issues in chromatographic processes. In *Bioseparation and Bioprocessing. A Handbook*, Ed. Subramanian, G. Wiley-VCH, Weinheim, Germany.

Sofer, G. **2001**. From R&D to licensing: what to do and when to do it. *BioPharm* (**August**),18-27.

Song, L., Elimelech., M, **1995.** Theory of concentration polarisation in crossflow microfiltration, *Journal Chemical Society Faraday Transactions*, **91**, 19, 3389-3398.

Spicer. C. 2005. Cambridge Antibody Technology Ltd. Personal communication.

Stamatakis, K., Tien, C., **1993.** A simple model of crossflow filtration based on particle adhesion, *American Institution of Chemical Engineers Journal*, **39,** 8, 1292-1302.

Storey, S. A. **2000**. Physical property indices to aid bioprocess synthesis and design. PhD Thesis, University of London.

Stratton, J. and Meagher, M.M. **1994**. Effect of membrane pore size and chemistry on the crossflow filtration of *Eschericia coli* and *Saccharomyces cerevisiae*: Simultaneous evaluation of different membranes using a versatile flat-sheet membrane module. *Bioseparation* **4**, 255-262.

Sweere, A.P.J., Luyben, K. C. A. M., and Kossen, N.W. F. **1987**. Regime-analysis and scale-down tools to investigate the performance of bioreactors. *Enzyme Microb. Technol* **9** (7), 386-398.

Tanaka, T., Kamimura, R., Itoh, K., and Nakanishi, K. **1993**. Factors affecting the performance of crossflow filtration of yeast cell suspension. *Biotechnology and Bioengineering* **41** (6), 617-624.

Tanaka, T., Abe, K., Asakawa, H., Yoshida, H., and Nakanishi, K. **1994**. Filtration characteristics and structure of cake in crossflow filtration of bacterial suspension. *Journal of Fermentation and Bioengineering* **78** (6), 455-461.

Tanaka, T., Itoh, H., Itoh, K., Nakanishi, K. **1995**. Crossflow filtration of baker's yeast with periodical stopping of permeation flow and bubbling. *Biotechnology and Bioengineering* **47** (3), 401-404.

Taniguchi, M., Kotani, N. and Kobayashi, T. **1987**. High concentration cultivation of lactic acid bacteria in fermenters with crossflow filtration. *J. Ferment. Technology*. **65**, 179-184.

Tarleton, E.S., and Wakeman, R. J. **1994**. Understanding flux decline in crossflow microfiltration: Part II - Effects on Process Parameters. *Trans IChemE* **72** (Part A), 431-440.

Titchener-Hooker, N J. **1998**. Radical ways to reduce biopharmaceutical development times. *BioPharm Europe*, Dusseldorf, Germany.

Titchener-Hooker, N.J. and Hoare, M. **2008**. Micro biochemical engineering to accelerate the design of industrial scale downstream processes for biopharmaceutical proteins. *Biotechnology and Bioengineering*, accepted January 2008.

Titchener-Hooker, N.J., Harri, S., Davies, E., Zhou, Y., Hoare, M. and Dunnill, P. **2001**. Biopharmaceutical process development Part 2, Methods of reducing development time. *Biopharm Europe* 68-74.

Tracy, E.M. and Davis, R.H. **1994**. Protein fouling of track-etched polycarbonate microfiltration membranes. *J. Colloid Interface Sci.* **167**, 104-116.

Turker, M. and Hubble, J. **1987**. Membrane fouling in a constant flux ultrafiltration cell. *J. Membrane Sci.* **34**, 267-281.

Turner, R. 2005. Cambridge Antibody Technology Ltd. Personal communication.

Tutunjian, R.S. **1986**. Cell separations with hollow fibre membranes. In *Comprehensive Biotechnology 2*, Ed. Cooney, C.L. and Humphrey, A, 383-409.

Van den Berg, G.B., Smolders, C.A., **1988.** Flux decline in membrane processes. *Filtration and Separation*, 115-121.

van Reis, R. and Saskena, S. **1997**. Optimisation diagram for membrane separations. *Journal of Membrane Science* **129**, 19-29.

van Reis, R. and Zydney, A. L. **2001**. Membrane separations in biotechnology. *Current Opinion in Biotechnology* **12**, 208-211.

van Reis, R., Leonard, L.C., Hsu, C.C. and Builder, S.E. **1991**.Industrial scale harvest of proteins from mammalian cell culture by tangential flow filtration. *Biotechnology and Bioengineering* **38**, 413-422.

van Reis, R., Gadam, S., Frautschy, L.N., Orlando, S., Goodrich, E.M., Saskena, S., Kuriyel, R., Simpson, C.M., Pearl, A. and Zydney, A.L. **1997**. High performance tangential flow filtration. *Biotechnology and Bioengineering* **56** (1), 71-82.

van Reis, R., Goodrich, E.M., Yson, C.L., Frautschy, L.N., Dzengeleski S. and Lutz, H. **1997**. Linear scale ultrafiltration. *Biotechnology and Bioengineering* **55** (5), 737-748.

van Reis, R., Goodrich, E.M., Yson, C.L., Frautschy, L.N., Whiteley, R., and Zydney, A.L. **1997**. Constant C wall ultrafiltration process control. *Journal of Membrane Science* **130**, 123-140.

van Reis, R., Brake, J.M, Charkoudian, J., Burns, D.B. and Zydney, A.L. et al. **1999**. High-performance tangential flow filtration using charged membranes. *Journal of Membrane Science* **159**, 133-142.

Vandanjon, L., Rossignol, N., Jaouen, P., et al. **1999**. Effects of shear on two microalgae species. Contribution of pumps and valves in tangential flow filtration systems. *Biotechnology and Bioengineering* **38** 63 (1), 1-9.

Varga, E. G., Titchener Hooker, N. J. and Dunnill, P. **1998**. Use of scale-down methods to rapidly apply natural yeast homogenisation models to a recombinant strain. *Bioproc. Eng.* **19**(5), 373-380.

Varga, E. G., Titchener-Hooker, N. J. and Dunnill, P. **2001**. Prediction of the pilot-scale recovery of a recombinant yeast enzyme using integrated models. *Biotechnology and Bioengineering* **74** (2).

Vasquez-AIvarez, E., Lienqueo, M. E. and Pinto, J. M. **2001**. Optimal synthesis of protein purification processes. *Biotechnol. Prog.* **17** (4), 685-696.

Vasan, S.S., Raja Ghosh and Zhanfeng Cui. **2002**. Design of cone-and-plate test cell for ultrafiltration. *Desalination* **146**, 219-224.

Vickroy, T.B., de-Vries, R.L. and Zabriskie, D.W. **1996**. Optimisation of cell culture process development for biopharmaceuticals. *Abstr. Pap. Am. Chem. Soc. 211th Meeting Pt. 1*, BIOT 042.

Vogel, J.H. and Kroner, K.H. **1999**. Controlled shear filtration: A novel technique for animal cell separation. *Biotechnology and Bioengineering* **63** (6), 663-674.

Vogel, J.H., Anspach, B., Kroner, K.H., Piret, J.M., and Haynes, C.A. **2002**. Controlled Shear Affinity Filtration (CSAF): A New Technology for Integration of Cell Separation and Protein Isolation from Mammalian Cell Cultures. *Biotechnology and Bioengineering* **78** (7), 806-814.

von Meien, O.F. and Nobrega, R. **1994**. Ultrafiltration model for partial solute rejection in the limiting flux region. *Journal of Membrane Science* **95**, 277-287.

Wheelwright, S.M. **1987**. Designing downstream processes for large-scale protein purification. *Bio/Technology* **5**, 790-793.

Wheelwright, S. M. **1991**. *Protein purification: design and scale-up of downstream processing*, Oxford University Press, New York, USA.

Wiley, D.E. and Fletcher, D.F. **2003**. Techniques for computational fluid dynamics modelling of flow in membrane channels. *Journal of Membrane Science* **211**, 127-137.

Willoughby, N., Martin, P., Titchener-Hooker, N.J. **2004**. Extreme scale-down of expanded bed adsorption: purification of an antibody fragment directly from recombinant *E.coli* culture. *Biotechnology & Bioengineering* **87**, 641-647.

Winkler. M. K, 0'Leary, R. et al. **2000**. Use of generic studies and scale-down models in process engineering. *ACS National Meeting*, San Francisco, USA.

Winzeler, H. B. and Belfort, G. **1993**. Enhanced performance for pressure-driven membrane processes: the argument for fluid instabilities. *Journal of Membrane Science* **80**, 35-47.

Woodley, J.M. and Titchener-Hooker, N. J.**1996**. The use of windows of operation as a bioprocess design tool. *Bioprocess Eng 1* **14**, 263-268.

Zahka, J. and Leahy, T.J. **1985**. Practical aspects of tangential flow filtration in cell separations. In *Purification of fermentation products*, ed. Leroith, D., Shiloach, J. and Leahy, T.J. *ACS Symposium Series* **271 ACS**, 51-69.

Zeman, L.J. and Zydney, A.L. **1996**. *Microfiltration and ultrafiltration: principles and applications*. Marcel Dekker Inc. N.Y.

Zhang, M. and Song, L. **2000**. Mechanisms and parameters affecting flux decline in crossflow microfiltration and ultrafiltration of colloids. *Environ. Sci. Technol.* **34**, 3767-3773.

Zhou, Y.H. and Titchener-Hooker, N.J. **1999**. Visualising integrated bioprocess designs through "windows of operation". *Biotechnology and Bioengineering.* **65**, 550-557.

Zhou, Y. H. and Titchener-Hooker, N. J. **1999a**. Simulation and optimisation of integrated bioprocesses: a case study. *J. Chem. Technol Biotechnol* **74**, 289-292.

Zhou, Y. H., Holwill, I.L.J. and Titchener-Hooker, N. J. **1997**. A study of the use of computer simulations for the design of integrated downstream processes. *Bioproc. Eng.* **16** (6), 67-374.

Zimmerer ,C.C., Kottke, V. **1996**. Effects of spacer geometry on pressure drop, mass transfer, mixing behaviour, and residence time distribution. *Desalination* **104** (1-2), *129-134.*

Zlokarnik, M. **1983**. Model scale-up in chemical engineering. *Chemical Engineering Technology* **55**, 362-372.

Zydney, A.L., Colton, C.K. **1986.** Concentration polarisation model for filtrate flux in crossflow microfiltration of particulate suspensions, *Chemical Engineering Communications*, **47,** 1-21.